UNIVERSIDADE DA BEIRA INTERIOR
Ciências da Saúde

Development of new antiepileptic drug candidates: a set of lamotrigine-related compounds

Mariana Ruivo Matias

Tese para obtenção do Grau de Doutor em
Ciências Farmacêuticas
(3º ciclo de estudos)

Orientador: Prof. Doutor Gilberto Lourenço Alves
Coorientador: Prof. Doutor Samuel Martins Silvestre
Coorientador: Prof. Doutor Amílcar Celta Falcão Ramos Ferreira

Covilhã, fevereiro de 2018

The experimental work presented in this thesis was performed under the scientific supervision of Professor Gilberto Lourenço Alves, Professor Samuel Martins Silvestre and Professor Amílcar Celta Falcão Ramos Ferreira at the Health Sciences Research Centre, Faculty of Health Sciences, University of Beira Interior, and at the Laboratory of Pharmacology, Faculty of Pharmacy, University of Coimbra.

O trabalho experimental apresentado nesta tese foi realizado, sob a orientação científica do Professor Doutor Gilberto Lourenço Alves, do Professor Doutor Samuel Martins Silvestre e do Professor Doutor Amílcar Celta Falcão Ramos Ferreira, no Centro de Investigação em Ciências da Saúde da Faculdade de Ciências da Saúde da Universidade da Beira Interior e no Laboratório de Farmacologia da Faculdade de Farmácia da Universidade de Coimbra.

The work developed under the scope of the present thesis was supported by Fundação para a Ciência e a Tecnologia (FCT), Portugal (SFRH/BD/85279/2012), involving the POPH–QREN, which is co-funded by FSE and MEC and by FEDER funds through the POCI - COMPETE 2020 - Operational Programme Competitiveness and Internationalisation in Axis I - Strengthening research, technological development and innovation (Project No. 007491) and National Funds by FCT (Project UID/Multi /00709).

Aos meus pais,

À minha irmã,

Aos meus sobrinhos

"Preferi a ciência ao ouro fino
porque a sabedoria vale mais que as pérolas
e tudo quanto há de apetecível
não se lhe pode comparar"

Anónimo

Agradecimentos

"Há um tempo em que é preciso abandonar as roupas usadas,
que já têm a forma do nosso corpo
e esquecer os nossos caminhos
que nos levam sempre aos mesmos lugares.
É o tempo da travessia;
e se não ousarmos fazê-la
teremos ficado, para sempre, à margem de nós mesmos."
Fernando Teixeira de Andrade

É sempre difícil chegar ao fim de uma etapa e olhar para trás, mesmo que este "fim" esteja envolto numa névoa de novas possibilidades e probabilidades correspondentes a um novo início. Embora atribulado, foi um percurso recheado de novidades e descobertas, de cansaço e sacrifício, de felicidade e satisfação. Seria impossível percorrer este caminho sozinha e, por essa razão, aqui deixo os meus agradecimentos:

Ao professor Gilberto Alves, meu orientador,

por me ter endereçado o convite para este grande desafio que é o Doutoramento, pelo voto de confiança que me deu e por ter acreditado sempre em mim e no meu potencial para realizar um trabalho tão aliciante. Obrigada por me ter permitido "abandonar as roupas usadas" e esquecer os "caminhos que nos levam sempre aos mesmos lugares". Quero expressar aqui a minha gratidão pela excelente orientação e apoio científico e pelas incessantes palavras de encorajamento e motivação. Preciso ainda de agradecer a incontestável disponibilidade que sempre manifestou e as imensas horas que dedicou no "terreno" a este trabalho, mesmo quando os resultados não eram animadores. Mas também não posso deixar de referir a imensa alegria que partilhámos quando todo o esforço parecia ser recompensado. Sei que nem sempre foi fácil e por vezes as emoções e o cansaço se evidenciavam, mas é com orgulho que hoje apresento esta tese, fruto desse trabalho, que não teria sido possível sem o seu enorme apoio e orientação.

Ao professor Samuel Silvestre, meu coorientador,

agradeço o inesgotável e incondicional apoio e companheirismo desde o início desta caminhada. Expresso ainda a minha gratidão pelo profissionalismo, disponibilidade e excelente orientação científica, não podendo omitir a sua simplicidade, humildade e humanismo com que sempre me identifiquei. E talvez por isso, por achar que me

compreendia, se tornou meu confidente e me ouviu nas horas mais difíceis, nunca esquecendo de me dar uma palavra de apoio e incentivo. Sem dúvida que desde os meus tempos de mestranda sempre nutri uma grande admiração pela sua capacidade de trabalho e conhecimentos científicos que são para mim um exemplo a seguir.

Ao professor Amílcar Falcão, meu coorientador,

agradeço imenso todo o apoio e ajuda que me foi dando ao longo da realização desta tese de doutoramento. A sua vasta experiência e reconhecimento científico são uma fonte de inspiração e fazem acreditar que podemos ir sempre mais além. Agradeço ainda por me ter aberto as portas da Faculdade de Farmácia da Universidade de Coimbra onde aprendi novas técnicas e procedimentos que valorizaram este trabalho. Resta-me referir que o seu contributo foi fundamental para a realização e conclusão desta tese a múltiplos níveis.

Aos meus colegas do grupo de doutoramento,

agradeço em particular ao Márcio, à Filipa, à Sandra, ao Paulo e à Beatriz, pelo apoio e confidências trocadas. Sem o espírito de entreajuda teria sido mais complicado. Dirijo ainda um agradecimento especial ao Gonçalo pelo apoio e disponibilidade que sempre manifestou e que contribuíram grandemente para o enriquecimento do meu trabalho. Por fim, não posso deixar de destacar o Daniel, companheiro de longa data, que para além do apoio académico, sempre me brindou com a sua amizade.

À professora Ana Fortuna e à Joana Bicker,

por me terem recebido no Laboratório de Farmacologia da Faculdade de Farmácia da Universidade de Coimbra e dado uma ajuda preciosa nos procedimentos experimentais de PAMPA.

Aos restantes colegas do laboratório,

por terem tornado esta minha passagem pelo Doutoramento muito mais simples e animada. Particularmente ao pessoal do laboratório de Química (que apenas não enumero por receio de esquecer alguém) que foram meus amigos e companheiros e de quem guardo um carinho e amizade muito especial. Tenho que realçar as vivências passadas no laboratório de síntese química, assim como na sala de cultura de células, destacando o fantástico e fundamental espírito de entreajuda.

À professora Ana Clara Cristóvão,

pela cedência das células N27 e pelo suporte que deu em relação à manipulação das mesmas.

Aos funcionários do CICS,

por contribuírem para a realização desta tese com o apoio logístico necessário para o desenrolar do trabalho. Um agradecimento especial para a Zé e para a D.ª Dulce com quem convivi quase diariamente e que nunca deixaram que faltasse nada a mim e aos meus animais de laboratório.

À Universidade da Beira Interior,

instituição que duplamente me acolheu, formou e preparou para a vida.

À Fundação para a Ciência e a Tecnologia,

pela atribuição de uma Bolsa de Doutoramento que tornou exequível este trabalho.

A todos os meus amigos e familiares,

pelos bons momentos de convívio proporcionados ao longo destes anos que muitas vezes me fizeram esquecer as preocupações e anseios próprios deste desafio.

À Catarina Canário,

que está sempre presente, nos bons e nos maus momentos. Nos agradecimentos da minha tese de mestrado em 2011 escrevi "Sei que uma amizade assim perdurará" e a prova disso é este agradecimento que hoje dirijo a uma grande amiga. Mesmo que estejamos longe, nos vejamos muito menos que em outros tempos, sei que está sempre lá para me apoiar. Porque já partilhámos muitos momentos, sentimentos, preocupações e alegrias. E porque terá sempre um lugar cativo na minha vida.

Ao Ricardo,

por me mostrar como eu consigo ser forte, superar barreiras e me superar a mim mesma. Por acreditar sempre em mim e nas minhas competências embora não compreenda exatamente o que faço; apenas sabe que irei conseguir e todo o esforço será recompensado. E porque sempre teve orgulho em mim e nunca deixou de me dar força durante este difícil desafio que é cumprir um projeto de Doutoramento. Agradeço principalmente por me fazer sonhar e por me fazer acreditar que vale a pena procurar a felicidade.

À minha irmã Joana, ao Bernardo e aos meus sobrinhos,

gostaria de agradecer tudo o que têm feito por mim. Porque o mundo sem a minha irmã simplesmente não existe e é com quem tenho partilhado não só anseios, preocupações ou alegrias, mas sim a minha vida inteira. Porque nos conhecemos desde sempre e sei que poderei contar com ela sob qualquer circunstância. Agradeço também ao Bernardo que faz

parte desta família e tem sido excelente e incansável sempre que preciso de alguma coisa. Por fim, agradeço aos meus pequenos sobrinhos que ainda não têm noção de como são importantes para mim e, mesmo sem saberem, me dão força para continuar e ir sempre mais além.

***Aos meus pais*,**

serão sempre poucas as palavras para lhes agradecer. Foram muitas horas de conversas, de lamentos e, principalmente de saudade e sentimento de falta. Mas, ao mesmo tempo, todas as alegrias, sucessos e pequenas vitórias também foram (e são) partilhados. Agradeço terem sempre acreditado em mim mesmo quando eu achava que não era capaz e estarem sempre lá para me segurar quando me faltava o chão. Agradeço o apoio, o amor incondicional, os conselhos, o carinho e a paciência que sempre demonstraram e nunca deixaram que me faltasse nada. Quem eu sou e o que conquistei apenas devo a eles e é por essa razão que a eles dedico esta tese. Porque são as pessoas mais importantes da minha vida.

A todos, o meu sincero e sentido OBRIGADA!

Table of Contents

List of Publications

Papers related to this thesis

I. *Gastrodia elata* and epilepsy: Rationale and therapeutic potential

Mariana Matias, Samuel Silvestre, Amílcar Falcão, Gilberto Alves

Phytomedicine, 2016, 23, 1511-1526

Doi: 10.1016/j.phymed.2016.09.001

II. Potential antitumoral 3,4-dihydropyrimidin-2-(1*H*)-ones: synthesis, *in vitro* biological evaluation and QSAR studies

Mariana Matias, Gonçalo Campos, Adriana O. Santos, Samuel Silvestre, Amílcar Falcão, Gilberto Alves

RSC Advances, 2016, 6, 84943-84958

Doi: 10.1039/C6RA14596E

III. Recent Highlights on Molecular Hybrids Potentially Useful in Central Nervous System Disorders

Mariana Matias, Samuel Silvestre, Amílcar Falcão, Gilberto Alves

Mini-Reviews in Medicinal Chemistry, 2017, 17, 486-512

Doi: 10.2174/1389557517666161111110121

IV. Synthesis, *in vitro* evaluation and QSAR modelling of potential antitumoral 3,4-dihydropyrimidin-2-(1*H*)-thiones

Mariana Matias, Gonçalo Campos, Adriana O. Santos, Samuel Silvestre, Amílcar Falcão, Gilberto Alves

Arabian Journal of Chemistry, 2017, *in press*

Doi: 10.1016/j.arabjc.2016.12.007

V. Early preclinical evaluation of dihydropyrimidin(thi)ones as potential anticonvulsant drug candidates

Mariana Matias, Gonçalo Campos, Samuel Silvestre, Amílcar Falcão, Gilberto Alves

European Journal of Pharmaceutical Sciences, 2017, 102, 264-274

Doi: 10.1016/j.ejps.2017.03.014

VI. Screening of pharmacokinetic properties of fifty dihydropyrimidin(thi)ones derivatives using a combo of *in vitro* and *in silico* assays

Mariana Matias, Ana Fortuna, Joana Bicker, Samuel Silvestre, Amílcar Falcão, Gilberto Alves

European Journal of Pharmaceutical Sciences, 2017, 109, 334-346

Doi: 10.1016/j.ejps.2017.08.023

VII. Selection of drug vehicles for evaluation of new drug candidates: focus on *in vivo* pharmaco-toxicological assays based on the rotarod performance test

Mariana Matias, Samuel Silvestre, Amílcar Falcão, Gilberto Alves

Submitted

Book chapter related to this thesis

I. Cytochrome P450-mediated toxicity of therapeutic drugs

Mariana Matias, Catarina Canário, Samuel Silvestre, Amílcar Falcão, Gilberto Alves

In book: Cytochrome P450 Enzymes: Biochemistry, Pharmacology and Health Implications, Publisher: Nova Science Publishers, 2014, Editor: Jian Wu, pp.13-50

Resumo Alargado/Abstract

Resumo Alargado

A epilepsia é uma perturbação neurológica crónica que afeta milhões de pessoas em todo o mundo. Esta perturbação é caracterizada por crises epiléticas espontâneas e recorrentes, muito variadas na sua origem e apresentação clínica, as quais têm um impacto significativo na qualidade de vida dos doentes. A farmacoterapia tem sido, e provavelmente continuará a ser, o pilar da terapia da epilepsia. Todavia, embora um número considerável de novos fármacos antiepiléticos tenha sido introduzido no mercado nos últimos anos, cerca de 30-40% dos doentes epiléticos não alcançam um controlo apropriado das suas crises, mesmo quando são adequadamente tratados com os fármacos antiepiléticos disponíveis atualmente. Por esta razão, a descoberta e desenvolvimento de novas possibilidades farmacoterapêuticas que sejam mais seguras e, principalmente, mais eficazes, constituem um desafio e são de extrema importância.

É neste contexto que surge o principal objetivo do presente trabalho; descobrir novos compostos com propriedades anticonvulsivantes para posterior desenvolvimento de novos fármacos antiepiléticos. Para atingir este objetivo, o *design* dos compostos selecionados baseou-se essencialmente na estrutura química da lamotrigina e levou à síntese de cinquenta dihidropirimidinonas/dihidropirimidinationas [DHPM(t)s] através da reação de Biginelli, a qual consiste numa reação de ciclocondensação entre um aldeído, um ß-cetoester/acetilacetona e ureia ou tioureia. Depois de sintetizados, todos os compostos foram purificados e caracterizados através de espetros de infravermelhos e de ressonância magnética nuclear (protão e carbono-13); espetros de massa de alta resolução também foram obtidos para os compostos novos, ou seja, aqueles que não se encontravam descritos. Posteriormente, a atividade anticonvulsivante dos compostos foi avaliada em modelos animais de crises agudas induzidas eletricamente [teste do eletrochoque máximo (MES)] e quimicamente [teste do pentilenotetrazole subcutâneo (scPTZ)]. O *screening* inicial da atividade anticonvulsivante foi realizado em murganhos CD-1 (n = 4/grupo) e os compostos foram avaliados aos 30 min e às 4 h após a sua administração intraperitoneal nas doses de 30, 100 e 300 mg/kg. Paralelamente, os compostos em investigação também foram avaliados em murganhos, quanto à sua toxicidade neuromotora (traduzida pelo deficit neurológico mínimo), através do teste do aparelho rotativo. Posteriormente, alguns dos compostos identificados previamente como anticonvulsivantes nos murganhos na mínima dose testada foram ainda selecionados e testados em ratos Wistar (n = 4/grupo) aos 30 min, 2 h e 4 h após administração oral de uma dose de 30 mg/kg. Adicionalmente, as cinquenta DHPM(t)s foram avaliadas relativamente à sua citotoxicidade em sistemas *in vitro* de linhas celulares, concretamente em células dopaminérgicas mesencefálicas de rato (N27), células de carcinoma hepatocelular humano (HepaRG), células de adenocarcinoma coloretal humano (Caco-2) e fibroblastos normais da derme humana (NHDF), através do ensaio bem estabelecido do brometo de 3-(4,5-

dimetiltiazol-2-il)-2,5-difeniltetrazólio (MTT) e a uma concentração de 30 μM. Além disso, como a eficácia de uma molécula está fortemente dependente da sua farmacocinética, várias propriedades cinéticas também foram investigadas em modelos *in vitro* e *in silico*. Assim, todos os compostos sintetizados foram sujeitos a um conjunto de ensaios de *screening in vitro* realizados numa linha celular que sob-expressa o transportador de efluxo glicoproteína-P (células MDCK-MDR1) e em dois modelos de ensaios de permeabilidade em membrana artificial paralela (PAMPA), preditivos da permeabilidade aparente dos compostos através da membrana intestinal (PAMPA intestinal) e da barreira hematoencefálica (PAMPA-BBB). Por último, diversas propriedades físico-químicas dos compostos também foram calculadas *in silico* e um conjunto de propriedades farmacocinéticas e de toxicidade foram estimados com a uma nova ferramenta computacional, pkCSM.

As moléculas alvo sintetizadas foram selecionadas principalmente com base na estrutura de fármacos antiepiléticos clinicamente relevantes, em particular a estrutura da lamotrigina, com o objetivo de descobrir novos candidatos para o desenvolvimento de fármacos antiepiléticos melhorados. A maioria das reações químicas ocorreram rapidamente e obtiveram-se bons rendimentos (acima de 60-70%) para grande parte dos produtos sintetizados. O procedimento de síntese química utilizado foi estendido também a reagentes específicos adicionais, tendo sido sintetizados com sucesso os produtos respetivos, os quais são novos (não descritos na literatura). Devido a questões práticas (baixos rendimentos na sua obtenção e fraca solubilidade aquosa), apenas quarenta e dois compostos (vinte e oito derivados de ureia e catorze derivados de tioureia) prosseguiram para os estudos *in vivo*. Os modelos animais usados foram os modelos *gold standard* para a identificação de novos compostos com propriedades anticonvulsivantes, sendo, desta forma, os modelos melhor validados. Os resultados do *screening* farmacológico inicial em murganhos revelaram proteção anticonvulsivante no modelo MES para vinte e quatro compostos, sendo nove deles ativos na dose mais baixa testada (30 mg/kg). Em termos estruturais, os compostos mais promissores apresentam cadeias mais curtas (provenientes da acetilacetona ou do acetoacetato de metilo) e um anel aromático não substituído ou substituído na posição *para* com um grupo metilo ligados, respetivamente, ao C5 e ao C4 do anel dihidropirimidínico. Referir também que os derivados tioureia apresentaram uma atividade anticonvulsivante ligeiramente superior comparativamente aos análogos correspondentes da série ureia. Os resultados de toxicidade neuromotora obtidos através do teste do aparelho rotativo evidenciaram que aproximadamente 52% dos compostos são menos tóxicos que a lamotrigina, carbamazepina e fenitoína. Os compostos **MM 17**, **MM 19** (derivados de ureia) e **MM 83** (derivado de tioureia) também protegeram contra as crises induzidas pelo MES em 50-75% dos ratos após administração oral (*gavage*) na dose de 30 mg/kg. Para além da atividade anticonvulsivante, os compostos mais ativos não exibiram citotoxicidade marcada nos estudos *in vitro* realizados nas diversas linhas celulares (proliferação celular relativa superior a 50% a 30 μM), o que pode ser relevante devido ao facto da toxicidade ser um problema comum aos fármacos antiepiléticos disponíveis. Neste contexto, as células N27 foram utilizadas por serem células

neuronais e os alvos de ação dos fármacos antiepiléticos estarem localizados no sistema nervoso central. Por outro lado, procedeu-se à avaliação da citotoxicidade em células hepáticas (HepaRG) e intestinais (Caco-2), respetivamente, porque alguns fármacos antiepiléticos têm sido associados a hepatotoxicidade severa e porque a via oral é a via de administração desejada. Como estas duas linhas celulares são cancerígenas, considerou-se incluir também uma linha celular humana não cancerígena (NHDF).

Relativamente aos estudos farmacocinéticos, os dados obtidos mostraram que 82% dos compostos investigados devem apresentar boa permeabilidade intestinal (Papp > $1{,}1\times10^{-6}$ cm/s), 66% dos quais poderão ter boa penetração cerebral (Papp > $2{,}0\times10^{-6}$ cm/s), o que pode sugerir uma elevada permeabilidade passiva transcelular passiva. Em ambos os ensaios, os derivados tioureia apresentaram valores de permeabilidade superiores em relação aos respetivos análogos da série ureia, o que pode estar associado à sua natureza mais lipofílica. Estes resultados podem explicar, pelo menos em parte, a maior atividade observada para os derivados tioureia no *screening* anticonvulsivante após as administrações por via intraperitoneal e via oral. Notar também que 44% dos compostos não modularam significativamente a glicoproteína-P (por inibição ou indução) a 10 μM e 50 μM. Este foi um achado importante porque a glicoproteína-P está fisiologicamente expressa em vários tecidos e órgãos relevantes de um ponto de vista farmacocinético. Finalmente, os estudos *in silico* indicaram que todos os compostos respeitam a regra dos cinco de Lipinski, sugerindo que eles possuem propriedades intrínsecas favoráveis de forma a preencher os critérios de *druglikeness*. A ferramenta *in silico* pkCSM também estimou que as DHPM(t)s têm boa absorção intestinal no homem (67,73-93,91%) e um volume aparente de distribuição no estado estacionário na mesma gama de valores encontrados para os fármacos antiepiléticos. As predições *in silico* também sugeriram uma percentagem baixa de ligação às proteínas plasmáticas para os compostos em estudo, o que é considerado favorável terapeuticamente, minimizando-se assim o risco de interações. Estes resultados corroboram os resultados obtidos no ensaio de PAMPA intestinal que mostrou que provavelmente nenhum dos compostos testados têm uma ligação às proteínas plasmáticas superior a 90% (Papp ≤ $1{,}0\times10^{-5}$ cm/s). Os derivados tioureia foram ainda considerados como os compostos que permeiam melhor através de barreiras biológicas (p.e., em monocamadas de células Caco-2 e barreira hematoencefálica), de modo similar ao obtido nos estudos experimentais de PAMPA. Contudo, o modelo preditivo utilizado sugeriu que 14% dos derivados ureia têm tendência para inibir o citocromo P450 *versus* 36% dos derivados tioureia. Por outro lado, preocupações com a disrupção da função hepática normal foram preditas para metade dos compostos.

Globalmente, os estudos levados a cabo fornecem novas informações sobre a atividade anticonvulsivante desta classe de heterociclos, bem como dados farmacocinéticos e de toxicidade. Mais de metade das moléculas investigadas apresentaram proteção anticonvulsivante contra as crises induzidas eletricamente (no modelo do MES), confirmando o interesse do modelo farmacofórico para o *design* de novos agentes anticonvulsivantes. Os

dados aqui reunidos permitiram a identificação de características estruturais importantes destas moléculas que podem ser responsáveis pela atividade anticonvulsivante, as quais devem ser mantidas ou melhor exploradas para produzir análogos mais ativos nos próximos passos do desenvolvimento destes candidatos a fármacos. No entanto, os resultados apresentados nesta tese constituem apenas a "ponta do iceberg" no que diz respeito à descoberta e desenvolvimento de DHPM(t)s como potenciais fármacos antiepiléticos.

Palavras-chave

Atividade anticonvulsivante, Descoberta e desenvolvimento de fármacos, Dihidropirimidinonas/Dihidropirimidinationas, Epilepsia, Farmacocinética, Fármacos Antiepiléticos, Toxicidade

Abstract

Epilepsy is one of the most common, chronic and serious neurological disorder, affecting million people worldwide. This brain disorder is characterised by recurrent spontaneous seizures, which have a considerable impact in the patients' quality of life. The pharmacological therapy has been, and is likely to remain, the mainstay of treatment for this disorder. Although a large number of new antiepileptic drugs (AEDs) has been introduced into the market in the last years, about 30-40% of epileptic patients are still inadequately controlled by standard drug therapy. For this reason, it continues to be important to develop new and improved chemical entities through which epilepsy could be effectively controlled.

In this context, the main objective of the present work was to discover new lead compounds with anticonvulsant properties for further development as AEDs. To achieve this goal, fifty dihydropyrimidin(thi)ones [DHPM(t)s] were synthesized through the Biginelli reaction, which consists in a one-pot cyclocondensation reaction among an aldehyde, a ß-ketoester/acetylacetone and urea or thiourea. The products were purified and characterised by infrared and ^{1}H- and ^{13}C-nuclear magnetic resonance spectroscopy. High resolution mass spectrum was also obtained for the novel compounds. Afterwards, the anticonvulsant activity of the compounds was evaluated against electrically [maximal electroshock seizure (MES) test] and chemically [subcutaneous pentylenetetrazole (scPTZ) test] induced seizures in rodent models. The initial anticonvulsant screening was performed in CD-1 mice (n = 4/group) at 30 min and 4 h after the intraperitoneal administration of 30, 100 and 300 mg/kg of each compound. The investigated compounds were also evaluated in mice for neuromotor impairment (as a surrogate of minimal neurological deficit) on the rotarod performance test. Then, selected compounds previously identified as anticonvulsants in mice at the minimum dose tested were further assessed in Wistar rats (n = 4/group) at 30 min, 2 h and 4 h after the oral administration of 30 mg/kg. Additionally, the fifty DHPM(t)s were evaluated for their *in vitro* cytotoxicity in rat mesencephalic dopaminergic (N27), human hepatocellular carcinoma (HepaRG), human colorectal adenocarcinoma (Caco-2) and normal human dermal fibroblasts (NHDF) cell lines, through the well-established 3-(4,5-dimethylthiazol-2-yl)-2,5-diphenyltetrazolium bromide (MTT) assay at the concentration of 30 µM. Moreover, as the efficacy of a molecule is strongly dependent on its pharmacokinetics, several kinetic properties were also investigated in *in vitro* and *in silico* models. Thus, all compounds were subjected to a set of *in vitro* screening assays performed on a cell line overexpressing the drug efflux transporter P-glycoprotein (MDCK-MDR1 cells) and on two models of parallel artificial membrane permeability assay (PAMPA) preditive of the apparent permeability (Papp) through intestinal membrane (intestinal PAMPA model) and blood-brain barrier (PAMPA-BBB model). Lastly, several physicochemical properties of the compounds were also

calculated *in silico* and a set of pharmacokinetic and toxicity properties were estimated employing the new computational tool, pkCSM.

The target molecules that were synthesized were mainly selected based on the structure of clinically relevant AEDs, in particular the structure of lamotrigine, aiming to discover new candidates for the development of improved AEDs. The majority of the chemical reactions occurred fastly and the products were obtained in good yields. The synthetic procedure used was also extended using additional specific reagents, being the respective products, which are new to the best of our knowledge, successfully synthesized. Due to practical considerations, only forty-two compounds (twenty-eight urea derivatives and fourteen thiourea derivatives) proceeded to *in vivo* experiments. The results of the initial pharmacological screening in mice revealed anticonvulsant protection in the MES model for twenty-four compounds showed anticonvulsant protection in the MES model, being nine of them active at the lowest dose tested (30 mg/kg). Structurally, the most promising compounds present smaller chains at the C5 of the dihydropyrimidine ring and an unsubstituted phenyl or a *para*-tolyl ring at the C4. In addition, the thiourea analogues also presented slightly increased anticonvulsant activity comparing with the corresponding urea analogues. The results of the minimal neuromotor impairment obtained through the rotarod assay showed that approximately 52% of the compounds are less toxic than lamotrigine, carbamazepine and phenytoin. Compounds **MM 17**, **MM 19** and **MM 83** also protected against MES-induced seizures in 50-75% of rats after the oral administration of 30 mg/kg. Furthermore, the most active compounds did not show notable cytotoxicity in *in vitro* experiments conducted in the several cell lines (relative cell proliferation higher than 50% at 30 μM), which can be relevant due to the fact that the toxicity is a common problem of the available AEDs. The data obtained showed that 82% of the investigated compounds are expected to have good intestinal permeability (Papp > 1.1×10^{-6} cm/s), and 66% of which good brain penetration (Papp > 2.0×10^{-6} cm/s), which can suggest a high passive transcellular permeability. In both cases, thiourea derivatives presented higher permeability values than the respective urea analogues, which can be associated with their higher lipophilicity. This finding can explain, at least in part, the higher activity of the thiourea derivatives in the anticonvulsant screening after both intraperitoneal and oral administrations. In addition, 44% of the compounds did not significantly modulate (inhibit or induce) P-glycoprotein at 10 and 50 μM. This is an interesting finding since P-glycoprotein is physiologically expressed in several tissues and organs relevant from a pharmacokinetics perspetive. Finally, *in silico* studies indicated that all compounds respect the Lipinski's rule-of-five, suggesting that they possess favourable properties that fulfil the druglikeness criteria. The pkCSM *in silico* tool also estimated that the DHPM(t)s have good human intestinal absorption (67.73-93.91%) and an apparent volume of distribution at the steady-state in the same range of values of the AEDs. The *in silico* predictions also suggested a low plasma protein binding percentage for the target compounds, which is considered to be therapeutically favourable, minimizing the risk of drug interactions. These results corroborate those obtained with the intestinal PAMPA

assay that showed that probably none of the tested compounds have a binding to plasma proteins higher than 90% (Papp ≤ 1.0×10^{-5} cm/s). The thiourea derivatives were also predicted as compounds that permeate better through biological barriers (e.g., Caco-2 cell monolayers and blood-brain barrier), similarly to the observed in the experimental PAMPA assays. However, the prediction model suggested that 14% of the urea derivatives have tendency for cytochrome P450 inhibition *versus* 36% of the thiourea derivatives. On the other hand, concerns on the disruption of normal liver function were predicted for half of the compounds.

Overall, the set of studies carried out provide new information about the anticonvulsant activity of this class of heterocycles, along with pharmacokinetic and toxicity data. More than half of the investigated molecules showed anticonvulsant protection against electrically-induced seizures (MES model), confirming the interest of the pharmacophoric model for the design of new anticonvulsant agents. The data gathered here allowed to identify important structural features of this attractive scaffold that can be responsible for the anticonvulsant activity, which should be maintained or better explored in order to produce more active analogues in further hit-to-lead optimization. However, the results presented in this thesis are just the "tip of the iceberg" in the discovery and development of the DHPM(t)s as potential AEDs.

Keywords

Anticonvulsant activity, Antiepileptic drugs, Dihydropyrimidin(thi)ones, Drug discovery and development, Epilepsy, Pharmacokinetics, Toxicity

List of Figures

Appendix

List of Tables

List of Abbreviations

l

A

Ab	10,000 units/mL penicillin G, 100 mg/mL streptomycin and 25 µg/mL amphotericin B
ABC	Adenosine triphosphate-binding cassette
ADME	Absorption, distribution, metabolism and excretion
ADMET	Absorption, distribution, metabolism, excretion and toxicity
AED	Antiepileptic drug
AMPA	α-Amino-3-hydroxy-5-methyl-4-isoxazolepropionic acid
ATP	Adenosine triphosphate

B

BBB	Blood-brain barrier
BCRP	Breast cancer resistance protein
Brs	Broad singlet

C

CMC	Carboxymethylcellulose
CNS	Central nervous system
CR	Component reaction
CYP450	Cytochrome P450

D

d	Doublet
dd	Double doublet
DDI	Drug–drug interactions
DHPM	3,4-Dihydropyrimidin-2(1*H*)-one
DHPMt	3,4-Dihydropyrimidin-2(1*H*)-thione
DMSO	Dimethyl sulfoxide
DMSO-d_6	Hexa deuterated dimethyl sulfoxide
dq	Double quartet

E

ED_{50}	Median effective dose
EEG	Electroencephalogram
EMA	European Medicines Agency

F

Fa	Intestinal absorption fraction
FBS	Fetal bovine serum
FDA	Food and Drug Administration
Fu	Unbound fraction

G

GABA	γ-Aminobutyric acid
GEPR	Genetically epilepsy-prone rats

H

HRMS	High resolution mass spectrometry

Hy	Hydrophilic factor
HTS	High throughput screening
Hz	Hertz

I

IC_{50}	Median inhibitory concentration
IL-1ß	Interleukin 1ß
ILAE	International League Against Epilepsy
IR	Infrared
ip	Intraperitoneal
iv	Intravenous

L

Log BB	Logarithm of the brain-to-blood concentration ratio
Log *P*	*n*-Octanol/water partition coefficient
Log PS	Logarithm of blood-brain permeability-surface area product

M

m	Multiplet
MCR	Multicomponent reaction
MDR1	Multidrug resistance 1
MES	Maximal electroshock seizure
MRP	Multidrug resistance protein
mTOR	Mammalian target of rapamycin
MTT	3-(4,5-Dimethylthiazol-2-yl)-2,5-diphenyltetrazolium bromide
MV	Molecular volume
MW	Molecular weight

N

NINDS	National Institute of Neurological Disorders and Stroke
NMDA	*N*-methyl-D,L-aspartate
NMR	Nuclear magnetic resonance
n-OH acceptors	Number of hydrogen bond acceptors
n-OHNH donors	Number of hydrogen bond donors
n-ROTB	Number of rotatable bonds

O

OD	Optical density

P

PAMPA	Parallel artificial membrane permeability assay
Papp	Apparent permeability
PBS	Phosphate buffer saline
PEG	Polyethylene glycol
PG	Propylene glycol
P-gp	P-glycoprotein
PPB	Plasma protein binding
ppm	Parts per million
PTZ	Pentylenetetrazole

Q

q	Quartet
QSAR	Quantitative structure-activity relationship

R

Rh123	Rhodamine 123

S

s	Singlet
SAR	Structure-activity relationship
sc	Subcutaneous
SD	Standard deviation
sp	10,000 units/mL penicillin G and 100 mg/mL of streptomycin
SV	Synaptic vesicle proteins

T

t	Triplet
TD_{50}	Median toxic dose
TPSA	Topological polar surface area
TSC	Tuberous sclerosis complex

U

USA	United States of America

V

VD	Apparent volume of distribution
VD_{ss}	Apparent volume of distribution at the steady-state

CHAPTER I

GENERAL INTRODUCTION

I.1. DRUG DISCOVERY AND DEVELOPMENT

I.1.1. Drug discovery and development process

Drug discovery and development is a challenging process that is expensive, time consuming, and troubled by failures at the same time that demands high standards of rigor, quality and ethics (Nierode et al., 2016). The need for novel and innovative therapeutic agents is not only associated with health disorders for which there are generally no effective medications (e.g. neurodegenerative/neurological diseases), but also with therapeutic areas that are historically well served, such as the discovery of new antibiotics due to the development of bacterial resistance (Ator et al., 2006). Despite the drug discovery and development process has shown a strong historical record for delivering life-saving medicines that have drastically improved individual and global public health cares, the metrics suggest that few or no gains have been made in the last two decades (Kaitin, 2010). In this way, continuous changes and improvements are both inevitable and needed.

The steps by which the drug discovery and development process leads to the generation of a new drug are typically categorized as follows: drug discovery, preclinical development, clinical development and marketing authorization. Therefore, a drug discovery project involves the development of a hypothesis that is relevant to the disease pathogenesis (e.g. target selection) and the discovery of small or large molecule drug candidates (i.e., screening, identification of "hits" and their optimization to lead compounds) that eventually become new chemical entities with the desired physicochemical, biological, safety and pharmacological preclinical characteristics. Further, some of these new chemical entities advance to extensive clinical drug development, involving numerous clinical trials to assess tolerability and pharmacokinetics (Phase I) and efficacy and safety (Phases II and III), until commercialization as drugs. The entire process usually lasts a decade or longer to produce a single new medicine and requires an organizationally networked environment (Caldwell, 2015). Although the pharmaceutical industry is the major driver of the discovery and development of new drugs, the role of academia in this context is also important, particularly in some therapeutic areas, as is highlighted in the final of this section.

I.1.1.1. Drug discovery

Drug discovery represents the first step in the generation of new drugs, and takes place in academic institutions, biotech companies, and large pharmaceutical corporations (Fishburn, 2013). These new chemical entities can be discovered, developed or optimized from several sources, such as natural products, exploitation of known pharmacophores, synthetic diversity libraries, rationally planned approaches (e.g. computer-assisted molecular design) and even by serendipity (Ator et al., 2006). The process of drug discovery includes several steps that take advantage of *in vitro* and *in vivo* screening models usually in combination with *in silico*

tools as selection criteria to advance drug candidates from one stage to another (Caldwell, 2015).

I.1.1.1.1. Target-based approach and network pharmacology

Since the early 1990s, the target-based drug discovery has been the prevalent approach in the pharmaceutical industry (Sams-Dodd, 2006). This strategy starts with the selection of a target (usually defined as a macromolecule to which the molecules bind and to promote their biological activities) that should be accessible to the putative drug molecule in order to induce the biological response that may be measured both in *in vitro* and *in vivo* assays (Hughes et al., 2011). These targets are of value for drug discovery only if they can be convincingly related to disease pathogenesis, maintenance or progression (Fishman and Porter, 2005). Thus, the target-based strategy enables the definition of specific molecular mechanisms or modes-of-action to be targeted by the molecules, which allows the use of molecular modelling techniques, structure-activity relationships (SARs) and automated screening technologies (Sams-Dodd, 2006).

However, incorrect or suboptimal selection of the molecular targets can lead to the lack of the expected efficacy, even in later phases of the drug development. In addition, potent molecules that are selective for a single target may increase the risk of adverse events or be limited by adaptive resistance (Andrade et al., 2016; Martínez-Jiménez and Marti-Renom, 2016). Thus, although often important, the knowledge of the target for a drug candidate is not necessarily an absolute requirement in initial drug development stages. For example, several diseases (e.g. neurological disorders) are complex and multifactorial and, therefore, drugs would require interaction with multiple targets to produce clinically meaningful effects (Andrade et al., 2016). In fact, the design of multitarget drugs, with multiple mechanisms of action, is one of the hottest topics and is becoming a new paradigm in drug discovery, which led to the appearing of the network pharmacology concept (Nicolaou, 2014).

A network approach relies on the systems biology view of the disease (Margineanu, 2014), focusing in the study of the biological pathways, rather than single drug targets, and in the identification of potential drugs capable of shifting the function of these pathways in order to produce the desirable action (Baggs et al., 2010). In fact, a target must be viewed not by itself, but as a part of a complex system. Thus, this approach affords a rational basis for useful strategies in drug design, providing a fresh perspective in the understanding of important nodes in a large molecular network that has the highest levels of connectivity associated with important functions and whose manipulation could lead to a significant perturbation of the network (Chandra and Padiadpu, 2013).

I.1.1.1.2. Hit-to-lead process

The next important step in the drug discovery pipeline is the hit identification and lead discovery. A "hit" molecule is defined as a compound that displays the desired activity and whose activity is confirmed upon retesting (Hughes et al., 2011). These hits will serve as the starting point for a medicinal chemistry optimization endeavour.

There are a variety of experimental and computational screening paradigms to identify hit molecules. Among them, high throughput screening (HTS) describes a set of technologies designed to permit a rapid and automated analysis of a library of compounds (Ator et al., 2006). Specifically, HTS includes the screening of the entire compound library directly against the drug target or in more complex assay systems (e.g. cell-based assays). The primary purpose of HTS is not to identify drug candidates, but rather to identify small subsets of molecules (functional groups or pharmacophores) that are associated with the bioactivity and can serve as a starting point for an iterative "hit-to-lead" campaign to optimize the efficacy and drug-like properties of a hit (Ator et al., 2006; Hughes et al., 2011). These molecules and their analogues can be further explored as possible lead compounds. A "lead" molecule is a compound that shows the most promising chemical structure, exhibiting high potency in biological assays that express the target mechanism, whose safety and pharmacokinetic profile usually have to be improved. Hence, its potential is established by a whole range of properties beyond its activity. For this reason, it is also characterised concerning a range of other physico-chemical (e.g. solubility) and biological (e.g. permeability, metabolic stability, target binding affinity) properties that are known to be relevant in drug candidates (Murray and Rees, 2009).

I.1.1.1.3. Lead optimization and candidate selection

After leads are identified, their activity, selectivity and pharmacokinetic features are optimized in an iterative and multifactorial process, leading to the selection of a suitable candidate for development. The employed assays are part of a critical path for compound characterisation and should be able to provide robust and useful information (Williams, 2011). Thus, lead optimization includes the process whereby the structures of the active molecules suffer chemical changes followed by biological studies in order to evaluate the impact of these modifications on "hitting the target". This process requires careful evaluation and appropriate time to select the final lead agents (Grever, 2013). Therefore, in this stage, there is also a generation of SAR data and defining the essential elements in the structure associated with activity, pharmacokinetics and safety. SARs for different properties of a molecule can be distinct, such that structural modifications improving one aspect (e.g. toxicity) can be detrimental for others (e.g. efficacy), making compound optimization a highly dynamic process (Ator et al., 2006).

The activity of new representatives of a lead series can be evaluated almost simultaneously in a variety of assay systems, such as *in vitro* activity assays against the molecular target (in both cell-free and cellular systems), selectivity profiling and *in vivo* efficacy and toxicity. *In vitro* assays designed to provide important information about absorption, distribution, metabolism and excretion (ADME) properties, as well as physicochemical characteristics, are also performed. It is also intended the selection of compounds that present good bioavailability and stability, with high chiral purity, and of easy and cost-effective production. In this context, issues of chemical synthesis have to be examined: ease of preparation, potential amenability to parallel synthesis and the ability to generate diversity from late-stage intermediates. Overall, in this phase, strengths and weaknesses of each series are revealed, which allows making decisions about the most promising series of compounds to be progressed (Ator et al., 2006; Hughes et al., 2011).

I.1.1.2. Preclinical development

Once obtaining a lead compound suitably optimized, a broad set of preclinical development studies are conducted and the results obtained are used in the decision-making process to determine the progression or not for the first-in-human studies.

In this stage, compounds should be examined through a more complex, integrated, hierarchical and pharmacological driven approach. All the information gathered about the molecule in terms of efficacy, toxicity and pharmacokinetic, pharmacodynamic and pharmaceutical properties will form the scientific basis of a regulatory submission previous to the beginning of the first clinical trials. The non-clinical evaluation of a new drug candidate can be carried out throughout all stages of drug development and is crucial to provide the basic knowledge on the pharmacodynamics and pharmacokinetics. Thus, the preclinical assessment usually includes the following tests:

- *In vitro and ex vivo assays*: Distinct *in vitro* models may reflect different levels of molecular and cellular organization, providing different levels of information. Particularly *in vitro* cell culture systems have proven to be valuable tools to study multiple biological, physiological and pathological cellular processes (Astashkina et al., 2012). A highlight goes to the three-dimensional cell culture models that are more complex and maintain several functions of the native tissue and, in some cases, represent the physiological response to drugs. Moreover, the potential drug candidates should also be evaluated in *ex vivo* models, in which also complex structures are considered. A continuous challenge in this aspect has allowed to acquire accurate information from *in vitro* assays to increase the success rate of potential drugs in clinical trials (Andrade et al., 2016; Nierode et al., 2016);

- *In vivo assays*: Despite the efforts for the standardization and validation of alternative methods to reduce the use of whole-animal models, *in vitro* assays have major limitations for the preclinical evaluation of several parameters and the use of laboratory animals in the process of drug development is still essential to meet the standards required by the drug regulatory agencies (Andrade et al., 2016). To be representative of the human condition, a good animal model should have predictive validity (Hendriksen and Groenink, 2015). Consequently, the animals are used with several purposes, for instance, to study different routes of administration, dosing regimens and appropriate formulations; to determine potential safety risks of the compounds; to discover and validate therapeutic targets; to estimate the potential therapeutic index; and to refine the pharmacokinetic profile and validate the pharmacodynamic effects (Ator et al., 2006; Grever, 2013).

Acquisition and assembly of the entire preclinical data package and compiling them for submission to the regulatory entities, such as Food and Drug Administration (FDA) and European Medicines Agency (EMA), takes years of work. In spite of the deep impact of the length of time needed for the development of new drug candidates, failure to establish the necessary preclinical information may result in an unsafe and ineffective clinical development (Grever, 2013).

I.1.1.3. Clinical development

Clinical research comprises the longest part of the entire drug development process, representing the largest expenditure (Glass et al., 2015). Clinical investigations are usually categorized in clinical trials of Phase I, Phase II and Phase III. Phase IV studies take place after the drug is approved for marketing.

- *Phase I*: Phase I studies, lasting 2 years on average, often represent the first human exposure to the new medicinal product and typically involves the participation of a small number of healthy volunteers (n = 20–80). Depending on the target disease and patient demographics, patients or targeted populations may also be included. Critically ill or terminal patients can also enter in phase I trials, depending on the assessed risk-benefit ratio (Ator et al., 2006; Ciociola et al., 2014). The studies in this phase are focused on tolerability and safety evaluation. They are designed to establish a nontoxic dosage range as well as to determine drug dosing, identify the most frequent side effects and determine the clinical pharmacokinetic properties of the drug candidate. These studies also intend to minimize the potential risk for subjects to be included in future studies, while providing sufficient information to enable the design of scientifically valid phase II studies (Ciociola et al., 2014; Williams, 2016);
- *Phase II*: Once the tolerability/safety, pharmacokinetics and dose range selection have been established for the potential drug in healthy volunteers, the next step is to

investigate its efficacy and safety in the target patient population. Hence, in this phase around 100 to 300 patients are included and, similarly to phase I, the average duration is about 2 years (Ciociola et al., 2014). Phase II is usually divided into Phase IIa and Phase IIb. The first refers to the exploratory clinical pharmacology (first indication of efficacy) in a small amount of patients (*n* = 12-100) and the tested candidate usually is given in a single-dose regimen at the maximum tolerated dose. In Phase IIb studies, several dose levels are tested in the target population to define the minimally effective or non-effective as well as the optimal doses, based on both clinical efficacy and safety (Shillingford and Vose, 2001; Tamimi and Ellis, 2009). Additional patients receiving a standard drug for the treatment of the disease can also be included for comparison, which may be important in the decision-making process (Ator et al., 2006). Good results in this phase are not always indicative of the progression for the next phase of clinical trials. Drug efficacy relative to standard drugs, safety profile, probability of technical and regulatory success, remaining patent life of the drug, global costs of production, potential market share and pricing and reimbursement are also taken into account. In the case of success in this phase, an "end of phase II" meeting takes place with regulatory agencies to discuss the results and agree the clinical and statistical analysis plans for Phase III studies. This negotiation is critical to ensure alignment between the regulatory agency and the sponsor (Tamimi and Ellis, 2009);

- *Phase III*: Phase III studies are large-scale clinical studies, involving several thousand patients (*n* = 1000-3000) and the average duration is 2-4 years (Ciociola et al., 2014). Before embarking on the costly Phase III programme, the sponsor should have a high level of confidence in the safety and efficacy of the potential drug in the target population at the dose range to be tested (Tamimi and Ellis, 2009). This is the final stage of drug development prior to registration application and will confirm the efficacy and validate the safety findings of previous studies. Additionally, the studies performed in this phase also evaluate diverse subpopulations, drug dosages and formulations, monitor adverse events related to long-term use and potentially important drug interactions (Williams, 2016).

I.1.1.4. Marketing authorization

Once the Phase III studies have been completed and delivered a positive outcome, the compilation of the data obtained about the efficacy (as a basis for the claimed indications), safety and a summary of the benefit-risk relationship for the new drug is submitted to the regulatory agencies. It can take 1 to 2 years for regulatory review and approval (Ciociola et al., 2014). After the drug is approved, the Phase IV process (post-marketing surveillance) starts and continues as long as the drug is on the market. This phase involves the monitoring of adverse effects (pharmacovigilance) and large-scale studies of drug efficacy/safety.

Additionally, Phase IV trials can be used to monitor additional indications for a new drug and gather information for pharmacoeconomic evaluations. When regulatory entities are notified of a change in the safety profile of an approved drug, the risk is assessed and managed by changes to drug labelling, implementation of a risk management plan, black box warnings, or even, if justified, withdrawal of the drug from the market (Ator et al., 2006; Williams, 2016).

I.1.1.5. The role of academia in drug discovery and development

The number of academic drug discovery centres has grown considerably in recent years, providing new opportunities to couple the curiosity-driven research culture in academia with the rigorous drug discovery practices used in industry (Dahlin et al., 2015). In Figure I.1 are represented the academic screening centres distributed in the world in 2016 from the information obtained in the website of the Society for Laboratory Automation and Screening (SLAS, 2016), where it is evident the predominance of these institutions in the North America [United States of America (USA) and Canada]. Unfortunately, just a small percentage of academic discovery centres are located in Europe, which means that there is a long way to go through by European universities in this area.

Indeed, academic research institutes are well-positioned to supply manpower, especially in the early phases of drug discovery and development. The freedom and flexibility offered by academia are conducive to risky ideas that can be pursued in collaboration with expert drug discoverers in the pharmaceutical and biotechnology industries for optimal success (Nicolaou, 2014). Thus, one of the core activities of academia could be gathering knowledge through fundamental research, such as unravel pathological mechanisms, discover new therapeutic targets and develop valid *in vivo* and *in vitro* test models. Particularly, in the case of the discovery and development of central nervous system (CNS)-active drugs, where large pharmaceutical companies have restricted their activity because of the low rates of success, academia could give a significant support, allowing the drug pipeline roar again (Hendriksen and Groenink, 2015).

On the other hand, to fully realize their own potential, it is important that academic researchers understand the inherent risks in preclinical drug discovery. Indeed, they are often not well-trained for some important clinical considerations or business strategies and have little access to the necessary funding for generating the proof-of-concept data needed to attract investment. Thus, a closer multidisciplinary collaboration between industry and academia may certainly lead to a new architecture in the field of drug discovery and development, creating a more efficient system (Dahlin et al., 2015; Fishburn, 2013).

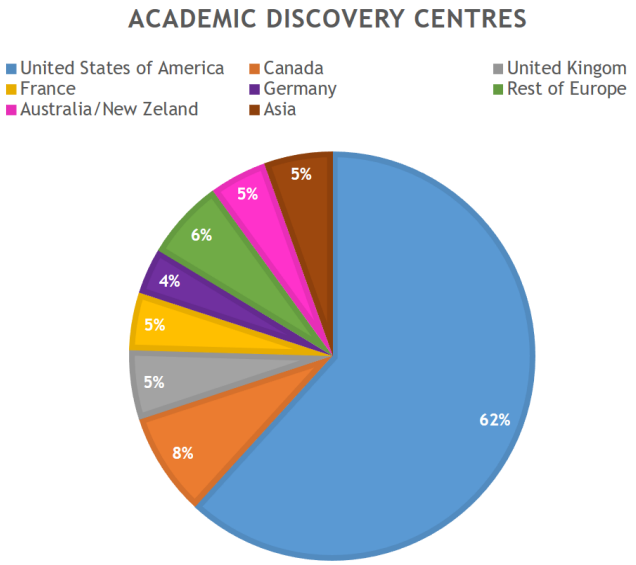

Figure I.1 - Geographical distribution of drug discovery facilities located in academic centres (in percentage) in the world. The data were obtained from the website of the Society for Laboratory Automation and Screening (SLAS, 2016).

Regarding the particular case of epilepsy, pharmaceutical industries have lost their enthusiasm in the search for new antiepileptic drugs (AEDs) (as specified in section I.2.6 of this chapter). In this context it seems to be very important the role of the "micropharma", which is represented by academia-originated, biotech start-up companies that are small, efficient, flexible, innovative and product-focused, and they are arising from universities, hospitals, or research institutes. Although "micropharma" corresponds to lower tier organizations within the hierarchy of the pharmaceutical ecosystem, and bigger pharmaceutical industries are required for large scale Phase III clinical trials, the rise of "micropharma" may represent an effective way for pursuing novel anticonvulsant/antiepileptic agents (Weaver, 2013). Also Bialer *et al.* highlighted the importance of the recent findings in epilepsy field from academia and pharmaceutical industries in the last Thirteenth Eilat Conference on New Antiepileptic Drugs and Devices (EILAT XIII) that took place in Madrid, on June 2016 (Bialer et al., 2017).

This doctoral thesis emerged in this context, being the main goal the discovery and development of new drug candidates in an academic environment. As the target disorder of this project is epilepsy, the next sections of this chapter are subordinated to this theme.

I.2. EPILEPSY

I.2.1. Historical overview

At around 2000 BC came to light the first known description of an epileptic seizure, written in Akkadian, the language spoken on the lands of Mesopotamia. Afterwards, the first rational study was undertaken around 400 BC by Hippocrates, who referred to epilepsy as a physical disorder of the brain, but, at that time, he was widely disbelieved. Thus, during millennia, epilepsy was "cured" by the means of prayers, magic and, often, exorcisms in order to make the evil spirit to go away. In the Renaissance, epileptic seizures were beginning to be redefined as symptoms of physical illness and, in the Enlightenment, there was the development of anatomy, physiology, pathology, chemistry and pharmacy fields, which allowed the evolution in the treatment and understanding of this disorder. In 1770, Tissot totally rejected the influence of the moon on epileptic seizures, and in the nineteenth century, the real breakthrough in perceiving epilepsy was brought by the study of the mind into the fields of neurology and psychiatry (Miziak et al., 2012; Varvel et al., 2015).

In 2005, the International League Against Epilepsy (ILAE) defined epilepsy as "a disorder of the brain characterised by an enduring predisposition to generate epileptic seizures, and by the neurobiologic, cognitive, psychological, and social consequences of this condition". More recently, this international organization has accepted a novel practical definition, by which epilepsy can be considered when any of the following conditions happen: at least two unprovoked (or reflex) seizures occurring more than 24 h apart; one unprovoked (or reflex) seizure and a probability of further seizures similar to the general recurrence risk (at least 60%) after two unprovoked seizures, occurring over the next 10 years; and the diagnosis of an epilepsy syndrome (Fisher et al., 2014).

With the avalanche of genetic, structural, and functional information, it has become evident that the term epilepsy is applied to an enormous variety of conditions, very heterogeneous about their aetiology, clinical expression, severity and prognosis and may involve cognitive, behavioural, motor, sleep, autonomic, and other systemic impairments and dysfunctions (Berg, 2015; Santulli et al., 2016).

I.2.2. Epidemiology

Epilepsy is one of the most common, chronic and serious neurological disorder, affecting around 50-60 million people worldwide. It is estimated that epilepsy occurrence varies substantially among populations studied, but, in sum, it is generally accepted that in resource-poor countries the incidence is likely to be higher than in developed countries (annual incidence of epilepsy of 700 per 100,000 *versus* 50 per 100,000 population, respectively) (Sander, 2003; Thurman et al., 2011). The predominance of the type of seizures (focal, generalised or unknown onset) seems to be related with the geographic location,

possibly due to genetic and environmental factors (Banerjee et al., 2009; Sander, 2003). Although studies are not in complete agreement, most reports show a general trend towards an increase in epilepsy prevalence during adolescence or early adulthood. On the other hand, the incidence seems to be higher in the childhood and elderly. In addition, although absolute difference in gender-specific prevalence is minimal, there are some evidence suggesting that the prevalence is higher in males than females (Banerjee et al., 2009). Alarming is the fact that people with epilepsy have a mortality rate 2–3 times higher than the general population. In addition, standardised mortality ratios are highest in the young people (due primarily to the low expected mortality in children) and during the first 5–10 years after diagnosis (Kerr, 2012).

I.2.3. Pathophysiology and clinical presentation

Asserting that the human brain is the most complex biological system in the universe, the complexity of epileptic pathology seems undisputed and remains an enormous challenge. The process that involves the development and extension of brain tissue capable of generating spontaneous seizures, resulting in development of an epileptic condition and/or progression for epilepsy is known as epileptogenesis (Łukawski et al., 2016). Epileptic dysfunctions involve brain physiology at all levels and probably many different mechanisms might contribute to epileptogenesis depending on aetiology, degree of cerebral maturation and duration of the disease. Thus, epilepsy is a dynamic and multifactorial disorder and generically can start from a congenital (e.g. a malformation of cortical development, a hypothalamic hamartoma, or a dysplastic tumour) or from an acquired lesion (e.g. prolonged febrile seizures, brain trauma, *status epilepticus*, or stroke), being also a percentage associated with no specific causes (idiopathic epilepsy) (Santulli et al., 2016).

The seizures, which typically characterise epilepsy, result from an excessive excitability or disordered inhibition of a large population of cortical neurons. Initially, a small number of neurons fire abnormally; after, the normal membrane conductances and inhibitory synaptic currents break down, and excessive excitability spreads to produce the seizures. Current theories have tried to explain the mechanism(s) for the abnormally increased propensity of the brain to develop excessive discharges of neurons: alterations in the distribution, number, type and biophysical properties of ion channels in the neuronal membranes; biochemical modifications of receptors; modulation of second messenger systems and gene expression; changes in extracellular ion concentrations; alterations in neurotransmitter uptake and metabolism in glial cells; and modifications in the ratio and function of inhibitory circuits. It is thought that particularly the transitory imbalance between the main neurotransmitters associated with excitability (glutamate) and inhibition [γ-aminobutyric acid (GABA)], as well as neuromodulators (e.g., acetylcholine, norepinephrine, and serotonin), may play a crucial role in precipitating seizures in susceptible patients (Wells et al., 2009).

Epileptic seizures show a very large variety of clinical manifestations and their recent classification is summarized in Figure I.2. Work-up with electroencephalogram (EEG), sleep/long-term EEG and magnet resonance imaging usually helps to differentiate between focal and generalised epilepsy (Gschwind and Seeck, 2016). Thus, focal seizures are originated within networks limited to one cerebral hemisphere and may be discretely localized or more widely distributed; these seizures are the most common, representing approximately 60% of all seizure types. On the other hand, generalised epileptic seizures are originated within bilaterally distributed networks that become rapidly engaged and can involve cortical and subcortical structures, but not necessarily the entire cortex. A distinct form of generalised seizures are absence seizures that are generated by thalamocortical loops. The characterisation of the different seizure types is presented in Table I.1. Usually, the most severe seizure type is *status epilepticus*, which is a continuous seizure, constituting a medical emergency and generally requiring aggressive medication therapy (Krasowski and Mcmillin, 2014; Łukawski et al., 2016).

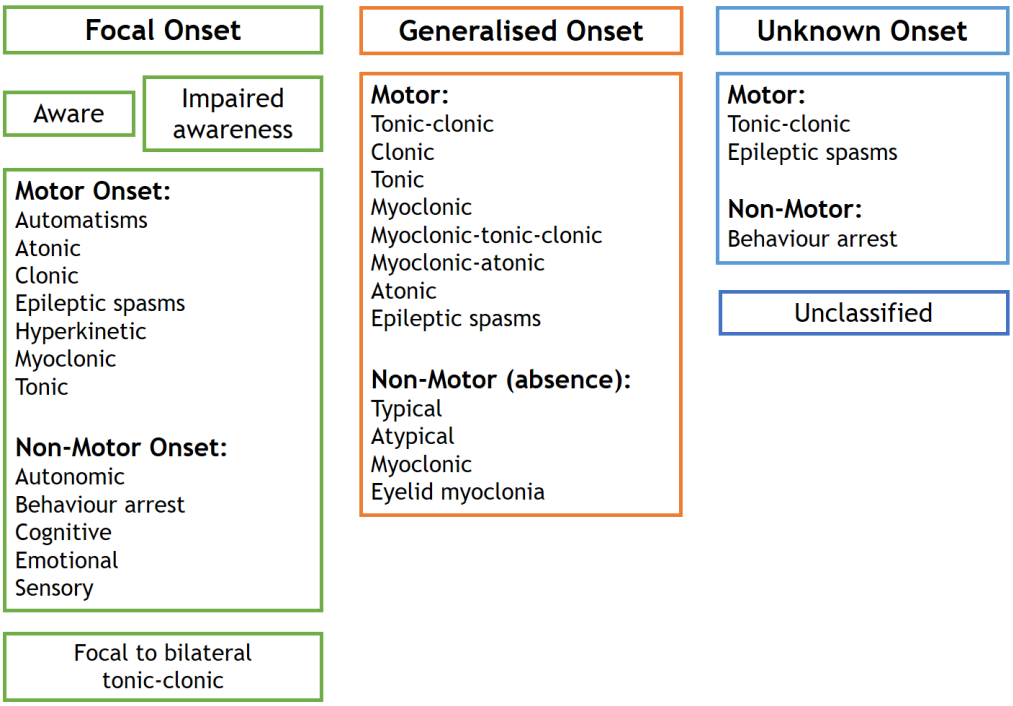

Figure I.2 – Categorisation of epileptic seizures according with the International League Against Epilepsy (Fisher, 2017a).

Table I.1 – Epileptic seizures characterisation accordingly with the International League Against Epilepsy 2017 Classification Seizure (Fisher, 2017b; Fisher et al., 2017).

Seizure characterisation
Focal onset seizures
• *Automatisms*: A seizure with automatic fumbling behaviour, such as lip-smacking, hand-rubbing, picking at objects, walking in circles, repeating meaningless phrases, or undressing.
• *Atonic*: Focal, for example in one arm or leg, sudden loss of muscle tone and strength, resulting in a transiently limp limb.
• *Clonic*: Sustained rhythmical jerking of one part of the body or face.
• *Epileptic spasms*: Sudden flexion or bending of the trunk with flexion or extension of the limbs lasting less than a few seconds. These often occur in clusters. The term infantile spasms applies to epileptic spasms occurring during infancy.
• *Hyperkinetic*: A seizure with vigorous thrashing or pedalling movements. Even though both sides of the body are usually involved with these seizures, the EEG often shows a focal and frontal lobe origin. Some people used to call these hypermotor seizures.
• *Myoclonic*: Irregular and brief lightning jerks of limbs or face on one side of the body.
• *Tonic*: Stiffening of arm, leg, or neck producing a forced posture during the seizure.
• *Autonomic*: A seizure whose primary effect is on autonomic nervous system functions, such as heart rate, blood pressure, sweating, skin colour, piloerection, and gastrointestinal sensations.
• *Behaviour arrest*: In this seizure type, movement stops, sometimes called a freeze or a pause. A seizure should only be classified as a focal behaviour arrest seizure if the behaviour arrest is the main feature through the entire seizure.
• *Cognitive*: This type of seizure refers to impaired cognition during a seizure. The impairment might affect language, spatial perception, ability to calculate math, or other cognitive functions. Do not count loss of awareness or memory (unless only memory is impaired) as a focal cognitive seizure, because awareness is used to describe other seizure types.
• *Emotional*: This seizure type begins with spontaneous fear, anxiety, or less often joy. There may be involuntary laughing or crying, each of which might or might not be accompanied by a subjective emotion. Gelastic and dacrystic seizures would fit into this group.
• *Sensory*: Sensory seizures can consist of tingling or numbness, visual symptoms, sounds, smells, tastes, tilting or vertigo, and hot-cold feelings.
Generalised onset seizures
• *Tonic–clonic*: Immediate loss of awareness, with stiffening of all limbs (tonic phase), followed by sustained rhythmic jerking of limbs and face (clonic phase). Duration is typically 1 to 3 min. The seizure may produce a cry at the start, falling, tongue biting, and incontinence.
• *Clonic*: Rhythmical sustained jerking of limbs and/or head with no tonic stiffening phase.
• *Tonic*: Stiffening of all limbs, without clonic jerking.
• *Myoclonic*: Irregular, unsustained jerking of limbs, face, eyes, or eyelids. The jerking of generalised myoclonus may not always be left–right synchronous, but it occurs on both sides. Myoclonus may be part of a seizure or a non-epileptic motor disorder.
• *Myoclonic–tonic–clonic*: Similar to a tonic–clonic seizure, but it is preceded by a few myoclonic jerks on both sides of the body.
• *Myoclonic–atonic*: This seizure presents with a few myoclonic jerks, followed by a limp drop.
• *Atonic*: This is an epileptic drop attack, with sudden loss of muscle tone and strength and a fall to the ground or a slump in a chair. Atonic seizures usually last only seconds.
• *Epileptic spasms*: Brief seizures with flexion at the trunk and flexion or extension of the limbs. Video-EEG recording may be required to determine focal *versus* generalised onset.
• *Typical absence*: Sudden cessation of activity with a brief pause and staring, sometimes with eye fluttering and head nodding or other automatic behaviours. In the more severe seizures, awareness and memory are impaired. Recovery is immediate.
• *Atypical absence*: Like typical absence seizures, but may have slower onset and recovery and more pronounced changes in tone. Atypical absence seizures can be difficult to distinguish from focal impaired awareness seizures, but absence seizures usually recover more quickly and the EEG patterns are different.
• *Myoclonic absence*: A seizure with a few jerks and then an absence seizure.
• *Eyelid myoclonia*: Eyelid myoclonia represents jerks of the eyelids and upward deviation of the eyes, often precipitated by closing the eyes or by light.
Unknown onset seizures
• The nature of seizure onset is known with less than 80% confidence by the clinician (the 80% level of confidence was arbitrarily chosen to match the usual acceptable false-negative beta error in an experiment). An unknown onset seizure later may be reclassified as focal or generalised as new information becomes available.
• The term unclassified comprises both seizures with patterns that do not fit into the other categories or seizures presenting insufficient information to allow categorization.

Finally, the impact of epilepsy is multifaceted and extensive, strongly affecting the patient's quality of life. The occurrence of seizures is unpredictable and often dangerous, increasing the risk of injury, hospitalization and mortality. Moreover, seizures can also result in stigmatization and social exclusion as well as in an increased probability of the development of medical and psychiatric comorbidities, such as depression and anxiety (Kerr, 2012).

I.2.4. Drug-resistant epilepsy

The ILAE proposed in 2010 a global consensus definition of drug-resistant (also known as "medically refractory/intractable" or "pharmacoresistant") epilepsy as the failure of adequate trials of two or more tolerated, appropriately chosen, and appropriately used AED regimens, whether administered as monotherapies or in combination, to achieve freedom from seizures. This definition is based on the fact that if seizure control is not achieved with trials of two appropriate drugs, the likelihood of success with subsequent AEDs is much more diminished (Kwan et al., 2010; Santulli et al., 2016).

An important percentage of patients shows a poor response to drugs from the onset of epilepsy or develops it over the time. Pharmacoresistance in epilepsy is associated with an increased mortality, morbidity, psychosocial disability and reduced quality of life as well as major financial implications (Santulli et al., 2016). When possible, epilepsy surgery and neuromodulation are effective treatments for patients with drug-resistant epilepsy (Gschwind and Seeck, 2016). Moreover, drugs with multiple mechanisms of action are usually broad spectrum and potentially useful in some cases of pharmacoresistant epilepsy (Brodie, 2016). However, an important issue to take into consideration is that some epileptic patients may not adequately respond to AEDs for other than drug-resistance reasons. They include, for example, the lack of compliance to pharmacotherapy and possible interactions that significantly affect the protective activity of AEDs. Moreover, after the failure of monotherapies, inappropriate combinations of AEDs may also generate false drug-resistance phenotypes (Miziak et al., 2012).

The phenomenon of drug-resistant epilepsy is complex in its nature and undoubtedly incompletely known; however, there are several theories:

- *Target hypothesis*: Genetic or acquired alterations in the structure and/or functionality of cellular targets of AEDs, leading to reduced response to drug treatment (e.g. changes in subunit compositions of voltage-gated sodium channels and $GABA_A$ receptors) (Löscher et al., 2013; Łukawski et al., 2016). To counteract a target mechanism of resistance, an appropriate approach would consist in developing drugs that specifically act on the modified target/other targets that are not downregulated in epilepsy (Löscher et al., 2013; Margineanu, 2014);

- *Transporter hypothesis*: Experimental and clinical evidence has accumulated for this hypothesis, which suggests an overexpression of drug efflux transporters at the blood-brain barrier (BBB) in focal tissue, limiting the penetration of AEDs to the epileptic focus in the brain. Drug efflux transporters are adenosine triphosphate (ATP)-binding cassette (ABC) transmembrane proteins, including P-glycoprotein (P-gp), multidrug resistance proteins (MRPs) and breast cancer resistance protein (BCRP) (Löscher et al., 2013; Łukawski et al., 2016). The transporter mechanism of resistance could be circumvented by AEDs that are not substrates of efflux transporters; alternatively, inhibitors of multidrug transporters might be used in combination to increase intraparenchymal AED concentration (Margineanu, 2014);
- *Network hypothesis*: This hypothesis suggests that there are structural brain alterations and/or network changes (e.g. hippocampal sclerosis) that can be involved in resistance to AEDs (Łukawski et al., 2016);
- *Intrinsic severity hypothesis*: Since the early phase of epilepsy there is an increase of severity. From a neurobiological perspective, this severity reflects the magnitude of the underlying epileptic process (Walker et al., 2015). Thus, this hypothesis suggests that an increased disease severity leads to drug intractability (Löscher et al., 2013);
- *Gene variant hypothesis*: There is an inherent resistance that is governed by genetic variants of proteins that can have a role in the pharmacokinetics and pharmacodynamics of AEDs. This hypothesis suggests that such variants can be associated to the target and/or transporters (Löscher et al., 2013).

None of these hypotheses is currently a stand-alone theory that is able to convincingly explain how drug resistance arises in human epilepsy. In fact, these mechanisms can coexist in epileptogenic brain. The cellular and molecular alterations involved in the epileptogenesis process may also contribute to pharmacoresistance in chronic epilepsy (Löscher et al., 2013). Effectively, there is a need to elucidate or better understand the neurobiological mechanisms responsible for pharmacoresistant epilepsy, which would help in the development of new AEDs and improve the treatment of epilepsy.

I.2.5. Therapeutic approaches

The main objective in the therapy of the epilepsy is to achieve a state of complete seizure freedom, and the treatment with AEDs is undoubtedly the most employed therapeutic approach. However, those patients that never become seizure free under AED polytherapy should be evaluated for non-pharmacological treatment options, such as surgery, neuromodulation (e.g. vagal nerve stimulation and deep brain stimulation) and ketogenic diet (Gschwind and Seeck, 2016; Koppel and Swerdlow, 2017; McGovern et al., 2016). As

pharmacotherapy is the main therapeutic option for epilepsy, the AEDs are extensively focused in the next sections.

I.2.5.1. Pharmacotherapy

Long-term AED therapy is the mainstay of epilepsy treatment, eliminating or reducing seizure frequency in around 60–70% of patients (Brown, 2016). Currently, more than twenty AEDs are available in clinical practice (Ben-Menachem, 2014). Since the exact mechanisms underlying epilepsy are not clear yet, the drug treatment remains mainly symptomatic. In fact, available drugs are effective to stop seizures (i.e. anticonvulsant drugs) but they are not curative and cannot stop the progression of epilepsy (i.e. they are not truly antiepileptic or antiepileptogenic drugs). Moreover, some seizures responsive to AEDs do not involve convulsive movements and, as referred to above, the current drugs are not able to alter the epileptogenesis process (Dalkara and Karakurt, 2012). Thus, although the term "anticonvulsant drug" is usually used as a synonym for AED, it is not entirely correct. However, due to the fact that the term "AED" is the most common and is widely accepted by the scientific community, it will be used throughout this thesis.

The choice of the right AED is often challenging and several parameters need to be taken into consideration, such as the type(s) of seizure(s) or epileptic syndrome, the pharmacological properties of the AED(s) (e.g. dosing regimen, potential for drug interactions and adverse effects profile) and the individual features of the patient (e.g. gender and age). Monotherapy is widely accepted as the *gold standard* strategy in epilepsy treatment; thus, alternative monotherapy should be considered when the first drug treatment fails. In fact, the use of a single drug facilitates the evaluation of the efficacy, reduces the toxicity, avoids the risk of pharmacological interactions between AEDs, improves compliance, minimizes the costs and allows the control of seizures in the majority of the responsive patients. However, in the cases of ineffective control of seizures with monotherapy, the polytherapy (adjunctive therapy) should be considered, being as "rational" as possible. This concept includes the fact that AEDs with different mechanisms of action can act in a synergistic manner, providing better seizure control than two drugs acting through a similar mechanism of action, which could still cause a potentiation of side effects (Ben-Menachem, 2014; Brodie, 2016; Santulli et al., 2016).

I.2.5.1.1. Antiepileptic drugs

A substantial armamentarium of AEDs is currently available, including drugs with structural variety, different mechanisms of action, pharmacokinetic properties, efficacy and tolerability profiles. Regarding efficacy, a strong evidence of any significant differences between the classic *versus* newer AEDs is not granted. However, the most recent AEDs usually present an

improved tolerability/safety profile and, generally, a more favourable pharmacokinetics and less potential for drug-drug interaction (DDI) (Brodie, 2016; Franco et al., 2016).

Due to the fact that several AEDs are able to control specific seizures, but can simultaneously exacerbate others, the choice of the AED must be a careful process. For this reason, according to the established by the National Institute for Health and Care Excellence ("NICE", 2016), a brief summary of the AEDs that are recommended towards each type of seizure is given in Table I.2. Concerning the AEDs that are approved for specific epilepsy syndromes, it will be mentioned throughout the description of the main characteristics of the respective AEDs.

Table I.2 – Recommended antiepileptic drugs for the different types of seizures, according to the National Institute for Health and Care Excellence ("NICE", 2016).

	Monotherapy First-line (second-line) [third-line]	**Adjunctive therapy**	**Avoid**
Focal seizures	Carbamazepine or lamotrigine (levetiracetam, oxcarbazepine or valproic acid)	Carbamazepine, clobazam, gabapentin, lamotrigine, levetiracetam, oxcarbazepine, valproic acid, topiramate, eslicarbazepine acetate, lacosamide, phenobarbital, phenytoin, pregabalin, tiagabine, vigabatrin, zonisamide, retigabine, brivaracetam or perampanel	
Absence seizures	Ethosuximide or valproic acid (lamotrigine)	Ethosuximide, lamotrigine, valproic acid, clobazam, clonazepam, levetiracetam, topiramate or zonisamide	Carbamazepine[1], gabapentin, oxcarbazepine, phenytoin, pregabalin, tiagabine or vigabatrin
Generalised tonic-clonic seizures	Valproic acid (lamotrigine) [carbamazepine or oxcarbazepine]	Clobazam, lamotrigine, levetiracetam, valproic acid or topiramate	Carbamazepine, gabapentin, oxcarbazepine, phenytoin, pregabalin, tiagabine or vigabatrin
Myoclonic seizures	Valproic acid (levetiracetam or topiramate)	Levetiracetam, valproic acid, topiramate, clobazam, clonazepam or zonisamide	Carbamazepine, gabapentin, oxcarbazepine, phenytoin, pregabalin, tiagabine or vigabatrin
Tonic or atonic seizures	Valproic acid	Lamotrigine, rufinamide or topiramate	Carbamazepine, gabapentin, oxcarbazepine, pregabalin, tiagabine or vigabatrin

[1]Suspicion of absence or myoclonic seizures or juvenile myoclonic epilepsy.

The chemical structures of the main AEDs in clinical use are illustrated in Figure I.3, emphasizing the structural diversity of the panoply of drugs that are currently available. The distribution of the AEDs into three consecutive generations was inspired in that described by Perucca *et al.* (Perucca et al., 2007), which was based in the chemical advances and structural modifications of the already existing AEDs to produce new and more promising agents. A brief overview of the AEDs in clinical use is given below:

Barbiturates: phenobarbital and analogues

Phenobarbital is a barbituric acid derivative and it is the oldest AED. The success of phenobarbital in the control of seizures led to the development of other barbiturates as subsequent AEDs including mephobarbital (*N*-methylphenobarbital) and primidone (deoxyphenobarbital), both being metabolized to phenobarbital in the organism (Bialer, 2012). Either phenobarbital or primidone are sometimes used in patients with major compliance problems, because of their long half-lives. Phenobarbital and its congeners have dose-related sedative effects (sometimes in subtherapeutic concentrations), which can be intolerable in a significant number of patients (Vajda and Eadie, 2014).

Hydantoins: phenytoin and derivatives

Phenytoin is a classical AED, whose chemical structure is related to barbiturates, and its major advantage is the fact that provides effective treatment without causing sedation. In fact, phenytoin was one of the mainstays of seizure therapy, leading to further investigations in the search for more promising compounds belonging to the class of hydantoins. In this context, fosphenytoin emerged as a parenteral water-soluble phenytoin prodrug (Bialer, 2012). Comparing with other AEDs, the phenytoin plasma levels have clinical interest as a guide for therapeutic drug monitoring. Hence, some patients, particularly those with newly-diagnosed epilepsy, often respond to plasma concentration levels below to the considered optimal therapeutic range, which is an interesting advantage of this drug (Vajda and Eadie, 2014).

Ethosuximide

The main antiepileptic succinimide currently in clinical use is ethosuximide. Originally, the discovery of this molecule was motivated by the necessity of more efficacious and safer chemical compounds for the treatment of absence or myoclonic seizures. In fact, although the succinimide core has no anticonvulsant activity, the introduction of both ethyl and methyl groups at position 3 of that nucleus led to ethosuximide, which is notably effective in controlling absence seizures (Bialer, 2012).

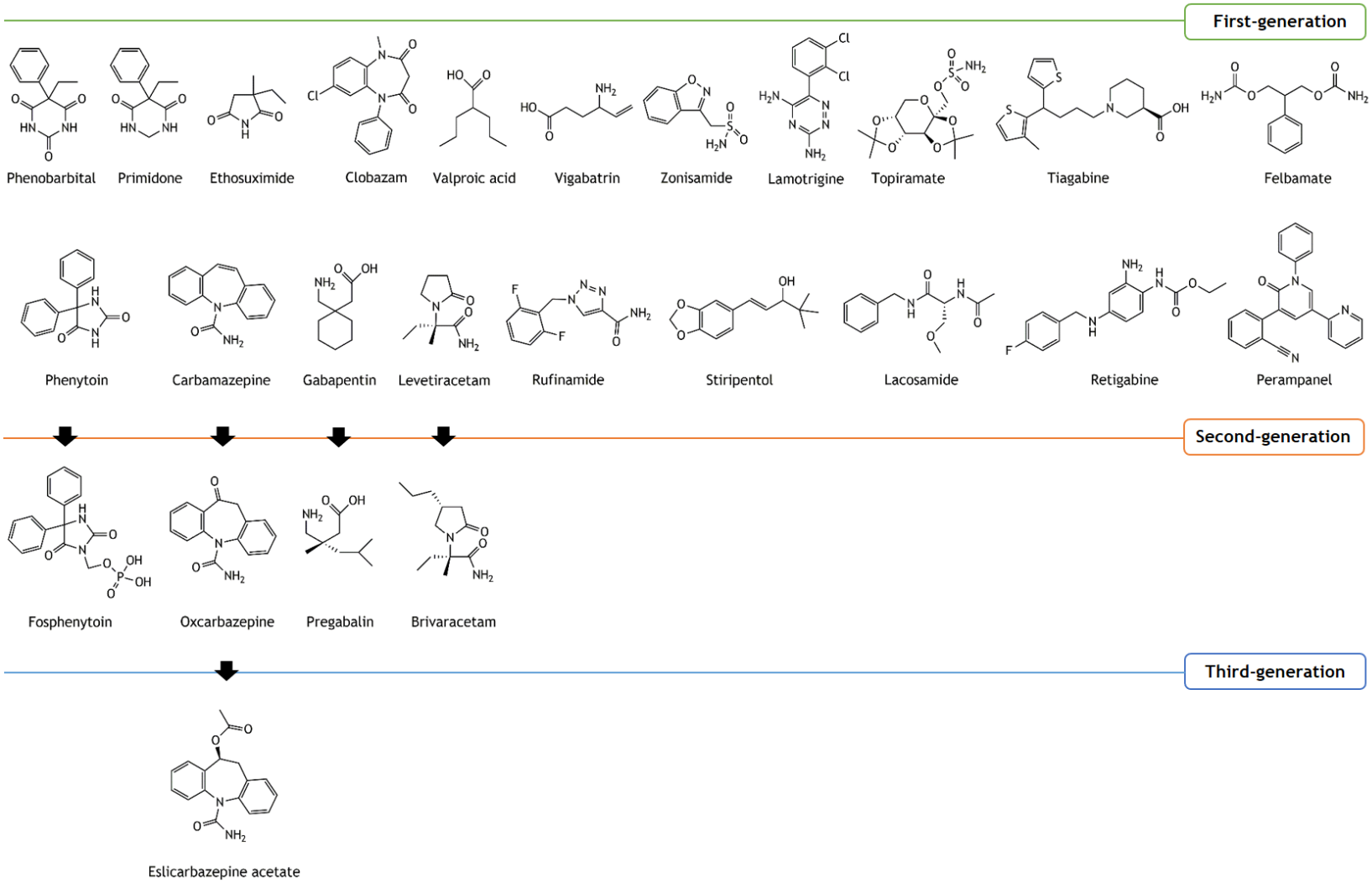

Figure I.3 – Structural diversity of chemical structures of the antiepileptic drugs (AEDs). They are distributed into three consecutive generations and are represented the main clinically available AEDs (Bialer, 2006; Perucca et al., 2007).

Benzodiazepines

Benzodiazepines are used as AEDs in particular conditions, such as *status epilepticus* (e.g. diazepam, clonazepam and midazolam) and in some paediatric syndromes (e.g. nitrazepam) (Vajda and Eadie, 2014). A highlight goes to clobazam that was approved in the USA in 2011 for adjunctive treatment of seizures associated with Lennox-Gastaut syndrome in adults and children over 2 years of age, but it had been approved since 1970 in Australia and further in Europe and Canada for use as a broad-spectrum agent (Chong and Lerman, 2016). Although the several benzodiazepines have different pharmacodynamic and pharmacokinetic properties and consequently distinct safety profiles, in general, their adverse effects include neurological and psychiatric events, sedation, memory problems, hyperactivity, withdrawal effects, and tolerance (Vajda and Eadie, 2014).

Carbamazepine, oxcarbazepine and eslicarbazepine acetate

Carbamazepine is an iminostilbene chemically related to tricyclic antidepressants and it is also approved for bipolar disorder. The most reactive site (chemically and metabolically) in this molecule is the double bond between C10 and C11, which is the point of the molecule involved in the metabolic conversion to its major and pharmacologically active metabolite (carbamazepine-10,11-epoxide). Carbamazepine is able to induce the metabolic capacity of cytochrome 450 (CYP450) system, enhancing its own metabolism, and it is also often involved in metabolism-based drug interactions particularly due to enzyme induction (Bialer, 2012). Oxcarbazepine is a keto-analogue of carbamazepine, with a similar spectrum of efficacy, but with a better tolerability and lower potential for clinically significant DDI. In humans, this AED is rapidly and enantioselectively metabolized to the pharmacologically active 10-hydroxycarbazepine (licarbazepine) at an approximate ratio of 4:1 for the *S*-licarbazepine and *R*-licarbazepine, respectively (Gschwind and Seeck, 2016; Krasowski and Mcmillin, 2014). Eslicarbazepine acetate is structurally a member of the third-generation of dibenz[*b,f*]azepine-5-carboxamide derivatives (Almeida and Soares-da-Silva, 2007). This chiral prodrug is rapidly metabolized almost exclusively to *S*-licarbazepine (Tatum, 2013). It shares with its precursors the dibenzazepine nucleus bearing the 5-carboxamide substituent but it is structurally different at the 10,11-position. This molecular variation results in differences in metabolism and seems to be responsible for improved tolerability and advantages of administration (Mula, 2016a).

Valproic acid and derivatives

Valproic acid possesses a wide spectrum of activity and it is the agent of first choice for idiopathic generalised epilepsy, being effective against all manifestations of the disorder, including absences. Moreover, it is recommended for patients with seizures that are difficult to classify and it is also used for treating psychiatric disorders and for migraine prevention.

The most important adverse effect associated with this drug is its well-known teratogenicity (Vajda and Eadie, 2014).

Gabapentin, pregabalin and vigabatrin

Gabapentin is an AED structurally related to the neurotransmitter GABA. It was originally approved as adjuvant therapy for focal seizures but has achieved greater popularity as an adjunctive therapy for peripheral neuropathic pain (Krasowski and Mcmillin, 2014). Pregabalin was designed to be a more potent analogue of gabapentin (Bialer, 2006). Thus, similarly to gabapentin, this drug is used much more for the management of neuropathic pain than for the treatment of seizure disorders (Krasowski and Mcmillin, 2014; Schulze-Bonhage, 2013). Vigabatrin is also a synthetic GABA derivative (Krasowski, 2010). The irreversible action of vigabatrin results in poor correlation between plasma/serum concentrations and therapeutic effect. It may produce serious irreversible visual deficits in any concentration (Ben-Menachem, 2014; Tatum, 2013).

Lamotrigine, zonisamide and topiramate

Lamotrigine belongs to the class of phenyltriazines and is structurally unrelated to other AEDs. It exhibits a broad spectrum of activity and one major advantage of lamotrigine, particularly in relation to the classic AEDs, is a good safety record in pregnancy. In fact, this AED is one of the best options for the management of epilepsy in pregnancy. However, rash is an important adverse effect, being the most common reason for discontinuing lamotrigine treatment (Yasam et al., 2016). Zonisamide is a benzisoxazole derivative with a sulphonamide side chain and has a wide spectrum of action. It is currently approved for use in both focal and generalised seizures in patients of all ages in Japan and Korea, as an adjunctive treatment for focal seizures in adults in the USA, and as add-on therapy or monotherapy for focal seizures in Europe (Cox et al., 2014). Topiramate is a sugar derivative synthesized from D-fructose and acetone and due its sulphamate moiety it was firstly tested as a hypoglycaemic agent (Bialer, 2012). It exhibits a broad spectrum of activity and their multiple pharmacological actions (as further described in section I.2.5.1.2) could contribute to its ability to protect against different types of seizures (Kaminski et al., 2014). Topiramate has been also used for prophylaxis of migraine. However, this drug does not show a good tolerability profile, being weight loss and cognitive slowing potential unacceptable side effects (Gschwind and Seeck, 2016).

Felbamate, stiripentol and tiagabine

Felbamate is a dicarbamate related to the anxiolytic agent meprobamate. It is approved for the treatment of focal seizures in adults and for Lennox–Gastaut syndrome. However, the

clinical use of this AED has been greatly limited by rare but severe adverse events (e.g. aplastic anaemia and severe liver failure). In fact, felbamate has remained on the market with revised labelling and a drastically restricted use, intended for use only in patients where the benefits clearly outweigh the risks and only under close monitoring. This drug is converted to multiple inactive metabolites, one or more of which are suspected to be underlying the severe adverse effects (Krasowski and Mcmillin, 2014). Stiripentol is an aromatic allylic alcohol that is approved in Europe as an orphan drug for the treatment of severe myotonic epilepsy (Dravet's syndrome) in infants. Although it is not approved in the USA, stiripentol may be obtained with a prescription originating in this country from a reputable international pharmacy, based on compassionate use (Krasowski and Mcmillin, 2014; Verrotti et al., 2016). Regarding tiagabine, although it is considered a well-tolerated AED, its use has been limited by adverse side effects, particularly a propensity to trigger seizures and rarely life-threatening, non-convulsive *status epilepticus* (Krasowski and Mcmillin, 2014).

Levetiracetam and brivaracetam

Levetiracetam is a heterocyclic amide structurally related to piracetam (Bialer, 2012). This successful AED is well tolerated and is nowadays one of the most widely used as first choice, including for *status epilepticus* (Gschwind and Seeck, 2016). Following the discovery of this drug, great efforts were developed to obtain more potent analogues. In this context, brivaracetam emerged and it was recently approved (in February 2016) for focal-onset seizures in epilepsy patients over 16 years old (Mula, 2016a).

Rufinamide, lacosamide, retigabine and perampanel

Rufinamide, a triazole derivative, is available as an adjunctive treatment of seizures associated with Lennox-Gastaut syndrome in children with 4 years or older (Ben-Menachem, 2014). Lacosamide is a unique functionalised amino acid specifically synthesized for use as an AED. It is restricted for specialist use in refractory epilepsy in people with epilepsy aged over 16 years. Given its intravenous formulation, lacosamide can be effectively used against non-convulsive and convulsive *status epilepticus* (Gschwind and Seeck, 2016). Retigabine, also known as ezogabine in USA, is a derivative of carbamic acid ethyl ester (Tatum, 2013). Due to its extensive profile of adverse effects, the use of retigabine has been restricted to patients who are already taking the drug and who have shown good efficacy without side effects (Ben-Menachem, 2014). Finally, perampanel is an AED that was recently approved. A special warning was issued concerning “serious psychiatric and behavioural adverse reactions including aggression, hostility, irritability, anger and homicidal ideation”; however long-term safety studies have demonstrated good tolerability (Gschwind and Seeck, 2016).

I.2.5.1.2. Mechanisms of action of antiepileptic drugs

The current understanding of the mechanisms of action of AEDs is undoubtedly incomplete. Nevertheless, a number of various hypothetical mechanisms may be targeted for the discovery of AEDs. As described in Table I.3, in addition to the mechanism of action that is thought to be the major (also illustrated in Figure I.4), many of the available AEDs have other putative mechanisms, which may also contribute to their antiepileptic activity. Moreover, the empirical (sometimes serendipitous) nature of the discovery of new AEDs in the last three decades coupled with their multiple mechanisms of action explains their diverse chemical structures and the fact that so far no clear correlation has been found between the chemical structures of the AEDs and their mechanisms of action (Bialer, 2012).

Thus, AEDs exert their effects in a number of ways. As shown in Table I.3, the main therapeutic targets of AEDs are sodium and calcium ion channels. The ligand- and voltage-dependent sodium, potassium, chloride and calcium channels, which form the basis of neuronal excitability and synaptic transmission, are membrane-spanning proteins that form selective pores with gates that open and close in response to stimuli (Brodie et al., 2011). The actions of AEDs at both sodium and calcium channels stabilize neuronal membranes, block action potential firing and propagation, reducing neurotransmitter release and preventing seizure spread (White et al., 2007). More specifically, a number of AEDs have their main site of action on sodium channels, most of them stabilise its fast-inactivated state. On the other hand, voltage-gated calcium channels are multimeric proteins, which can be broadly classified into high-voltage-activated channels (L-, R-, P/Q-, and N-types) and low-voltage-activated channels (T-type). Inhibition of these channels probably translates into a reduction in excitatory neurotransmission (Perucca and Mula, 2013). In addition, retigabine was the first AED developed as a neuronal potassium channel opener. It enhances the activity of KV7.2/KV7.3 potassium M-type current maintaining channels in the open position to stabilize neuronal membranes during repetitive firing (Tatum, 2013).

Additionally, as the most important neurotransmitters in the brain are glutamate (excitatory neurotransmitter) and GABA (inhibitory neurotransmitter), an alteration of the balance between GABAergic and glutamatergic neurotransmission can contribute to increase or decrease seizure activity. Thus, several of the available AEDs either directly or indirectly shift this balance away from excitatory neurotransmission in favour of inhibitory neurotransmission (Rowley et al., 2012).

Table I.3 - Putative mechanisms of action of the clinically available antiepileptic drugs (Perucca and Mula, 2013; Santulli et al., 2016).

AEDs	Sodium channel blockade (channel state)	Calcium channel blockade (channel subtype)	Potassium channel activation	GABA potentiation	Inhibition of glutamate transmission (receptor type)	Synaptic vesicle modulation
Barbiturates	-	?	-	++	?	-
Phenytoin	++ (F)	?	-	?	?	-
Ethosuximide	-	++ (T)	-	-	-	-
Benzodiazepines	-	-	-	++	-	-
Carbamazepine	++ (F)	+ (L)	-	?	+ (NMDA)	-
Valproate	?	+ (T)	-	+	+ (NMDA)	-
Vigabatrin	-	-	-	++	-	-
Zonisamide	++	++ (N, P, T)	-	+	?	-
Lamotrigine	++ (F)	++ (N, P/Q, R, T)	-	+	++ (NMDA, AMPA)	-
Felbamate	++	+ (L)	-	+	++ (NMDA)	-
Gabapentin	-	++ (N, P/Q)	-	?	-	-
Topiramate	++	+ (L)	-	++	++ (AMPA)	-
Tiagabine	-	-	-	++	-	-
Oxcarbazepine	++ (F)	+ (N, P/Q)	?	?	+ (NMDA)	-
Levetiracetam	-	+ (N)	-	?	?	++
Stiripentol	-	-	-	++	-	-
Pregabalin	-	++ (N, P/Q)	-	-	-	-
Rufinamide	++ (F)	-	-	-	?	-
Lacosamide	++ (S)	-	-	-	-	-
Eslicarbazepine acetate	++ (S)	-	-	-	-	-
Retigabine	-	-	++	?	-	-
Brivaracetam	-	+	-	?	-	++
Perampanel	-	-	-	-	++ (AMPA)	-

"++" primary action; "+" secondary action; "–"not described; "?" controversial; AEDs, antiepileptic drugs; AMPA, α-amino-3-hydroxy-5-methyl-4-isoxazolepropionic acid; F, fast-inactivated state; NMDA, *N*-methyl-D,L-aspartate; S, slow-inactivated state.

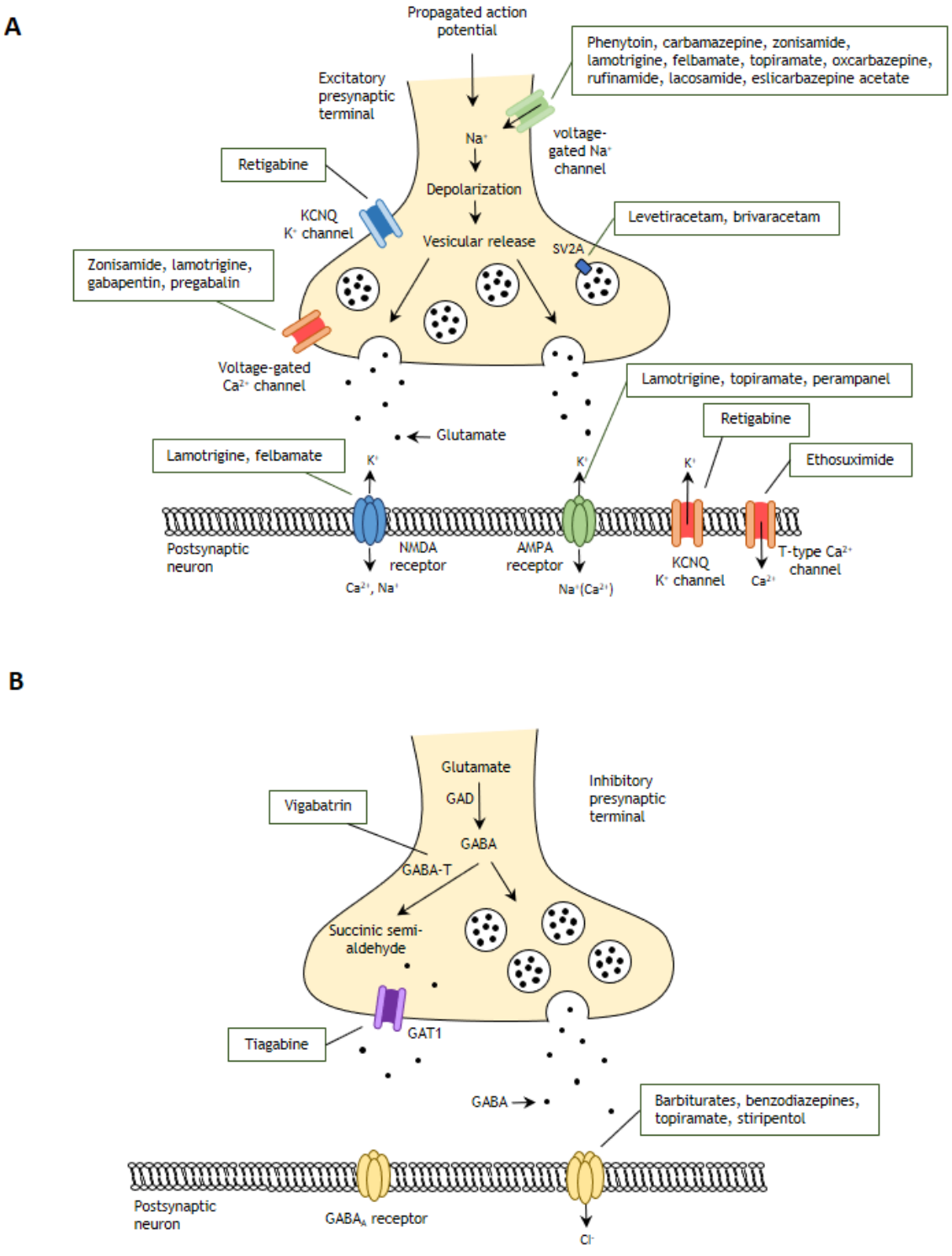

Figure I.4 – Main putative molecular targets of currently available antiepileptic drugs. **A** - Excitatory synapse; **B** - Inhibitory synapse. AMPA, α-amino-3-hydroxy-5-methyl-4-isoxazolepropionic acid; GABA-T, GABA transaminase; GAT, GABA transporter; NMDA, N-methyl-D-aspartate. Adapted from (Bialer and White, 2010).

The first information on the existence of GABA in the CNS appeared in 1950, particularly when it was shown that the intracerebral administration of GABA led to anticonvulsant effects. Unfortunately, brain GABA levels cannot be increased by exogenous administration of this neurotransmitter because it does not cross the BBB due to its high hydrophilicity. Hence, the search for GABAergic agonists that would penetrate the CNS system emerged (Miziak et al., 2012). Several clinically used AEDs enhance GABA-mediated inhibitory activity, such as benzodiazepines and barbiturates. Moreover, tiagabine and stiripentol block synaptic GABA reuptake, and vigabatrin inhibits GABA transaminase, which is one enzyme involved in GABA degradation (Brodie et al., 2011). On the other hand, the glutamate pathway is targeted by perampanel. This AED is a novel non-competitive selective antagonist at the postsynaptic ionotropic α-amino-3-hydroxy-5-methyl-4-isoxazolepropionic acid (AMPA) glutamate receptor, which is suggested to inhibit seizure generation and spread (Greenwood and Valdes, 2016).

The modulation of synaptic vesicle proteins is another mechanism of action ascribed to some AEDs, which particularly modulate the synaptic vesicle protein SV2A that selectively enhances low-frequency neurotransmission and maintains the readily releasable pool of transmitters (Rowley et al., 2012). Indeed, it is thought that the synaptic vesicle protein SV2A is the specific binding site for the levetiracetam as well as for the brivaracetam that has 20-fold higher affinity than levetiracetam for this target (Bialer et al., 2015). In fact, the discovery of this new mechanism of action led that the presynaptic terminal in general, and synaptic vesicles in particular, represent promising therapeutic targets for the development of new AEDs (Löscher and Schmidt, 2006).

Other mechanisms of action involve, for instance, the serotoninergic (increase in extracellular serotonin by valproic acid, carbamazepine, oxcarbazepine, topiramate and zonisamide) and dopaminergic (stimulation of brain dopamine turnover by valproic acid and increase of extracellular dopamine levels by carbamazepine, oxcarbazepine, topiramate and zonisamide) systems (Perucca and Mula, 2013). Moreover, topiramate and zonisamide are also carbonic anhydrase inhibitors (Chong and Lerman, 2016).

Overall, AEDs act by a variety of molecular mechanisms and probably many of them remain unknown. The multiple mechanisms of action result in some disadvantages, including increased side effects and metabolic DDI; however, being “pharmacologically rich” and having a broad spectrum of activities these can also be considered advantages (Dalkara and Karakurt, 2012). In fact, due to their wide spectrum of action in CNS, AEDs have also been successfully used to treat non-epilepsy disorders, such as neurological and psychiatric conditions, including bipolar disorder, panic attacks, aggression, addiction, migraine, autism, Parkinson's disease and a variety of movement disorders (Krasowski and Mcmillin, 2014). In addition, in the last years, new mechanisms of action have been discovered, which can also add more knowledge about the epileptogenesis process. Probably, identifying these mechanisms may open new doors for the discovery and development of more effective AEDs.

I.2.6. Need for new antiepileptic drugs

Despite the large therapeutic arsenal of old and new AEDs, a high proportion of epileptic patients develops drug resistance during the course of their condition, and many patients are not seizure-free even under appropriate pharmacotherapy with the currently available AEDs. Given the current *status*, the effective therapy for epilepsy is undoubtedly an unmet clinical need and it is urgent to continue developing new AEDs with improved efficacy spectra and more favourable safety profiles. In addition, it is essential to reverse the lack of interest that has been demonstrated by pharmaceutical industry in the discovery and development of new AEDs. Hence, there are several hurdles that have to be overcomed to obtain better AED therapies (Golyala and Kwan, 2017). The three main hurdles are highlighted and discussed below: lack of efficacy, poor safety profile and loss of industry interest.

I.2.6.1. Lack of efficacy

When the new wave of the modern era of AEDs started to become available in the early 90s, there were widespread expectations that these new agents would prove effective in achieving complete seizure freedom in a considerable number of patients, who were refractory to older drugs. Unfortunately, these expectations were not fulfilled and the overall probability of achieving seizure freedom in 2015, with over 25 AEDs available in the market, was approximately 70%, similarly to that in the early 70s when physicians had only a handful of AEDs to use. In fact, the introduction of newer AEDs did not bring the expected incremental value to the pharmacological armamentarium; although they present a reduced toxicity burden and less potential for adverse drug interactions, they are not more efficacious than older agents (Franco et al., 2016).

The limited impact of newer AEDs in reducing the problem of drug resistance can be explained through different factors. One of them is the discovery of new anticonvulsant agents using the traditional animal models. This aspect will be discussed in more detail further ahead. Problems with broad-spectrum approaches are another reason. Indeed, an important aim of previous research and development efforts was to discover novel AEDs that exhibited a broad spectrum of activity against different seizure types. However, none of the broad-spectrum AEDs existing to be used in the clinical practice (e.g. valproate or topiramate) is more efficacious for specific seizure types or epilepsy syndromes than narrow-spectrum drugs. Thus, in view of the different mechanisms and possible aetiologies underlying the specific epileptic disorders, there is a growing concern that the broad-spectrum concept may not be the best suited to identify drugs with higher efficacy in difficult-to-treat patient populations. Additionally, issues associated with clinical trial designs may have also contributed to the lack of progress in the development of more effective AEDs. The frequent use of clinically irrelevant controls, problems with placebo and issues in the selection of the

participants have prevented previous trial designs from identifying agents with improved efficacy for drug-resistant epilepsy. Finally, AEDs have been developed for the symptomatic suppression of seizures and not for the prevention of epilepsy or for disease modification. Although the molecular mechanisms underlying epileptogenesis and ictogenesis probably differ, some mechanisms (e.g. inflammatory processes) might be relevant for both conditions (Löscher et al., 2013).

I.2.6.2. Poor safety profile

In spite of the advances in terms of tolerability and safety of newer AEDs, the pharmacological treatment of epilepsy is often accompanied by dose-related severe side effects, long-term toxicity and DDI, which can prevent the administration of the dose required for adequate seizure control. Indeed, severe adverse effects may result in poor treatment adherence in a substantial proportion of patients, and discontinuation of the therapy (Dalkara and Karakurt, 2012; Kowski et al., 2016). A serious concern in this scope is the fact that some severe adverse events of the new AEDs have been identified only in late stages after their widespread clinical use because they are difficult to be identified and/or predicted in preclinical and even clinical development programmes (Löscher et al., 2013).

In terms of toxicity, CNS effects are a transversal problem to all AEDs. A possible explanation for this relates to the fact that all current AEDs have been developed to counteract the neuronal hyperexcitability by targeting mechanisms that also interfere with normal neurotransmission (Löscher et al., 2013). These adverse effects usually are dose-dependent and, in general, it is recognized that AEDs potentiating GABAergic neurotransmission have more detrimental effects on cognition than those modulating voltage-gated channels (Mula and Cock, 2015). On the other hand, there is no doubt that the lower risk of hypersensitivity reactions and the lower potential for detrimental drug interactions may explain why some new AEDs (e.g. levetiracetam and gabapentin) are better tolerated and easier to use than some of the classical AEDs (e.g. carbamazepine and phenytoin). However, serious idiosyncratic adverse effects have also been reported for several new AEDs such as vigabatrin (concentric visual field defects) and felbamate (aplastic anaemia and hepatic failure), which have restricted their use, as early referred. In addition, among the older AEDs, the teratogenicity provoked by valproic acid continues to be one of the main concerns. Thus, regulatory authorities strongly recommend that this drug should only be used in women of childbearing age when no suitable alternative exists or effective birth control measures are in use (Löscher and Schmidt, 2011; Mula and Cock, 2015).

Finally, labelling for AEDs as adjunctive therapy does not differentiate tolerability and safety profiles according to their specific individual characteristics. In fact, adverse events tend to be less frequent, and often less severe, with AED monotherapy, because of the absence of adverse pharmacokinetic and/or pharmacodynamic interactions. However, a lower incidence

of adverse events with monotherapy *versus* adjunctive therapy is not clear yet (Mintzer et al., 2015).

I.2.6.3. Loss of industry interest

As previously referred, the development of new drugs is costly and risky. Even when a new drug candidate is at the first-in-man stage (phase I) and an investigational new drug application has been filled, the chance to be successfully completed its clinical development and be approved by the regulatory authorities is only about 10% (Perucca et al., 2007). Prior incentives for investment in AED development are now negatively balanced by overall challenges facing the industry for the drug development. Moreover, up to date, none AED has convincingly demonstrated to be superior in efficacy to any other, and differentiation by safety profile is not a principal component for enhancing pricing and reimbursement. Thus, payer reimbursement requires that future AEDs bring additional value or differentiation (mainly with regard to efficacy) to an already crowded, highly generic AED field (Löscher et al., 2013; Perucca et al., 2007). Other problematic issue is the fact that commercialization models indicate that an adjunctive indication alone for a marginally differentiated product is not adequate. However, although an indication in monotherapy can move a drug earlier into the epilepsy treatment paradigm, the approval of an AED as monotherapy has so far required its prior approval as add-on therapy, which causes a considerable time delay (Löscher et al., 2013).

On the other hand, it is also important to highlight that the clinical heterogeneity observed in epilepsy could represent an opportunity for the pharmaceutical industry rather than a limitation. Indeed, many epilepsies frequently are associated with drug resistance and for which unmet needs are greatest fulfil the criteria for an orphan disease. Therefore, the development of a treatment for these indications can benefit from facilitated regulatory pathways, availability of data sharing programmes and in some settings also from financial incentives from governmental agencies or other sources. Importantly, for some epilepsy syndromes no licensed treatments exist, and therefore any new compound that has shown any degree of efficacy in a controlled clinical trial in such indications would enjoy virtual exclusivity in terms of regulatory approval (Franco et al., 2016). This notably reduces the level of investment necessary for discovery and development, and also potentially diminishes the technical hurdles and regulatory data requirements. In addition, another more immediate business opportunity may involve the repurposing of drugs from other therapeutic areas (e.g. mood disorders, migraine and neuropathic pain) (Löscher et al., 2013). In fact, it has been estimated that a new AED with additional approved indications in bipolar disorder and neuropathic pain might have a potential market size three times larger than that of epilepsy alone (Franco et al., 2016).

I.2.7. Discovery of new antiepileptic drugs

An AED is considered well-succeed when it has at least one of the following properties: higher efficacy than other drugs in the treatment of refractory epilepsies; the ability to prevent or delay the onset of epilepsy or modify its progression; broad usefulness in non-epileptic CNS disorders; fewer adverse effects than available drugs; and ease of use, such as rapid titration, linear pharmacokinetics, lack of drug interactions, or a longer half-life (Perucca et al., 2007). Until now an ideal AED that are capable to fulfil all of these requirements remains undisclosed. However, constant efforts have been made in order to discover new more efficacious and safer AEDs.

I.2.7.1. Historical background

The story of the modern pharmacological treatment of epilepsy starts on May 1857 when the chairman Sir Charles Locock shared with the audience his enthusiasm for potassium bromide in young women with "hysterical epilepsy connected with the menstrual period". Indeed, treatment of seizures with bromides is considered as the first attempt for AED therapy (Miziak et al., 2012).

In 1911, phenobarbital was synthesized for the first time and a year after it was introduced in the market as a hypnotic. In the same year, Alfred Hauptmann discovered serendipitously its anticonvulsant properties. This young resident psychiatrist lived over a ward of people with epilepsy and, due to the seizures, the patients kept him awake. Thus, Hauptmann sedated his patients with phenobarbital so that he could get a good night of sleep. After, he noticed that phenobarbital did not only alleviate the attacks, but also decreased their number. Subsequent tests confirmed the antiepileptic properties of phenobarbital and it was recognized that this drug was efficient in severe cases of epilepsy, even when the highest doses of bromide did not work. However, it was only at the beginning of 1920 that phenobarbital was introduced on a larger scale as an AED. Nowadays, this drug is still the most widely prescribed AED in the developing world and remains the first popular choice in many industrialized countries partly because of its modest cost (Brodie, 2010; Miziak et al., 2012).

In 1934, when Tracy Putnam was appointed to the directorship of the neurological unit at the Boston City Hospital, he set out to discover a less sedative AED than phenobarbital. With the help of Frederic Gibbs, he established the first electroencephalographic laboratory for the routine study of "brain waves". A makeshift piece of apparatus was assembled to demonstrate that phenobarbital markedly raised the convulsive threshold in cats. Thus, several phenyl derivatives were then investigated and only one of them, phenytoin, was not too toxic for routine administration. Fortunately, it was markedly effective in protecting cats from electrically induced convulsions. Putnam gave this drug to one of his young assistants,

Houston Merritt, for clinical evaluation in 1936. The first patient to receive the drug had suffered daily seizures for many years and became permanently seizure-free on commencing treatment. The subsequent publication established this new drug in the therapeutic armamentarium (Brodie, 2010). At the same time, in 1935, mephobarbital was discovered and, after, primidone was introduced in the market in 1952. It proved to have anticonvulsant properties as well and did not cause sedation in the patient, but after 60 consecutive years of clinical studies, it was demonstrated that primidone does not have advantages over phenobarbital (Miziak et al., 2012).

In 1945, trimethadione was developed and it was the first drug to be specifically used in absence seizures (Dalkara and Karakurt, 2012). Subsequently, major researches were initiated to find a less toxic drug for this indication, which resulted in the licensing of ethosuximide in 1958. The next major drug to be licensed was carbamazepine, which became widely available in the mid-1960s and is arguably supported by the best available evidence. It was synthesized by Schindler at Geigy in 1953 as a possible competitor for the recently introduced antipsychotic chlorpromazine. The first study with this drug in epilepsy was not carried out until 1963, after which it was rapidly licensed as AED (Brodie, 2010).

Additionally, valproic acid, firstly synthesized in 1882, was re-examined and its anticonvulsant properties were discovered only 80 years later. During this time period, valproic acid was used as a metabolically neutral solvent for organic compounds. In 1962, a research student Pierre Eymard encountered some difficulties in dissolving certain compounds in the usual solvents. In order to solve this problem, Meunier suggested to try valproic acid as solvent, and then he noticed that regardless the dissolved substance the resulting solution had anticonvulsant properties. In 1964, the first clinical study was published, and in 1967, its sodium salt was approved as a drug in France, and then in the rest of the world (Miziak et al., 2012).

Regarding benzodiazepines, their value for the treatment of epilepsy was rapidly recognised following their synthesis and development by Leo Sternbach in the 1960s. In 1965 Henry Gastaut published a report regarding the efficacy of diazepam in treating *status epilepticus*. His follow up paper with clonazepam 6 years later was even more positive and nowadays the most recent benzodiazepine, clobazam, is probably the most widely used oral benzodiazepine for a range of refractory epilepsies (Brodie, 2010).

The known modern era of AED discovery began in 1975 when the National Institute of Neurological Disorders and Stroke (NINDS) in the USA established the Anticonvulsant Screening Program. Many thousands of new chemical entities from academic and pharmaceutical industry were systematically screened for their potential anticonvulsant activity, resulting in the licensing of an increasing list of AEDs (Łukawski et al., 2016). Oxcarbazepine is sold in the world market since 1990, but it was only approved by the FDA as late as 2000. Felbamate was first synthesized in 1954, but the development of clinical studies took place as late as in 1982. However, it was just approved by FDA in 1993. In this year, gabapentin was approved as

well as lamotrigine a year later. It was followed by topiramate, tiagabine, levetiracetam, pregabalin, zonisamide, eslicarbazepine acetate and lacosamide, clobazam, retigabine, stiripentol, rufinamide, brivaracetam and perampanel in the last twenty years (Holmes and Hernandez-Diaz, 2012; Löscher and Schmidt, 2011; Miziak et al., 2012).

I.2.7.2. Design strategies

As the historical background documents, some of the older AEDs have been serendipitously discovered. However, according to Löscher (Löscher et al., 2013), three main strategies have been used in AED discovery:

- *Structural variation of known AEDs*. Derivatives or analogues of the existing drugs can be regarded as second or third-generation or follow-up agents of the parent compounds. Through this fruitful strategy many of newer AEDs (e.g. eslicarbazepine acetate and brivaracetam) as well as candidates under development have been designed. This strategy generally results in "me-too/me better drugs" especially with better tolerability and improved pharmacokinetic properties such as enhanced oral absorption, less toxic metabolites, extended duration of activity and lower potential for DDI (Dalkara and Karakurt, 2012);
- *Random, phenotypic screening of newly synthesized compounds of diverse structural classes*. In this case, new potential anticonvulsant agents found in screening tests represent various structures for which the precise mechanism of action needs to be further specified. Numerous groups of compounds undergo intensive screening in seizure models. This kind of research is performed in many laboratories worldwide, as every years many papers have been published on new chemicals possessing clear-cut anticonvulsant potential in experimental models of seizures (Miziak et al., 2012);
- *Mechanism-based approach or "rational" drug design*. By means of this approach, it was identified a small number of AEDs and is based on previously presumed mechanisms of seizure generation. As example, the development of vigabatrin and tiagabine was directed to the potentiation of GABAergic inhibitory neurotransmission and perampanel was developed aiming at inhibiting the glutamatergic excitatory neurotransmission. However, the old reductionist view that seizures or epilepsy are due to an imbalance between GABAergic and glutamatergic neurotransmission ignores the complexity of this disorder. Following this strategy, gabapentin was designed considering GABA structure so that, unlike GABA, it penetrates the BBB but retains as much as possible GABA properties. However, it was verified that this drug and its second-generation pregabalin do not exert their activity through the GABAergic system.

The strategy of targeting mechanisms not related to the associated with the existing AEDs is another method for searching novel AEDs, and it may deliver new and more disruptive options

for the treatment of drug-resistant epilepsy (Łukawski et al., 2016). For this approach, the hard task to understand the pathophysiology of epilepsy is crucial. Additionally, the use of quantitative structure-activity relationship (QSAR) techniques constitute another strategy, but it has some limitations. Although there are many SARs established and used for development of new anticonvulsant compounds, there have been many difficulties to improve the understanding of the main mechanisms underlying the chemical diversity of structures of the known AEDs. Moreover, the demonstration of a simple and successful quantitative relationship between interatomic distance and activity took time and requires experimental data for a relatively large number of molecules. However, the modern QSAR techniques have made possible to extend the knowledge on anticonvulsant mechanisms to the molecular level and to support some programmes of rational design and development of new AEDs (Dalkara and Karakurt, 2012).

I.2.7.3. Novel potential targets

It is thought that the major hurdle to the development of preventative AEDs is the lack of understanding of the mechanisms underlying the generation and perpetuation of seizures following an initial insult to the brain (Walker et al., 2015). Currently, there is an intense research effort focused on understanding the scientific basis of the epileptogenesis. Thus, a wide range of new molecular targets are being identified and, in many cases, they are entirely different from those that are already known. The strategy is to "repurpose" therapeutic agents designed for different purposes, for example to modulate immune function, reduce oxidative stress, or stimulate red cell production. The fact that many of these agents are already approved for use in other disease indications will facilitate the evaluation of the novel strategies in clinical studies (Kaminski et al., 2014). Thus, some particularly interesting target mechanisms have been described below:

- *Immune and inflammatory mechanisms*. Experimental evidence and clinical observations indicate an important role of inflammation in the pathogenesis of epilepsy. Chronic brain inflammation comprises the activation of microglia, astrocytes, endothelial cells of the BBB and peripheral immune cells, as well as the concomitant production of inflammatory mediators. A large number of inflammatory mechanisms have been implicated, but only relatively few have been experimentally investigated using pharmacological tools in animal epilepsy models. Among them are the cytokine interleukin 1ß (IL-1ß) pathway that is one of the best characterised inflammatory pathways in epilepsy; leukocyte trafficking and anti-leukocyte adhesion mechanisms; sphingosine 1-phosphate receptors; and prostaglandin E2/E-prostanoid 2 receptor signaling pathway (Löscher et al., 2013; Łukawski et al., 2016; Varvel et al., 2015);
- *Oxidative stress mechanisms*. This biochemical state in which harmful reactive oxygen species are generated has been hypothesized to occur in epilepsy and to be a cause of

treatment refractoriness. Several antioxidant strategies have been proposed as a treatment approach, such as the use of resveratrol, melatonin, vitamin E, selenium and allopurinol and the participation of the nuclear factor erythroid-2-related factor 2 transcription factor (Kaminski et al., 2014; Łukawski et al., 2016);

- *Signaling pathways*. Some positive data in terms of anticonvulsant and antiepileptogenic activity also exist in relation to agents inhibiting mammalian target of rapamycin (mTOR). This signaling pathway controls many cellular events in the brain including neurite growth, synaptic plasticity and cell survival by regulating metabolism and protein synthesis. A strong association between mTOR and epilepsy occurs in tuberous sclerosis complex (TSC), a genetic disease due to mutations in TSC1 (hamartin) and TSC2 (tuberin) tumour suppressor genes. Increasing evidence also implicates mTOR dysregulation in the pathogenesis of acquired forms of epilepsy, such as temporal lobe epilepsy. In addition, the peroxisome proliferator-activated receptors could also constitute a target and their agonism can lead to protection against seizures (Łukawski et al., 2016; Varvel et al., 2015);
- *Thrombolysis, haematopoiesis, and angiogenesis*. Reduction of the activity of brain tissue-type plasminogen activator or increase of the activity of neuroserpin or amount of erythropoietin could be potential antiepileptogenic possibilities. Moreover, vascular endothelial growth factor receptors could also represent a potential target (Kaminski et al., 2014);
- *3-Hydroxy-3-methylglutaryl-coenzyme A reductase*. Statins are a class of drugs used to reduce cholesterol levels by inhibiting this enzyme. Interestingly, there has been a flurry of reports providing evidence that statins could be useful in the treatment of epilepsy (Banach et al., 2014);
- *Neurotrophic factors*. Emerging evidence suggests that the enhanced activation of the neurotrophic factor receptor TrkB in the mature brain may be a requisite for limbic epileptogenesis following prolonged seizures (Varvel et al., 2015);
- *α2 Adrenergic receptor blockade*. Several decades of research have demonstrated that pharmacological activation or blockade of the various adrenergic receptor types can influence seizure susceptibility. Specifically, the stimulation of α2 adrenergic receptors is generally anticonvulsant (Kaminski et al., 2014);
- *Cannabinoid receptor*. Many studies have demonstrated that cannabinoid agonists are acutely anticonvulsant, whereas cannabinoid antagonists are acutely proconvulsant agents. The observation that the cannabinoid system can regulate epileptogenesis indicates that caution is warranted when contemplating the use of agents that interact with cannabinoid signaling in epilepsy therapy (Kaminski et al., 2014);

- *Adenosine kinase*. Adenosine is released directly from activated neurons and metabolically cleared by astrocytic adenosine kinase, and it has long been recognized as a powerful endogenous anticonvulsant neuromodulator. Administration of an adenosine kinase inhibitor could represent a potential future clinical direction (Varvel et al., 2015).

After identification, the new druggable targets should be extensively validated by pharmacological and genetic approaches before the onset of substantial drug discovery efforts. To facilitate this goal, major attention should be devoted to biomarker identification and validation, which would allow rapid translation to early clinical proof-of-concept trials (Löscher et al., 2013).

I.2.7.4. Molecules in clinical development

The past two decades have witnessed an unprecedented expansion in pharmacological treatment options for epilepsy; however, there is limited evidence to suggest that clinical outcomes have substantially improved over that period (Brodie et al., 2011). Thus, nowadays, there are several molecules in various stages of clinical development as AEDs candidates (Table I.4). These include compounds with chemical structures that do not resemble existing AEDs, and derivatives of existing drugs that are developed as follow-up compounds with potentially improved properties. For some compounds, the clinical development has advanced substantially and extensive published information is already available. For others, data are limited, and the results of clinical trials are not yet in the public domain, including compounds that have undergone only preliminary clinical assessment and those that have been in clinical development for many years but remain in a dormant state (Perucca et al., 2007); these were not included in the table below.

In addition to synthetic molecules, which represent the main amount of new therapeutic candidates, it is worth to refer that over the years, patients with epilepsy have used a variety of herbs for controlling the seizures (Ekstein, 2015). Actually, extracts of plants and/or their single constituents have shown to act on the same pharmacological targets as those of the most commonly used AEDs (Matias et al., 2016b; Sucher and Carles, 2015). According to the progress report on new AEDs published as a summary of the Twelfth Eilat Conference (EILAT XII) that took place in Madrid (Spain) in 2014 (Bialer et al., 2015), at least three of the AED candidates in clinical development are herb-derived compounds (cannabidiol, cannabidivarin and huperzine A).

Moreover, through the Table I.4, it is also possible to notice that several molecules in clinical trials have novel and distinct putative mechanisms of action, which can represent a greater chance of success to control refractory seizures, and a potential for discovering antiepileptogenic drugs. One example is VX-765 that is an orally active IL-converting enzyme/caspase-1 inhibitor, blocking IL-1β secretion and producing a strong anti-

inflammatory effect (Kaminski et al., 2014). Another case is huperzine A that is a dual inhibitor of acetylcholinesterase and glutamate [*N*-methyl-D,L-aspartate (NMDA)] receptors.

Table I.4 – Antiepileptic drug candidates in clinical development (Bialer et al., 2015; Doumlele et al., 2016; "Epilepsy Foundation," 2017; Faught, 2014; Leo et al., 2016; Mula, 2016b; Zaccara and Schmidt, 2016).

Drug candidate	Company	Indication	Putative mechanism of action	Phase of development
2-Deoxy-D-glucose	NeuroGenomeX	Refractory seizures, Lennox-Gastaut syndrome, seizure clusters and *status epilepticus*	Glycolytic inhibition	Phase IIa
Allopregnanolone	Marinus Pharmaceuticals	Super-refractory *status epilepticus*	$GABA_A$ receptor modulation	Phase III
Beprodone	MarcoPolo Pharmaceuticals	Refractory focal epilepsies	Melatonin type 3 receptor agonism	Phase II
Cannabidiol	GW Pharmaceuticals	Paediatric drug refractory epilepsy, Dravet and Lennox-Gastaut syndromes	Adenosine uptake inhibition, voltage dependent anion channel-1 expression modulation and activity at transient receptor potential channels	Phases I, II and III
Cannabidivarin	GW Pharmaceuticals	Focal seizures	Activity at transient receptor potential channels	Phase IIa
CPP-115	Catalyst Pharmaceuticals	Infantile spasms	GABA-transaminase inhibition	Phase I
Everolimus	Novartis	Tuberous sclerosis complex-related epilepsy	Selective mechanistic target of rapamycin (mTOR) inhibition	Phase III
Ganaxolone	Marinus Pharmaceuticals	Female paediatric epilepsy and adult drug-refractory focal epilepsy	$GABA_A$ receptor modulation	Phases I, IIa and III
Huperzine A	Biscayne Pharmaceuticals	Complex focal seizures and Dravet syndrome	Acetylcholinesterase and glutamate receptor inhibition	Phase I
Nalutozan	Proximagen	Drug-refractory focal epilepsy	$5HT_{1A}$ receptor agonism	Phase IIa
Pitolisant	Bioprojet Pharma	Photosensitive epilepsies	Histamine 3 receptor antagonism	Phase II
UCB0942	UCB	Pharmacoresistant epilepsy	Unknown	Phase I
VX-765	Vertex Pharmaceuticals	Drug resistant focal epilepsies	Selective caspase-1 inhibition	Phase IIb
YKP3089	SK Life Sciences	Photosensitive epilepsy	Sodium channel blockage and GABAergic transmission enhancement	Phase IIb

However, it should not be forgotten that the mechanisms of action in almost all the cases of these compounds is ascertain. In general, these molecules show several putative mechanisms through which play their action and to discern which of them is/are responsible for the anticonvulsant/antiepileptic potential is a very hard task.

I.3. CHEMICAL STRUCTURES RELATED TO ANTICONVULSANT ACTIVITY

I.3.1. Pharmacophores related to anticonvulsant activity

As referred before, a large number of AEDs is available for the treatment of different types of seizures and more than a dozen are under clinical trials. However, the search for new molecules having high tolerability, good pharmacokinetic properties and clinical efficacy remains as a subject of intensive research, particularly in academia (Dong et al., 2017; Liao et al., 2017; Obniska et al., 2016). Hence, as shown in Figure I.5, the literature has been enriched with progressive findings about the association of various pharmacophores with anticonvulsant activity.

In this context, heterocyclic scaffolds should be highlighted due to the fact that they represent the central framework of many biologically active compounds. These structures are known to contain at least one or more hetero atoms in a cyclic system and they have received considerable attention as drug precursors, having become useful materials in drug research programmes (Taylor et al., 2016). In fact, there are several reports also associating diverse heterocyclic systems with the anticonvulsant activity (Asif, 2015; Nusrat et al., 2014) and, for this reason, in the following sections, the most relevant heterocyclic as well as non-heterocyclic scaffolds were presented. The selection criteria included the frequency of appearance of the pharmacophores in the literature (Figure I.5) and, mainly, the incorporation of these groups in AEDs already used in the clinical practice, whose activity and efficacy is well-established. Moreover, in this section, different chemical strategies to produce new anticonvulsant candidates are also addressed, such as the molecular hybridization and the employment of multicomponent reactions (MCRs).

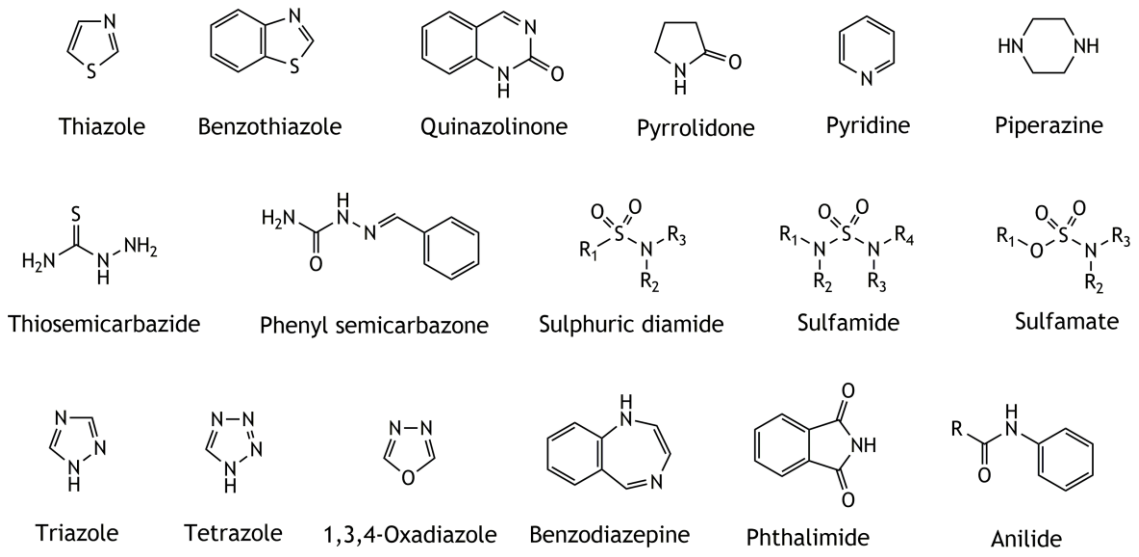

Figure I.5 – Chemical structures of several pharmacophoric groups usually associated with anticonvulsant activity and/or found in clinically available antiepileptic drugs.

I.3.1.1. Non-heterocyclic structures

Valproic acid is one of the structurally simplest drugs and probably is the AED with linear structure more used as starting material to search for novel anticonvulsant candidates. For instance, several valproate analogues were synthesized by Shekh-Ahmad and collaborators, which developed a prodrug of valproic acid, *N*,*N*-dimethylethanolamine valproate **(1)** (Figure I.6), to originate a drug seven times more potent than the original AED (Shekh-Ahmad et al., 2012). Also the interesting analogue *N*-methoxy-valnoctamide **(2)** (Figure I.6) showed an improved profile of efficacy in several animal models when comparing with valproate, without exhibiting teratogenic effects (Pessah et al., 2011).

(1)
N,*N*-dimethylethanolamine valproate

(2)
N-methoxy-valnoctamide

Figure I.6 – Chemical structures of *N*,*N*-dimethylethanolamine valproate **(1)** and *N*-methoxy-valnoctamide **(2)** (Pessah et al., 2011; Shekh-Ahmad et al., 2012).

I.3.1.2. Thiazole and benzothiazole

Thiazoles and benzothiazoles are found in a wide variety of bioactive synthetic molecules and natural products (Rouf and Tanyeli, 2015). A prominent example that includes the benzothiazole moiety is riluzole (Figure I.7), which was developed in the 80 years as anticonvulsant, having been tested in several seizures/epilepsy animal models (Mizoule et al., 1985). However, it did not gain significant footing in the treatment of epileptic patients, being currently applied in several neurologic and psychiatric conditions, involving aberrant sodium metabolism or glutamatergic excitotoxicity as a presumed underlying pathologic mechanism (Wilson and Fehlings, 2014). Despite this change of therapeutic indication, riluzole continues to be a starting point for the design of new AED candidates. An example is given by Hassan *et al.* who searched anticonvulsant and neuroprotective molecules developing a series of *N*-(substituted benzothiazol-2-yl)amide derivatives **(3)** (Figure I.7) after incorporating the GABA structure into the benzothiazole nucleus (Hassan et al., 2012). In addition, various benzothiazol-2-yl-aminoacetamide analogues **(4)** (Figure I.7) also reinforced the anticonvulsant role of this nucleus due to the fact that 85% of these molecules shown to be active in animal models of chemically and electrically induced seizures (Ali and Siddiqui, 2015). Regarding the anticonvulsant activity of thiazole derivatives, Nikalje and collaborators synthesized a series of *N*-(2-oxo-2((4-oxo-2-substituted thiazolidin-3-yl)amino)ethyl) benzamides **(5)** (Figure I.7) and moderate to high activity was observed (Nikalje et al., 2014).

Several conjugates of 4-[3-(aryl/heteroaryl)-3-oxo-propenyl]-benzaldehyde **(6)** (Figure I.7) with thiazole and thiazolidinones were also developed and structures incorporating the naphthalene ring and the 5-bromo-thiophene showed high levels of anticonvulsant protection (96 and 93%, respectively) (Pandey et al., 2016).

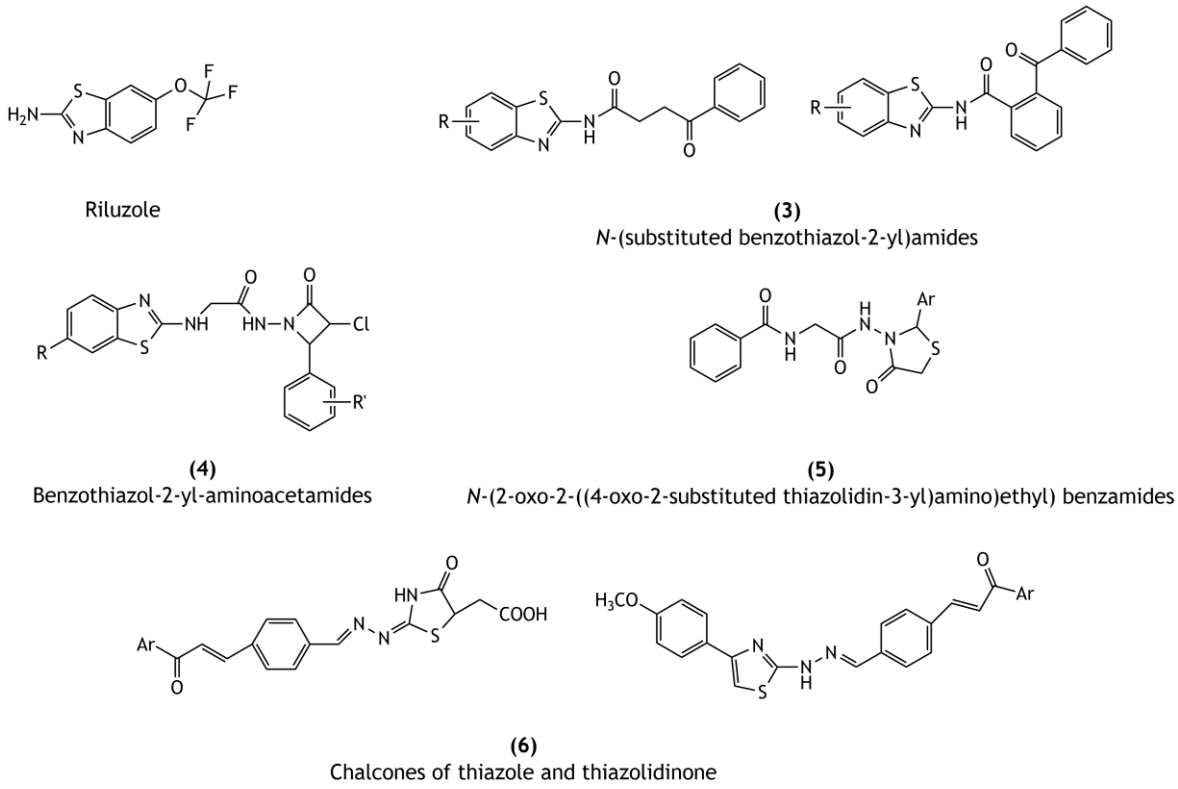

Figure I.7 – Chemical structures of riluzole and derivatives including benzothiazole or thiazole rings (Ali and Siddiqui, 2015; Hassan et al., 2012; Nikalje et al., 2014; Pandey et al., 2016).

I.3.1.3. Quinazolin-4(3*H*)-one

The discovery of methaqualone (Figure I.8) represented a relevant landmark in the field of synthetic anticonvulsant agents (El-Azab and Eltahir, 2012). This compound contains the quinazolin-4(3*H*)-one nucleus, which is thought to be important for its anticonvulsant activity and it was suggested that it acts through the selective modulation of the $GABA_A$ receptors (Hammer et al., 2015). In fact, there are numerous reports in the literature describing the synthesis and anticonvulsant evaluation of molecules incorporating the quinazolinone nucleus. For instance, a series of new 6-iodo-quinazolin-4(3*H*)-one derivatives **(7)** (Figure I.8) was developed, exhibiting moderate to high protection levels in animal models of seizures (Ibrahim et al., 2015). More recently, novel 3-substituted-2-phenylquinazolin-4(3*H*)-ones and similar 7-chloro-quinazolin-4(3*H*)-one derivatives **(8)** (Figure I.8) were synthesized and some of them presented 100% of protection against induced seizures (Patel et al., 2016).

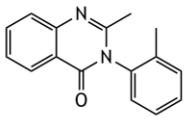

Methaqualone

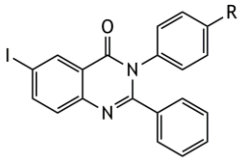

(7)
6-Iodinated-quinazolin-4(3*H*)-ones

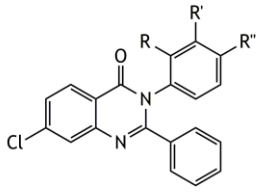

(8)
7-Chlorinated-quinazolin-4(3*H*)-ones

Figure I.8 – Chemical structures of methaqualone and quinazolin-4(3*H*)-one derivatives (Ibrahim et al., 2015; Patel et al., 2016).

I.3.1.4. Pyrrolidone

The pyrrolidone nucleus is a cyclic imide system and constitutes the basic pharmacophore of several AEDs (e.g., levetiracetam and ethosuximide; Figure I.3). Considering this, various pyrrolidine-2,5-dione derivatives **(9)** (Figure I.9) were synthesized, presenting good activity, whose mechanism of anticonvulsant action could be partially associated with the influence on voltage-sensitive sodium and L-type calcium channels (Obniska et al., 2016). In addition, the same group also showed that the pyrrolidinedione derivatives elevated considerably the electroconvulsive threshold in mice, confirming their outstanding anticonvulsant activity against the electrically induced seizures in animals (Rapacz et al., 2016).

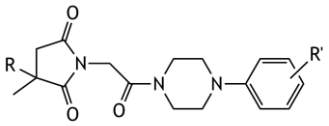

(9)
Pyrrolidine-2,5-dione derivatives

Figure I.9 – General skeleton of pyrrolidone-2,5-diones **(9)** as potential anticonvulsant agents (Obniska et al., 2016).

I.3.1.5. Pyridine

Perampanel (Figure I.3) is an AED that contains a pyridine ring in its structure. The discovery of this new drug opened new doors for the search of new AED candidates containing pyridine as a potential pharmacophoric moiety. A good example is given by Amato *et al.*, who

synthesized a group of *N*-pyridyl benzamide derivatives which were active on KCNQ2/Q3 channels (Amato et al., 2011). Further studies demonstrated that the compound 4-chloro-*N*-(6-chloro-pyridin-3-yl)-benzamide **(10)** (Figure I.10) reduced the neuronal excitability and was also effective in an animal model of chronic epilepsy (rat amygdala kindling model) (Boehlen et al., 2013).

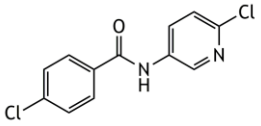

(10)
4-Chloro-*N*-(6-chloro-pyridin-3-yl)-benzamide

Figure I.10 – Chemical structure of 4-chloro-*N*-(6-chloro-pyridin-3-yl)-benzamide **(10)** (Boehlen et al., 2013).

I.3.1.6. Other chemical structures associated with anticonvulsant activity

Apart from the groups already described, the literature counts with many other heterocycles associated with anticonvulsant potential and some of them are also mentioned here. In this context, for example, the piperazine ring is frequently found in the design of new drugs for epilepsy (Habib et al., 2015; Kumari et al., 2016; Obniska et al., 2012). Aryl thiosemicarbazides and phenyl semicarbazones also should be highlighted, because they have been incorporated in several compounds with interesting anticonvulsant activity (Kulandasamy et al., 2010; Tripathi et al., 2012). Additionally, molecules containing a sulphonyl as functional group have been studied, as proved by Li *et al*. who incorporated the sulphonamide group in molecules with anticonvulsant properties (Li et al., 2015), and Villalba and collaborators who synthesized sulphuric diamide and sulphamates derivatives and evaluated their anticonvulsant activity (Villalba et al., 2016). The specific heterocyclestriazole (Ayati et al., 2016) and tetrazole (Malik and Khan, 2014; S.-B. Wang et al., 2014) have also gained importance in the discovery and development of new anticonvulsant drugs as well as oxadiazole (Siddiqui et al., 2014) which, for instance, was linked to phenytoin (Botros et al., 2013). Additionally, taking into consideration the effects of the benzodiazepine nucleus in the CNS, this pharmacophore has also been incorporated in the design of new drug candidates for epilepsy (Auta et al., 2010; Ghogare et al., 2010). Finally, it was described the combination of GABA structure with phthalimide and anilide/hydrazone nucleus (Ragavendran et al., 2007) and with ameltolide (Yogeeswari et al., 2007) in order to obtain molecules with improved anticonvulsant properties.

I.3.2. Molecular hybridization

The efforts to increase the knowledge about the mechanisms involved in the pathogenesis of the diseases combined with the evolution of the technology have offered multiple possible drug targets in the perspective of drug discovery, particularly in the case of complex diseases such as CNS disorders. As aforementioned, this refined knowledge that has been achieved throughout the years is changing the drug discovery paradigm from the traditional approach of the generation of a compound that shows higher selectivity and potency for a single-target ("one-disease-one-target" approach) to the development of molecules that are able to simultaneously modulate two or more drug targets involved in the disease process (Geldenhuys and Schyf, 2013). For this reason, the design and preparation of molecular hybrids currently represents an encouraging research strategy in the development of new drug candidates. Conceptually, hybrid molecules are a result of the union of two or more distinct pharmacophores, which are covalently linked in order to produce a single compound that acts simultaneously on the same or different pharmacological targets. The combination of distinct structural moieties allows the production of molecules with potential dual activity, having one or multiple pharmacological actions (Bansal and Silakari, 2014; Meunier, 2008). As expected, these new agents are proving to be more efficacious, economical and safer than the single-target directed drugs (Meunier, 2008). The proof of proficiency of this strategy is given by some examples of hybrid molecules that are already commercially available in clinical practice, such as vilazodone (Milelli et al., 2016) and indinavir (Patrick, 2009).

Therefore, the development of new drugs through molecular hybridization attracted the interest of medicinal chemists. For this reason, currently, several molecular hybrids are under exploitation, namely as antibacterial (Pavlović et al., 2010), antimalarial (Bellot et al., 2010), anticancer (Berube, 2016), antidiabetic (Hidalgo-Figueroa et al., 2013), anti-inflammatory (Almasirad et al., 2014), anti-obesity (Kinfe et al., 2013), anti-osteoporosis (Sashidhara et al., 2013) and cardioprotective agents (Bisi et al., 2003). In addition, new hybrid molecules were also developed to treat cystic fibrosis (Mills et al., 2010), chronic obstructive pulmonary disease (Liu et al., 2013), human immunodeficiency virus (Zeng et al., 2010), gastrointestinal disorders (Theoduloz et al., 2013) and skin diseases (Kim et al., 2009). Due to the wide spectrum of biological and pharmacological activities, this topic has also gained an increasing interest in the context of complex CNS disorders (Matias et al., 2017c), which are multifaceted and in general there is a lack of satisfactory pharmacotherapeutic options. In the area of neurodegenerative diseases, there are considerable endeavours to discover new hybrid molecules with higher potential than the existing drugs. In this field, the focus goes to Alzheimer's disease where the molecular hybridization strategy has been explored mainly using the tacrine and donepezil pharmacophores to develop new drug candidates (Singh et al., 2015). Moreover, there are also several reports about the development of hybrid molecules directed for Parkinson's disease (Ghosh et al., 2010) and other neurodegenerative disorders (Yoo et al., 2011).

Due to the increasing importance of this strategy in drug research, together with the necessity of development of new and improved AEDs, it is frequent to find in the literature the design of new compounds combining two or more pharmacophores associated with anticonvulsant potential. Some examples were already described in the previous section. Others can be found, for instance, in the work of Kaminski *et al*. who developed a new series of compounds combining chemical fragments of lacosamide, ethosuximide and levetiracetam **(11)** (Figure I.11) obtaining interesting results (Kamiński et al., 2015). A group of structures linking semicarbazones and the pyridine ring **(12)** (Figure I.11) was also developed (Mehta et al., 2006), as well as molecules combining the quinazolin-4(3*H*)-one from methaqualone and substituted 1*H*- and 2*H*-tetrazoles from YKP3089 **(13)** (Figure I.11) (Malik and Khan, 2014).

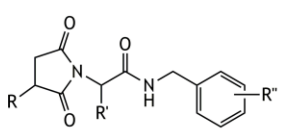

(11)
N-Benzyl-2-(2,5-dioxopyrrolidin-1-yl)propanamides

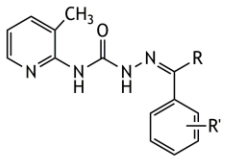

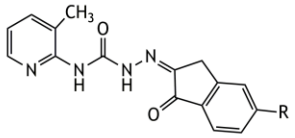

(12)
N-(3-Methylpyridin-2-yl) semicarbazones

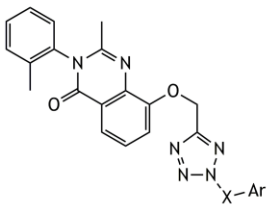

(13)
Quinazolin-4(3*H*)-one substituted 1*H* and 2*H*-tetrazoles

Figure I.11 – Chemical structures of hybrid compounds with anticonvulsant properties (Kamiński et al., 2015; Malik and Khan, 2014; Mehta et al., 2006).

I.3.3. Multicomponent reactions

MCRs (so-called "tandem", "domino", or "cascade" reactions) are usually defined as "one-pot" processes, combining three or more reactants either simultaneously or through a sequential-addition procedure that does not involve any change of solvent (Touré and Hall, 2009) The product that is obtained in this single operation contains essentially all of the atoms of the starting materials (with the exception of condensation by-products, such as molecules of water, hydrochloric acid, or methanol). During the reactional step intermediate molecules are frequently in equilibrium reactions and only the last step is irreversible, leading to the final products (Ruijter et al., 2011).

It is difficult to identify the first example of a MCR. However, one of the oldest known is the Hantzsch synthesis, which was reported in 1881. In this MCR, Hantzsch heated acetoacetic

ester, an ammonia source, and an aldehyde to obtain dihydropyridines. A decade later, Biginelli reacted acetoacetic ester, aldehyde and urea to obtain a new class of compounds, the 3,4-dihydropyrimidin-2(1*H*)-ones (DHPMs), also designed Biginelli products (Suresh and Sandhu, 2012). The first isocyanide-based MCRs were disclosed by Passerini [3 component reaction (CR)] in 1921 and after by Ugi (4CR) in 1959. Surprisingly, MCR strategies remained underexploited for many decades, as illustrated in Figure I.12. However, they gained prominence in the early 1990s with the advent of combinatorial chemistry, for which MCRs were considered as ideal reactions to assemble large compound libraries in medicinal chemistry endeavours (Toure□ and Hall, 2009) Actually, nowadays, MCRs fill an important place in library synthesis by providing direct access to library compounds and by serving as starting points for diversity-oriented synthesis (Biggs-Houck et al., 2010).

MRCs became very popular due to their numerous advantages over conventional linear-type synthesis. In fact, MRCs are highly economical reactions, being possible a reduction of the number of synthetic operations and the maximization of the build-up of structural and functional complexity (Touré and Hall, 2009) In addition, MCRs provide the highest number of compounds for the least synthetic effort. In other words, a 3CR can provide 1000 compounds when 10 variants of each component are employed in a full matrix of combinations. Hence, they can allow the fast generation of SAR information by providing sets of compounds with related core structures (Biggs-Houck et al., 2010). Overall, MCRs can afford products with the diversity needed for the discovery of new lead compounds and lead optimization, employing combinatorial chemistry techniques (Kappe, 2003).

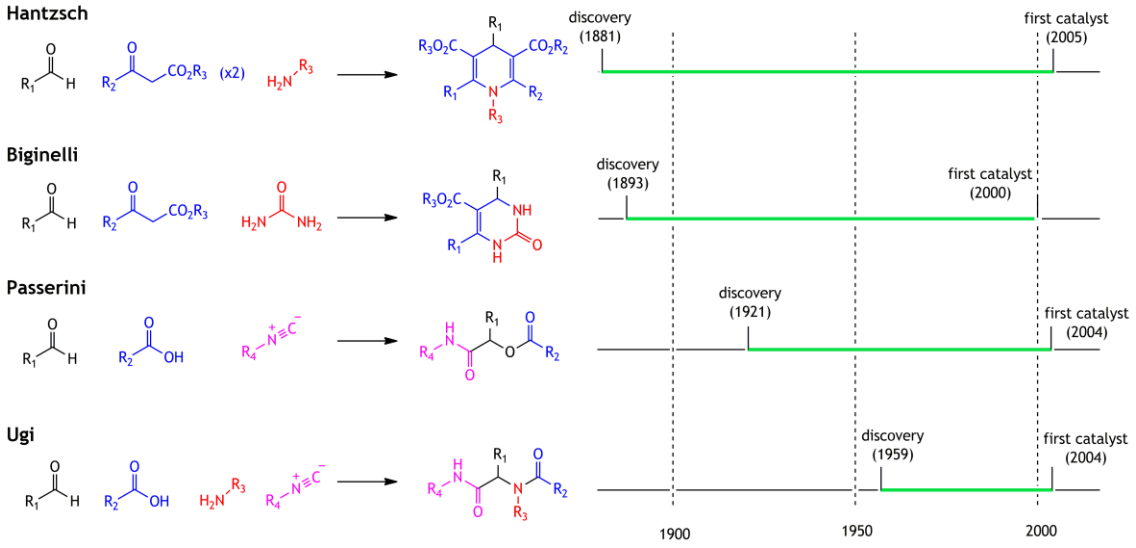

Figure I.12 – General scheme of multicomponent reactions and the timeline of their discovery and the first catalysts for these reactions. Adapted from (Biggs-Houck et al., 2010).

On the other hand, in spite of the high number of molecules that can be produced through a MCR, there is a limited scaffold diversity and, usually, a poor stereocontrol. The first limitation can be overcomed by the continuous discovery of novel MCRs and/or by combination of existing MCRs with complexity-generating reactions, such as cyclization reactions. Regarding the lack of stereocontrol, the study adequate catalysts to be used in these reactions can be an option. In addition, the exploitation of the intrinsic diastereoselectivity of certain MCRs is another attractive strategy for the development of stereoselective MCRs (Ruijter et al., 2011).

I.3.3.1. Biginelli reaction

Biginelli reaction or Biginelli condensation is a prominent MCR that offers a straightforward approach to produce multifunctionalized dihydropyrimidines and related heterocyclic compounds. The original reaction was reported for the first time by the Italian chemist Pietro Biginelli, who described the cyclocondensation reaction of ethyl acetoacetate, urea, and benzaldehyde, using ethanol as solvent in the presence of hydrochloric acid at reflux temperature (Kappe, 2003). As the Biginelli scaffold has shown a great value from the pharmaceutical point of view, over the years a plethora of different methods and conditions for the synthesis of DHPMs has been explored, involving namely the use of microwaves (Chaudhary et al., 2014), sonication (Li et al., 2003), ionic liquids (Dong et al., 2007), and a large panoply of different catalysts (Kolosov et al., 2009).

After the discovery of this reaction, it was largely ignored in the following decades; therefore, the pharmacological properties of this interesting heterocyclic scaffold remained relatively unexplored. However, since the early 1980s, the interest in DHPMs significantly increased due to their apparent structural similarity with the well-known dihydropyridine calcium channel modulators of the Hantzsch type. For this reason, it was then established that DHPMs exhibit a pharmacological profile similar to the attributed for the Hantzsch products as calcium channel modulators (Cernecka et al., 2012; Jetti et al., 2014; Singh et al., 2012). In addition, several members of this class of heterocycles have shown, for example, anticancer (Prashantha Kumar et al., 2009), antimicrobial (Hamdi et al., 2017), anti-inflammatory (Gireesh et al., 2013), antioxidant (Gangwar and Kasana, 2012) and anti-thyroid (Lacotte et al., 2013) properties.

An interesting aspect of the Biginelli products is the fact that these compounds have an inherent stereogenic centre and its configuration can influence the biological activity of the molecules (the individual enantiomers can exhibit different or even opposite pharmacological activities). For instance, the (*R)*-enantiomer of SQ 32926 **(14)** (Figure I.13), a calcium channel blocker, is more potent (> 400-fold) as antihypertensive in *in vitro* experiments than the corresponding (*S)*-enantiomer (Atwal et al., 1991). On the other hand, (*S*)-monastrol **(15)**

(Figure I.13) is 15-fold more potent in the Eg5 ATPase inhibition than (*R*)-monastrol (Mayer et al., 1999).

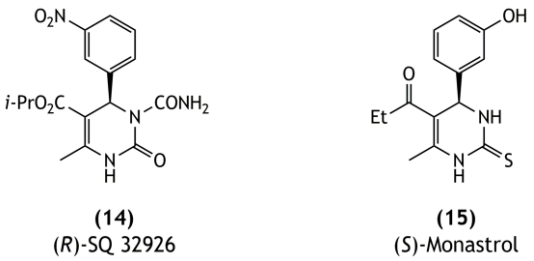

(14)
(*R*)-SQ 32926

(15)
(*S*)-Monastrol

Figure I.13 – Chemical structures of (*R*)-SQ 32926 **(14)** and (*S*)-monastrol **(15)** (Mayer et al., 1999; Schnell et al., 2000).

With the finding that individual enantiomers of the Biginelli adducts exhibit different pharmacological properties, the use of asymmetric synthetic approaches to obtain optically pure DHPMs has been a powerful tool with an effective impact on the Biginelli products and it has increased their potencies and applications as drug agents (Gong et al., 2007).

I.4. EVALUATION OF ANTIEPILEPTIC DRUG CANDIDATES

I.4.1. Preclinical evaluation of new antiepileptic drug candidates

The discovery and preclinical development of a new AED almost exclusively relied on the employment of animal models to establish anti-seizure efficacy and safety of compounds prior to first clinical trials. This approach has contributed to the development of numerous clinically effective AEDs. Indeed, animal models with a similar high predictive value do not exist for other CNS disorders, such as bipolar disorder or migraine (Löscher et al., 2013). On the other hand, new advances in *in vitro* and *in silico* methodologies for predicting pharmacokinetic properties and toxicity of drug candidates have served to significantly reduce the drug failure rate (Andrade et al., 2016). In this context, *in vitro* and *in silico* models can provide substantive information and, ideally, these data should be integrated with those obtained from *in vivo* tests. Additionally, in advanced phases of preclinical drug development, *in vitro*/*ex vivo* systems are also of high value to support mechanistic studies. Furthermore, nowadays, preclinical pharmacokinetic/pharmacodynamic modelling and simulation are also essential parts of any drug development programme (Löscher, 2016). For example, computational models for biopharmaceutical and ADME predictions could represent a starting point for further preclinical and clinical studies (Leucuta, 2014). Thus, research and preclinical studies using animal models in combination with *in vitro* assays and computer predictions is the best procedure to find the most promising molecules.

Considering the current state of the art, the use of whole-animal models of acute seizures and epilepsy is still essential in the early stages of discovery and preclinical development of novel AEDs. However, an important principle that should be always remembered is the fact that, in early studies of drug discovery and development, animal models provide data to mainly determine which compounds deserve to be developed.

I.4.1.1. Animal models

Since 1975, the NINDS has facilitated the development of novel chemical entities for the treatment of epilepsy disorders. Through the Anticonvulsant Screening Program (which recently was renamed as Epilepsy Therapy Screening Program) of the University of Utah, potential compounds undergo an initial identification, characterisation, and differentiation of anticonvulsant efficacy and toxicity using a battery of well-defined animal models. The screening protocol of this programme includes well-characterised models that might provide clinically relevant information (NINDS, 2016; Smith et al., 2007). Since its initiation, this programme has been upgraded and various additional models have been implemented apart from the well-established maximal electroshock seizure (MES) model and subcutaneous pentylenetetrazole (scPTZ) seizure model. The new recommended animal models to use in

the initial phases of the drug discovery and development process include the 6-Hz model and a chronic model of epilepsy (kindling seizure model), in order to identify potentially interesting and effective compounds that may be missed when only using the MES and scPTZ tests. Furthermore, the scPTZ test is being abandoned as an initial screening model because it has been suggested that this test did not correctly predict the effects of several AEDs, including lamotrigine and levetiracetam, which shall abolish the seizures provoked by PTZ (as they are indicated in absence seizures in humans, Table I.2) and also provided false positive data for other AEDs (e.g., tiagabine, vigabatrin). In addition to anticonvulsant evaluation, this programme also includes tests to detect "minimal neurological deficit" such as the rotarod test, which allows the calculation of the "protective (or therapeutic) index" [ratio between the median toxic dose (TD_{50}) and the median effective dose (ED_{50})] of the compounds (Löscher, 2016).

To be used with confidence, the animal models need to be systematically validated using the known clinically effective drugs (Kupferberg, 2001). The workflow that is currently proposed by NINDS (in PANAChE website) is illustrated in Figure I.14. The project of this thesis intended to accomplish the first studies of anticonvulsant evaluation and neurotoxicity (minimal motor impairment) that take place in the phase of "identification" of new AED candidates.

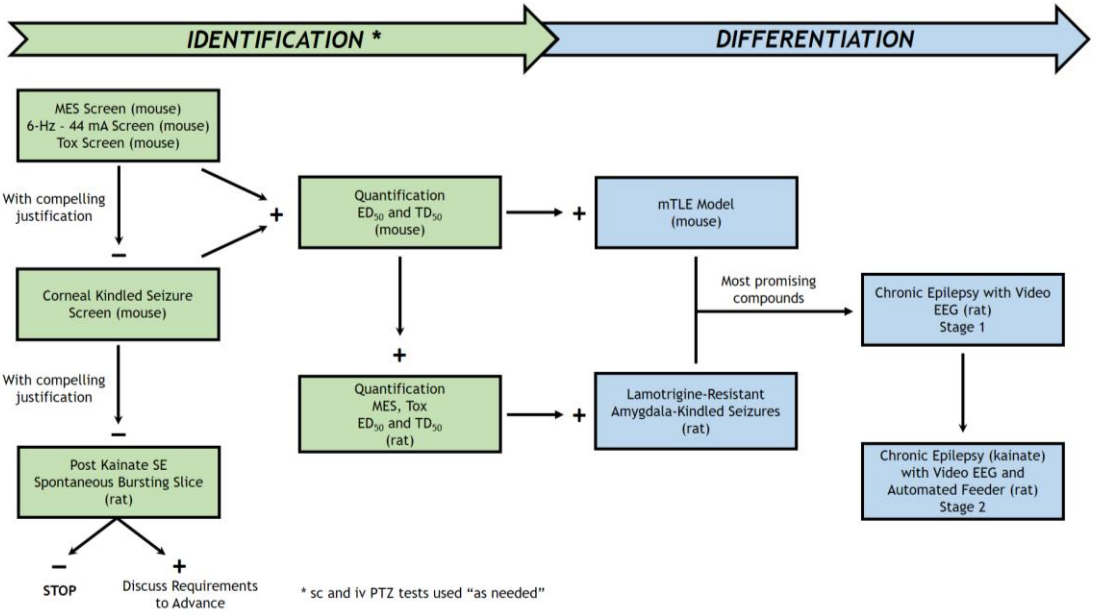

Figure I.14 – Workflow proposed in the Epilepsy Therapy Screening Program from National Institute of Neurological Disorders and Stroke to encourage and facilitate the discovery and development of antiepileptic drug candidates. Tox screen includes rotarod assessment (mouse) and minimal motor impairment assessment and/or automated locomotor activity assessment (rat); spontaneously bursting hippocampal slice is an *in vitro* model; and mTLE is a model of mesial temporal lobe epilepsy induced by focal chemoconvulsant injection. ED_{50}, median effective dose; EEG, electroencephalogram; iv, intravenous; MES, maximal electroshock seizure; PTZ, pentylenetetrazole; sc, subcutaneous; SE, *status epilepticus*; TD_{50}, median toxic dose assessed by motor impairment (PANACHE, 2017).

Whole-animal models only select compounds that are inherently anticonvulsants and able to access to the relevant brain targets. Novel chemical structures identified in screening animal models may act on a well-recognized target or by novel combinations of actions on more than one target (knowns or unknowns). Moreover, they can be considered non-mechanistic in nature (i.e. any biomolecule could, in principle, be detected as a target); thus, they are useful for determining whether a compound prevents seizure spread or raises seizure threshold, but they do not provide insight into the mechanism by which the compounds elicit their pharmacodynamic effects. Consequently, *in vivo* animal models offer an opportunity to uncover drugs that act in new ways and through new targets. These models have been efficiently used to identify new anticonvulsant compounds with clinical potential. Indeed, most of the currently approved AEDs (with their diverse and often distinctive clinical activities) would have not been identified if they had not exhibited activity in animal models.

I.4.1.1.1. Purposes and selection

According to Löscher (Löscher, 2011), during the discovery and development of new AEDs, animal models of seizures or epilepsy serve a variety of purposes:

a. Identification of novel AEDs (the main aim);
b. Characterisation of the spectrum of anticonvulsant activity of new AEDs (evaluation of possible specific efficacies of the compound against different types of seizures or epilepsy);
c. Investigation whether the novel drug has advantages towards clinically established AEDs for therapy of difficult-to-treat types of seizures or epilepsies, using specific models of AED-resistant seizures;
d. Evaluation whether preclinical efficacy of novel compounds changes during chronic administration;
e. Comparison of adverse effects of new AEDs in epileptic *versus* non-epileptic animals (study whether epileptogenesis alters the adverse effect potential of a given compound);
f. Estimation of effective plasma concentrations of new AEDs for first clinical trials;
g. Discovery of therapies that may prevent or modify the development of epilepsy after brain insults.

Additionally, animal models for seizures and epilepsy have played a fundamental role to understand the physiological and behavioural changes associated with human epilepsy, allowing the investigation of the mechanisms underlying the epileptogenesis and also giving information about normal brain function (Sarkisian, 2001).

Different options of animal models exist for the preclinical evaluation studies of AEDs candidates. The selection of the suitable animal models strongly depends on the intention of the study (not all animal models of seizures and/or epilepsy can be used for all of the above

described purposes) (Löscher, 2011). Animal models range in diversity from drosophila and zebrafish to nonhuman primates (Easter et al., 2009; Sarkisian, 2001). However, for practical reasons, rodents (rats, mice and Mongolian gerbils) are, by far, the most commonly used species in the discovery and development of new AEDs. Only one gender may be sufficient for a particular study (Simonato et al., 2014); however, gender differences are emerging amongst some types of epilepsies (e.g. epilepsy syndromes). Moreover, the age range varied according to the model (usually chronic models) because seizure susceptibility and manifestation of epilepsies in some cases are age-dependent. Other factors to be considered are the high mortality rates, variability between animals and the financial cost. A judgment needs to be made about what is acceptable in terms of type, duration, intensity and frequency of seizures, recovery time and the level of suffering following the initiation of seizures (Lidster et al., 2015). Finally, none of the approved AEDs required the presence of a second drug to confer seizure protection in such models, nor there are any known examples in which an approved AED is inactive unless a second, so-called helper AED, is present (Mintzer et al., 2015).

Generically, animal models have been categorized into two main categories: models of acute seizures (non-epileptic animals are induced to have a seizure) and models of chronic epilepsy (animals that have enhanced seizure susceptibility or spontaneous seizures) (Rogawski, 2006; Simonato et al., 2014). Innumerable models of epilepsy and epileptic seizures have been described. In Figure I.15 there is represented the chronological emergence of the main and more frequently used animal models. For practical reasons, these are also the models that are mainly focused in the next sections.

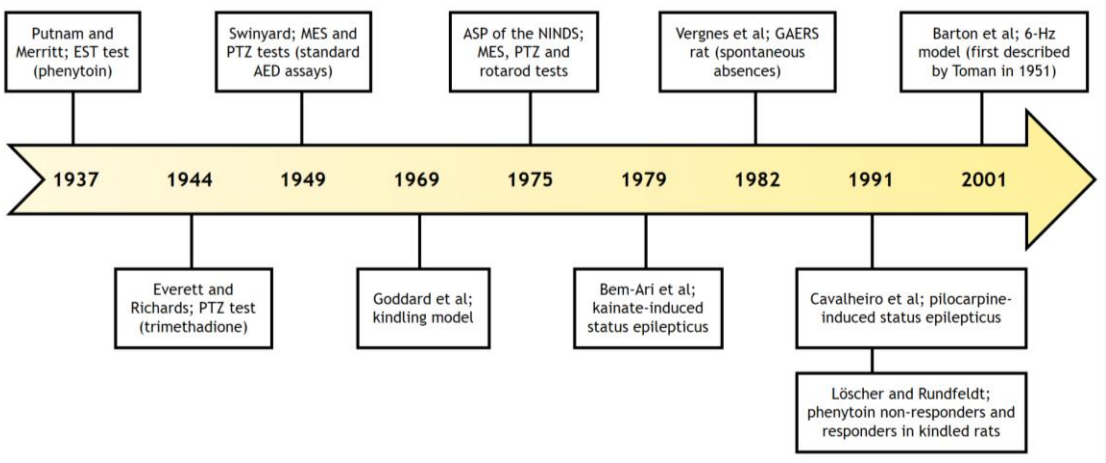

Figure I.15 – Milestones in the development of animal models for the discovery and development of new antiepileptic drugs. AED, antiepileptic drug; ASP, Anticonvulsant Screening Program; EST, electroshock threshold; GAERS, genetic absence epilepsy rat from Strasbourg; MES, maximal electroshock seizure; NINDS, National Institute of Neurological Disorders and Stroke; PTZ, pentylenetetrazole. Adapted from (Löscher et al., 2013).

I.4.1.1.2. Acute seizure models

In acute seizure models the seizures are induced in laboratory animals, usually rodents, mainly through the use of chemoconvulsants (chemical stimulation) or electrical stimulation (Simonato et al., 2014). These models are considered the ideal models for AED discovery because they allow the anticonvulsant screening of a large number of compounds, are easy to perform, time- and cost-efficient, and predictive of clinical activity (Löscher et al., 2013). The most representative acute seizure models are MES and scPTZ tests that have constituted, for several decades, the two key preclinical models for random anticonvulsant screening aiming the identification of new candidates to AEDs. Compounds that are active in one or both of these tests have generally shown efficacy in clinical trials, with exception of NMDA receptor antagonists, which are highly active in the MES test but have poor clinical efficacy (Rogawski, 2006).

Maximal electroshock seizure model

Despite the nearly 70 years of use and many criticisms, the MES test in rodents remains the *gold standard* in the search for new AEDs, particularly because it is well suited for anticonvulsant screening and is quite effective in identifying drugs that block tonic–clonic seizures in patients. The MES test has also repeatedly been proposed to identify drugs that are active against focal seizures in humans, but this test failed to detect several AEDs (e.g. levetiracetam, tiagabine and vigabatrin) that are effective against focal seizures in patients (Löscher, 2016). It is probably the best-validated preclinical model of seizures and permits the evaluation of the ability of a substance to prevent seizure spread through neural tissue. The test is easily conducted, presents low mortality and high reproducibility, requires a minimal investment in equipment and technical expertise, and is well standardized. Moreover, this model can provide insight into pharmacokinetic-pharmacodynamic relationship of potential new AEDs. In the traditional MES test, rodents receive an electrical stimulus of appropriate intensity, applied through corneal or auricular electrodes, to induce maximal seizures characterised by the tonic extension hind limbs. The electrical stimulus is about 5-10 times higher than the electrical seizure threshold of the animals in order to avoid bias in the induction of tonic seizures due to daily fluctuations in seizure threshold (Castel-Branco et al., 2009; Kandratavicius et al., 2014; Łukawski et al., 2016).

6-Hz model

The 6-Hz test in mice was first described more than 60 years ago. However, due to the lack of consistency with the clinical profile of known AEDs in the treatment of psychomotor seizures, it was subsequently abandoned. Fifty years later, Barton *et al*. re-evaluated the utility of the

6-Hz model as a potential screen for therapy-resistant epilepsy (Loscher, 2016). For this reason, this acute seizure model is detailed further ahead (section I.4.1.1.4).

Subcutaneous pentylenetetrazole test

The scPTZ test, also known as metrazole test, is a validated model of chemoconvulsant induced seizures for the early detection of compounds with anti-seizure activity, which is thought to be useful to identify drugs that block generalised non-convulsive seizures. However, the effectiveness of a compound against this seizure type needs to be checked in other models of non-convulsive seizures (e.g. genetic epilepsy models) because a number of AEDs that protect against non-convulsive seizures in people with epilepsy failed in the PTZ test (Łukawski et al., 2016). Once it is considered a GABA selective antagonist, *via* the blockade of $GABA_A$ receptor, it is thought that effective compounds in this test act through the GABAergic system (Rubio et al., 2010). In spite of the sc route is the most used, timed intravenous (iv) PTZ infusion is also used to determine seizure threshold, particularly when testing investigational drugs for proconvulsant activity during safety evaluation (Loscher, 2016).

Other seizure models

Although less used, there are other acute seizure models that can be used to evaluate the seizures suppression mediated by investigational compounds. Some of these examples are models of seizures induced by the administration of high-fixed doses of strychnine, bicuculline, camphor, NMDA, tetanus toxin, kainic acid, mercaptopropionic acid, picrotoxin, isoniazid, aminophylline or penicillin. However, none of these models are fully clinically validated (Kandratavicius et al., 2014; Kupferberg, 2001; Rubio et al., 2010). An important aspect is the fact that the models are not “static” but are highly dependent of the dose level and number of administrations, i.e. the repeated administration of some convulsants (e.g., PTZ, kainic acid, tetanus toxin and penicillin) in subconvulsant doses can result in chronic epilepsy models, as discussed below.

I.4.1.1.3. Chronic epilepsy models

Once the identification of the anticonvulsant efficacy of a compound is generally established using the standard acute seizure tests, a battery of other assays needs to be performed to characterise the anticonvulsant potential of the drug candidates. This allows to predict whether an active compound possesses a narrow or broad spectrum of activity and provides the sponsor with a sense of how the compound compares with prototype “marketed” drugs. Of the diversity of tests that one might elect, the kindling model is the only chronic model of epilepsy that has been routinely employed by most AED discovery programmes (Smith et al.,

2007). In general, chronic models of epilepsy are models of epileptogenesis with documented spontaneous seizures (acquired or genetic) in long-term video-EEG studies (Simonato et al., 2014). Thus, these models should better reflect the pathophysiology and phenomenology associated with human epilepsy. In addition to the discovery of new AEDs, these models are also very useful to understand the process of epileptogenesis and the progressive nature by which epilepsy is developed (Barker-Haliski et al., 2015).

Kindling model

Kindling model is a chronic model of epilepsy produced by repeated administration of an initially subconvulsive electrical or chemical stimulus (preferentially in limbic system, such as amygdala or hippocampus) that induces initially nonconvulsive epileptiform discharges, which gradually increase in duration, complexity and severity. Ultimately, it culminates in emergence of spontaneous seizures by the establishment of a permanent enhanced seizure susceptibility and other enduring brain alterations that are similar to those occurring in human temporal lobe epilepsy (Kupferberg, 2001; Löscher, 2016). The behavioural response in the kindling model is characterised into five progressive and cumulative behavioural states: facial movements such as blinking or mastication movements, oscillatory movements of the head, mioclonic movements of the forelimbs (first contralaterally, then bilaterally), erection of the body and standing on hinds legs, and finally generalised tonic-clonic seizures occur and there is a loss of posture (Rubio et al., 2010). This model possibly offers the best predictive model, predicting adequately the clinical utility of most AEDs, including tiagabine and vigabatrin, as well as the lack of clinical efficacy of NMDA antagonists (Smith et al., 2007).

Kainic acid and pilocarpine models

Kainic acid is an L-glutamate analogue, having potent epileptogenic and excitatory effect on rat cortical neurons. Its systemic or intracerebral administration produces an extensive brain damage by causing neuronal depolarization and recurrent seizures, usually secondarily generalised seizures. Kainic acid has the advantage of causing usually hippocampus-restricted injuries, unlike pilocarpine, which can also produce lesions in neocortical areas (Kandratavicius et al., 2014; Lévesque and Avoli, 2013; Rubio et al., 2010). As in human temporal lobe epilepsy extrahippocampal areas are also significantly compromised, the use of pilocarpine as chemoconvulsant can generate a useful model of epilepsy; pilocarpine is a muscarinic acetylcholine receptor agonist, which systemic or intracerebral injection induces seizures that build up progressively into a limbic *status epilepticus*. Structural damages and subsequent development of spontaneous recurrent seizures resemble those of human complex focal seizures (Curia et al., 2008; Kandratavicius et al., 2014; Rubio et al., 2010).

Genetic models

In addition to the models of acquired epilepsy, numerous genetic mouse models have been developed in recent years, recapitulating many of the phenotypic features of human genetic epilepsy. These models have not been widely used in the stage of AED discovery. However, they have provided a plenty of information regarding the pathophysiology of epilepsy at the molecular and genetic levels (Bialer and White, 2010). Examples of whole-animal models that have emerged from knowledge of human genetic mutations include:

- *Audiogenic seizure-prone mice*. When these animals are exposed to high-frequency and high-intensity sound, they exhibit wild running, followed by generalised clonic–tonic seizures. Despite the similarities among strains, behavioural features of audiogenic seizures are strain-specific, being the DBA/2J mice the most commonly used for anticonvulsant identification. Levetiracetam was discovered using this model and subsequently was found to be active in the 6-Hz and kindling models, but not in the traditional anticonvulsant screening models of acute seizures (MES and scPTZ) (Kupferberg, 2001; Rogawski, 2006);
- *Genetic absence epilepsy rat from Strasbourg and WAG/Rij*. These models present electrographic waves characteristic of seizures and a pharmacological profile consistent with generalised absence epilepsy, showing a good correlation with clinically effective drugs (Kupferberg, 2001; Simonato et al., 2014);
- *Genetically epilepsy-prone rats (GEPR)*. GEPR-3 and GEPR-9 differ primarily in the intensity of convulsions. The seizure pattern of the GEPR-3 consists of an initial running phase followed by clonic seizures, whereas the GEPR-9 exhibit a seizure pattern similar to the DBA/2J mice, characterised by a terminal, complete tonic phase. Both noradrenergic and serotonergic deficits appear to be important in the seizure aetiology of the GEPR (Kupferberg, 2001).

I.4.1.1.4. Animal models of pharmacoresistant seizures

Based on the operational definition of drug-resistant epilepsy, the term “pharmacoresistant” applied in the context of animal models is used to describe persistent seizure activity not responding or with very poor response to monotherapy with at least two AEDs at the maximum tolerated doses (Löscher, 2016). In recent years there have been described several animal models that display a seizure phenotype consistent with pharmacoresistant epilepsy. These whole-animal models tend to better mimic the human condition of the disorder (e.g., presence of responders and nonresponders) and, for instance, include the phenytoin-resistant kindled rat, the lamotrigine-resistant kindled rat, and the 6-Hz psychomotor seizure model of focal epilepsy (Smith et al., 2007). Some of these models have been of the utmost importance to elucidate potential mechanisms underlying the AED-resistance (Loscher, 2016).

6-Hz model

In the 6-Hz model, electrical stimulation by low-frequency (6-Hz) and long duration (3 s) is delivered through corneal electrodes, inducing seizures that are reminiscent of "psychomotor seizures" occurring in human limbic epilepsy. At 22 mA, this test did not discriminate between clinical classes of AEDs; however, increasing the current intensity by 50% (i.e., 32 mA) decreases the sensitivity of the 6-Hz seizure to phenytoin and lamotrigine and at a current intensity of 44 mA, only levetiracetam (at high doses) and valproate, display complete anticonvulsant protection (Löscher, 2011). Other clinically established AEDs (e.g. retigabine, phenobarbital, and brivaracetam) also potently suppress 6-Hz seizures induced by 44 mA, but there is no clinical evidence that these drugs are particularly effective in patients with drug-refractory focal seizures. In addition, the discrimination is strongly affected by the genetic background of mice (Loscher, 2016).

Lamotrigine- and phenytoin-resistant kindled rat models

In the amygdala-kindling model induced in male Sprague-Dawley rats was reported that early exposure to low doses of lamotrigine and further carbamazepine during the critical period of kindling acquisition may lead to pharmacoresistance. Lamotrigine-resistant kindled rats are also resistant to carbamazepine, phenytoin and topiramate, but not to valproate, felbamate and retigabine (Löscher, 2016; Löscher, 2011; Łukawski et al., 2016). On the other hand, levetiracetam is the only AED that is highly effective in phenytoin-resistant kindled rats, whereas all other AEDs are significantly less efficacious or not efficacious (Löscher et al., 2013).

I.4.1.1.5. Limitations of animal models

As previously stated, AED discovery programmes are based primarily on the use of animal models of seizures (e.g. MES and scPTZ) rather than models of epilepsy for initial candidate selection. This approach has been highly effective in identifying new AEDs and predicting clinical anticonvulsant activity. However, the value of acutely induced seizure models has been under intensive discussion. The fact that the AEDs discovered by MES and scPTZ models do not work in about 30-40% of epilepsy patients, suggests that these models lack sufficient predictability for pharmacoresistant seizures (Löscher and Schmidt, 2011). Indeed, one of the main limitations of these acute seizure models is the fact that they do not represent the development of epilepsy. Thus, the compounds identified using these classic models exert a seizure-suppressing effect but they do not affect or prevent the underlying epilepsy or associated comorbidities (Simonato et al., 2014). Additionally, it is thought that they fail the identification of compounds that act in mechanistically new ways and, as result, do not offer therapeutic advantages over the presently available AED agents. An example is levetiracetam

that is inactive both in the MES and scPTZ tests, but is effective in the 6-Hz and kindling models (Łukawski et al., 2016). The discovery of this AED also showed that novel drugs that are not effective in the MES test should not be immediately discarded because they may be effective in more sophisticated models (Loscher, 2016). Notwithstanding, the acute models also seem to uncover drugs with unique and unexpected clinical utilities. For example, while the older sodium channel blockers phenytoin and carbamazepine are inactive, and in some cases may worsen absence seizures and juvenile myoclonic epilepsy, lamotrigine surprisingly is effective for these epileptic disorders, what distinguishes lamotrigine from others sodium channel blockers AEDs (Rogawski, 2006).

However, due to the logistical problems that arise when large numbers of compounds are to be tested, the more laborious models of epilepsy such as kindling models are usually employed only at late stages of the process of preclinical drug development (Löscher and Schmidt, 2011). Chronic models are much more labour-intensive and require adequate facilities and resources, robust sample sizes, long periods of handling and observation, including after treatment washout, and extensive testing with continuous video-EEG and/or additional behavioural endpoints. Unfortunately, the development of similar reliable models in mice has proven difficult, mainly as a result of genetic interstrain and intrastrain differences in sensitivity to chemical or electrical induction of epilepsy. Although such differences may help to further explain the contribution of genetic factors to the pharmacology of seizure disorders, it is also true that there is a considerable risk of false-negative data when using certain strains of mice for preclinical testing (Simonato et al., 2012). Moreover, none of the emerging models of drug-resistant epilepsy has been properly validated for predicting clinical success in patients with pharmacoresistant epilepsy, remaining to be established whether the use of these models leads to the identification of more effective AEDs (Löscher et al., 2013). Moreover, taking into consideration the highly heterogeneous nature of seizure disorders, the complexity of the seizure phenotypes, and the syndromes involved, it is highly unlikely that a single animal model can always predict the full therapeutic potential of an AED candidate (Smith et al., 2007). In addition, no therapy was introduced into clinic solely on the basis of efficacy data achieved in a chronic model of epilepsy, which can be explained by the fast turnover of screening in the acute seizure models or due to constraints in the use of chronic models in drug discovery (Simonato et al., 2014).

Overall, it is expected that the acute seizure models will continue to be pivotal in the discovery of new AEDs. However, to achieve further progresses, the design and evaluation of novel AEDs candidates have to progressively include chronic models of epilepsy.

I.4.1.2. *In vitro models*

Ideally, one promising option in the discovery of new AEDs could be a multistep approach, in which putative drugs would be screened in *in vitro* assays (e.g. binding assays and electrophysiological techniques in brain slices preparations) before being tested in more expensive and time-consuming *in vivo* models (Easter et al., 2009; Simonato et al., 2013). However, currently, the available *in vitro* procedures are not likely to replace the screening assays in animal models. Firstly, these assays are limited to recognized targets; therefore, the possibility of serendipitously finding a novel mechanism of action or compounds that act by unknown mechanisms cannot occur (Kupferberg, 2001). In addition, many AEDs act on various molecular targets, which complicates the optimization process since stronger interactions with one target would have unpredictable effects on the others. Moreover, for ion channel targets, it is not possible to predict anticonvulsant activity simply on the basis of binding affinity or even with more complex studies; for instance, sodium channel blockers AEDs as phenytoin bind with relatively low affinity to sodium channels, whereas a very large number of drugs that does not have clinically useful anticonvulsant activity (e.g. tricyclic antidepressants) modulate these channels more potently than such AEDs. Thus, optimizing binding affinity usually is not employed to identify molecules with useful anticonvulsant properties (Rogawski, 2006). Additionally, the screening against protein targets is not likely to lead to clinically useful AEDs because *in vitro* assays cannot model the specific pharmacodynamic actions required for seizure protection, and do not predict with accuracy the bioavailability and brain accessibility (Kupferberg, 2001). Having defined a novel target on the basis of studies in animal models, it should theoretically be possible to use *in vitro* systems to optimize the activity of a lead compound and detect related chemical structures with anticonvulsant properties. However, as already mentioned, *in vitro* systems have only limited utility in AED discovery and it is always necessary to validate the compounds activity using animal models (Kupferberg, 2001; Rogawski, 2006).

Whereas the identification of AED candidates is mainly assessed using *in vivo* models, the *in vitro* methods can also be applied for both screening and mechanistic studies. As it is possible to use tissues from a vast array of animals, including humans, the flexibility to assess how drugs affect target systems in *in vitro* conditions sometimes allows the quick and rigorous obtainment of useful data about the investigated compound (Allen et al., 2005). Thus, exploitation of *in vitro* cell culture systems has proven to be valuable to study biological, physiological and pathological processes, but the *in vitro* models are subject to limitations, artefacts and misleading results when removed from physiological and dynamic *in vivo* environment. In fact, all cell, tissue, or organ cultures can be seen as minimalist approaches and there is a general agreement that no *in vitro* culture will ever completely represent whole animal experiments (Astashkina et al., 2012).

Regarding the epilepsy area, *in vitro* systems are commonly used in advanced stages of the drug development, particularly for mechanistic studies with the most promissory compounds previously identified in *in vivo* models. In this context, some examples of *in vitro* mechanistic assays reported in the literature are: sodium and calcium channel binding assays (Kamiński et al., 2016), inhibition of sodium uptake by rat cortical synaptosomes (Benes et al., 1999), inhibition of the GABA transporter subtypes mGAT1-mGAT4 (Kowalczyk et al., 2014) and inhibition of glutamate release (Ambrósio et al., 2001). Moreover, studies of toxicity in cell lines and *in vitro* pharmacokinetic assays (e.g. permeability studies and P-gp modulation) can and must be carried out during the evaluation of new AED candidates. These assays are better explored in the next sections.

I.4.1.2.1. Cytotoxicity assays

From the perspective of pharmaceutical drug development, cytotoxicity studies are intended to identify: safe concentrations and subsequent extrapolation to dose-escalation scheme in humans; potential target organs of toxicity and reversibility of toxicity; and parameters for clinical monitoring (Baumstark-Khan et al., 2010). For *in vitro* cell culture systems, a compound or treatment is considered to be cytotoxic if it interferes with cellular attachment, significantly alters morphology, adversely affects cell growth rate, or causes cell death (Niles et al., 2008). Depending on the research scopes and on the further aims that are expected to be met, cytotoxicity may or may not be an endpoint on its own. For instance, in studies trying to decipher the pharmacological activity of new compounds (i.e., for which no or low toxic effects are expected), toxicity towards *in vitro* cell cultures should be limited, notably in using proper concentrations and incubation times. On the other hand, in screening works for potential anticancer compounds, cytotoxicity should be sought at the lowest concentration possible (Bunel et al., 2014). Thus, the results of cytotoxicity screening assays will help to decide which compounds will proceed for further experiments.

In fact, cytotoxicity data is an important kind of information that can be obtained in early biological evaluation. An example is given by Ambrósio *et al*. (Ambrósio et al., 2000) who assessed the neuronal injury of eslicarbazepine acetate (formerly known as BIA 2-093) by using the 3-(4,5-dimethylthiazol-2-yl)-2,5-diphenyltetrazolium bromide (MTT) assay. This assay is currently the most commonly used method to test cell growth rate and cytotoxicity of a compound (Li et al., 2015). The MTT-based assay determines the ability of viable cells, with active mitochondria, to reduce the soluble tetrazolium salt into an insoluble dark purple formazan precipitate, which can in turn be dissolved for spectrophotometric assessment (Figure I.16) (Baumstark-Khan et al., 2010; Mosmann, 1983). The amount of crystals formed is considered to have a positive correlation to the number of viable cells and their activity, and consequently the measurement of the absorbance colorimetric value reflects the number of surviving cells and their metabolic activity (Li et al., 2015). This *in vitro* assay revolutionized

cell-based drug screening of cytotoxicity, namely because it can be adapted to HTS as enables miniaturization in several multi-well plate formats, involves a simplified sample processing and do not require radioisotopes. This allows that many compounds in several concentrations and combinations to be tested simultaneously using identical experimental conditions while consuming very small amount of cells and compounds. Moreover, the procedure does not require special qualifications or equipment (Hayon et al., 2003). The MTT assay is extremely well characterised and referenced to this day in the literature, and is often considered a *gold standard* with which that new viability/cytotoxicity assay methods are compared (Niles et al., 2008).

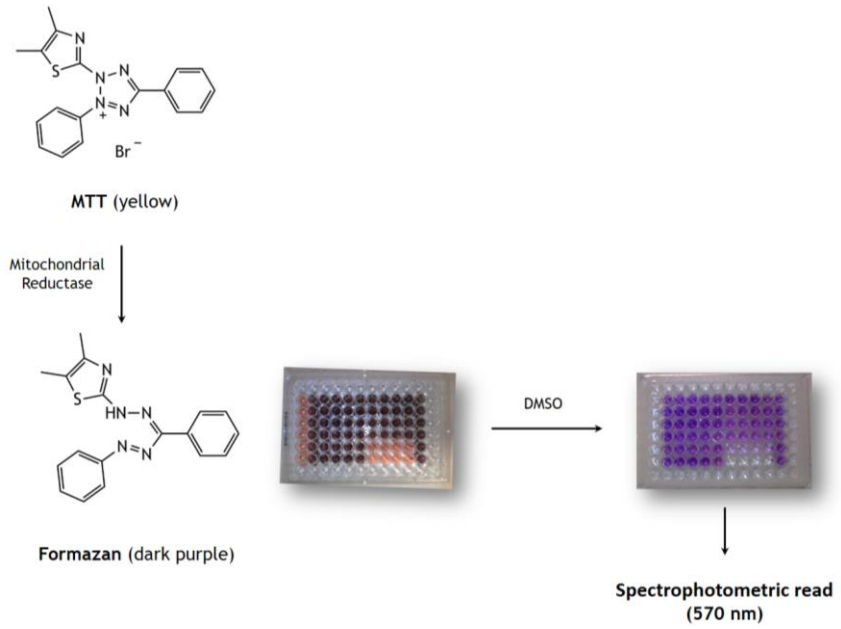

Figure I.16 – Conversion of yellow 3-(4,5-dimethylthiazol-2-yl)-2,5-diphenyltetrazolium bromide (MTT) to dark purple formazan by mitochondrial reductase. Images collected from an experimental MTT assay using Caco-2 cells.

Despite the above-mentioned advantages, this popular assay also has limitations. For example, a decrease in the concentration of D-glucose, NADH or NADPH in culture medium may be accompanied by a decrease in MTT-formazan production. Furthermore, in cells undergoing apoptosis, there may be some MTT reduction at early stages of apoptosis since the mitochondria remain almost intact. Moreover, some compounds might exert different effects on cell metabolism which could result in undesirable changes in mitochondrial activity, influencing the results (Hayon et al., 2003).

I.4.1.2.2. Pharmacokinetic properties: screening assays

Pharmacokinetic features should always be included as a part of the screening process in the selection of drug candidates, since poor pharmacokinetic properties is considered one of the main causes of compound failure in drug development programmes (Page, 2016). In fact, many highly potent lead compounds with optimized pharmacodynamic properties produced through pharmaceutical research and development strategies, present weak solubility and low bioavailability because of their relatively suboptimal intrinsic biopharmaceutical properties (Leucuta, 2014).

In this context, the evaluation of intestinal absorption should be included in the early screening of drug candidates due to their great impact on bioavailability and potential risks of DDI (Alqahtani et al., 2013; Page, 2016). Also the crossing of the BBB is a crucial parameter of all drug candidates whether are designed or not to act in the CNS. Here, one of the most known drug efflux transporter is P-gp, which is recognized to limit the intracellular levels of drugs and toxic substances (Alqahtani et al., 2013). Due to the importance of this thematic in the drug development process, it is deeper explored in the next sections.

I.4.1.2.2.1. Permeability assays

The oral route is the most common route of delivering drugs to patients, allowing self-administration and enhancing the chances of good compliance. Thus, although other routes of administration (e.g. iv, inhalation, intramuscular) are important, the design of drugs capable of being administered orally remains the focus of the majority of small molecule drug discovery projects (Page, 2016).

Drug candidates must fulfil several physicochemical properties in order to be successful candidates for oral administration. The intestinal absorption process is a combination of multiple events that are governed by many factors, which can be divided into three major groups: physicochemical properties of the drug (e.g. solubility, lipophilicity, pKa and particle size); physiological factors (e.g. gastrointestinal pH, gastric emptying, small intestinal transit time and absorption mechanism); and dosage form properties (e.g. solution, capsule, tablet and suspension) (Zakeri-Milani and Valizadeh, 2014).

After oral drug intake, the solid dosage forms undergo dissolution, releasing the drug and allowing its solubilisation, which makes it ready for absorption across the intestinal wall formed by enterocytes that control nutrients and drugs transport. Several transport mechanisms are involved in drugs absorption through enterocytes via active and/or passive processes (Alqahtani et al., 2013). Particularly for lipophilic compounds, transporters are thought to play a limited role in absorption because the passive transcellular diffusion is generally high across the biomembrane barriers. Conversely, for hydrophilic compounds,

transport typically occurs by the passive paracellular diffusion for low molecular weight compounds or transcellularly via carrier-mediated processes (Feng et al., 2014).

Due to the fact that small intestine is extensively involved in drug transport, metabolism and toxicity after oral administration, the preclinical investigation of intestinal absorption is required in this context. Nowadays huge amount of research works is directed toward modifying physicochemical properties of drugs to increase their gastrointestinal absorption (Zakeri-Milani and Valizadeh, 2014). In fact, candidates with poor biopharmaceutical and pharmacokinetic properties tend to take more time and efforts to progress through development, and most likely may lead to safety and efficacy failures (Kostewicz et al., 2014). Moreover, a detailed knowledge about drug candidates and their interaction with physiological barriers would also aid in optimizing drug's efficacy and in avoiding adverse effects (Alqahtani et al., 2013).

In addition to intestinal permeability, the brain penetration of drug candidates is another important kinetic aspect that deserves to be early assessed. The BBB is a dynamic interface, which displays a strong regulatory control over the influx and efflux of molecules between the brain and the bloodstream (Banerjee et al., 2016). The BBB is formed by brain capillary endothelial cells, which are characterised by highly developed tight junctions between adjacent cells and a paucity of fenestra and pinocytic vesicles (Kikuchi et al., 2013). Similarly to intestinal absorption, molecules can reach the CNS by two different pathways: the paracellular or the transcellular pathway. The first consists in a diffusion process between two endothelial cells through the tight junctions and is limited to small hydrophilic molecules. However, due to the presence of tight junctions, this route is extremely limited and nearly non-existent at the BBB, although under some pathological conditions tight junctions and adherens junctions between endothelial cells may be altered. On the other hand, molecules reaching the CNS via the transcellular pathway can diffuse passively, can be actively transported by specific transporters or can undergo endocytosis (Passeleu-Le Bourdonnec et al., 2013) (Figure I.17). Therefore, the transcellular route is the major pathway for the exchange of compounds between the two compartments (Kikuchi et al., 2013).

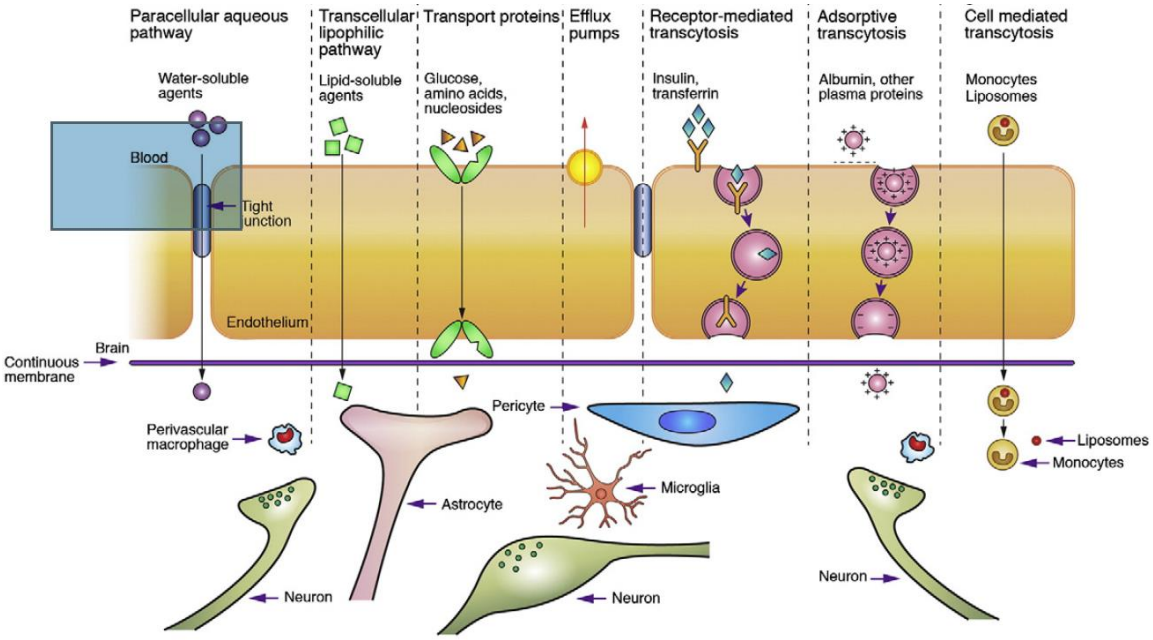

Figure I.17 – Schematic representation of transport routes across the blood–brain barrier (Chen and Liu, 2012).

The permeation of drugs through the BBB is also subject to strong selection depending on the physicochemical properties of the compound and/or their affinity to specific transporters (efflux or influx transporters) that are present in the cellular space. Hence, drug molecules are subject to varying degrees of CNS restriction, presenting both challenges and opportunities to drug discovery projects. On the one hand, if pharmacological activity in the CNS is required, considerable drug design efforts might be applied to ensure that the brain exposure to drugs is achieved at sufficient concentrations to engage with the pharmacological target and evoke the intended therapeutic response. On the other hand, when a drug target is located peripherally, the required systemic exposure may result in CNS concentrations high enough to engage with receptors in the brain other than those targeted (off-target), leading to undesirable toxicity (Bagal and Bungay, 2014). Thus, it is important to evaluate the drug distribution to CNS of any new molecular entity, regardless of its therapeutic area (Kikuchi et al., 2013).

I.4.1.2.2.2. Drug efflux transport: the role of P-glycoprotein

The bioavailability of a wide variety of compounds, including endogenous substances and xenobiotics, is dependent of the influx and the efflux transporters that facilitate their movement across membranes. These transporters are important to maintain cellular homeostasis and also to detoxify potentially toxic substances. There are numerous classes of efflux transporters, each with different substrate specificity, affinity and capacity, as well as specific tissue and cellular expression patterns. Among them, the ABC transporters are the

most extensively studied. The ABC transporters use energy from ATP hydrolysis to move their substrates across biological membranes against their concentration gradients, thereby limiting their cellular accumulation. These proteins pump substrates in a single direction, typically out of the cytoplasm and cellular organelles (Silva et al., 2015).

P-gp, a product of the *ABCB1* (also known as multidrug resistance 1; *MDR1*) gene, is a glycosylated membrane protein of 170 kDa that is broadly expressed, but particularly in the luminal membrane of the small intestine and BBB, and in the apical membranes of excretory cells such as hepatocytes and kidney proximal tubule epithelial cells (Giacomini et al., 2010; Hitchcock, 2012). P-gp is a highly permissive transporter, recognizing and effluxing a vast diversity of small molecules and peptides, which are chemically, structurally and pharmacologically unrelated. They include natural compounds, chemotherapeutic drugs, calcium channel blockers, steroids, linear and cyclic peptides, fluorescent dyes and pesticides, among many others. Most of these substrates are weakly amphipathic and relatively hydrophobic, often containing aromatic rings and a positively charged nitrogen atom (Silva et al., 2015).

P-gp was originally identified as a key factor for multidrug resistance in treatment of certain cancers, but its constitutive expression in many normal tissues also demonstrates its protective role against xenobiotics/toxins in limiting drug absorption, determining pharmacokinetic behaviours, and potentially impacting pharmacodynamic and toxicity. In addition, interactions of drugs with P-gp have received attention for facilitating or complicating DDI and their role in adverse drug events and interpatient variability. Moreover, several single nucleotide polymorphisms for P-gp have been documented and shown to influence the pharmacokinetics. The impact of P-gp–mediated drug efflux in oral drug absorption is not likely to be quantitatively important unless it is in combination with low dose, low aqueous solubility, slow passive diffusion, and/or marked first-pass mucosal metabolism. However, compounds with CNS targets are often quantitatively influenced by P-gp-mediated efflux because the exposure to free drug concentrations in plasma is typically undersaturated relative to efflux pump activity, including those predicted to have brain accumulation on the basis of their physicochemical properties such as lipophilicity (DeGorter et al., 2012; Hitchcock, 2012; Raub, 2006). The level of expression and functionality of P-gp can be modulated by inhibition and induction, which can affect the pharmacokinetics, efficacy, safety or tissue levels of P-gp substrates (Giacomini et al., 2010).

In addition to P-gp role in ADME properties of the drugs, the overexpression of multidrug transporters, primarily P-gp, is a plausible hypothesis to explain multidrug resistance in epilepsy. In fact, since AEDs must traverse the BBB to enter the brain and exert their desired effects, the overexpression of multidrug transporters in the endothelial cells of the BBB may contribute to drug resistance. Furthermore, it has been also demonstrated that the P-gp expression is higher in drug-resistant than in drug-responsive patients (Zhang et al., 2012). This overexpression may be the consequence of genetic variation, for example. In this

context, genetic polymorphisms may explain why different patients with the same type of epilepsy may have different response to AEDs: as the drug efflux transporter P-gp is highly expressed at BBB, genetic variation in its expression or functionality could directly affect brain uptake and extrusion of AEDs. However, there is still substantial controversy whether polymorphisms in the *ABCB1* gene encoding P-gp could influence drug-response and seizure frequency (Aronica et al., 2012; Stępień et al., 2012). Moreover, several studies have investigated other possible mechanisms underlying the upregulation of efflux transporters such as P-gp in the brain. These studies revealed a complex regulation that could involve inflammation, oxidative stress, ligand-activated nuclear receptors, ß-amyloid, glutamate and components of the innate immune response (Aronica et al., 2012).

The development of novel strategies to overcome transporter-mediated resistance in epilepsy has been considered based on the previous experience with targeting drug efflux of cytostatic drugs in cancer therapy. Thus, experimental data confirmed that inhibition of P-gp can improve AED efficacy and help to overcome drug-resistance (Potschka, 2012).

I.4.1.3. *In silico* models

In recent decades, *in silico* modelling has emerged as a tool for rational drug design and has received considerable attention from pharmaceutical scientists (Garro Martinez et al., 2015; Kuhlmann et al., 2015; Raies and Bajic, 2016; Zanni et al., 2015). Thus, the '*in silico*' term defines the experimentation performed in computers, which use information for the creation of computational models or simulations that can be used to make predictions, suggest hypotheses, and ultimately provide discoveries or advances in medicine and therapeutics (Andrade et al., 2016). The high-throughput and low-cost of these models allow a more streamlined drug development process in which the identification of hits or their structural optimization can be guided based on a parallel investigation of bioavailability, safety and activity (Wang et al., 2015). Indeed, the computational approaches have application in all stages in the discovery and development pipeline: target identification, lead discovery, lead optimization, preclinical or clinical trials but also other objectives like synthesis route prediction and simulation of cellular or organ complex systems (Leucuta, 2014).

An important aspect to mention is the fact that while computational models are presently used in virtually all fields of drug discovery, computational approaches for the screening or design of novel AEDs have been underexplored in comparison with other therapeutic areas. This may be due to a persistent and major obstacle to apply structure-based approaches in the field of AED development: most validated molecular targets for AEDs are either voltage- or ligand-based ion channels whose structure has not been experimentally solved yet, which forces drug designers in the epilepsy field to resort to homology modelling or ligand-based approximations. In addition, as aforementioned, the most AEDs are multi-target agents. In this context, it is expected that the application of *in silico* screening models to identify this

type of molecules yields lower hit rates than virtual screening campaigns oriented to single-target drug candidates (Talevi, 2016).

At present, *in silico* modelling is based on experimental training sets (Elder and Holm, 2013). It is recommended to consider *in vitro* biological data only, since *in vivo* data reflects a number of parallel processes, such as transport, binding to multiple targets, biotransformation and bioactivation. However, this approach could be excessively reductionist when dealing with complex disorders such as epilepsy. Thus, very commonly, biological data obtained from phenotypic models are used to build QSAR models. Indeed, on the basis of already alleged advantages of multi-target ligands over single-target agents against epilepsy, building predictive models from biological responses obtained in phenotypic screening might be the best choice to obtain novel AEDs (Talevi, 2016).

Other type of studies including *in silico* models are directed to early predict absorption, distribution, metabolism, excretion and toxicity (ADMET) properties for a broad number of drug candidates. In fact, it is impractical and not rational to perform intricate and costly procedures to experimentally assess the ADMET properties (*in vitro* and *in vivo* experiments) of a large number of compounds. The establishment of high-quality *in silico* ADMET models permits the parallel optimization of compound efficacy and druggability properties, which is expected to improve not only the overall quality of drug candidates and therefore the probability of their success, but also to detect and eliminate, at an early stage of drug discovery, compounds with inappropriate ADMET properties to avoid financial burden (Mishra, 2011; Wang et al., 2015). The relationships between important ADMET properties and molecular structures have been used to develop *in silico* models in order to enable the early estimation of several biopharmaceutical and ADMET properties using molecular descriptors. In fact, the application of informatics to anticipate pharmacokinetics and toxicity can provide a general guidance, but it is also worthy to note that there is still a long way to go before use these informatics tools without the need to perform nonclinical experimental procedures.

I.5. AIMS

I.5.1. Aims of this thesis

The pharmacological therapy has been, and is likely to remain, the mainstay of treatment for the epileptic patients. A large number of new AEDs was introduced into the market in the last years; however, they did not have shown significant advantages of efficacy in comparison with the older AEDs that continue to be used in the clinic practice. Hence, none of the current AEDs, including those that act on newly identified targets, can be considered a "magic bullet" that cures patients with epilepsy. In this context, the main goal of the present work was the discovery of new lead compounds with anticonvulsant properties that should be developed and elected for further development.

To this end, the following specific objectives were outlined for the implementation of this doctoral work:

- *Design, synthesis, purification and structural characterisation of new candidates to AEDs based on the structure of lamotrigine*. Taking into account several factors, such as the basic structure of DHPMs and 3,4-dihydropyrimidin-2(1*H*)-thiones (DHPMts), the advantages of MCRs and the interesting data on the bioactivity of Biginelli products, the chemical synthesis proposed in this project aimed the discovery of potential anticonvulsant molecules among the class of DHPM(t)s. Specifically, it involved the synthesis and further characterisation of several products through a one-pot Biginelli reaction, with focus on halogenated molecules due to their structural similarity with lamotrigine (Figure I.18).

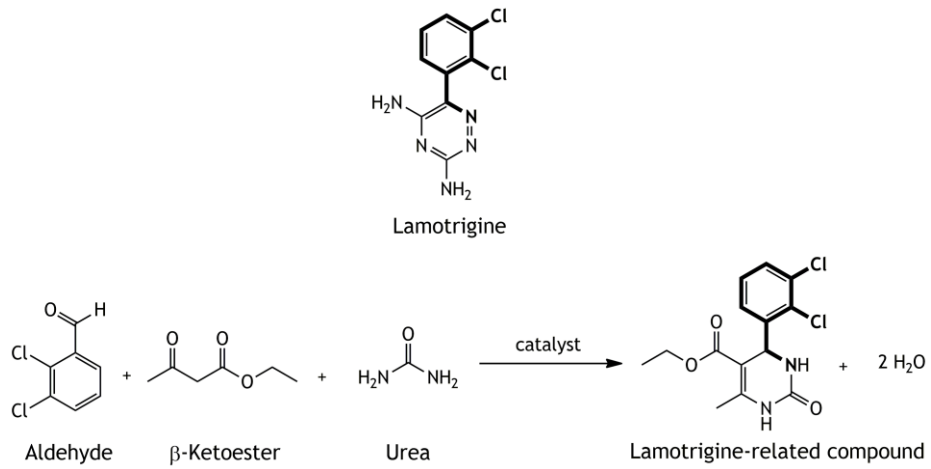

Figure I.18 - Chemical structure of lamotrigine and a schematic example of a Biginelli reaction using 2,4-dichlorobenzaldehyde, ethyl acetoacetate and urea as reagents.

- *In vivo screening of anticonvulsant activity and neurotoxicity in rodents*. Previously to the *in vivo* evaluation of the synthesized compounds, a set of drug vehicle was experimentally studied in order to select the most suitable one. Afterwards, the initial screening of the anticonvulsant activity of the compounds, administered by intraperitoneal (ip) route, was performed in acute models of seizures (MES and scPTZ) induced in mice. Simultaneously, the motor impairment (as a surrogate of minimal neurological deficit) was also assessed in mice through the rotarod performance test. The second stage of evaluation of the anticonvulsant potential was carried out in rats after oral administration of selected promising compounds.
- *In vitro screening of cytotoxicity of the synthesized compounds*. Since the toxicity assessment is an important aspect to be considered as early as possible, this work also aimed to evaluate the cytotoxicity of the synthesized compounds in *in vitro* conditions, through the well-established MTT assay. The cell lines were chosen according to their importance for the development of AED candidates and consisted of neuronal (N27), hepatic (HepaRG) and intestinal (Caco-2) cell lines; in addition, normal dermal fibroblasts (NHDF) were also used for the evaluation of cytotoxicity.
- *In vitro evaluation of pharmacokinetic properties*. Apart from studies of anticonvulsant efficacy and toxicity, the early assessment of the pharmacokinetic properties of new drug candidates is a key part of any rational strategy to support the continuous structural optimization and decision-making process. Considering the relevance of the intestinal permeability and BBB penetration of the AED candidates, the ability of the synthesized compounds to permeate the intestinal membrane and the BBB was investigated and predicted using validated PAMPA assays. Moreover, due to the impact of P-gp either in the determination of the ADME profile of the compounds or its possible role in drug-resistant epilepsy, the study of the modulation of P-gp by DHPM(t)s was also carried out in a suitable cell-based screening model.
- *In silico predictions of ADMET properties*. The drugabillity of the synthesized molecules is an important aspect to consider since the early stages of the drug discovery process. Thus, a set of physicochemical, pharmacokinetic and toxicity parameters of the DHPM(t)s in investigation was also estimated using a predictive computational tool in order to better understand the ADMET properties of the target compounds.

CHAPTER II

DESIGN AND CHEMICAL SYNTHESIS

II.1. Introduction

As previously referred, a MCR is generally defined as the process in which three or more reactants are combined in a single step to form a product that incorporates structural characteristics of each reagent and can allow the synthesis of small drug-like molecules with several degrees of structural diversity (Ganem, 2009). MCRs can represent a form of combinatorial chemistry and diversity-oriented synthesis, and their interest has increased in the development of modern synthetic methodology in drug discovery research. MCRs offer simplicity, economical advantages and can enable the synthesis of a wide amount of molecules, which generally are purer than the final products from multi-step reactions (Biggs-Houck et al., 2010; Hulme and Gore, 2003).

One of the most famous MCR is the Biginelli reaction that has been applied to synthesize multiple bioactive molecules during drug discovery programmes (Rashid et al., 2013; Suresh and Sandhu, 2012). Although the first reaction of this cyclocondensation process typically involved a ß-ketoester, an aromatic aldehyde and urea, the scope of this heterocycle synthesis has been considerably extended by variation of all the three constituents, allowing the access to a large number of pyrimidine derivatives (Kappe, 2003). The aldehyde is the component that can be varied to the largest extent. In general, the most used are the aromatic aldehydes, which can be substituted in the *o*-, *m*- or *p*-positions with either electron-withdrawing or electron-donating atoms (Litvić et al., 2010). However different aldehydes can also be used such as aliphatic aldehydes (Jenner, 2004) and bisaldehydes (Azizian et al., 2010), and interesting products containing a sugar-like moiety can also be obtained (Ali, 2013). Regarding the ß-ketoester, traditionally, simple alkyl acetoacetates are employed, but different ketones were also used to prepare 5-unsubstituted DHPMs derivatives (Wang et al., 2004). Other examples are benzyl esters (Desai et al., 2006), acetophenone (Liang et al., 2007), cyclic or bicyclic structures (Sabitha et al., 2003), α-cyanoketones (Val et al., 2013), and primary, secondary and tertiary acetoacetamides (Stadler and Kappe, 2001). Finally, urea is the component in the Biginelli reaction with more restrictions in terms of structural diversity. Thiourea and substituted thioureas follow the same general rules of ureas (Quan et al., 2009), leading to the production of DHPMts. Simple monosubstituted alkyl ureas are also described (Jenner, 2004) as well as reactions using guanidine (Ahmed et al., 2009).

Over the years, the possible mechanism of the reaction was explored and it could proceed in very different ways as described in the article published by Suresh and Sandhu (Suresh and Sandhu, 2012). However, the most acceptable mechanism describes the initiation of the condensation of the aldehyde with urea or thiourea in the presence of the catalyst, generating an activated *N*-acyliminium, which is subsequently attacked by acetoacetate *via* the Mannich reaction to generate the reactive intermediate. After, this intermediate cyclizes to afford the DHPMs, with the concomitant release of water (Figure II.1) (Gong et al., 2007).

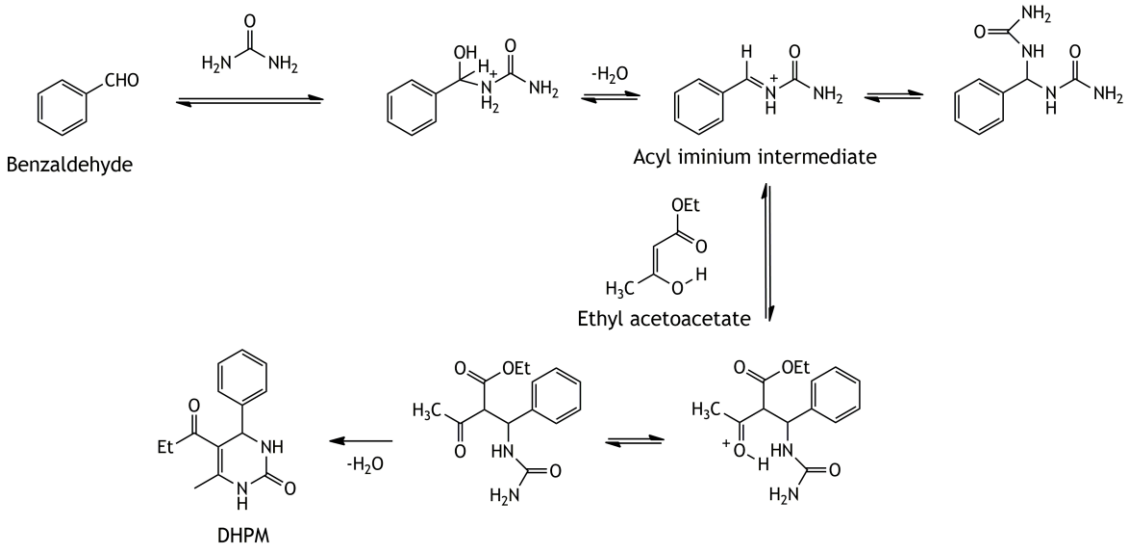

Figure II.1 - Formation of 3,4-dihydropyrimidinone (DHPM) via the proposed iminium-based mechanism (Suresh and Sandhu, 2012).

DHPM(t)s and their derivatives have attracted considerable attention in organic and medicinal chemistry because they display several pharmacological and therapeutic properties (De Fátima et al., 2015). For this reason, many improved procedures with new catalysts and experimental conditions have been reported in the literature (Kolosov et al., 2009).

Taking advantage of this prominent MCR, in this chapter is reported the synthesis of a set of DHPM(t)s, which were posteriorly subjected to pharmacological evaluation.

II.2. Experimental section

II.2.1. General remarks

The reagents urea, thiourea, benzaldehyde, *p*-tolualdehyde, *p*-nitrobenzaldehyde, 2,4-dichlorobenzaldehyde, 2,3-difluorobenzaldehyde, 5-methylfuraldehyde, 3-pyridinealdehyde, 5-chloro-2-furaldehyde, 2-thiophenaldehyde, anhydrous sodium sulphate and zirconium tetrachloride ($ZrCl_4$) were purchased from Acros Organics (New Jersey, USA); ethyl acetoacetate, methyl acetoacetate, acetylacetone and anisaldehyde were acquired from Merck (Hohenbrunn, Germany); 2,3-dichlorobenzaldehyde, furaldehyde and bismuth (III) nitrate pentahydrate [$Bi(NO_3)_3.5H_2O$] were purchased from Sigma-Aldrich (St. Louis, MO, USA). The ethanol 99.9% was purchased from Manuel Vieira & C^a (Torres Novas, Portugal); ethyl acetate and hydrochloric acid were acquired from Fisher Scientific (New Hampshire, USA); sodium hydroxide was purchased from Vencilab (Vila Nova de Gaia, Portugal); 5-chloro-2-thiophenaldehyde was acquired from Maybridge (Altrincham, United Kingdom) and hexa

deuterated dimethyl sulfoxide (DMSO-d_6) was purchased from Armar Chemicals (Leipzig, Germany). The evaporation was carried out in a rotavapor (Büchi, Switzerland). Infrared (IR) spectra were collected on a Thermoscientific Nicolet iS10: smart iTR, equipped with a diamond ATR crystal. For ATR data acquisition, a sample of the solid compound was placed onto the crystal and the spectrum was recorded. An air spectrum was used as a reference in absorbance calculations. The sample spectra were collected at room temperature in the 4000-400 cm^{-1} range by averaging 16 scans at a spectral resolution of 2 cm^{-1}. Nuclear magnetic resonance (NMR) spectra (^{1}H-NMR and ^{13}C-NMR) were acquired on a Bruker Avance 400 MHz spectrometer and were processed with the software TOPSPIN 3.1 (Bruker, Fitchburg, WI, USA). DMSO-d_6 was used as solvent. Chemical shifts are reported in parts per million (ppm) relative to deuterated solvent as an internal standard. Coupling constants (*J* values) are reported in hertz (Hz) and splitting multiplicities are described as s=singlet; brs=broad singlet; d=doublet; dd=double doublet; t=triplet; q=quartet; dq=double quartet and m=multiplet. High resolution mass spectrometry (HRMS) spectra were performed by the microanalysis service on a QSTAR XL instrument (Salamanca, Spain).

II.2.2. Chemical synthesis

General procedure: To a mixture of an aldehyde (1 mmol), a ß-ketoester/acetylacetone (1 mmol) and urea/thiourea (1.3 mmol) was added $Bi(NO_3)_3.5H_2O$ (10 mol%) for urea series and $ZrCl_4$ (5 mol%) for thiourea series. The reaction was heated with stirring at 70 ºC in a preheated oil bath for the appropriate time (Tables II.1, II.2 and II.3). The reaction was considered completed when solidified and, after being cooled to room temperature, was poured onto cold water and stirred from 20-30 min. The solid separated was filtered under suction, washed with ice-cold water, dried and then recrystallized from ethanol 99.9% to afford the pure products.

Alternative procedure for chlorinated compounds for urea series: A mixture containing the aldehyde (1 mmol), the ß-ketoester/acetylacetone (1 mmol), urea (1.3 mmol) and $ZrCl_4$ (10 mol%) in ethanol (5 mL) was refluxed for the appropriate time (Appendix A). After completion of the reaction, as monitored by thin layer chromatography, the solvent was removed under reduced pressure to obtain a solid, which was washed with cold water and recrystallized from ethanol 99.9% to afford the pure products.

*Procedure for the synthesis of **MM 95**:* To a mixture of 3-pyridinealdehyde (1 mmol), ethyl acetoacetate (1 mmol) and urea (1.3 mmol) was added $Bi(NO_3)_3.5H_2O$ (10 mol%). The reaction was heated with stirring at 70 ºC in a preheated oil bath for 46 h. The reaction was considered completed when the mixture solidified and, after being cooled to room temperature, was poured onto cold water with 5% hydrochloric acid until complete dissolution. Then, the resulting solution was alkalinized to basic pH using sodium hydroxide, extracted with ethyl acetate (4 x 50 mL), dried with anhydrous sodium sulphate and

evaporated under vacuum to give the crude product. The purification was done by recrystallization using ethanol 99.9%. Then, the product was characterised by IR and ^{1}H- and ^{13}C-NMR.

II.2.2.1. Structural characterisation

All compounds were structurally characterised by IR, ^{1}H- and ^{13}C-NMR and additional HRMS data were also acquired for the new compounds. The compounds were identified accordingly to the order that they were synthesized. Further, they were organized in accordance with their molecular functional groups into the two series (urea and thiourea series). This order is used throughout the thesis.

Urea series:

Ethyl 6-methyl-2-oxo-4-phenyl-1,2,3,4-tetrahydropyrimidine-5-carboxylate (compound **MM 18**). White solid, yield: 81%, IR (υ_{max}/cm^{-1}): 3233, 3111, 2978, 1697, 1642, 1217, 1086; ^{1}H-NMR (400 MHz, DMSO-d_6) δ: 1.09 (t, 3H, *J* = 7.05 Hz, OCH_2CH_3), 2.24 (s, 3H, CH_3), 3.98 (q, 2H, *J* = 7.05 Hz, OCH_2), 5.14 (d, 1H, *J* = 3.04 Hz, CH), 7.20-7.36 (m, 5H, ArH), 7.73 (brs, 1H, NH), 9.18 (brs, 1H, NH); ^{13}C-NMR (100 MHz, DMSO-d_6) δ: 14.06, 17.77, 53.95, 59.17, 99.25, 126.23, 127.25, 128.38, 144.86, 148.35, 152.12, 165.33.

Methyl 6-methyl-2-oxo-4-phenyl-1,2,3,4-tetrahydropyrimidine-5-carboxylate (compound **MM 72**). White solid, yield: 80%, IR (υ_{max}/cm^{-1}): 3328, 3213, 3103, 1692, 1664, 1412, 1236, 1092; ^{1}H-NMR (400 MHz, DMSO-d_6) δ: 2.25 (s, 3H, CH_3), 3.53 (s, 3H, CH_3OCO), 5.14 (d, 1H, *J* = 3.35 Hz, CH), 7.21-7.35 (m, 5H, ArH), 7.75 (brs, 1H, NH), 9.22 (brs, 1H, NH); ^{13}C-NMR (100 MHz, DMSO-d_6) δ: 17.83, 50.78, 53.80, 99.00, 126.17, 127.29, 128.45, 144.67, 148.67, 152.18, 165.84.

5-Acetyl-6-methyl-4-phenyl-3,4-dihydropyrimidin-2(1*H*)-one (compound **MM 17**). Yellow solid, yield: 93%, IR (υ_{max}/cm^{-1}): 3329, 3253, 1700, 1673, 1597, 1234; ^{1}H-NMR (400 MHz, DMSO-d_6) δ: 2.10 (s, 3H, CH_3), 2.29 (s, 3H, CH_3CO), 5.26 (d, 1H, *J* = 3.39 Hz, CH), 7.21-7.36 (m, 5H, ArH), 7.82 (brs, 1H, NH), 9.18 (brs, 1H, NH); ^{13}C-NMR (100 MHz, DMSO-d_6) δ: 18.90, 30.31, 53.80, 109.58, 126.42, 127.33, 128.51, 144.24, 148.12, 152.12, 194.25.

Ethyl 6-methyl-2-oxo-4-*p*-tolyl-1,2,3,4-tetrahydropyrimidine-5-carboxylate (compound **MM 22**). White solid, yield: 74%, IR (υ_{max}/cm^{-1}): 3238, 3112, 2981, 1700, 1645, 1217, 1086; ^{1}H-NMR (400 MHz, DMSO-d_6) δ: 1.10 (t, 3H, *J* = 7.05 Hz, OCH_2CH_3), 2.24 (s, 3H, CH_3), 2.26 (s, 3H, CH_3), 3.98 (q, 2H, *J* = 7.04 Hz, OCH_2), 5.10 (d, 1H, *J* = 3.23 Hz, CH), 7.12 (s, 4H, ArH), 7.68 (brs, 1H, NH), 9.15 (brs, 1H, NH); ^{13}C-NMR (100 MHz, DMSO-d_6) δ: 14.09, 17.75, 20.63, 53.61, 59.14, 99.40, 126.13, 128.87, 136.35, 141.95, 148.14, 152.16, 165.35.

Methyl 6-methyl-2-oxo-4-*p*-tolyl-1,2,3,4-tetrahydropyrimidine-5-carboxylate (compound **MM 73**). White solid, yield: 72%, IR (υ_{max}/cm^{-1}): 3331, 3212, 3105, 2955 1694, 1665, 1238, 1090; ^{1}H-NMR (400 MHz, DMSO-d_6) δ: 2.24 (s, 3H, CH_3), 2.26 (s, 3H, CH_3), 3.52 (s, 3H, CH_3OCO), 5.10 (d, 1H, *J* = 3.17 Hz, CH), 7.11 (s, 4H, ArH), 7.70 (brs, 1H, NH), 9.18 (brs, 1H, NH); ^{13}C-NMR (100 MHz, DMSO-d_6) δ: 17.81, 20.64, 50.76, 53.48, 99.12, 126.08, 128.95, 136.40, 141.76, 148.47, 152.17, 165.85.

5-Acetyl-6-methyl-4-*p*-tolyl-3,4-dihydropyrimidin-2(1*H*)-one (compound **MM 19**). Orange solid, yield: 60%, IR (υ_{max}/cm^{-1}): 3285, 3118, 2918, 1697, 1615, 1234; ^{1}H-NMR (400 MHz, DMSO-d_6) δ: 2.08 (s, 3H, CH_3), 2.26 (s, 3H, CH_3), 2.27 (s, 3H, CH_3CO), 5.21 (d, 1H, *J* = 3.22 Hz, CH), 7.12 (s, 4H, ArH), 7.77 (brs, 1H, NH), 9.14 (brs, 1H, NH); ^{13}C-NMR (100 MHz, DMSO-d_6) δ: 18.85, 20.64, 30.21, 53.56, 109.54, 126.35, 129.02, 136.49, 141.30, 147.91, 152.11, 194.58.

Ethyl 6-methyl-4-(4-nitrophenyl)-2-oxo-1,2,3,4-tetrahydropyrimidine-5-carboxylate (compound **MM 23**). Yellow solid, yield: 67%, IR (υ_{max}/cm^{-1}): 3228, 3113, 2976, 1698, 1640, 1517, 1210, 1084; ^{1}H-NMR (400 MHz, DMSO-d_6) δ: 1.09 (t, 3H, *J* = 7.09 Hz, OCH_2CH_3), 2.26 (s, 3H, CH_3), 3.98 (q, 2H, *J* = 7.10 Hz, OCH_2), 5.27 (d, 1H, *J* = 3.15 Hz, CH), 7.50 (d, 2H, *J* = 8.71 Hz, ArH), 7.88 (brs, 1H, NH), 8.22 (d, 2H, *J* = 8.70 Hz, ArH), 9.35 (brs, 1H, NH); ^{13}C-NMR (100 MHz, DMSO-d_6) δ: 14.05, 17.86, 53.68, 59.38, 98.17, 123.83, 127.65, 146.72, 149.39, 151.73, 151.99, 165.05.

Methyl 6-methyl-4-(4-nitrophenyl)-2-oxo-1,2,3,4-tetrahydropyrimidine-5-carboxylate (compound **MM 82**). Yellow solid, yield: 61%, IR (υ_{max}/cm^{-1}): 3364, 3221, 3114, 2950, 1689, 1638, 1514, 1225, 1093; ^{1}H-NMR (400 MHz, DMSO-d_6) δ: 2.27 (s, 3H, CH_3), 3.54 (s, 3H, CH_3OCO), 5.27 (d, 1H, *J* = 3.27 Hz, CH), 7.51 (d, 2H, *J* = 8.78 Hz, ArH), 7.90 (brs, 1H, NH), 8.21 (d, 2H, *J* = 8.78 Hz, ArH), 9.37 (brs, 1H, NH); ^{13}C-NMR (100 MHz, DMSO-d_6) δ: 17.93, 50.92, 53.53, 97.97, 123.88, 127.61, 146.75, 149.64, 151.78, 165.57.

5-Acetyl-6-methyl-4-(4-nitrophenyl)-3,4-dihydropyrimidin-2(1*H*)-one (compound **MM 24**). Orange solid, yield: 71%, IR (υ_{max}/cm^{-1}): 3247, 3110, 2945, 1672, 1606, 1514, 1234; ^{1}H-NMR (400 MHz, DMSO-d_6) δ: 2.18 (s, 3H, CH_3), 2.31 (s, 3H, CH_3CO), 5.38 (d, 1H, *J* = 3.42 Hz, CH), 7.50 (d, 2H, *J* = 8.64 Hz, ArH), 7.98 (brs, 1H, NH), 8.20 (d, 2H, *J* = 8.64 Hz, ArH), 9.33 (brs, 1H, NH); ^{13}C-NMR (100 MHz, DMSO-d_6) δ: 19.18, 30.70, 53.20, 109.54, 123.88, 127.75, 146.75, 149.17, 151.60, 152.06, 194.07.

Ethyl 4-(4-methoxyphenyl)-6-methyl-2-oxo-1,2,3,4-tetrahydropyrimidine-5-carboxylate (compound **MM 34**). White solid, yield: 79%, IR (υ_{max}/cm^{-1}): 3235, 3104, 2956, 1703, 1647, 1218, 1085; ^{1}H-NMR (400 MHz, DMSO-d_6) δ: 1.10 (t, 3H, *J* = 7.12 Hz, OCH_2CH_3), 2.24 (s, 3H, CH_3), 3.72 (s, 3H, OCH_3), 3.98 (q, 2H, *J* = 7.12 Hz, OCH_2), 5.09 (d, 1H, *J* = 3.20 Hz, CH), 6.87 (d, 2H, *J* = 8.67 Hz, ArH), 7.14 (d, 2H, *J* = 8.67 Hz, ArH), 7.66 (brs, 1H, NH), 9.14 (brs, 1H, NH); ^{13}C-NMR (100 MHz, DMSO-d_6) δ: 14.10, 17.74, 53.32, 55.04, 59.14, 99.55, 113.69, 127.38, 137.05, 148.00, 152.14, 158.43, 165.36.

Methyl 4-(4-methoxyphenyl)-6-methyl-2-oxo-1,2,3,4-tetrahydropyrimidine-5-carboxylate (compound **MM 74**). Yellow solid, yield: 81%, IR (υ_{max}/cm^{-1}): 3240, 3108, 2955, 1710, 1680, 1651, 1236, 1095; ^{1}H-NMR (400 MHz, DMSO-d_6) δ: 2.24 (s, 3H, CH_3), 3.52 (s, 3H, CH_3OCO), 3.72 (s, 3H, OCH_3), 5.09 (d, 1H, *J* = 3.25 Hz, CH), 6.87 (d, 2H, *J* = 8.63 Hz, ArH), 7.14 (d, 2H, *J* = 8.63 Hz, ArH), 7.68 (brs, 1H, NH), 9.17 (brs, 1H, NH); ^{13}C-NMR (100 MHz, DMSO-d_6) δ: 17.80, 50.76, 53.18, 55.05, 99.28, 113.76, 127.33, 136.85, 148.34, 152.16, 158.46, 165.86.

5-Acetyl-4-(4-methoxyphenyl)-6-methyl-3,4-dihydropyrimidin-2(1*H*)-one (compound **MM 35**). Orange solid, yield: 64%, IR (υ_{max}/cm^{-1}): 3298, 3218, 1694, 1609, 1511, 1248, 1175; ^{1}H-NMR (400 MHz, DMSO-d_6) δ: 2.07 (s, 3H, CH_3), 2.27 (s, 3H, CH_3CO), 3.72 (s, 3H, OCH_3), 5.20 (d, 1H, *J* = 3.18 Hz, CH), 6.88 (d, 2H, *J* = 8.56 Hz, ArH), 7.16 (d, 2H, *J* = 8.56 Hz, ArH), 7.75 (brs, 1H, NH), 9.14 (brs, 1H, NH); ^{13}C-NMR (100 MHz, DMSO-d_6) δ: 18.83, 30.16, 53.31, 55.06, 109.60, 113.85, 127.63, 136.37, 147.79, 152.08, 158.50, 194.36.

Ethyl 4-(2,3-dichlorophenyl)-6-methyl-2-oxo-1,2,3,4-tetrahydropyrimidine-5-carboxylate (compound **MM 55**). White solid, yield: 32%, IR (υ_{max}/cm^{-1}): 3305, 3235, 3100, 2968, 1697, 1638, 1558, 1215, 1085; ^{1}H-NMR (400 MHz, DMSO-d_6) δ: 0.97 (t, 3H, *J* = 7.08 Hz, OCH_2CH_3), 2.30 (s, 3H, CH_3), 3.89 (q, 2H, *J* = 7.08 Hz, OCH_2), 5.68 (dd, 1H, *J* = 2.67 Hz, CH), 7.29 (dd, 1H, J_1 = 7.81 Hz, J_2 = 1.58 Hz ArH), 7.35 (t, 1H, *J* = 7.81 Hz, ArH), 7.54 (dd, 1H, J_1 = 7.81 Hz, J_2 = 1.57 Hz, ArH), 7.78 (brs, 1H, NH), 9.32 (brs, 1H, NH); ^{13}C-NMR (100 MHz, DMSO-d_6) δ: 13.86, 17.68, 52.37, 59.11, 97.63, 127.31, 128.64, 129.48, 129.85, 131.74, 144.42, 149.59, 151.11, 164.85.

5-Acetyl-4-(2,3-dichlorophenyl)-6-methyl-3,4-dihydropyrimidin-2(1*H*)-one (compound **MM 54**). Yellow solid, yield: 45%, IR (υ_{max}/cm^{-1}): 3230, 3108, 2961, 1636, 1520, 1236; ^{1}H-NMR (400 MHz, DMSO-d_6) δ: 2.09 (s, 3H, CH_3), 2.35 (s, 3H, CH_3CO), 5.70 (d, 1H, *J* = 3.23 Hz, CH), 7.23 (dd, 1H, J_1 = 7.83 Hz, J_2 = 1.49 Hz, ArH), 7.34 (t, 1H, *J* = 7.83 Hz, ArH), 7.55 (dd, 1H, J_1 = 7.83 Hz, J_2 = 1.49 Hz, ArH), 7.81 (brs, 1H, NH), 9.32 (brs, 1H, NH); ^{13}C-NMR (100 MHz, DMSO-d_6) δ: 18.96, 30.34, 52.33, 108.63, 126.94, 128.69, 129.65, 129.99, 131.96, 143.53, 149.11, 151.39, 193.82. HRMS (ESI-TOF): *m/z* [M^+ + Na] calcd for $C_{13}H_{12}N_2O_2Cl_2Na$: 321.0176; found 321.0168.

Ethyl 4-(2,4-dichlorophenyl)-6-methyl-2-oxo-1,2,3,4-tetrahydropyrimidine-5-carboxylate (compound **MM 57**). White solid, yield: 46%, IR (υ_{max}/cm^{-1}): 3356, 3217, 3098, 2972, 1693, 1638, 1560, 1225, 1092; ^{1}H-NMR (400 MHz, DMSO-d_6) δ: 1.00 (t, 3H, *J* = 7.03 Hz, OCH_2CH_3), 2.29 (s, 3H, CH_3), 3.90 (q, 2H, *J* = 7.03 Hz, OCH_2), 5.59 (d, 1H, *J* = 2.83 Hz, CH), 7.32 (d, 1H, *J* = 8.34 Hz, ArH), 7.41 (dd, 1H, J_1 = 8.34 Hz, J_2 = 2.11 Hz, ArH), 7.56 (d, 1H, *J* = 2.11 Hz, ArH), 7.74 (brs, 1H, NH), 9.31 (brs, 1H, NH); ^{13}C-NMR (100 MHz, DMSO-d_6) δ: 13.92, 17.69, 51.17, 59.13, 97.47, 127.97, 128.68, 130.27, 132.54, 132.65, 140.95, 149.57, 151.13, 164.83.

Methyl 4-(2,4-dichlorophenyl)-6-methyl-2-oxo-1,2,3,4-tetrahydropyrimidine-5-carboxylate (compound **MM 81**). White solid, yield: 51%, IR (υ_{max}/cm^{-1}): 3360, 3219, 3096, 2944, 1695, 1641, 1227, 1099; ^{1}H-NMR (400 MHz, DMSO-d_6) δ: 2.29 (s, 3H, CH_3), 3.46 (s, 3H, CH3OCO), 5.58 (d, 1H, *J* = 2.59 Hz, CH), 7.31 (d, 1H, *J* = 8.41 Hz, ArH), 7.41 (dd, 1H, J_1 = 8.42

Hz, J_2 = 1.72 Hz, ArH), 7.56 (d, 1H, *J* = 1.72 Hz, ArH), 7.75 (brs, 1H, NH), 9.34 (brs, 1H, NH); ^{13}C-NMR (100 MHz, DMSO-d_6) δ: 17.77, 50.77, 51.10, 97.34, 127.99, 128.80, 130.18, 132.59, 132.63, 140.81, 149.70, 151.20, 165.35.

5-Acetyl-4-(2,4-dichlorophenyl)-6-methyl-3,4-dihydropyrimidin-2(1*H*)-one (compound **MM 56**). Yellow solid, yield: 50%, IR (υ_{max}/cm^{-1}): 3332, 3100, 2976, 1637, 1559, 1226, 1040; ^{1}H-NMR (400 MHz, DMSO-d_6) δ: 2.08 (s, 3H, CH_3), 2.33 (s, 3H, CH_3CO), 5.62 (d, 1H, *J* = 2.91 Hz, CH), 7.26 (d, 1H, *J* = 8.39 Hz, ArH), 7.40 (dd, 1H, J_1 = 8.38 Hz, J_2 = 1.87 Hz, ArH), 7.59 (d, 1H, *J* = 1.87 Hz, ArH), 7.78 (brs, 1H, NH), 9.30 (brs, 1H, NH); ^{13}C-NMR (100 MHz, DMSO-d_6) δ: 18.96, 30.30, 51.17, 108.39, 128.02, 128.96, 129.94, 132.75, 132.83, 140.12, 149.03, 151.40, 193.83.

Ethyl 4-(2,3-difluorophenyl)-6-methyl-2-oxo-1,2,3,4-tetrahydropyrimidine-5-carboxylate (compound **MM 59**). White solid, yield: 37%, IR (υ_{max}/cm^{-1}): 3228, 3106, 2982, 1694, 1651, 1480, 1232, 1101; ^{1}H-NMR (400 MHz, DMSO-d_6) δ: 1.04 (t, 3H, *J* = 7.13 Hz, OCH_2CH_3), 2.28 (s, 3H, CH_3), 3.94 (dq, 2H, J_1 = 7.12 Hz, J_2 = 2.38 Hz, OCH_2), 5.50 (d, 1H, *J* = 2.83 Hz, CH), 7.08-7.14 (m, 1H, ArH), 7.16-7.22 (m, 1H, ArH), 7.28-7.37 (m, 1H, ArH), 7.77 (brs, 1H, NH), 9.33 (brs, 1H, NH); ^{13}C-NMR (100 MHz, DMSO-d_6) δ: 13.83, 17.72, 48.32, 59.15, 97.08, 116.10, 116.27, 123.88, 124.90, 134.44, 134.55, 149.31, 151.31, 164.85. HRMS (ESI-TOF): *m*/*z* [M$^+$ + H] calcd for $C_{14}H_{15}N_2O_3F_2$: 297.1052; found 297.1045.

Methyl 4-(2,3-difluorophenyl)-6-methyl-2-oxo-1,2,3,4-tetrahydropyrimidine-5-carboxylate (compound **MM 75**). White solid, yield: 58%, IR (υ_{max}/cm^{-1}): 3373, 3219, 3095, 2956, 1692, 1644, 1482, 1228, 1096; ^{1}H-NMR (400 MHz, DMSO-d_6) δ: 2.27 (s, 3H, CH_3), 3.48 (s, 3H, CH_3OCO), 5.47 (d, 1H, *J* = 2.84 Hz, CH), 7.06-7.11 (m, 1H, ArH), 7.14-7.20 (m, 1H, ArH), 7.28-7.36 (m, 1H, ArH), 7.78 (brs, 1H, NH), 9.35 (brs, 1H, NH); ^{13}C-NMR (100 MHz, DMSO-d_6) δ: 17.84, 48.35, 50.81, 96.92, 116.21, 116.39, 123.75, 124.93, 134.18, 134.29, 149.52, 151.41, 165.40. HRMS (ESI-TOF): *m*/*z* [M$^+$ + H] calcd for $C_{13}H_{13}N_2O_3F_2$: 283.0896; found 283.0889.

5-Acetyl-4-(2,3-difluorophenyl)-6-methyl-3,4-dihydropyrimidin-2(1*H*)-one (compound **MM 58**). White solid, yield: 52%, IR (υ_{max}/cm^{-1}): 3305, 3218, 3119, 1693, 1607, 1487, 1240; ^{1}H-NMR (400 MHz, DMSO-d_6) δ: 2.13 (s, 3H, CH_3), 2.31 (s, 3H, CH_3CO), 5.55 (d, 1H, *J* = 3.08 Hz, CH), 7.03-7.08 (m, 1H, ArH), 7.12-7.196 (m, 1H, ArH), 7.27-7.36 (m, 1H, ArH), 7.84 (brs, 1H, NH), 9.30 (brs, 1H, NH); ^{13}C-NMR (100 MHz, DMSO-d_6) δ: 19.02, 30.42, 48.30, 108.14, 116.25, 116.41, 123.60, 124.95, 133.80, 133.91, 148.82, 151.53, 193.72. HRMS (ESI-TOF): *m*/*z* [M$^+$ + H] calcd for $C_{13}H_{13}N_2O_2F_2$: 267.0947; found 267.0940.

Ethyl 4-(furan-2-yl)-6-methyl-2-oxo-1,2,3,4-tetrahydropyrimidine-5-carboxylate (compound **MM 65**). Brown solid, yield: 81%, IR (υ_{max}/cm^{-1}): 3351, 3233, 3115, 2976, 1694, 1644, 1230, 1098; ^{1}H-NMR (400 MHz, DMSO-d_6) δ: 1.14 (t, 3H, *J* = 7.19 Hz, OCH_2CH_3), 2.23 (s, 3H, CH_3), 4.03 (dq, 2H, J_1 = 7.20 Hz, J_2 = 1.92 Hz, OCH_2), 5.20 (d, 1H, *J* = 3.34 Hz, CH), 6.09 (d, 1H, *J* = 3.14 Hz, ArH), 6.34-6.37 (m, 1H, ArH), 7.55 (brs, 1H, ArH), 7.75 (brs, 1H, NH),

9.24 (brs, 1H, NH); ^{13}C-NMR (100 MHz, DMSO-d_6) δ: 14.15, 17.74, 47.73, 59.22, 96.75, 105.28, 110.34, 142.15, 149.36, 152.41, 155.93, 165.01.

Methyl 4-(furan-2-yl)-6-methyl-2-oxo-1,2,3,4-tetrahydropyrimidine-5-carboxylate (compound **MM 76**). Brown solid, yield: 74%, IR (υ_{max}/cm^{-1}): 3313, 2954, 1672, 1637, 1432, 1237, 1087; ^{1}H-NMR (400 MHz, DMSO-d_6) δ: 2.24 (s, 3H, CH_3), 3.57 (s, 3H, CH_3OCO), 5.20 (d, 1H, *J* = 3.39 Hz, CH), 6.35 (d, 1H, *J* = 3.13 Hz, ArH), 6.34-6.36 (m, 1H, ArH), 7.56 (brs, 1H, ArH), 7.78 (brs, 1H, NH), 9.27 (brs, 1H, NH); ^{13}C-NMR (100 MHz, DMSO-d_6) δ: 17.77, 47.63, 50.88, 96.55, 105.30, 110.37, 142.21, 149.67, 152.39, 155.83, 165.49.

5-Acetyl-4-(furan-2-yl)-6-methyl-3,4-dihydropyrimidin-2(1*H*)-one (compound **MM 66**). Brown solid, yield: 76%, IR (υ_{max}/cm^{-1}): 3277, 3151, 2954, 1675, 1595, 1235; ^{1}H-NMR (400 MHz, DMSO-d_6) δ: 2.16 (s, 3H, CH_3), 2.24 (s, 3H, CH_3CO), 5.31 (d, 1H, *J* = 3.33 Hz, CH), 6.12 (d, 1H, *J* = 3.17 Hz, ArH), 6.34-6.37 (m, 1H, ArH), 7.56 (brs, 1H, ArH), 7.84 (brs, 1H, NH), 9.23 (brs, 1H, NH); ^{13}C-NMR (100 MHz, DMSO-d_6) δ: 18.88, 29.95, 47.84, 105.61, 107.22, 110.34, 142.36, 148.80, 152.44, 155.87, 193.79.

Ethyl 6-methyl-4-(5-methylfuran-2-yl)-2-oxo-1,2,3,4-tetrahydropyrimidine-5-carboxylate (compound **MM 93**). Yellow solid, yield: 69%, IR (υ_{max}/cm^{-1}): 3225, 3100, 2982, 2923, 1703, 1652, 1218, 1090; ^{1}H-NMR (400 MHz, DMSO-d_6) δ: 1.14 (t, 3H, *J* = 7.06 Hz, OCH_2CH_3), 2.21 (s, 3H, CH_3), 2.23 (s, 3H, CH_3), 3.98-4.07 (m, OCH_2), 5.13 (d, 1H, *J* = 3.24 Hz, CH), 5.92-5.96 (m, 2H, ArH), 7.71 (brs, 1H, NH), 9.18 (brs, 1H, NH); ^{13}C-NMR (100 MHz, DMSO-d_6) δ: 13.39, 14.16, 17.74, 47.71, 59.18, 96.81, 106.00, 106.33, 149.21, 150.70, 152.38, 154.21, 165.06.

Ethyl 6-methyl-2-oxo-4-(pyridin-3-yl)-1,2,3,4-tetrahydropyrimidine-5-carboxylate (compound **MM 95**). Yellow solid, yield: 36%, IR (υ_{max}/cm^{-1}): 3344, 3225, 3108, 2978, 1682, 1640, 1223, 1102; ^{1}H-NMR (400 MHz, DMSO-d_6) δ: 1.07 (t, 3H, *J* = 7.11 Hz, OCH_2CH_3), 2.27 (s, 3H, CH_3), 3.98 (dq, 2H, J_1 = 7.11 Hz, J_2 = 1.04 Hz, OCH_2), 5.19 (d, 1H, *J* = 3.22 Hz, CH), 7.36 (dd, 1H, J_1 = 8.04 Hz, J_2 = 4.62 Hz ArH), 7.61 (d, *J* = 7.94 Hz 1H, ArH), 7.80 (brs, 1H, NH), 8.43-8.47 (m, 2H, ArH), 9.30 (brs, 1H, NH); ^{13}C-NMR (100 MHz, DMSO-d_6) δ: 14.03, 17.80, 52.14, 59.29, 98.32, 123.78, 133.91, 140.10, 147.91, 148.57, 149.13, 151.85, 165.06.

Ethyl 6-methyl-2-oxo-4-(thiophen-2-yl)-1,2,3,4-tetrahydropyrimidine-5-carboxylate (compound **MM 96**). White solid, yield: 83%, IR (υ_{max}/cm^{-1}): 3235, 3104, 2981, 1711, 1650, 1208, 1088; ^{1}H-NMR (400 MHz, DMSO-d_6) δ: 1.14 (t, 3H, *J* = 7.09 Hz, OCH_2CH_3), 2.22 (s, 3H, CH_3), 4.06 (q, 2H, *J* = 7.10 Hz, OCH_2), 5.41 (d, 1H, *J* = 3.46 Hz, CH), 6.89 (d, 1H, *J* = 3.27 Hz, ArH), 6.92-6.95 (m, 1H, ArH), 7.35 (dd, 1H, J_1 = 5.03 Hz, J_2 = 1.17 Hz, ArH), 7.90 (brs, 1H, NH), 9.31 (brs, 1H, NH); ^{13}C-NMR (100 MHz, DMSO-d_6) δ:14.16, 17.68, 49.35, 59.36, 99.77, 123.50, 124.63, 126.66, 148.66, 148.79, 152.24, 165.02.

Ethyl 4-(5-chlorofuran-2-yl)-6-methyl-2-oxo-1,2,3,4-tetrahydropyrimidine-5-carboxylate (compound **MM 99**). Brown solid, yield: 67%, IR (υ_{max}/cm^{-1}): 3351, 3233, 3115, 2976, 1694, 1644, 1230, 1098; ^{1}H-NMR (400 MHz, DMSO-d_6) δ: 1.14 (t, 3H, *J* = 7.08 Hz, OCH_2CH_3), 2.24 (s, 3H, CH_3), 3.97-4.10 (m, 2H, OCH_2), 5.16 (d, 1H, *J* = 3.33 Hz, CH), 6.19 (d, 1H, *J* = 3.30 Hz,

ArH), 6.36 (d, 1H, *J* = 3.33 Hz, ArH), 7.82 (brs, 1H, NH), 9.30 (brs, 1H, NH); ^{13}C-NMR (100 MHz, DMSO-d_6) δ: 14.13, 17.76, 47.78, 59.31, 95.93, 107.51, 107.98, 133.54, 149.88, 152.13, 155.98, 164.85. HRMS (ESI-TOF): *m/z* [M^+ + H] calcd for $C_{12}H_{14}N_2O_4Cl$: 284.6956; found 285.0637

Ethyl 4-(5-chlorothiophen-2-yl)-6-methyl-2-oxo-1,2,3,4-tetrahydropyrimidine-5-carboxylate (compound **MM 106**). White solid, yield: 81%, IR (υ_{max}/cm^{-1}): 3230, 3107, 2976, 1704, 1648, 1215, 1084; ^{1}H-NMR (400 MHz, DMSO-d_6) δ: 1.17 (t, 3H, *J* = 7.10 Hz, OCH_2CH_3), 2.22 (s, 3H, CH_3), 4.08 (q, 2H, *J* = 7.10 Hz, OCH_2), 5.31 (d, 1H, *J* = 3.53 Hz, CH), 6.74 (d, 1H, *J* = 3.82 Hz, ArH), 6.94 (d, *J* = 3.82 Hz, 1H, ArH), 7.95 (brs, 1H, NH), 9.39 (brs, 1H, NH); ^{13}C-NMR (100 MHz, DMSO-d_6) δ: 14.15, 17.68, 49.56, 59.49, 98.99, 123.25, 126.39, 126.59, 147.74, 149.28, 152.06, 164.87. HRMS (ESI-TOF): *m/z* [M^+ + H] calcd for $C_{12}H_{14}N_2O_3SCl$: 300.7612; found 301.0408.

Thiourea series:

Ethyl 6-methyl-4-phenyl-2-thioxo-1,2,3,4-tetrahydropyrimidine-5-carboxylate (compound **MM 26**). White solid, yield: 70%, IR (υ_{max}/cm^{-1}): 3325, 3170, 3104, 2980, 1666, 1572, 1175, 1117; ^{1}H-NMR (400 MHz, DMSO-d_6) δ: 1.10 (t, 3H, *J* = 7.04 Hz, OCH_2CH_3), 2.29 (s, 3H, CH_3), 4.01 (q, 2H, *J* = 7.06 Hz, OCH_2), 5.17 (d, 1H, *J* = 3.68 Hz, CH), 7.19-7.38 (m, 5H, ArH), 9.64 (brs, 1H, NH), 10.32 (brs, 1H, NH); ^{13}C-NMR (100 MHz, DMSO-d_6) δ: 14.00, 17.15, 54.02, 59.58, 100.70, 126.37, 127.67, 128.55, 143.49, 145.01, 165.11, 174.22.

Methyl 6-methyl-4-phenyl-2-thioxo-1,2,3,4-tetrahydropyrimidine-5-carboxylate (compound **MM 83**). White solid, yield: 60%, IR (υ_{max}/cm^{-1}): 3312, 3179, 3116, 2996, 1661, 1579, 1178, 1112; ^{1}H-NMR (400 MHz, DMSO-d_6) δ: 2.29 (s, 3H, CH_3), 3.56 (s, 3H, CH_3OCO), 5.18 (d, 1H, *J* = 3.71 Hz, CH), 7.19-7.38 (m, 5H, ArH), 9.67 (brs, 1H, NH), 10.36 (brs, 1H, NH); ^{13}C-NMR (100 MHz, DMSO-d_6) δ: 17.22, 51.09, 53.89, 100.42, 126.31, 127.70, 128.64, 143.29, 145.31, 165.64, 174.27.

1-(6-Methyl-4-phenyl-2-thioxo-1,2,3,4-tetrahydropyrimidin-5-yl)ethanone (compound **MM 25**). Orange solid, yield: 80%, IR (υ_{max}/cm^{-1}): 3275, 3176, 2994, 1610, 1574, 1181; ^{1}H-NMR (400 MHz, DMSO-d_6) δ: 2.16 (s, 3H, CH_3), 2.33 (s, 3H, CH_3CO), 5.30 (d, 1H, *J* = 3.86 Hz, CH), 7.20-7.38 (m, 5H, ArH), 9.75 (brs, 1H, NH), 10.27 (brs, 1H, NH); ^{13}C-NMR (100 MHz, DMSO-d_6) δ: 18.27, 30.44, 53.78, 110.47, 126.57, 127.72, 128.66, 142.94, 144.56, 174.10, 194.78.

Ethyl 6-methyl-2-thioxo-4-*p*-tolyl-1,2,3,4-tetrahydropyrimidine-5-carboxylate (compound **MM 28**). White solid, yield: 44%, IR (υ_{max}/cm^{-1}): 3322, 3172, 3105, 2982, 1670, 1574, 1464, 1175, 1118; ^{1}H-NMR (400 MHz, DMSO-d_6) δ: 1.10 (t, 3H, *J* = 7.07 Hz, OCH_2CH_3), 2.26 (s, 3H, CH_3), 2.28 (s, 3H, CH_3), 4.00 (q, 2H, *J* = 7.08 Hz, OCH_2), 5.13 (d, 1H, *J* = 3.60 Hz, CH), 7.07-7.16 (m, 4H, ArH), 9.60 (brs, 1H, NH), 10.29 (brs, 1H, NH); ^{13}C-NMR (100 MHz, DMSO-d_6) δ: 14.01, 17.12, 20.65, 53.71, 59.54, 100.80, 126.27, 129.04, 136.88, 140.58, 144.86, 165.13, 174.14.

Methyl 6-methyl-2-thioxo-4-*p*-tolyl-1,2,3,4-tetrahydropyrimidine-5-carboxylate (compound **MM 84**). White solid, yield: 33%, IR (υ_{max}/cm^{-1}): 3166, 2996, 1714, 1654, 1572, 1186, 1102; ^{1}H-NMR (400 MHz, DMSO-d_6) δ: 2.26 (s, 3H, CH_3), 2.28 (s, 3H, CH_3), 3.55 (s, 3H, CH_3OCO), 5.13 (d, 1H, *J* = 3.65 Hz, CH), 7.07-7.159 (m, 4H, ArH), 9.62 (brs, 1H, NH), 10.32 (brs, 1H, NH); ^{13}C-NMR (100 MHz, DMSO-d_6) δ: 17.18, 20.66, 51.07, 53.59, 100.52, 126.23, 129.14, 136.96, 140.40, 145.16, 165.64, 174.15.

1-(6-Methyl-2-thioxo-4-*p*-tolyl-1,2,3,4-tetrahydropyrimidin-5-yl)ethanone (compound **MM 29**). Orange solid, yield: 50%, IR (υ_{max}/cm^{-1}): 3282, 3174, 3002, 1617, 1582, 1451, 1180; ^{1}H-NMR (400 MHz, DMSO-d_6) δ: 2.13 (s, 3H, CH_3), 2.26 (s, 3H, CH_3), 2.32 (s, 3H, CH_3CO), 5.25 (d, 1H, *J* = 3.94 Hz, CH), 7.09-7.17 (m, 4H, ArH), 9.71 (brs, 1H, NH), 10.24 (brs, 1H, NH); ^{13}C-NMR (100 MHz, DMSO-d_6) δ: 18.19, 20.65, 30.30, 53.55, 110.41, 126.49, 129.15, 136.96, 139.99, 144.36, 173.95, 194.81.

1-(6-Methyl-4-(4-nitrophenyl)-2-thioxo-1,2,3,4-tetrahydropyrimidin-5-yl)ethanone (compound **MM 30**). Orange solid, yield: 17%, IR (υ_{max}/cm^{-1}): 3266, 3171, 3011, 1574, 1519, 1344; ^{1}H-NMR (400 MHz, DMSO-d_6) δ: 2.23 (s, 3H, CH_3), 2.36 (s, 3H, CH_3CO), 5.41 (d, 1H, *J* = 3.99 Hz, CH), 7.48 (d, 2H, *J* = 8.48 Hz, ArH), 8.22 (d, 2H, *J* = 8.48 Hz, ArH), 9.87 (brs, 1H, NH), 10.44 (brs, 1H, NH); ^{13}C-NMR (100 MHz, DMSO-d_6) δ: 18.45, 30.74, 53.11, 110.24, 123.95, 127.80, 145.54, 146.90, 149.98, 174.54, 194.56.

Ethyl 4-(4-methoxyphenyl)-6-methyl-2-thioxo-1,2,3,4-tetrahydropyrimidine-5-carboxylate (compound **MM 36**). Yellow solid, yield: 79%, IR (υ_{max}/cm^{-1}): 3309, 3166, 2982, 1664, 1573, 1508, 1169, 1121, 1026; ^{1}H-NMR (400 MHz, DMSO-d_6) δ: 1.10 (t, 3H, *J* = 7.05 Hz, OCH_2CH_3), 2.28 (s, 3H, CH_3), 3.72 (s, 3H, OCH_3), 4.00 (q, 2H, *J* = 7.04 Hz, OCH_2), 5.11 (d, 1H, *J* = 3.66 Hz, CH), 6.90 (d, 2H, *J* = 8.76 Hz, ArH), 7.12 (d, 2H, *J* = 8.75 Hz, ArH), 9.59 (brs, 1H, NH), 10.28 (brs, 1H, NH); ^{13}C-NMR (100 MHz, DMSO-d_6) δ: 14.02, 17.13, 53.42, 55.08, 59.54, 100.94, 113.87, 127.60, 135.68, 144.73, 158.73, 165.15, 174.01.

Methyl 4-(4-methoxyphenyl)-6-methyl-2-thioxo-1,2,3,4-tetrahydropyrimidine-5-carboxylate (compound **MM 85**). Yellow solid, yield: 31%, IR (υ_{max}/cm^{-1}): 3324, 3280, 2958, 1662, 1553, 1509, 1172, 1110, 1020; ^{1}H-NMR (400 MHz, DMSO-d_6) δ: 2.29 (s, 3H, CH_3), 3.55 (s, 3H, CH_3OCO), 3.72 (s, 3H, OCH_3), 5.11 (d, 1H, *J* = 3.76 Hz, CH), 6.90 (d, 2H, *J* = 8.56 Hz, ArH), 7.13 (d, 2H, *J* = 8.58 Hz, ArH), 9.61 (brs, 1H, NH), 10.31 (brs, 1H, NH); ^{13}C-NMR (100 MHz, DMSO-d_6) δ: 17.18, 51.07, 53.30, 55.09, 100.65, 113.94, 127.55, 135.48, 145.04, 158.75, 165.65, 174.03.

1-(4-(4-Methoxyphenyl)-6-methyl-2-thioxo-1,2,3,4-tetrahydropyrimidin-5-yl)ethanone (compound **MM 37**). Orange solid, yield: 89%, IR (υ_{max}/cm^{-1}): 3308, 3230, 3002, 1618, 1564, 1509, 1179, 1024; ^{1}H-NMR (400 MHz, DMSO-d_6) δ: 2.12 (s, 3H, CH_3), 2.32 (s, 3H, CH_3CO), 3.72 (s, 3H, OCH_3), 5.23 (d, 1H, *J* = 3.78 Hz, CH), 6.90 (d, 2H, *J* = 8.72 Hz, ArH), 7.14 (d, 2H, *J* = 8.70 Hz, ArH), 9.69 (brs, 1H, NH), 10.23 (brs, 1H, NH); ^{13}C-NMR (100 MHz, DMSO-d_6) δ: 18.18, 30.26, 53.33, 55.11, 110.46, 113.99, 127.87, 135.08, 144.25, 158.79, 173.83, 194.90.

Ethyl 4-(2,3-dichlorophenyl)-6-methyl-2-thioxo-1,2,3,4-tetrahydropyrimidine-5-carboxylate (compound **MM 46**). White solid, yield: 21%, IR (υ_{max}/cm^{-1}): 3170, 2994, 1545, 1477, 1194; ^{1}H-NMR (400 MHz, DMSO-d_6) δ: 0.99 (t, 3H, J = 7.03 Hz, OCH_2CH_3), 2.33 (s, 3H, CH_3), 3.92 (q, 2H, J = 7.03 Hz, OCH_2), 5.70 (d, 1H, J = 2.9 Hz, CH), 7.28 (dd, 1H, J_1 = 7.76 Hz, J_2 = 1.43 Hz, ArH), 7.38 (t, 1H, J = 7.85 Hz, ArH), 7.58 (dd, 1H, J_1 = 7.76 Hz, J_2 = 1.42 Hz, ArH), 9.65 (brs, 1H, NH), 10.42 (brs, 1H, NH); ^{13}C-NMR (100 MHz, DMSO-d_6) δ: 13.83, 17.03, 52.42, 59.51, 99.50, 127.92, 128.70, 129.89, 130.05, 131.91, 143.26, 145.87, 164.67, 173.84.

Methyl 4-(2,3-dichlorophenyl)-6-methyl-2-thioxo-1,2,3,4-tetrahydropyrimidine-5-carboxylate (compound **MM 90**). White solid, yield: 19%, IR (υ_{max}/cm^{-1}): 3173, 3004, 1544, 1478; ^{1}H-NMR (400 MHz, DMSO-d_6) δ: 2.33 (s, 3H, CH_3), 3.48 (s, 3H, CH_3OCO), 5.69 (d, 1H, J = 3.01 Hz, CH), 7.27 (dd, 1H, J_1 = 7.91 Hz, J_2 = 1.21 Hz, ArH), 7.38 (t, 1H, J = 7.84 Hz, ArH), 7.58 (dd, 1H, J_1 = 7.92 Hz, J_2 = 1.21 Hz, ArH), 9.65 (brs, 1H, NH), 10.45 (brs, 1H, NH); ^{13}C-NMR (100 MHz, DMSO-d_6) δ: 17.14, 51.07, 52.35, 99.31, 127.83, 128.42, 128.75, 129.97, 132.01, 143.03, 146.05, 165.23, 137.98. HRMS (ESI-TOF): m/z [M^+ + H] calcd for $C_{13}H_{13}N_2O_2SCl_2$: 331.0077; found 331.0069.

1-(4-(2,3-Dichlorophenyl)-6-methyl-2-thioxo-1,2,3,4-tetrahydropyrimidin-5-yl)ethanone (compound **MM 48**). Orange solid, yield: 47%, IR (υ_{max}/cm^{-1}): 3220, 2998, 1625, 1576, 1198, 1013; ^{1}H-NMR (400 MHz, DMSO-d_6) δ: 2.14 (s, 3H, CH_3), 2.38 (s, 3H, CH_3CO), 5.72 (d, 1H, J = 3.62 Hz, CH), 7.21 (dd, 1H, J_1 = 7.97 Hz, J_2 = 1.41 Hz, ArH), 7.36 (t, 1H, J = 7.91 Hz, ArH), 7.58 (dd, 1H, J_1 = 7.95 Hz, J_2 = 1.42 Hz, ArH), 9.68 (brs, 1H, NH), 10.39 (brs, 1H, NH); ^{13}C-NMR (100 MHz, DMSO-d_6) δ: 18.26, 30.49, 52.35, 109.88, 127.55, 128.72, 130.01, 130.12, 132.13, 142.35, 145.22, 174.01, 194.43. HRMS (ESI-TOF): m/z [M^+ + H] calcd for $C_{13}H_{13}N_2OSCl_2$: 315.0127; found 315.0120.

Ethyl 4-(2,4-dichlorophenyl)-6-methyl-2-thioxo-1,2,3,4-tetrahydropyrimidine-5-carboxylate (compound **MM 60**). White solid, yield: 19%, IR (υ_{max}/cm^{-1}): 3406, 3192, 3076, 3023, 1534, 1473, 1100, 1048; ^{1}H-NMR (400 MHz, DMSO-d_6) δ: 1.02 (t, 3H, J = 7.05 Hz, OCH_2CH_3), 2.32 (s, 3H, CH_3), 3.92 (q, 2H, J = 7.05 Hz, OCH_2), 5.60 (d, 1H, J = 3.05 Hz, CH), 7.30 (d, 1H, J = 8.39 Hz, ArH), 7.44 (dd, 1H, J_1 = 8.40 Hz, J_2 = 2.09 Hz, ArH), 7.59 (d, 1H, J = 2.08 Hz, ArH), 9.62 (brs, 1H, NH), 10.40 (brs, 1H, NH); ^{13}C-NMR (100 MHz, DMSO-d_6) δ: 13.86, 17.03, 51.24, 59.52, 99.31, 128.06, 128.83, 130.81, 132.80, 133.03, 139.82, 145.86, 164.63, 173.83.

Methyl 4-(2,4-dichlorophenyl)-6-methyl-2-thioxo-1,2,3,4-tetrahydropyrimidine-5-carboxylate (compound **MM 92**). White solid, yield: 34%, IR (υ_{max}/cm^{-1}): 3406, 3178, 3090, 3025, 1545, 1470, 1101, 1047; ^{1}H-NMR (400 MHz, DMSO-d_6) δ: 2.31 (s, 3H, CH_3), 3.48 (s, 3H, CH3OCO), 5.59 (d, 1H, J = 3.10 Hz, CH), 7.29 (d, 1H, J = 8.47 Hz, ArH), 7.44 (dd, 1H, J_1 = 8.49 Hz, J_2 = 2.12 Hz, ArH), 7.59 (d, 1H, J = 2.14 Hz, ArH), 9.63 (brs, 1H, NH), 10.43 (brs, 1H, NH); ^{13}C-NMR (100 MHz, DMSO-d_6) δ: 17.10, 51.03, 51.21, 99.20, 128.08, 128.93, 130.71, 132.76, 133.07, 139.71, 145.93, 165.16, 173.93.

1-(4-(2,4-Dichlorophenyl)-6-methyl-2-thioxo-1,2,3,4-tetrahydropyrimidin-5-yl)ethanone (compound **MM 64**). Orange solid, yield: 42%, IR (υ_{max}/cm^{-1}): 3393, 3225, 3086, 2977, 1631, 1556, 1465 1179, 1097; ^{1}H-NMR (400 MHz, DMSO-d_6) δ: 2.13 (s, 3H, CH_3), 2.36 (s, 3H, CH_3CO), 5.64 (d, 1H, J = 3.46 Hz, CH), 7.24 (d, 1H, J = 8.42 Hz, ArH), 7.42 (dd, 1H, J_1 = 8.42 Hz, J_2 = 2.07 Hz, ArH), 7.61 (d, 1H, J = 2.08 Hz, ArH), 9.66 (brs, 1H, NH), 10.37 (brs, 1H, NH); ^{13}C-NMR (100 MHz, DMSO-d_6) δ: 18.26, 30.44, 51.22, 109.64, 128.06, 129.08, 130.52, 132.93, 133.19, 138.98, 145.11, 173.96, 194.42. HRMS (ESI-TOF): m/z [M$^+$ + H] calcd for $C_{13}H_{13}N_2OSCl_2$: 315.0127; found 315.0119.

Ethyl 4-(2,3-difluorophenyl)-6-methyl-2-thioxo-1,2,3,4-tetrahydropyrimidine-5-carboxylate (compound **MM 61**). Yellow solid, yield: 16%, IR (υ_{max}/cm^{-1}): 3318, 3177, 3104, 2984, 1713, 1654, 1570, 1485, 1194, 1100; ^{1}H-NMR (400 MHz, DMSO-d_6) δ: 1.04 (t, 3H, J = 7.09 Hz, OCH_2CH_3), 2.30 (s, 3H, CH_3), 3.95 (dq, 2H, J_1 = 7.13 Hz, J_2 = 3.08 Hz, OCH_2), 5.48 (d, 1H, J = 2.97 Hz, CH), 7.04-7.10 (m, 1H, ArH), 7.17-7.24 (m, 1H, ArH), 7.32-7.40 (m, 1H, ArH), 9.62 (brs, 1H, NH), 10.43 (brs, 1H, NH); ^{13}C-NMR (100 MHz, DMSO-d_6) δ: 13.77, 17.07, 48.33, 59.55, 98.94, 116.62, 116.79, 124.22, 125.06, 133.24, 133.36, 145.68, 164.62, 174.06. HRMS (ESI-TOF): m/z [M$^+$ + H] calcd for $C_{14}H_{15}N_2O_2SF_2$: 313.0824; found 313.0817.

Methyl 4-(2,3-difluorophenyl)-6-methyl-2-thioxo-1,2,3,4-tetrahydropyrimidine-5-carboxylate (compound **MM 86**). Yellow solid, yield: 19%, IR (υ_{max}/cm^{-1}): 3305, 3192, 3102, 1665, 1564, 1484, 1186, 1126; ^{1}H-NMR (400 MHz, DMSO-d_6) δ: 2.30 (s, 3H, CH_3), 3.51 (s, 3H, CH_3OCO), 5.48 (d, 1H, J = 3.08 Hz, CH), 7.03-7.09 (m, 1H, ArH), 7.17-7.24 (m, 1H, ArH), 7.31-7.40 (m, 1H, ArH), 9.64 (brs, 1H, NH), 10.46 (brs, 1H, NH); ^{13}C-NMR (100 MHz, DMSO-d_6) δ: 17.17, 48.36, 51.10, 98.76, 116.70, 116.86, 124.10, 125.06, 132.96, 133.09, 145.82, 165.21, 174.15. HRMS (ESI-TOF): m/z [M$^+$ + H] calcd for $C_{13}H_{13}N_2O_2SF_2$: 299.0668; found 299.0660.

1-(4-(2,3-Difluorophenyl)-6-methyl-2-thioxo-1,2,3,4-tetrahydropyrimidin-5-yl)ethanone (compound **MM 63**). White solid, yield: 61%, IR (υ_{max}/cm^{-1}): 3289, 3177, 3117, 3000, 1607, 1578, 1190; ^{1}H-NMR (400 MHz, DMSO-d_6) δ: 2.18 (s, 3H, CH_3), 2.35 (s, 3H, CH_3CO), 5.56 (d, 1H, J = 3.5 Hz, CH), 7.00-7.06 (m, 1H, ArH), 7.15-7.22 (m, 1H, ArH), 7.31-740 (m, 1H, ArH), 9.71 (brs, 1H, NH), 10.38 (brs, 1H, NH); ^{13}C-NMR (100 MHz, DMSO-d_6) δ: 18.30, 30.52, 48.32, 109.29, 116.68, 116.86, 124.01, 125.05, 132.56, 132.67, 144.99, 174.13, 194.33. HRMS (ESI-TOF): m/z [M$^+$ + H] calcd for $C_{13}H_{13}N_2OSF_2$: 283.0718; found 283.0711.

Ethyl 4-(furan-2-yl)-6-methyl-2-thioxo-1,2,3,4-tetrahydropyrimidine-5-carboxylate (compound **MM 68**). Brown solid, yield: 23%, IR (υ_{max}/cm^{-1}): 3308, 3173, 3126, 2983, 1659, 1573, 1182; ^{1}H-NMR (400 MHz, DMSO-d_6) δ: 1.13 (t, 3H, J = 6.82 Hz, OCH_2CH_3), 2.28 (s, 3H, CH_3), 4.04 (q, 2H, J_1 = 7.17 Hz, J_2 = 3.09 Hz, OCH_2), 5.23 (d, 1H, J = 2.89 Hz, CH), 6.14 (d, 1H, J = 3.16 Hz, ArH), 6.36-6.41 (m, 1H, ArH), 7.58 (brs, 1H, ArH), 9.64 (brs, 1H, NH), 10.398 (brs, 1H, NH); ^{13}C-NMR (100 MHz, DMSO-d_6) δ: 14.07, 17.14, 47.69, 59.62, 98.19, 106.25, 110.50, 142.67, 146.03, 154.57, 174.88.

Methyl 4-(furan-2-yl)-6-methyl-2-thioxo-1,2,3,4-tetrahydropyrimidine-5-carboxylate (compound **MM 88**). Brown solid, yield: 28%, IR (υ_{max}/cm^{-1}): 3309, 3183, 1655, 1569, 1183, 1114; ^{1}H-NMR (400 MHz, DMSO-d_6) δ: 2.28 (s, 3H, CH_3), 3.59 (s, 3H, CH_3OCO), 5.23 (d, 1H, *J* = 3.74 Hz, CH), 6.14 (d, 1H, *J* = 3.12 Hz, ArH), 6.36-6.39 (m, 1H, ArH), 7.58 (brs, 1H, ArH), 9.66 (brs, 1H, NH), 10.42 (brs, 1H, NH); ^{13}C-NMR (100 MHz, DMSO-d_6) δ: 17.18, 47.60, 51.22, 98.01, 106.30, 110.53, 142.74, 146.31, 154.45, 165.30, 174.92.

1-(4-(Furan-2-yl)-6-methyl-2-thioxo-1,2,3,4-tetrahydropyrimidin-5-yl)ethanone (compound **MM 67**). Brown solid, yield: 57%, IR (υ_{max}/cm^{-1}): 3285, 3192, 1606, 1573, 1179, 1012; ^{1}H-NMR (400 MHz, DMSO-d_6) δ: 2.20 (s, 3H, CH_3), 2.30 (s, 3H, CH_3CO), 5.34 (d, 1H, *J* = 3.37 Hz, CH), 6.17 (d, 1H, *J* = 2.53 Hz, ArH), 6.35-6.40 (m, 1H, ArH), 7.59 (brs, 1H, ArH), 9.74 (brs, 1H, NH), 10.35 (brs, 1H, NH); ^{13}C-NMR (100 MHz, DMSO-d_6) δ: 18.20, 30.05, 47.70, 106.51, 108.05, 110.45, 142.80, 145.18, 154.47, 174.83, 194.30.

II.3. Results and discussion

Firstly, fulfilling the initial objective of the project of the research grant, we intended to prepare hybrid AED candidates, combining lamotrigine and several GABA analogues/modulators, including linear (e.g. GABA) and cyclic (e.g. isonipecotic acid) aminoacids as well as sodium valproate, through molecular hybridization. Lamotrigine was chosen because it is a first-line AED with a broad spectrum of action, and acts mainly by voltage-dependent inhibition of sodium channels (Chong and Lerman, 2016). As GABA is a primary neurotransmitter inhibitor playing an important role in the arrest of seizures, the design, synthesis and evaluation of a series of new compounds prepared by a molecular hybridization approach combining lamotrigine with several known GABA analogues/modulators was proposed. However, unfortunately, the chemical synthesis of these molecular hybrids was not well succeeded (Appendix B).

Therefore, based on the chemical structure of lamotrigine, an alternative option was the development of compounds with the dihydropyrimidine nucleus linked to a phenyl ring containing chlorine atoms. This led us to the Biginelli reaction (a MCR), which fulfilled the desired requirements. Additionally, the AEDs in clinical use contain several structural features that could play a role in their pharmacological activity; these aspects were also found in the structures of the tested compounds (as illustrated in Figure II.2).

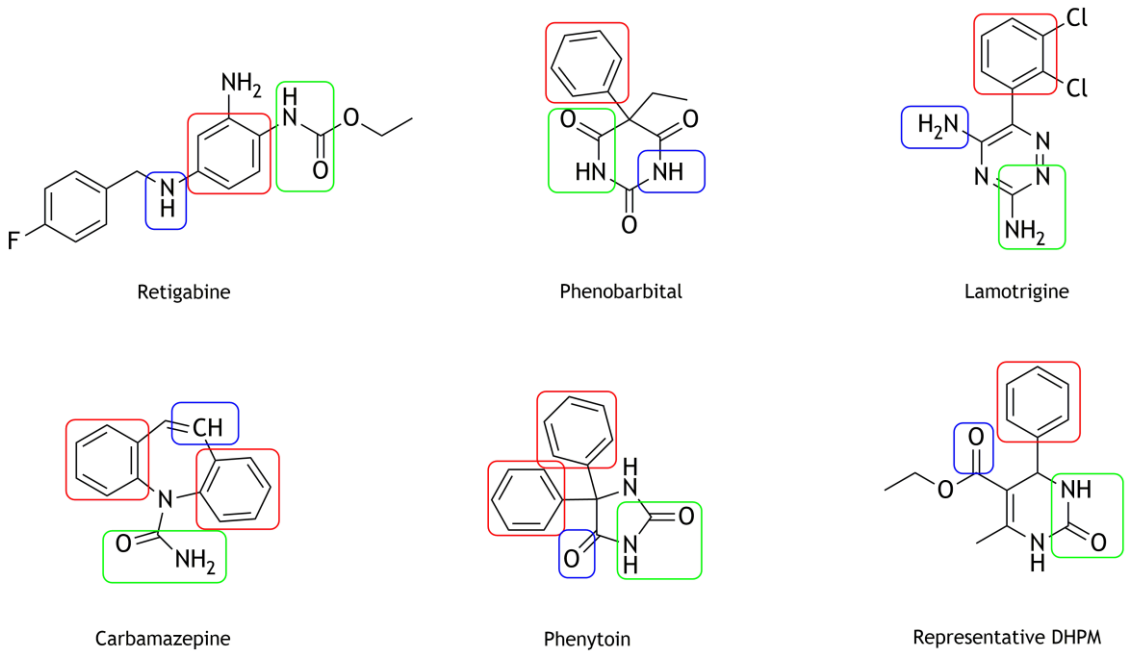

Figure II.2 – Essential pharmacophoric pattern of well-known antiepileptic drugs and a representative dihydropyrimidinone (DHPM): red rectangle represents hydrophobic domain; green rectangle represents hydrogen bond acceptor/donor domain; and blue rectangle represents electron donor moiety.

The use of Biginelli reaction was still reinforced by the advantages of this kind of reaction. In fact, as referred above, the MCRs can provide a diverse spectrum of compounds and have become an active and challenging topic in modern organic and medicinal chemistry. As compared with traditional multioperational synthesis, these one-step reactions exhibit synthetic advantages in regard to simplicity, efficiency, selectivity and can dramatically reduce the generation of chemical waste and costs of starting materials. Additionally, a wide variety of heterocycles with considerable structural complexity can be readily synthesized, resulting frequently in a broad scope of applications (Jiang et al., 2010), such as the discovery and development of new drug candidates for multiple therapeutic purposes.

In this context, twenty "standard" DHPMs (Table II.1), nineteen "standard" DHPMts (Table II.2) and eleven DHPM(t)s combining two heterocyclic rings (Table II.3) were successfully synthesized through the Biginelli reaction, which consisted in a one-pot cyclocondensation reaction among an aldehyde (benzaldehyde, *p*-tolualdehyde, 4-nitrobenzaldehyde, anisaldehyde, 2,3-dichlorobenzaldehyde, 2,4-dichlorobenzaldehyde, 2,3-difluorobenzaldehyde, furaldehyde, 5-methylfuraldehyde, 5-chloro-2-furaldehyde, 2-thiophenaldehyde, 5-chloro-2-thiophenaldehyde and 3-pyridinaldehyde), a ß-ketoester (ethyl acetoacetate and methyl acetoacetate)/acetylacetone and urea or thiourea (Figure II.3). Although many products were found in the literature, this synthetic procedure included other reagents as starting material, being the respective products, which are new to the best of our knowledge, successfully synthesized (compounds **MM 48**, **MM 54**, **MM 58**, **MM 59**, **MM 61**, **MM 63**, **MM 64**, **MM 75**, **MM 86**, **MM 90** and **MM 99**).

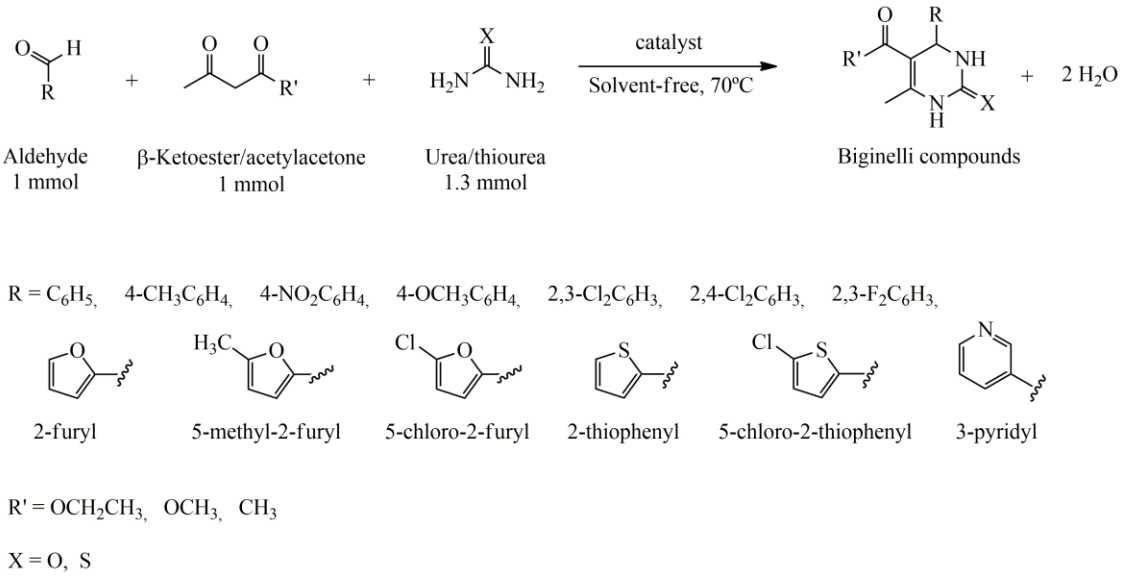

Figure II.3 – General scheme of one-pot synthesis of 3,4-dihydropyrimidin-2-(1*H*)-(thi)ones, under solvent-free conditions. The reaction to synthesize compounds belonging to urea series (X=O) was catalysed by $Bi(NO_3)_3.5H_2O$, while the reaction to synthesize thiourea derivatives (X=S) was catalysed by $ZrCl_4$ (Matias et al., 2016a, 2017a).

After a study of process and a partial optimization of the Biginelli reaction (Appendix A), the final procedure for the DHPMs (urea series) was carried out under solvent-free conditions and the catalyst used to promote the reaction was $Bi(NO_3)_3.5H_2O$, similarly to the reported by Khodaei and collaborators (Khodaei et al., 2004). The bismuth salt was chosen because bismuth compounds have been widely applied in synthetic medicinal chemistry due to the fact that they are economical, nontoxic and easy to handle (Salvador et al., 2012). Moreover, several bismuth salts have been successfully explored as catalysts in Biginelli reaction (Chari et al., 2005; Khodaei et al., 2004; Reddy et al., 2004).

For the series of DHPMs, it was observed that the reactions occurred quickly (5-30 min) and half of them were considered complete in no more than 7 min. In fact, it is described that the Biginelli reaction is usually very rapid, namely when it occurs in solvent-free conditions, and similar results can be found in the literature (Bose et al., 2004; Khodaei et al., 2004). Overall the yields of the reactions were moderate to high and the lowest yields were obtained with the compounds containing halogen atoms in their structures (32-58%, entries 13-20, Table II.1). These results were also in agreement with the works of other authors regarding the good yields obtained for the majority of compounds already described in the literature (Kalita and Phukan, 2007; Salim and Akamanchi, 2011). Regarding some urea derivatives containing chlorine atoms (entries 13-17, Table II.1), a further alternative procedure was employed for their synthesis, as described by Reddy *et al.* (Reddy et al., 2002). Although the longer reaction times (25-48 h *versus* 5-8 min) and the slight reduction of the yields (28-45% *versus* 32-51%), this alternative procedure was employed in the cases where considerable quantities

of the compounds were needed for the *in vivo* experiments and little impurities were present in NMR spectra of the compounds produced by the general procedure.

Table II.1 – $Bi(NO_3)_3.5H_2O$-catalyzed synthesis of 3,4-dihydropyrimidin-2-(1*H*)-ones under solvent-free conditions at 70 ºC.[a]

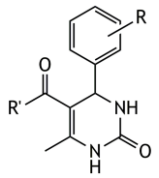

Entry	Compound	R	R'	Time (min)	Yield[b,c] (%)
1	**MM 18**	H	OCH_2CH_3	7	81
2	**MM 72**	H	OCH_3	14	80
3	**MM 17**	H	CH_3	6	93
4	**MM 22**	4-CH_3	OCH_2CH_3	12	74
5	**MM 73**	4-CH_3	OCH_3	9	72
6	**MM 19**	4-CH_3	CH_3	7	60
7	**MM 23**	4-NO_2	OCH_2CH_3	5	67
8	**MM 82**	4-NO_2	OCH_3	8	61
9	**MM 24**	4-NO_2	CH_3	5	71
10	**MM 34**	4-OCH_3	OCH_2CH_3	7	79
11	**MM 74**	4-OCH_3	OCH_3	7	81
12	**MM 35**	4-OCH_3	CH_3	30	64
13	**MM 55**	2,3-Cl_2	OCH_2CH_3	8	32 (28)[d]
14	**MM 54**	2,3-Cl_2	CH_3	8	45 (37)[d]
15	**MM 57**	2,4-Cl_2	OCH_2CH_3	5	46
16	**MM 81**	2,4-Cl_2	OCH_3	6	51 (45)[d]
17	**MM 56**	2,4-Cl_2	CH_3	5	50
18	**MM 59**	2,3-F_2	OCH_2CH_3	5	37
19	**MM 75**	2,3-F_2	OCH_3	8	58
20	**MM 58**	2,3-F_2	CH_3	7	52

[a]Reaction conditions: aldehyde (1 mmol), ß-ketoester/acetylacetone (1 mmol), urea (1.3 mmol) and $Bi(NO_3)_3.5H_2O$ (10 mol%) at 70ºC.
[b]Yields of isolated pure products after purification.
[c]All products were characterised by ^1H- and ^{13}C-NMR, IR spectra and compared with available data in the literature. The new products were also characterised by HRMS.
[d]Yields obtained through the alternative procedure.

Following the procedure proposed by Rodríguez-Domínguez and collaborators (Rodríguez-Domínguez et al., 2007), several DHPMts (thiourea series) were also synthesized, using $ZrCl_4$ as catalyst and, similarly to DHPM, the reactions were considered concluded when solidified. The catalysts used were different in the two series because initial experimental reactions (Appendix A) showed that the catalyst $Bi(NO_3)_3.5H_2O$ was ineffective in the production of the DHPMts, which was in accordance with the literature (Khodaei et al., 2004). Generally, these reactions were very fast; however, particularly in the case of the products containing halogens (entries 11-19, Table II.2), longer times were needed to obtain complete reactions and, in some of them, lower yields were observed compared with the respective analogues of the urea series. These low yields could be related with the high lipophilicity of these compounds as well as with the substituents in *ortho* position, which can partially provide steric hindrance. Interestingly, the DHPMts synthesized using acetylacetone (entries 3, 6, 7,

10, 13, 16 and 19, Table II.2) as reagent were generally obtained with higher yields than the respective analogues with longer lateral chains.

Table II.2 – $ZrCl_4$-catalyzed synthesis of 3,4-dihydropyrimidin-2-(1*H*)-thiones under solvent-free conditions at 70 ºC.[a]

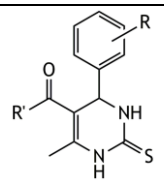

Entry	Compound	R	R'	Time	Yield (%)[b,c]
1	**MM 26**	H	OCH_2CH_3	14 min	70
2	**MM 83**	H	OCH_3	15 min	60
3	**MM 25**	H	CH_3	8 min	80
4	**MM 28**	4-CH_3	OCH_2CH_3	21 min	44
5	**MM 84**	4-CH_3	OCH_3	10 min	33
6	**MM 29**	4-CH_3	CH_3	7 min	50
7	**MM 30**	4-NO_2	CH_3	35 min	17
8	**MM 36**	4-OCH_3	OCH_2CH_3	58 min	79
9	**MM 85**	4-OCH_3	OCH_3	43 min	31
10	**MM 37**	4-OCH_3	CH_3	1 h 40 min	89
11	**MM 46**	2,3-Cl_2	OCH_2CH_3	45 min	21
12	**MM 90**	2,3-Cl_2	OCH_3	4 h	19
13	**MM 48**	2,3-Cl_2	CH_3	1 h	47
14	**MM 60**	2,4-Cl_2	OCH_2CH_3	17 h	19
15	**MM 92**	2,4-Cl_2	OCH_3	3 h	34
16	**MM 64**	2,4-Cl_2	CH_3	6 h	42
17	**MM 61**	2,3-F_2	OCH_2CH_3	7 h	16
18	**MM 86**	2,3-F_2	OCH_3	1 h	19
19	**MM 63**	2,3-F_2	CH_3	15 min	61

[a]Reaction conditions: aldehyde (1 mmol), ß-ketoester/acetylacetone (1 mmol), thiourea (1.3 mmol) and $ZrCl_4$ (5 mol%) at 70 ºC.
[b]Yields of isolated pure products after purification.
[c]All products were characterised by ^{1}H- and ^{13}C-NMR and IR spectra and compared with available data in the literature. The new products were also characterised by HRMS.

As stated before, heterocycles are present in a large variety of organic molecules with chemical, biomedical, and industrial interest. They are among the most frequently encountered scaffolds in drugs and pharmaceutically relevant substances. As previously reported, the large majority of the anticonvulsant pharmacophores (many of them present in the structures of the approved AEDs) have at least one heterocycle, which can display a role in the anticonvulsant activity. For this reason, several Biginelli products were developed incorporating a second heteroaromatic ring. Either five-membered heterocycles bearing one heteroatom (furan and thiophene) or six-membered *N*-heterocycle (pyridine) were included in this study (Table II.3). When the furan ring was introduced, it was observed that the reactions were slower in the case of the thiourea series and the yields were lower than the obtained with their urea analogues. This motivated us to synthesize the remaining heterocycles, using urea as reactant. Within these, compound **MM 95** (pyridine derivative) was the product that needed the longest reaction time (46 h). Contrarily to other compounds, this product dissolved in water during the work up step. For this reason, the processing of the reaction

needed to be optimized, resulting in the chemical synthesis procedure described in section II.2.2 (*Procedure for the synthesis of **MM 95***).

Table II.3 – Synthesis of 3,4-dihydropyrimidin-2-(1*H*)-(thi)ones including two heterocycles under solvent-free conditions at 70 ºC.[a]

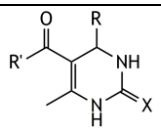

Entry	Compound	R	R'	X	Time	Yield (%)[b,c]
1	**MM 65**	2-furyl	OCH_2CH_3	O	13 min	81
2	**MM 68**	2-furyl	OCH_2CH_3	S	60 min	23
3	**MM 76**	2-furyl	OCH_3	O	12 min	74
4	**MM 88**	2-furyl	OCH_3	S	60 min	28
5	**MM 66**	2-furyl	CH_3	O	18 min	76
6	**MM 67**	2-furyl	CH_3	S	60 min	57
7	**MM 93**	5-methylfuryl	OCH_2CH_3	O	10 min	69
8	**MM 95**	3-pyridil	OCH_2CH_3	O	46 h	36
9	**MM 96**	2-thiophenyl	OCH_2CH_3	O	8 min	83
10	**MM 99**	5-chlorofuryl	OCH_2CH_3	O	12 min	67
11	**MM 106**	5-chlorothiophenyl	OCH_2CH_3	O	15 min	81

[a]Reaction conditions: aldehyde (1 mmol), ß-ketoester/acetylacetone (1 mmol), urea/thiourea (1.3 mmol) and $Bi(NO_3)_3.5H_2O$ (10 mol%) for urea series and $ZrCl_4$ (5 mol%) for thiourea series at 70 ºC.
[b]Yields of isolated pure products after purification.
[c]All products were characterised by ^1H- and ^{13}C-NMR and IR spectra and compared with available data in the literature. The new products were also characterised by HRMS.

Other aldehydes (2-pyrrolealdehyde and 3-indolealdehyde), which were selected because of the potential interest of pyrrole and indole as anticonvulsant pharmacophores (Wei et al., 2015), were also used as initial reactants to synthesize DHPM(t)s including these different heterocycles. Several conditions were applied beyond the general procedure. Using 3-indolealdehyde as starting material, the alternative procedure (experimental section) as well as the use of another catalyst [cerium (III) chloride heptahydrate] were tested, according to what was described in the literature (Shanmugam et al., 2007). In the case of 2-pyrrolaldehyde as reagent, the product (a robust black "stone") was formed in seconds after the addition of the catalyst (general procedure). Although the efforts in the step of recrystallization, plus mechanical strength, the product did not dissolve or split. For this reason, new reactions without or with solvent (ethanol) and both without catalyst were performed. Unfortunately, the products incorporating these two interesting heterocycles were not synthesized with success as demonstrated by NMR spectra.

Several other efforts were also performed in order to synthesize additional Biginelli adducts or Biginelli-like compounds structurally closer to lamotrigine. However, the desired products were not successfully synthesized (Appendix C).

It is noteworthy that the reactions described for the production of the compounds successfully synthesized involved a true one-pot procedure without intermediate work up or solvent change (alternative procedure); indeed, the products incorporated essentially all of the atoms of the reactants, with the exception of the small condensation product (water

molecules) and involved only inputs that could be independently varied. In addition, the majority of the reactions did not require organic solvents and one liquid reactant (usually the ß-ketoester/acetylacetone and some aldehydes) directly served as the reaction medium. Thus, this type of reaction offered important opportunities for synthesis of both chemically and medicinally useful compounds, having environmentally friendly characteristics and employing the green chemistry principles (Narahari et al., 2012).

Overall, twenty-eight DHPMs and twenty-two DHPMts were successfully synthesized through the fast and simple Biginelli reaction. These synthesized and characterised compounds were further submitted to pharmacological evaluation as described in the next chapters.

CHAPTER III

IN VIVO STUDIES:

Selection of delivery vehicle

III.1. Introduction

In the discovery and development of new drug candidates the solubility of the test compounds is one of the physicochemical properties that must be considered and assessed since the early stages of the drug research (Caron and Ermondi, 2017). Indeed, nowadays, it is widely accepted by the scientific community that solubility of the drug compounds, especially its aqueous solubility, is a major indicator for the drug dissolution in physiological fluids, which is the limiting step for drug absorption and consequently to achieve the pharmacological activity (Di et al., 2012; Stegemann et al., 2007). In fact, even for first *in vivo* preclinical screening studies a suitable formulation strategy is required in order to enable an appropriate administration of the test compounds with acceptable tolerability and maintaining the stability for a sufficient period of time with no adverse effects in animal tests that could be attributed to the delivery vehicles (Banfor et al., 2016; Gad et al., 2006). Particularly, when the compound of interest is developed to act in the CNS, its solubility is a very relevant challenge because, usually, is necessary a considerable degree of lipophilicity to cross the BBB. In this context, the selection of the administration/delivery vehicle to be employed for solubilisation/suspension of test compounds continues to be a challenge in order to appropriately conduct pharmacokinetics and/or pharmaco-toxicological experiments in *in vivo* conditions.

Whenever possible, the choice of the delivery/administration vehicle falls in isotonic physiological saline solutions which are considered innocuous vehicles. However, often, the test compounds are not soluble in this type of aqueous solvents due to their intrinsic lipophilicity and other options have to be considered. Dimethyl sulfoxide (DMSO), a polar organic solvent, often emerges as a relevant alternative, and many studies about its pharmacological and toxicological effects have been carried out over the years (Galvao et al., 2014; Larsen et al., 1996; Santos et al., 2003). Indeed, DMSO has been frequently included in different percentages in the administration vehicles of compounds tested in whole-animal assays (Li et al., 2013; Mozaffari et al., 2012; Wang et al., 2014). Other examples of delivery vehicles widely used in different formulations by pharmaceutical industry are propylene glycol (PG) (Auta et al., 2010) and polyethylene glycol (PEG) (Amir et al., 2013; Goodfellow et al., 2013), which have the advantages of being soluble in polar and non-polar solvents and are quite inexpensive. In addition, they have been considered non-toxic (Abbasi et al., 2014; Vafaeezadeh and Hashemi, 2015). Furthermore, carboxymethylcellulose (CMC) is also one of the most commonly used biopolymers in biomedical applications because it is considered environmentally friendly and non-toxic (Bao et al., 2014; Thore et al., 2015; Yang et al., 2015).

The preclinical assessment of the “minimal neurological deficit” in rodents (mice and rats) is an essential task in primary and secondary pharmacological screening either in the early stages of drug development of new CNS-active drugs to screen out less promising compounds

(Amenta et al., 2012; Cao et al., 2016; Harada et al., 2017; Torregrosa et al., 2015; Zhang et al., 2014) or also during the safety evaluation of peripheral-acting drugs in order to investigate adverse/toxic effects that could later cause impairments (Bagal and Bungay, 2014; Harford-Wright et al., 2010; Hasebe et al., 2008). Overall, the rotarod performance test has been widely used to indirectly assess the minimal neurological deficit in rodents induced by test compounds through the evaluation of the impairment of functions of balance and/or motor coordination. This behavioural assay has gained increasing importance in the discovery and development programmes of new drug candidates as it is very simple to perform and allows the evaluation of a large set of compounds and/or formulation vehicles. Furthermore, the rotarod performance test is a versatile whole-animal assay that can be used for the assessment of any new molecular entity, regardless of its therapeutic area (Kikuchi et al., 2013).

An analysis of the literature concerning the solvents and/or mixtures of solvents that have been used to evaluate potential anticonvulsant compounds in the *gold standard* assays of efficacy (MES and scPTZ models) and toxicity (rotarod test) (Amir et al., 2013; Kshirsagar et al., 2009; Kumar et al., 2013; Mozaffari et al., 2012) revealed that the impact of the administration vehicles on the obtained results has not been clearly evaluated and discussed. Although the influence of the delivery vehicle may be negligible in many pharmaco-toxicological assays, we suspected that this might not be the case in more sensitive behavioural assays, such as the rotarod performance test aimed at detecting minimal neurological deficit. Thus, the aim of this study was to assess the minimal neuromotor impairment (neurotoxicity) induced by a set of the most common vehicles and their mixtures using the rotarod performance test.

III.2. Experimental section

III.2.1. Chemicals and reagents

DMSO, CMC sodium and PG were obtained from Sigma (St. Louis, MO, USA). Sodium chloride (NaCl) 0.9% was obtained from B. Braun (Bethlehem, PA, USA). PEG-400 was obtained from Merck Schuchardt (Hohenbrunn, Germany).

III.2.2. Animals

Adult male CD-1 mice, aged between 6-7 weeks, were obtained from local certified animal facilities (Faculty of Health Sciences of the University of Beira Interior, Covilhã, Portugal). Four mice per cage were housed under controlled environmental conditions [12 h light/dark cycle (lights on at 8:00 AM) at 20 ± 2 ºC and relative humidity 50 ± 5%] with free access to tap

water and standard rodent diet (4RF21, Mucedola, Italy). All experimental and care procedures were conducted in accordance with the European Directive (2010/63/EU) regarding the protection of laboratory animals used for scientific purposes.

III.2.3. Administration/delivery vehicles

Mice were intraperitoneally injected with each delivery/administration vehicle (10 µL/g of body weight). The vehicles assessed included the individual solvents (DMSO, NaCl 0.9%, CMC 0.5%, PEG-400 and PG) and also solutions of NaCl 0.9%, CMC 0.5%, PEG-400 and PG containing 5% and 10% DMSO. Formulations of CMC 0.5% containing 20, 30 and 50% of DMSO were also evaluated.

III.2.4. Minimal motor impairment (rotarod) test

Minimal motor impairment was established in mice by standard rotarod performance assay as previously reported (Pandeya et al., 2000). Mice were previously trained to balance on an accelerating rotarod apparatus (rod diameter: 3 cm) that rotated at a constant speed of 10 revolutions per minute (Rota-rod, Ugo Basile, Varese, Italy). During the training sessions, the animals were placed on the rotating rod at least three consecutive trials for 90 s. On the day of the test, trained mice were injected with each delivery/administration vehicle and the motor/neurological toxicity was indicated by the inability of the animals to maintain equilibration on the rod for at least 60 s (primary endpoint). The mice were placed on the rod at predefined time-points (0.5 h, 1 h, 1.5 h, 2 h, 2.5 h, 3 h, 3.5 h and 4 h) after the administration of each vehicle and fall off time was recorded (n = 4 per group). In this assay the number of animals that performed the test with success (primary endpoint) was recorded and, additionally, it was also obtained the number of seconds that each animal remained on the rod (secondary endpoint).

III.2.5. Statistics

Data were reported as the mean ± standard error of the mean. Comparison among groups was analysed by using the one-way ANOVA with the post hoc Dunnett's multiple comparison test to judge significance of the observed effect. Differences were considered statistically significant for a p-value lower than 0.05 ($p < 0.05$).

III.3. Results and discussion

In this study, different administration vehicles were evaluated, which were chosen based on their potential usefulness for the solubilisation/suspension and delivery of drug candidates in the first steps of nonclinical *in vivo* pharmaco-toxicological assays. The evaluation of the neurotoxic effects of the test set of administration vehicles was performed by means of the rotarod assay that has proved to have a remarkable value in the screening of potential side effects of drugs or drug candidates in the CNS, which are manifested on the balance and motor coordination required to successfully achieve the primary endpoint of the assay. In this comparative study we evaluated not only the potential neurotoxicity of the vehicles themselves (NaCl 0.9%, DMSO, PEG-400, PG and CMC 0.5%) but also solutions of these vehicles with different percentages of DMSO (5% and 10%).

Regarding the discovery and development of new drug candidates, DMSO has become the solvent of choice to dissolve potential neuroprotective and neurotoxic hydrophobic substances used in both biological and medical research (Yuan et al., 2014). It has been suggested that DMSO can be safely used, being generally well-tolerated by the experimental animals (Authier et al., 2002; Bakar et al., 2012). However, there are also several case reports revealing severe neurotoxicity associated with DMSO, indicating the importance of its careful use in certain circumstances, including as administration vehicle, to avoid confounding factors that can bias the study results and lead to seriously erroneous conclusions (Cavaletti et al., 2000; Hanslick et al., 2009; Yuan et al., 2014). Because of these contradictions and the established importance of this solvent as drug vehicle, it was of high interest to evaluate its neurological toxicity in *in vivo* nonclinical studies using the rotarod performance test. Thereby, it was verified that the administration of a vehicle (10 µL/g) consisting of 100% DMSO originates motor impairment (a surrogate of neurotoxicity or minimal neurological deficit) on the rotarod assay, with animals falling from the rod at all post-dose time-points considered in the study (Table III.1). In addition, it was observed that, at the first time-points, the animals receiving vehicles (10 µL/g) containing PEG-400 showed a notable toxicity, but at 4 h after the intraperitoneal injection, 100% of the animals successfully reached the primary endpoint of the assay. On the other hand, until 2.5 h after the injection of the vehicles containing PG, 75-100% of the mice showed inability to maintain equilibration on the rod for at least 60 s (primary endpoint). Moreover, considering the evaluation data for PG, it was verified that the animals receiving this delivery vehicle containing 10% of DMSO recovered the motor coordination faster than the animals receiving only PG or PG with 5% of DMSO (neurotoxicity in 25% *versus* 75-100% of the animals at 4 h).

Table III.1 – Time-course of minimal neurological impairment (neurotoxicity) of the vehicles administered intraperitoneally to mice in the rotarod performance test (number of animals exhibiting neurological impairment/number of animals tested).

Vehicle	0.5 h	1 h	1.5 h	2 h	2.5 h	3 h	3.5 h	4 h
DMSO	4/4	4/4	4/4	4/4	4/4	3/4	3/4	3/4
NaCl 0.9%	0/4	0/4	0/4	0/4	0/4	0/4	0/4	0/4
NaCl 0.9%/DMSO (95%/5%, *v*/*v*)	0/4	0/4	0/4	0/4	0/4	0/4	0/4	0/4
NaCl 0.9%/DMSO (90%/10%, *v*/*v*)	0/4	0/4	0/4	0/4	0/4	0/4	0/4	0/4
PEG-400	4/4	4/4	4/4	3/4	2/4	1/4	1/4	0/4
PEG-400/DMSO (95%/5%, *v*/*v*)	4/4	3/4	3/4	3/4	1/4	0/4	0/4	0/4
PEG-400/DMSO (90%/10%, *v*/*v*)	4/4	3/4	2/4	2/4	2/4	0/4	0/4	0/4
PG	4/4	4/4	4/4	4/4	4/4	4/4	4/4	3/4
PG/DMSO (95%/5%, *v*/*v*)	4/4	4/4	4/4	4/4	4/4	4/4	4/4	4/4
PG/DMSO (90%/10%, *v*/*v*)	4/4	4/4	3/4	3/4	3/4	2/4	1/4	1/4
CMC 0,5%	0/4	0/4	0/4	0/4	0/4	0/4	0/4	0/4
CMC 0.5%/DMSO (95%/5%, *v*/*v*)	0/4	0/4	0/4	0/4	0/4	0/4	0/4	0/4
CMC 0.5%/DMSO (90%/10%, *v*/*v*)	0/4	0/4	0/4	0/4	0/4	0/4	0/4	0/4
CMC 0.5%/DMSO (80%/20%, *v*/*v*)	0/4	0/4	0/4	0/4	0/4	0/4	0/4	0/4
CMC 0.5%/DMSO (70%/30%, *v*/*v*)	0/4	0/4	0/4	0/4	0/4	0/4	0/4	0/4
CMC 0.5%/DMSO (50%/50%, *v*/*v*)	0/4	0/4	0/4	0/4	0/4	0/4	0/4	0/4

CMC, carboxymethylcellulose; DMSO, dimethyl sulfoxide; PEG-400, polyethylene glycol-400; PG, propylene glycol.

Besides the number of animals that achieve with success the primary endpoint of the rotarod performance test (maintaining equilibrium on the rod for at least 60 s), it was also recorded the exact time in seconds (secondary endpoint) that each animal remained on the rod during the time set for the test. The results are illustrated in Figure III.1. As can be seen, at the first time-points of the study it is possible to notice that the toxicity triggered by the pure DMSO was lower than the observed with PEG-400 alone (1 h) and with formulations containing PG.

Concerning the reasons explaining the DMSO-induced neurotoxicity, some evidence suggest that its mechanism of toxicity can involve neurophysiological and pathological changes including myelin disruption and uncompacted myelin lamelle (Cavaletti et al., 2000). In addition, DMSO could also be able to produce widespread, dose-dependent neurodegeneration in the developing mouse brain at several ages and this toxicity probably results from a direct cellular effect. Furthermore, the DMSO-induced apoptosis might produce significant learning and memory deficits (Hanslick et al., 2009). However, these studies just had focus on chronic neurotoxicity exhibited by DMSO and they probably could not explain the acute toxicity observed in this preliminary research.

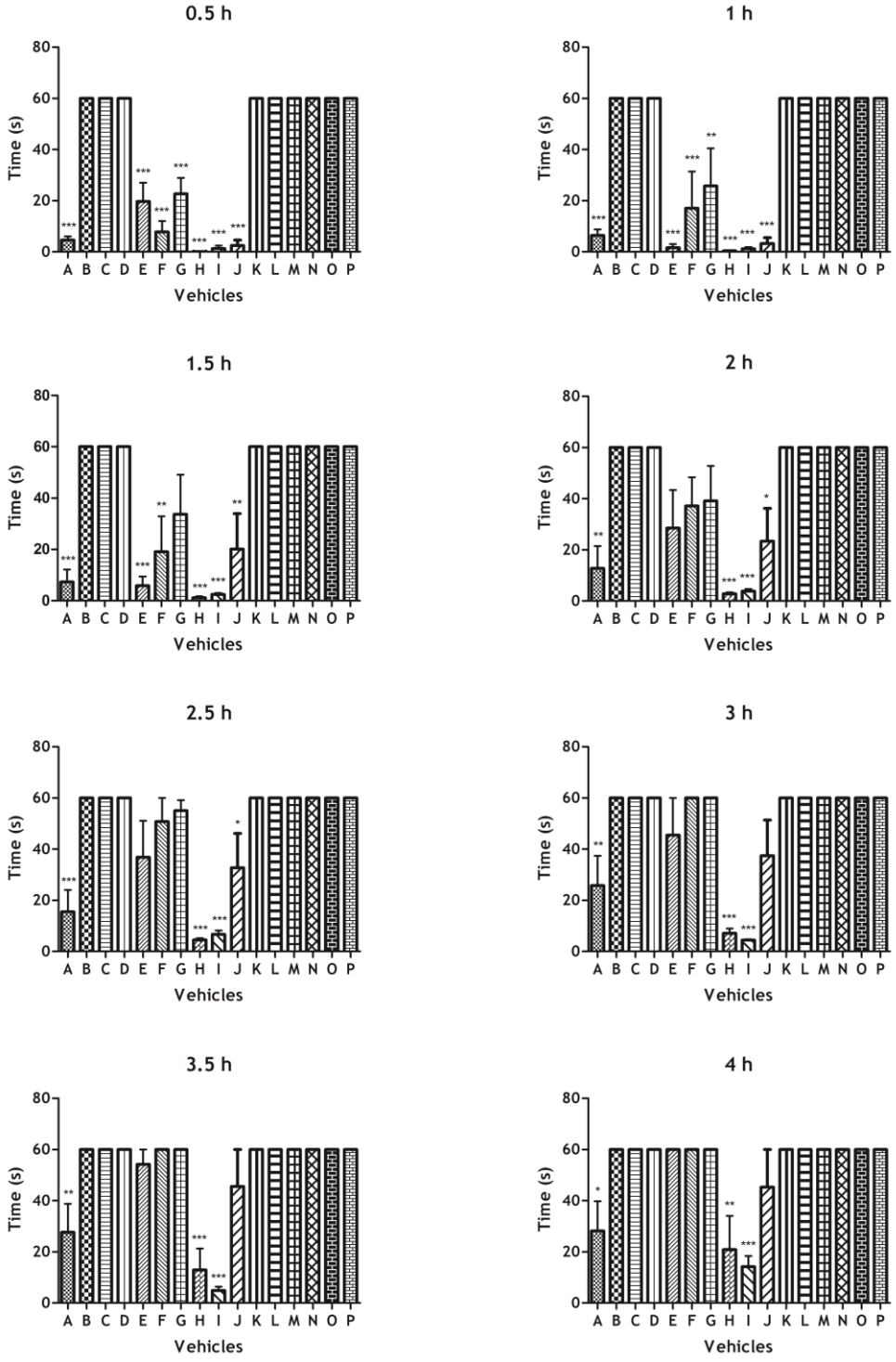

Figure III.1 – Effect of the vehicles during 4 hours and evaluated each thirty minutes. Data are presented as the mean ± standard error of the mean (n = 4). Mice were intraperitoneally administration of each vehicle: **A**, DMSO; **B**, NaCl 0.9%; **C**, NaCl 0.9%/DMSO (95%/5%); **D**, NaCl 0.9%/DMSO (90%/10%); **E**, PEG-400; **F**; PEG-400/DMSO (95%/5%); **G**, PEG-400/DMSO (90%/10%); **H**, PG; **I**, PG/DMSO (95%/5%); **J**, PG/DMSO (90%/10%); **K**, CMC 0.5%; **L**, CMC 0.5%/DMSO (95%/5%); **M**, CMC 0.5%/DMSO (90%/10%); **N**, CMC 0.5%/DMSO (80%/20%); **O**, CMC 0.5%/DMSO (70%/30%); **P**, CMC 0.5%/DMSO (50%/50%). *p < 0.05, **p < 0.01, ***p < 0.001 compared to control group (**B**).

In this study, it was also observed that all solutions of PG possibly reached the brain rapidly because a strong neuromotor impairment in rotarod performance test was noted. Particularly, the vehicles consisting of PG (100%) and PG/DMSO (95%/5%, *v*/*v*) in all steps of the study led to higher neuromotor impairment than the observed with DMSO (100%). On the other hand, although the solution of PG/DMSO (90%/10%, *v*/*v*) led to evident neuromotor deficit in the early steps of the study, the recovery of the animals was faster than those receiving DMSO and the other vehicles containing PG. As demonstrated for DMSO, PG also has been suggested to produce apoptotic neurodegeneration in a dose-dependent manner. Furthermore, the observed damage was dependent on age at the time of exposure and probably PG does not produce damage through GABA receptors. It is still unknown whether apoptosis results in long-term cognitive and behavioural abnormalities (Lau et al., 2012).

After the administration of the PEG-400–containing formulations, interestingly, it was verified that with the increase of the DMSO percentage in the vehicle, the neuromotor toxicity seems to be reduced. In fact, 3 hours after the administration of PEG-400 with the highest percentage of DMSO (10%) all the animals performed the test without any evident neuromotor deficit. Actually, DMSO was reported as having anti-nociceptive and anti-inflammatory effects in male CD-1 mice when given orally (10 mL/kg) or by intracerebroventricular route (5 µL/mouse) (Colucci et al., 2008), which could be a possible explanation for our results. Regarding the PG-containing vehicles, another possible explanation for the neuromotor toxicity observed could be associated with the hyperosmolality effects and increase of the anion gap metabolic acidosis (due to lactic acidosis) that was observed in humans. For instance, after an injection of lorazepam was observed that PG had a much greater contribution than PEG for the hyperosmolar metabolic acidosis (Zar et al., 2007). This information can be useful to understand the differences between PG and PEG-400 in our results.

Moreover, it should be highlighted that after the injections of PEG-400, PG and DMSO (100%) hypoactivity and immobility was noticed in the animals, which was consequently expressed in the performance on the rod. These results were in accordance with the observations of a previous study which analysed several solvents administered intravenously in female CD-1 mice, which aimed to understand the tolerability and recommended solvent dose limits for pharmacokinetic studies (Thackaberry et al., 2014).

Independently of the causes underlying the neuromotor toxicity observed with these delivery vehicles, this preliminary study showed that their use to evaluate the neurotoxicity of new drug candidates through the rotarod assay can be debatable. In fact, during the revision of literature, it was frequently found the usage of PEG-400 (100%) (Alam et al., 2010; Amir et al., 2013; Kashaw et al., 2009; Kumar et al., 2013) and even DMSO (100%) (Dawood et al., 2006; Mozaffari et al., 2012) as vehicles to assess the neurotoxicity of new AED candidates administered intraperitoneally, using the rotarod test. It was surprising the fact that the majority of the animals injected with testing compounds have been reported as exhibiting no

deficit motor at least at some doses tested, when this preliminary study showed that these vehicles have a huge toxicity themselves, which certainly would influence the results.

However, on the other hand, all vehicles containing NaCl 0.9% and CMC 0.5% with or without DMSO (5 and 10%) did not produce any motor impairment. Probably this occurred due to the fact that these vehicles consisted in aqueous solvents and, therefore, they seem to be the safest whenever they can be considered. Particularly, the vehicles containing CMC 0.5%, with a little percentage of DMSO may offers a good option to formulate compounds that show poor solubilisation in NaCl 0.9% solutions. This motivated us to evaluate vehicles with higher percentages of DMSO (20, 30 and 50%) and the results were identical, with all the trained animals performing the test successfully.

Hence, the vehicle selected as appropriate for the initial screening of the synthesized compounds against the minimal neurological impairment (neurotoxicity) in the rotarod assay was CMC 0.5%/DMSO (50%/50%, *v*/*v*).

CHAPTER IV

IN VIVO STUDIES:

Anticonvulsant evaluation and neurotoxicity

IV.1. Introduction

Epilepsy is a complex disorder of the brain function that affects around 60 million people worldwide (Shetty and Upadhya, 2016) and has a considerable impact in the patients' quality of life (Hosseini et al., 2016). A range of structurally diverse drugs is currently used for controlling both convulsive and non-convulsive epileptic seizures, which act through several molecular mechanisms and have different efficacy, pharmacokinetic and safety profiles (Santulli et al., 2016). Nevertheless, despite the availability of many AEDs already in clinical use, just 60–70% of the patients with epilepsy remains seizure-free when properly treated with current drugs (Bidwell et al., 2015). Therefore, the development of safer and more effective AEDs is critical and remains a challenge for medicinal chemists (Dalkara and Karakurt, 2012; Kowski et al., 2016).

In the process of discovery and development of new drug candidates, heterocyclic nucleus has received considerable attention in almost all drug classes (Taylor et al., 2016). In fact, there are several reports associating diverse heterocyclic systems, including pyrimidine ring systems, with anticonvulsant effects (Asif, 2015; Nusrat et al., 2014). In this context, the Biginelli reaction is a prominent MCR that offers a straightforward approach to produce multifunctionalized dihydropyrimidines and related heterocyclic compounds (Kappe, 2003). Although this interesting chemical reaction has remained underexploited for decades, it gained prominence in the early 1990s with the advent of combinatorial chemistry, since this type of reaction was considered ideal to prepare large compound libraries in medicinal chemistry endeavours. Currently, the Biginelli scaffold has shown great pharmaceutical value and, for this reason, the search for novel dihydropyrimidines with important biological properties has been under intensive exploitation (Kaur et al., 2017). Indeed, several members of this class of heterocycles have shown anticancer (Sośnicki et al., 2014), anti-malarial (Chiang et al., 2009), antifungal and antibacterial (Ghodasara et al., 2013; Godhani et al., 2014), and antithyroid (Lacotte et al., 2013) properties. Additionally, some of these compounds have also been shown to inhibit human immunodeficiency virus replication (Kim et al., 2012), antagonize melanin concentrating hormone receptor (Goss and Schaus, 2008), and have hyaluronidase (Gireesh et al., 2013) and ß-glucuronidase (Ali et al., 2016) inhibitory properties. Regarding CNS disorders, several Biginelli derivatives have been developed as inhibitors of the acetylcholinesterase enzyme, which represents an important therapeutic target for Alzheimer's disease (Arunkhamkaew et al., 2013). Moreover, there are some reports describing the antioxidant activity of this type of molecules (Da Silva et al., 2012; Gangwar and Kasana, 2012) and also a potential role in the treatment of Parkinson's disease (Kang et al., 2013). Concerning their potential anticonvulsant activity, up to date, to the best of our knowledge, only one *in vitro* study showed the ability of these compounds to modulate the GABAergic system (Lewis et al., 2010).

Taking into consideration the value of DHPM(t)s scaffolds, this work aimed to find novel anticonvulsant drug candidates structurally related to lamotrigine (Figure I.18). Thus, after the synthesis of the Biginelli products, their anticonvulsant properties were screened against rodent models of electrically and chemically-induced seizures, the MES test and the scPTZ seizure test, respectively. Moreover, the neurotoxicity of these compounds was also explored *in vivo* on the rotarod performance test.

IV.2. Experimental section

IV.2.1. General remarks

Anticonvulsant activity and minimal motor impairment evaluation were performed based on the procedures of the Anticonvulsant Screening Program pursued originally in the NINDS, National Institute of Health, Rockville, USA (NINDS, 2016). The initial screening studies were carried out in adult male CD-1 mice (25-40 g) and involved the use of the MES and scPTZ tests for anticonvulsant activity and the rotarod test to identify minimal motor and/or neurological impairment. Additionally, the most promising compounds identified as anticonvulsants in mice were further tested in adult male Wistar rats (350-450 g). The animals were obtained from local certified animal facilities (Faculty of Health Sciences, University of Beira Interior, Covilhã, Portugal) and they were kept in cages and housed under controlled environmental conditions (12 h light/dark cycle at 20 ± 2 ºC and relative humidity 50 ± 5%) with free access to tap water and standard rodent diet (4RF21, Mucedola, Italy). All experimental and care procedures were conducted in accordance with the European Directive (2010/63/EU) regarding the protection of laboratory animals used for scientific purposes.

In the initial screening experiments conducted in mice, the compounds to be tested were incorporated in the selected vehicle constituted by CMC 0.5%/DMSO (50%/50%, *v*/*v*) and were injected intraperitoneally (10 μL/g). Mice were administered with doses of 30, 100 and 300 mg/kg (test compounds, lamotrigine, carbamazepine, phenytoin and sodium valproate) and 0.1 and 0.3 mg/kg (clonazepam) (Bum et al., 2009), and then, the anticonvulsant activity and neurotoxicity was assessed at 0.5 and 4 h after injection. Lamotrigine, carbamazepine, phenytoin and sodium valproate were also tested in the MES and clonazepam and lamotrigine were also assayed against scPTZ test as standard drugs (positive controls). All the aforementioned drugs were also evaluated as positive controls in the rotarod assay. The vehicle itself was tested in a similar amount (10 μL/g) as negative control.

In the experiments performed in rats, the selected compounds and lamotrigine (as positive control) were further evaluated in the MES test at 0.5, 2 and 4 h after the oral administration of a dose of 30 mg/kg (10 mL per kg body weight); in this case the vehicle was constituted by 0.5% CMC/DMSO (95%/5%, *v*/*v*).

IV.2.2. Maximal electroshock seizure test

The MES test was performed according to procedures already described (Ibrahim et al., 2015; Kumar et al., 2011). Briefly, the animals received an electrical stimulus of suprathreshold current (50 mA, 60 Hz, 0.2 s for mice and 150 mA, 60 Hz, 0.2 s for rats) delivered by the electroconvulsometer (ECT Unit, Ugo Basile, Varese, Italy) to induce maximal seizures. Electroconvulsions were produced with the use of auricular electrodes in mice and corneal electrodes in rats. The auricular electrodes were placed in 0.9% NaCl solution before application. In the case of corneal stimulation, a drop of an ocular electrolyte solution containing oxybuprocaine hydrochloride as anaesthetic agent (Anestocil™, eye drop solution 4 mg/mL) was applied in the eyes of rats immediately before the electrical stimulus. The endpoint was the tonic extension of the hind limbs (Figure IV.1). In the negative control group, the procedure caused immediate hind-limb tonic extension. Animals not displaying hind-limb tonic extension were considered to be protected from seizure.

Figure IV.1 – Representative image of the endpoint (tonic extension of the hind limbs) in the maximal electroshock seizure test in mice. Image collected after the electric stimulation of a mouse 0.5 h after intraperitoneal administration of the negative control (vehicle).

IV.2.3. Subcutaneous pentylenetetrazole seizure test

PTZ (Sigma-Aldrich, St. Louis, MO, USA) was dissolved in isotonic saline solution (7 mg/mL) and scPTZ-induced seizures were produced in mice by sc injection of PTZ (70 mg/kg), following the procedure reported by Siddiqui *et al.* (Siddiqui et al., 2014). This produced clonic convulsions lasting for at least five seconds, with accompanying loss of the righting reflex (Figure IV.2). The animals were observed for a period of 30 min and the absence of clonic convulsions in this time period was interpreted as the ability of compounds to protect against scPTZ-induced seizures.

Figure IV.2 – Representative image of the endpoint (clonic convulsions lasting at least five seconds) in the subcutaneous pentylenetetrazole seizure test in mice. Image collected during the 30 min of observation, 0.5 h after intraperitoneal administration of the negative control (vehicle).

IV.2.4. Rotarod test

Minimal motor impairment was established in mice by standard rotarod performance assay as previously reported (Pandeya et al., 2000). Mice were previously trained to balance on an accelerating rotarod apparatus (rod diameter: 3 cm) that rotated at a constant speed of 10 revolutions per minute (Rota-rod, Ugo Basile, Varese, Italy). During the training sessions, the animals were placed on the rotating rod at least three consecutive trials for 90 s (Figure IV.3). On the day of the test, trained mice were intraperitoneally pretreated with the compounds and the motor/neurological toxicity was indicated by the inability of the animal to maintain equilibration on the rod for at least 60 s.

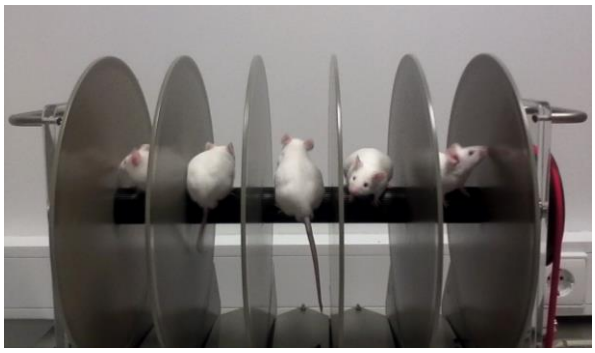

Figure IV.3 – Representative image of a training session in the rotarod apparatus.

IV.3. Results and discussion

As previously referred, the preclinical development of new chemical agents for the management of epileptic seizures is still based on the empirical screening of compounds against acute seizure rodent models (Löscher, 2016). Despite the diversity of models that could potentially be used in the screening of anticonvulsant activity, the MES and the scPTZ tests have been considered for decades as *gold standard* models for discovery and development of new AEDs, probably because they are simple and allow the evaluation of a large number of compounds in a relatively short period of time (Löscher et al., 2013). Nowadays, the scPTZ test is not highly recommended to be used in the first approach of anticonvulsant evaluation (only when needed) because the problems with clinical validation. However, in the beginning of this research work, the MES and scPTZ animal models were still employed as the recommended models to be used in order to start the anticonvulsant evaluation of new candidates together with the rotarod assay to evaluate the potential neurological toxicity (classic Anticonvulsant Screening Program that was further revised). Following this original programme, the 6-Hz animal model would be used in the cases of failure of efficacy in the initial seizure models (Löscher, 2011; Simonato et al., 2014). In fact, nowadays this classical programme continues to be followed by a large amount of scientists (Dong et al., 2017; Łączkowski et al., 2016; Liao et al., 2017; Villalba et al., 2016).

All the *in vivo* experiments were performed on adult males, aiming to reduce possible confounding contributions of the oestrus cycle on seizure susceptibility. For anticonvulsant and neurotoxic evaluations just 42 out of the 50 synthesized compounds were tested. The reasons to exclude 8 compounds were essentially limitations at the level of chemical synthesis, such as the obtainment of very low yields of the products (**MM 30**, **MM 85**, **MM 90**, **MM 60** and **MM 61**), and/or strong problems of solubility (**MM 67**, **MM 68** and **MM 88**). Therefore, the 42 synthesized compounds were screened for their anticonvulsant activity against both MES and scPTZ tests, at 0.5 and 4 h after ip administration in mice, at the standard doses of 30, 100 and 300 mg/kg (Table IV.1).

The data obtained in the MES screening showed that compounds **MM 26**, **MM 83**, **MM 17**, **MM 28**, **MM 84**, **MM 19**, **MM 29**, **MM 82** and **MM 86** exhibited 50% or more protection at the lowest dose tested (30 mg/kg). Additionally, other derivatives provided anti-MES protection at the dose of 100 mg/kg (compounds **MM 22**, **MM 35**, **MM 37**, **MM 56**, **MM 64** and **MM 58**) or 300 mg/kg (**MM 72**, **MM 73**, **MM 74**, **MM 55**, **MM 54**, **MM 81**, **MM 92** and **MM 65**). Apart from compounds **MM 64**, **MM 59** and **MM 65**, which only exhibited anticonvulsant activity at 0.5 h post-dose, in general, a higher anticonvulsant activity was found at 4 h after ip administration. These results can suggest a slow onset of action and a long duration of action for the majority of these compounds.

Table IV.1 – *In vivo* anticonvulsant activity and neurotoxicity following intraperitoneal administration in mice of the synthesized compounds and standard antiepileptic drugs. The compounds are grouped as urea and thiourea series.[a]

Entry	Compound	MES[b]		scPTZ[c]		Toxicity[d]		Entry	Compound	MES		scPTZ		Toxicity	
		0.5 h	4 h	0.5 h	4 h	0.5 h	4 h			0.5 h	4 h	0.5 h	4 h	0.5 h	4 h
	Urea series								**Thiourea series**						
1	MM 18	—	—	—	—	300	—	29	MM 26	300	30	—	—	—	100
2	MM 72	—	300	—	—	—	—	30	MM 83	—	30	—	—	30	100
3	MM 17	—	30	—	—	300	—	31	MM 25	—	—	—	—	30	—
4	MM 22	—	100	—	—	30	—	32	MM 28	—	30	—	—	100	—
5	MM 73	—	300	—	—	30	—	33	MM 84	—	30	—	—	30	100
6	MM 19	—	30	—	—	30	—	34	MM 29	30	300	—	—	—	300
7	MM 23	—	—	—	—	300	—					—	—		
8	MM 82	300	30	—	—	—	—					—	—		
9	MM 24	—	—	—	—	—	—								
10	MM 34	—	—	—	—	100	—	35	MM 36	—	—	—	—	—	100
11	MM 74	—	300	—	—	100	—								
12	MM 35	—	100	—	—	300	—	36	MM 37	—	100	—	—	30	—
13	MM 55	—	300	—	—	—	—	37	MM 46	—	—	—	—	30	—
14	MM 54	—	300	—	—	—	—	38	MM 48	—	—	—	—	30	—
15	MM 57	—	—	—	—	30	—								
16	MM 81	—	300	—	—	30	300	39	MM 92	—	300	—	—	30	30
17	MM 56	—	100	—	—	300	—	40	MM 64	100	—	—	—	100	300
18	MM 59	300	—	—	—	—	—								
19	MM 75	—	—	—	—	30	—	41	MM 86	—	30	—	—	30	30
20	MM 58	—	100	—	—	—	—	42	MM 63	—	—	—	—	—	—
21	MM 65	300	—	—	—	—	—								
22	MM 76	—	—	—	—	30	—								
23	MM 66	—	—	—	—	300	—		**Antiepileptic drugs**						
24	MM 93	—	—	—	—	30	—	43	Lamotrigine	30	30	—	—	30	100
25	MM 99	—	—			30	—	44	Carbamazepine	30	100	NT	NT	30	100
26	MM 96	—	—	—	—	30	—	45	Phenytoin	30	30	NT	NT	100	100
27	MM 106	—	—	—	—	30	—	46	Clonazepam[e]	NT	NT	0.1	0.1	0.1	—
28	MM 95	—	—	—	—	30	—	47	Sodium valproate	300	—	NT	NT	30	—

[a]Doses of 30, 100, and 300 mg/kg were administered. The data in the table indicate the minimal dose whereby bioactivity was demonstrated at least in half of three-four animals. They were examined at 0.5 and 4 h after intraperitoneal injection of each compound. A dash indicates the absence of activity at maximum dose administered (300 mg/kg); NT = not tested. [b]Maximal electroshock seizure test. [c]Subcutaneous pentylenetetrazole seizure test. [d]Neurotoxicity screening (rotarod) test. [e]Drug tested at doses of 0.1 and 0.3 mg/kg

Considering the results, it was difficult to obtain a clear structure-anticonvulsant activity relationship among the compounds. However, the MES screening in mice enables to draw some general conclusions concerning the relations between the structure and the observed activity. In this point, it was observed that all the compounds belonging to the set with a methyl group attached to a phenyl ring (entries 4-6 and 32-34, Table IV.1) presented protection against seizures, with around 67% of them revealing activity at the lowest dose tested (30 mg/kg). Regarding the derivatives that have an unsubstituted phenyl ring at the 4 position of the dihydropyrimidine heteroring (entries 1-3 and 29-31, Table IV.1), four compounds exhibited anticonvulsant properties, being three of them active at 30 mg/kg (compounds **MM 26**, **MM 83** and **MM 17**). On the other hand, except of one nitro derivative that was effective at 30 mg/kg (compound **MM 82**), the introduction of a methoxy or a nitro groups did not seem crucial for a potent anticonvulsant activity. Surprisingly, in general, the introduction of halogens (chlorine and fluorine atoms) at 2,3- and 2,4-positions of the phenyl ring (entries 13-20 and 37-42, Table IV.1) decreased the activity in comparison to unsubstituted compounds. This was not expected because there are several reports in the literature associating an increased anticonvulsant activity with the introduction of chlorine atoms in the structure of the molecules (Habib et al., 2015; Hassan et al., 2012). However, it is worthy to note that in these halogenated derivatives the halogen atoms are attached to positions C2 and C3 or C2 and C4 of the aromatic ring, and therefore steric hindrance effects (particularly the atoms at *ortho* position) can influence the relative spatial positions of the two rings and influence target binding. Thus, it seems that an unsubstituted phenyl ring or a *para*-substituted phenyl with a lipophilic electron-donating substituent at the position 4 of the pyrimidin(thi)one ring is favouring the anticonvulsant effects. The lack of efficacy of the compounds incorporating two heterocycles in their structure (entries 21-28, Table IV.1), which was accompanied by high motor deficit, was another unexpected result, because these compounds were intentionally designed considering described pharmacophores with anticonvulsant activity. However, in the case of the compounds including the 5-methyl-2-furyl, 5-chloro-2-furyl, 2-thiophenyl, 5-chloro-2-thiophenyl and 3-pyridyl, only one derivative was synthesized (i.e. the lateral chain was not changed and the thiourea analogues were also not synthesized), which is not enough to establish a reliable relation between the structure and the activity of this group of compounds.

It was not found marked differences between the two series (urea and thiourea) regarding the anticonvulsant activity. However, in the group of molecules possessing the basic scaffold [unsubstituted phenyl at the position 4 of the pyrimidin(thi)one ring] or having the methyl group at *para*-position of the phenyl ring (the most potent compounds), the DHPMts appeared to be more potent than the corresponding urea analogues. However, in general, a slightly higher neurological toxicity was observed in the rotarod test in the animals that received thiourea derivatives. Finally, analysing all the results, this study can also suggest that the anticonvulsant activity seems to increase with the reduction of the size of the chain at the position 5 of the dihydropyrimidine ring (i.e. compounds synthesized using acetylacetone and

methyl acetoacetate seem to be more potent than the analogues synthesized using the ethyl acetoacetate).

In the scPTZ test, contrarily to the standard drug clonazepam, clonic seizures lasting more than 5 s were observed in the treated mice, which indicated that the investigated compounds as well as lamotrigine do not protect the animals against chemically-induced seizures by a subcutaneous injection of PTZ. Seizure profiles consisted in immobility, abnormal limb splay, ataxia, Straub tail, clonic/tonic seizures, muscle fasciculation, loss of righting reflex, *status epilepticus*, and ultimately release of sperm (Figure IV.4).

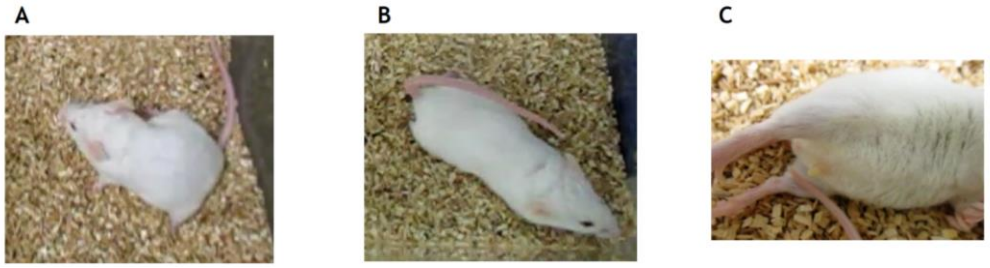

Figure IV.4 – Some characteristic signs manifested by mice during the observation period of 30 min after subcutaneous pentylenetetrazole administration. **A** - abnormal limb splay; **B** - Straub tail; **C** - release of sperm.

Furthermore, in addition to the anticonvulsant screening, the minimal motor and/or neurological impairment was determined in mice by the rotarod performance test. Interestingly, contrasting with the anticonvulsant activity, the neurotoxic effects of the tested compounds were mainly noticed at 0.5 h post administration, with the exception of some thiourea derivatives (**MM 26**, **MM 29** and **MM 36**). The most neurotoxic derivatives were compounds **MM 92** and **MM 86**, for which neurotoxicity was observed at 30 mg/kg in both time-points of evaluation. This finding is particularly important for compound **MM 86** that was one of the most potent compounds at the lowest dose evaluated (30 mg/kg). Moreover, compounds **MM 83** and **MM 84** exhibited a neurotoxic profile similar to the AEDs lamotrigine and carbamazepine. The remaining compounds showed lesser motor/neurological impairment and faster time of recuperation than the AEDs tested. Within these, compounds **MM 72**, **MM 82**, **MM 24**, **MM 55**, **MM 54**, **MM 59**, **MM 58**, **MM 63** and **MM 65** seem to be devoid of relevant neurological toxicity in these experimental conditions.

Therefore, after integrating the data obtained in the ip screening in mice (anticonvulsant activity and neurotoxicity), three compounds (**MM 83**, **MM 17** and **MM 19**) were selected and evaluated for their anticonvulsant activity in the MES test in a different rodent species (rats) after oral administration at a single dose of 30 mg/kg. This assay evaluated the ability of the most promising compounds to inhibit seizures when administered via the oral route, which is the desired route of administration for anticonvulsant drug candidates. All the three

compounds displayed some degree of anticonvulsant protection, with the highest activity observed at 0.5 h post-dose for compound **MM 17** (50%) and at 4 h post-dose for compounds **MM 83** (75%) and **MM 19** (50%) as demonstrated in Table IV.2. These findings also indicated that these compounds are absorbed from the gastrointestinal tract of rats.

Table IV.2 – Anticonvulsant evaluation of compounds **MM 83**, **MM 17** and **MM 19**, as well as lamotrigine (positive control), in the maximal electroshock seizure (MES) test, after oral administration to rats at 30 mg/kg.

Compound	MES activity[a]		
	0.5 h	**2.0 h**	**4.0 h**
MM 83	1/4	2/4	3/4
MM 17	2/4	1/4	1/4
MM 19	1/4	1/4	2/4
Lamotrigine	4/4	4/4	4/4

[a]The data indicate: number of rats protected/number of rats tested

These seizure rodent models are not only used to identify novel anticonvulsants, but they also enable to predict the efficacy of the compounds against different types of seizures. Taking into account that MES test is thought to be an experimental model of human generalised tonic–clonic seizures, whereas scPTZ model generally refers to non-convulsive seizures, the efficacy of the investigated compounds in the MES model and the lack of anticonvulsant protection demonstrated in scPTZ test suggest that these compounds might be potentially effective in human generalised clonic-tonic seizures and not in absence or myoclonic seizures.

In spite of animal models are considered non-mechanistic (Kupferberg, 2001), the efficacy profile of the compounds could suggest the main potential mechanism of action. Indeed, drugs acting by blockade of voltage-gated sodium and also calcium channels, with the exception of ethosuximide, usually are effective in the protection against seizures induced by MES test, and they frequently show no anticonvulsant protection in the scPTZ model (e.g. phenytoin, carbamazepine, lamotrigine), while numerous GABAergic AEDs (e.g. benzodiazepines, tiagabine) and the calcium channel blocker ethosuximide are effective in the scPTZ model (Löscher and Schmidt, 2011). In fact, it was described that T-type calcium channels have been implicated in the pathology of both the genetic and acquired epilepsies and several AEDs in clinical use are known to suppress seizures *via* inhibition of T-type calcium channels (Powell et al., 2013). Moreover, the blockade of this type of calcium channels has been associated to the prevention of tonic-clonic seizures in the MES model (Sakkaki et al., 2016). In addition, there is evidence about the potential interest of the L-type calcium channel antagonist verapamil in drug-resistant epilepsy (Nicita et al., 2016). Bearing this in mind, it can be expected the interference of the tested compounds with the ion channels as a potential mechanism underlying the anticonvulsant activity. In fact, previous studies have demonstrated the calcium channel blocking activity in general or the L-type calcium channel in particular of DHPMs (Cernecka et al., 2012; Putatunda et al., 2012; Singh et al., 2009).

On the other hand, it was also previously demonstrated *in vitro* the potentiation of $GABA_A$ receptors by this class of molecules (Lewis et al., 2010). For this reason, some degree of anticonvulsant protection against the scPTZ model was expected, which did not happen. This could suggest the weak correlation between *in vitro* and *in vivo* experiments in the discovery process of new AED candidates. Overall, it is important to mention that the elucidation of the mechanisms of action of the evaluated compounds was outside the scope of the current work, but it should be considered in further extended mechanistic studies.

In conclusion, the results obtained in this study provide new information on the anticonvulsant activity of the DHPM(t)s, which still remain underexploited. A number of compounds showed interesting *in vivo* anticonvulsant activity, even at the lowest dose tested (30 mg/kg) against electrically-induced seizures. Based on the initial anticonvulsant screening in mice, this study allows the selection of important structural features of this attractive scaffold, which could be responsible for the anticonvulsant activity obtained. In fact, compounds with small or intermediate chains at the position 5 of the dihydropyrimidine ring and possessing an unsubstituted or substituted phenyl ring at the *para*-position with a methyl group seem to be the most promising structures to consider in further studies of the development of new AED candidates.

CHAPTER V

IN VITRO STUDIES:

Cytotoxicity and kinetic properties

V.1. Introduction

A successful drug discovery and development programme requires selecting the right therapeutic target to an unmet clinical need and a flawless set of methodologies that early and accurately predict not only efficacy, but also the pharmacokinetic and toxicological behaviour of new chemical compounds. Screening assays should, hence, be performed in an attempt of selecting the compounds with better binding properties to the therapeutic target, but which should simultaneously be able to reach the site of action in adequate concentrations to produce the therapeutic effect. For these reasons, HTS of ADME properties together with the *in vitro* cytotoxicity evaluation of drug candidates is an integrated part of the drug development process to enhance the success rate when drug candidates are administered to animals or humans (Leucuta, 2014; Wan, 2013).

In addition, biopharmaceutical and *in vitro* pharmacokinetic screening assays most typically comprise the evaluation of solubility, membrane permeability, metabolic stability, interaction with drug transporters, and DDI mediated by CYP450 enzymes. Among the key factors influencing ADME properties, permeability has been widely recognized as an important characteristic of drug candidates as it strongly determines gastrointestinal absorption, BBB permeation and cell-membrane penetration to reach intracellular targets (Lennernäs et al., 2014). Intestinal absorption should also be predicted early, particularly when the new drug is intended to be administered by oral route, since it has a great impact on the bioavailability of the compound and, consequently, on its efficacy (Alqahtani et al., 2013; Page, 2016). In addition, the screening of permeation compounds through BBB models should always be conducted as early as possible in drug development programmes, independently of the biophase. Indeed, for a CNS-acting drug to be successful it must cross the BBB to reach the therapeutic target site; in opposition, a peripheral-acting drug should exhibit a low permeation through the BBB in order to avoid potential undesired CNS side-effects (Bagal and Bungay, 2014; Lanevskij et al., 2013).

P-gp is also considered to be responsible for limiting the penetration of AEDs into CNS and appearance of side-effects, and it has been suggested to be overexpressed in the BBB of patients diagnosed with intractable epilepsy, contributing to the pharmacoresistance phenomenon (Stępień et al., 2012; Wang et al., 2016). Thus, it is not surprising that P-gp is of particular interest to medicinal chemists and pharmaceutical scientists because of its ability to influence whether an optimal lead candidate is chosen to potentially become a drug or need to be modified or even rejected. Actually, the importance of routinely evaluate the interference with P-gp in early stages of drug development is reinforced by the revised guidance entitled “Drug Interaction Studies – Study Design, Data Analysis, Implications for Dosing, and Labeling Recommendations” released by FDA (FDA, 2012) and by the revised guideline titled “Guideline on the Investigation of Drug Interactions” issued by EMA (EMA, 2012).

In spite of some cytotoxic data have been reported in the literature (Prashantha Kumar et al., 2009; Russowsky et al., 2006; Sachdeva and Dwivedi, 2012), the kinetic properties of the DHPM(t)s must also be investigated as a rational strategy to support a continuous structural optimization of these drug candidates. Hence, additionally to the evaluation of the cytotoxic potential of DHPM(t)s in different cell lines, the ability of these molecules to permeate the intestinal membrane and the BBB was also investigated using two parallel artificial membrane permeability assay (PAMPA) models, and their interference on P-gp–mediated efflux transport was evaluated through Madin-Darby canine kidney type II cell line transfected with the *MDR1* gene (MDCK-MDR1) cell-based accumulation assays.

V.2. Experimental section

V.2.1. General cytotoxicity evaluation

V.2.1.1. Cell culture

N27 cells were kindly donated by Dr. Ana Clara Cristóvão (CICS-UBI, Covilhã, Portugal); NHDF and Caco-2 cell lines were obtained from American Type Culture Collection (ATCC; Manassas, VA, USA) and HepaRG cell line was obtained from Life Technologies – Invitrogen™ (through Alfagene, Portugal). The cells were maintained in 75 cm^2 culture flasks at 37 ºC in a humidified air incubator with 5% CO_2. N27 cells were cultured in RPMI 1640 medium with 10% fetal bovine serum (FBS; Sigma-Aldrich, St. Louis, MO, USA) and 1% of the antibiotic mixture of 10,000 units/mL penicillin G and 100 mg/mL of streptomycin (sp; Sigma-Aldrich, St. Louis, MO, USA); NHDF cells have grown in RPMI 1640 medium supplemented with 10% FBS, 2 mM L-glutamine (Sigma-Aldrich, St. Louis, MO, USA), 10 mM HEPES (Fisher Scientific, New Hampshire, USA), 1 mM sodium pyruvate (Sigma-Aldrich, St. Louis, MO, USA) and 1% antibiotic/antimycotic (10,000 units/mL penicillin G, 100 mg/mL streptomycin and 25 µg/mL amphotericin B) (Ab; Sigma-Aldrich, St. Louis, MO, USA); Caco-2 cells were cultured in high-glucose Dulbecco's modified Eagle medium supplemented with 10% FBS and 1% sp, and HepaRG cells were seeded in Williams' E medium supplemented with 10% FBS, 1% sp, 5 µg/mL insulin, and 5×10^{-5} M hydrocortisone hemisuccinate (Sigma–Aldrich, St. Louis, MO, USA). For all cell lines, the medium was renewed every 2-3 days until cells reach approximately 90-95% confluence. Then, they were detached by gentle trypsinization (trypsin-EDTA; Sigma-Aldrich, St. Louis, MO, USA) and, before the experiments, viable cells were counted by the trypan-blue exclusion assay and suitably diluted in the adequate complete culture medium.

V.2.1.2. Preparation of compound solutions

All compounds were dissolved in DMSO in a concentration of 10 mM and stored at 4-8 ºC. From this stock solution, the various working solutions of the compounds in study in different concentrations were prepared by adequate dilutions in complete culture medium before each experiment. The maximum DMSO concentration in the studies was 1% and previous experiments revealed that this solvent level has no significant effects in cell proliferation.

V.2.1.3. MTT assay

The *in vitro* cytotoxicity was evaluated by the MTT (Sigma-Aldrich, St. Louis, MO, USA) assay. After the trypsinization and count of the cells, 100 µL of cell suspension with an initial density of 2×10^4 cells/mL were seeded in each well of 96-well culture plates and left to adhere for 48 h. After adherence, the medium was replaced by the several solutions of the compounds in study (30 µM for preliminary studies and 0.01, 0.1, 1, 10, 50 and 100 µM for concentration-response studies) in the appropriate culture medium for approximately 72 h. Untreated cells were used as the negative control, 5-fluorouracil (Sigma-Aldrich, St. Louis, MO, USA) was used as positive control, and lamotrigine, carbamazepine, phenytoin and clonazepam were also used for comparison. Each experiment was performed in quadruplicate and at least two independent experiments were performed. Then, the medium was removed, 100 µL of phosphate buffer saline (PBS, NaCl 137 mM, KCl 2.7 mM, Na_2HPO_4 10 mM and KH_2PO_4 1.8 mM, pH 7.4) were used to wash the cells and 100 µL of the MTT solution (5 mg/mL), prepared in the serum-free medium, was added to each well, followed by incubation for approximately 4 h at 37 ºC. Afterwards, the MTT containing medium was removed and the formazan crystals were dissolved in DMSO. The absorbance was measured at 570 nm using a microplate reader Bio-rad Xmark spectrophotometer. After background subtraction, cell proliferation values were expressed as percentage relatively to the absorbance determined in negative control cells.

V.2.2. Permeability assays through artificial lipid membranes

V.2.2.1. Intestinal PAMPA model

The PAMPA method herein applied to predict the intestinal absorption of the test compounds was previously optimized and validated (Fortuna et al., 2012). Stock solutions of each compound were prepared in DMSO at 10 mM and then diluted with Tris buffer pH 6.5 to obtain the donor drug solution with the final concentration of 500 µM. The assay procedure was

initiated by filling each well of the microtiter plate (MultiScreen®, catalogue no. MATRNPS50, Millipore Corporation, Bedford, MA, USA) with 300 µL of each donor drug solution. Carefully, and avoiding the pipette tip contact with the filter, the hydrophobic filter (0.45 µm) of each acceptor well of the 96-well microfilter plate (MultiScreen®-IP, catalogue no. MAIPNTR10, Millipore Corporation, Bedford, MA, USA) was impregnated with 6 µL of the artificial lipid solution composed of 2% of L-α-phosphatidylcholine from soybean (Sigma–Aldrich, St. Louis, MO, USA) in *n*-dodecane (Acros Organics, MA, USA). Immediately after this application, 150 µL of Tris buffer pH 7.4 containing 5% of DMSO were added to the acceptor well. Then, receptor plate was gently placed onto the donor plate, making sure that the underside of the membrane was in contact with donor solution without entrapment of air bubbles. The assembled donor–acceptor plates were incubated at room temperature for 16 h under constant slight shaking. Afterwards, plates were separated and test compounds were quantified by ultraviolet–visible spectrophotometry in the receiver solution, using a microplate reader Bio-rad Xmark spectrophotometer. Experiments were carried out in replicate (n = 6) and the apparent permeability (Papp) of each drug, in centimetre per second, was calculated applying the equation previously reported by Fortuna *et al.* (Fortuna et al., 2012).

V.2.2.2. PAMPA-BBB model

V.2.2.2.1. Lipid extraction from pig brain tissue

As previously reported by Bicker *et al.* (Bicker et al., 2016), 0.01% butylated hydroxytoluene (Acros Organics, MA, USA) was added to solvents as antioxidant and all protocol stages were performed with glass material. Fresh pig brain tissue (0.3 g) was firstly homogenized with 2 mL of methanol (Fisher Scientific, Leicestershire, UK) using a glass-teflon homogenizer. Then, 4 mL of chloroform (Fisher Scientific, Leicestershire, UK) were added, ensuring a 20-fold dilution of the tissue weight. The homogenates were transferred to tubes for overnight rotation at 4 ºC. Following this time period, 1.5 mL of 0.15 M ammonium acetate aqueous solution (Panreac, Barcelona, Spain) were added in order to achieve the critical ratios between the solvents [chloroform:methanol:ammonium acetate (8:4:3, *v*/*v*/*v*)]. The sample was vortexed, centrifuged (2000 g/4 ºC/10 min) and the lower chloroform phase was gently aspirated into a new test tube. Subsequently, 6 mL of chloroform:methanol (2:1, *v*/*v*) were added to the original homogenate, vortexed and centrifuged as above. The lower phase was combined with the first chloroform extract and a second phase extraction was initiated by adding 1.5 mL of 0.15 M ammonium acetate, vortexing and centrifuging as formerly stated. Lastly, the organic phase was transferred to a new test tube and evaporated. According to the weight of lipid residue, *n*-dodecane was added to redissolve the lipid in the final concentration of 2% and the lipid solution was applied in the PAMPA filter.

V.2.2.2.2. Phosphorus assay

In order to determine the concentration of phospholipids extracted as described in the previous section, 0.1 mL of each lipid sample were dried completely under vacuum and added of 0.65 mL of perchloric acid 60% (Panreac, Barcelona, Spain) and, then, placed in a heated-block at 100 ºC for 45 min. After cooling, 3.3 mL of water, 0.5 mL of a 25 mg/mL ammonium molybdate (Fisher Scientific, Leicestershire, UK) aqueous solution and 0.5 mL of a 100 mg/mL ascorbic acid (Sigma–Aldrich, St. Louis, MO, USA) aqueous solution were added to the tubes, vortexing after each addition. The tubes were then placed in a boiling water bath for 10 min and the absorbance of the cold samples was read at 800 nm, using a microplate reader Bio-rad Xmark spectrophotometer. The phospholipid content of the extracts was estimated according to the equation previously reported by Bicker *et al.* (Bicker et al., 2016).

V.2.2.2.3. PAMPA-BBB procedure

After the lipid extraction, the procedure of PAMPA-BBB was similar to that described in section IV.2.2.2.1. However, in this case, the donor and acceptor solutions were prepared using PBS buffer pH 7.4 and the Papp was obtained through the equation previously reported by Bicker *et al.* (Bicker et al., 2016).

V.2.3. Cell-based P-glycoprotein assay

V.2.3.1. Cell line and culture conditions

MDCK-MDR1 cell line, transfected with the *MDR1* gene encoding the P-gp efflux transporter, was obtained from the Netherlands Cancer Institute (NKI-AVL, Amsterdam, Netherlands). The cells were cultured in high-glucose Dulbecco's modified Eagle medium supplemented with 10% fetal bovine serum and 1% spand maintained in 75 cm^2 culture flasks at 37 ºC in a humidified air incubator with 5% CO_2. Medium was renewed every 2-3 days until cells reached approximately 90-95% confluence. At that moment, cells were gently detached by trypsinization and, immediately before carrying on the following experiments, viable cells were counted by the trypan-blue exclusion assay and suitably diluted in the adequate complete culture medium.

V.2.3.2. MTT assay

In this case, the *in vitro* cytotoxicity was also evaluated by the MTT assay similarly to that described in section V.2.1.3. Briefly, after reaching 90-95% confluence, 200 µL of cell

suspension/well with an initial density of 2 × 10^4 cells/mL were seeded in 96-well culture plates and left to adhere and grow during 4 days (medium changed after 48 h). Afterwards, the medium was replaced by the solutions of the compounds in study (10 and 50 μM prepared in medium, from a stock solution of 10 mM in DMSO) for approximately 4 h. Then, the medium was removed, 100 μL of PBS (pH 7.4) were used to wash the cells and 100 μL of the MTT solution (5 mg/mL), prepared in the serum-free medium, were added to each well and followed by an incubation period of approximately 4 h at 37 ºC. Then, the MTT containing medium was removed and the formazan crystals were dissolved in DMSO. Each experiment was performed in quadruplicate and independently repeated (n = 4). The absorbance was measured as described in section V.2.1.3.

V.2.3.3. Intracellular rhodamine 123 accumulation assay

MDCK-MDR1 cells were seeded at an initial density of 1.3 × 10^5 cells/mL in 96-well plates and cultured for 4 days. At confluence, the medium was removed, the cells were washed with 200 μL of PBS at 37 ºC and then 100 μL of the compounds [DHPM(t)s, lamotrigine, carbamazepine and phenytoin] and the positive control (verapamil) at the tested concentrations (10 and 50 μM), prepared in the serum-free medium, were added to each well, as well as the serum-free medium in the negative control (untreated cells), followed by incubation for approximately 30 min at 37 ºC. Untreated cells, exposed only to the test compound vehicle (serum-free medium) with the same percentage of DMSO (0.5%, *v*/*v*), were used as the negative control and verapamil was used as positive control as it is a well-recognized P-gp inhibitor. Lamotrigine, carbamazepine and phenytoin were also used for comparison purposes. Finally, 5 μM of Rh123 (prepared at the initial concentration of 5 mM in DMSO from a 20 mM stock solution) was added to each well and the plates were incubated for 2 h at 37 ºC. At this step, the accumulation of Rh123 was stopped by washing the cells three times with cold PBS and the cells were lysed with 100 μL of 0.1% Triton X-100 aqueous solution at room temperature for 30 min. The fluorescence of cell lysates was measured with a Spectramax Gemini XS spectrofluorometer (Molecular Devices LLC, US) at a wavelength of 485 nm for excitation and 538 nm for emission. The concentration of Rh123 was determined by comparing the experimental absorbance values with a calibration curve (0.01–0.5 μM of Rh123 with standards prepared from the 5 mM intermediate solution) and then compared with the negative control. Experiments were carried out in replicate (n = 6).

V.2.4. Statistics

The data are expressed as mean ± SD. Comparison among groups of one factor was analysed by using the t-student test (two groups) and one-way ANOVA (three groups) followed by Dunnett's post hoc tests to find statistically significant differences among the means. Difference between groups was considered statistically significant for a *p*-value lower than 0.05 ($p < 0.05$).

V.3. Results and discussion

V.3.1. General cytotoxicity

The pharmacological treatment of epilepsy is often accompanied by adverse effects, which are one of the main reasons for the failure in the achievement of the required dose for an adequate seizure control and they have a significant negative impact on the quality of life of the patients (Kowski et al., 2016). Thus, the toxicological evaluation is a relevant aspect to consider since the early stages of the preclinical development of new anticonvulsant drug candidates. The well-established MTT assay was used to evaluate the general cytotoxicity of the synthesized compounds in several cell lines: rat mesencephalic dopaminergic (N27), human hepatocellular carcinoma (HepaRG), human colorectal adenocarcinoma (Caco-2) cell lines and normal human dermal fibroblasts (NHDF).

Unlike what happened in *in vivo* experiments, in *in vitro* tests all synthesized compounds were evaluated, because these assays do not require substantial amounts of each compound and the concentrations used in *in vitro* assays allowed a good dissolution of the compounds, even in aqueous solutions (e.g. culture mediums). Specifically, the fifty compounds were submitted to a screening assay with a single concentration of 30 μM and the results correspond to the relative cell proliferation, in percentage, after 72 h of incubation with the compounds of interest (Tables V.1, V.2, V.4 and V.5).

The evaluation of the potential neuronal cytotoxicity was considered bearing in mind that the target of action of AEDs is the CNS. In fact, for new agents that are designed for CNS disorders, it is of paramount importance that the potential effects of these drug candidates on the brain are known. For this reason, the synthesized compounds as well as the AEDs lamotrigine, carbamazepine, phenytoin and clonazepam were evaluated in dopaminergic neuronal (N27) cells (Table V.1). By analysing the results, it is clear that compounds with halogen atoms in their structure (entries 13, 14, 16, 17, 19, 25 and 40-43, Table V.1) and the product bearing the heterocycle 5-methyl-furan (entry 24, Table V.1) led to a relatively marked cytotoxicity in the tested concentration (relative cell proliferation lower than 50%). Compounds **MM 46**, **MM 57** and **MM 106** (with chlorine atoms), **MM 86** (with fluorine atoms)

and **MM 95** (pyridine ring) led to values of relative cell proliferation between 50 and 60%. However, these values were relatively closer to those obtained for clonazepam (60.54%).

Table V.1 – Relative cell proliferation in percentage of the synthesized compounds, distributed respectively into the urea and thiourea series, and standard antiepileptic drugs (lamotrigine, carbamazepine, phenytoin and clonazepam), at 30 μM, in dopaminergic neuronal (N27) cells.

Entry	Compound	Relative cell proliferation (%)	Entry	Compound	Relative cell proliferation (%)
	Urea series			**Thiourea series**	
1	MM 18	73.39 ± 8.17	29	MM 26	71.11 ± 6.05**
2	MM 72	99.15 ± 7.49	30	MM 83	72.08 ± 4.93**
3	MM 17	91.68 ± 17.17	31	MM 25	76.54 ± 10.75
4	MM 22	77.95 ± 6.30	32	MM 28	91.16 ± 14.46
5	MM 73	89.31 ± 14.96	33	MM 84	79.98 ± 9.87**
6	MM 19	96.35 ± 13.30*	34	MM 29	90.52 ± 12.17
7	MM 23	78.59 ± 13.51			
8	MM 82	74.30 ± 14.27*			
9	MM 24	93.32 ± 8.45	35	MM 30	98.49 ± 7.77
10	MM 34	97.04 ± 9.76	36	MM 36	81.43 ± 10.58*
11	MM 74	88.14 ± 15.78	37	MM 85	86.55 ± 9.90
12	MM 35	91.92 ± 9.42	38	MM 37	77.58 ± 14.40
13	MM 55	**46.32 ± 9.80****	39	MM 46	54.40 ± 11.53***
			40	MM 90	**39.60 ± 3.41*****
14	MM 54	**47.60 ± 4.43*****	41	MM 48	**38.20 ± 0.21*****
15	MM 57	53.08 ± 7.88*	42	MM 60	**42.88 ± 2.59*****
16	MM 81	**47.95 ± 1.94****	43	MM 92	**36.34 ± 2.06*****
17	MM 56	**48.92 ± 2.76****	44	MM 64	72.88 ± 11.59
18	MM 59	68.14 ± 12.26	45	MM 61	71.57 ± 1.34**
19	MM 75	**47.43 ± 2.48*****	46	MM 86	52.98 ± 4.56***
20	MM 58	76.13 ± 4.11	47	MM 63	89.24 ± 8.63*
21	MM 65	92.59 ± 14.44	48	MM 68	79.72 ± 15.47
22	MM 76	73.36 ± 9.04**	49	MM 88	90.03 ± 8.10
23	MM 66	89.14 ± 4.73	50	MM 67	83.07 ± 16.06
24	MM 93	**38.66 ± 5.78*****			
25	MM 99	**46.07 ± 3.44***		**Antiepileptic drugs**	
26	MM 96	63.51 ± 8.88	51	Lamotrigine	95.60 ± 2.03***
27	MM 106	56.63 ± 9.78**	52	Carbamazepine	82.94 ± 4.20**
28	MM 95	56.69 ± 3.93	53	Phenytoin	84.29 ± 9.46
			54	Clonazepam	60.54 ± 4.65

Results are expressed as mean ± SD (standard deviation) after 72 h of treatment. Each experiment was performed in quadruplicate and at least two independent experiments were carried out. The control were untreated cells. *p < 0.05 *versus* control; **p < 0.01 *versus* control; ***p < 0.001 *versus* control. Bold values correspond to the compounds that exhibited a relative cell proliferation lower than 50%.

Taking into consideration that hepatotoxicity is associated with some AEDs in clinical use (Björnsson, 2008) and it has been recognized as a serious safety problem, the hepatic cytotoxicity of the compounds was also investigated, using the HepaRG cell line (Table V.2). This is a recent model of hepatic cells that is now considered the most promising hepatoma cell line as a surrogate for primary human hepatocytes in *in vitro* assessments, including hepatotoxicity studies (Gómez-Lechón et al., 2014). This cell line was used in its non-differentiated form.

Table V.2 – Relative cell proliferation in percentage of the synthesized compounds, distributed respectively into the urea and thiourea series, and standard antiepileptic drugs (lamotrigine, carbamazepine, phenytoin and clonazepam), at 30 μM, in hepatic (HepaRG) cells.

Entry	Compound	Relative cell proliferation (%)	Entry	Compound	Relative cell proliferation (%)
	Urea series			**Thiourea series**	
1	MM 18	51.95 ± 9.16***	29	MM 26	72.86 ± 6.03**
2	MM 72	66.13 ± 7.90*	30	MM 83	74.01 ± 9.30***
3	MM 17	69.12 ± 3.66**	31	MM 25	58.80 ± 9.39***
4	MM 22	56.56 ± 6.26***	32	MM 28	54.84 ± 6.50***
5	MM 73	86.64 ± 8.84*	33	MM 84	65.98 ± 7.87***
6	MM 19	61.12 ± 12.65***	34	MM 29	50.84 ± 4.61***
7	MM 23	50.32 ± 4.23***			
8	MM 82	78.33 ± 9.63**			
9	MM 24	58.51 ± 12.51***	35	MM 30	74.04 ± 10.03*
10	MM 34	55.94 ± 11.67***	36	MM 36	**45.78 ± 5.31***
11	MM 74	72.01 ± 6.69*	37	MM 85	63.69 ± 6.00***
12	MM 35	72.30 ± 9.95***	38	MM 37	75.38 ± 10.18*
13	MM 55	**15.19 ± 1.29*****	39	MM 46	**20.06 ± 6.28*****
			40	MM 90	**25.83 ± 3.39*****
14	MM 54	**36.36 ± 11.00*****	41	MM 48	**37.40 ± 2.31*****
15	MM 57	**15.50 ± 0.45*****	42	MM 60	**21.35 ± 1.23*****
16	MM 81	**36.81 ± 1.81*****	43	MM 92	**14.62 ± 2.34*****
17	MM 56	**29.62 ± 2.57*****	44	MM 64	**46.58 ± 4.43***
18	MM 59	53.67 ± 8.34***	45	MM 61	55.54 ± 16.43***
19	MM 75	54.97 ± 12.32***	46	MM 86	51.66 ± 3.24***
20	MM 58	81.42 ± 7.92	47	MM 63	76.14 ± 5.10*
21	MM 65	62.87 ± 14.47**	48	MM 68	83.98 ± 4.00*
22	MM 76	52.96 ± 8.18***	49	MM 88	77.55 ± 4.50**
23	MM 66	67.80 ± 6.71***	50	MM 67	83.36 ± 12.76
24	MM 93	60.16 ± 4.53***			
25	MM 99	76.34 ± 3.75		**Antiepileptic drugs**	
26	MM 96	84.54 ± 4.67	51	Lamotrigine	75.06 ± 9.44**
27	MM 106	52.34 ± 10.93	52	Carbamazepine	67.71 ± 10.87***
28	MM 95	92.66 ± 6.85***	53	Phenytoin	66.94 ± 7.93*
			54	Clonazepam	73.41 ± 7.59*

Results are expressed as mean ± SD (standard deviation) after 72 h of treatment. Each experiment was performed in quadruplicate and at least two independent experiments were carried out. The control were untreated cells. *p < 0.05 *versus* control; **p < 0.01 *versus* control; ***p < 0.001 *versus* control. Bold values correspond to the compounds that exhibited a relative cell proliferation lower than 50%.

As shown in Table V.2, in general, compounds without substituents in the phenyl group (entries 1-3 and 29-31, Table V.2) and with methyl (entries 4-6 and 32-34, Table V.2), nitro (entries 7-9 and 35, Table V.2) and methoxy (entries 10-12 and 36-38, Table V.2) groups introduced in the aromatic moiety at *para*-position did not exhibit marked cytotoxic activity. On the other hand, the molecules containing chlorine atoms attached to the aromatic ring belonging to urea (**MM 55**, **MM 54**, **MM 57**, **MM 81** and **MM 56**) and thiourea (**MM 46**, **MM 90**, **MM 48**, **MM 60**, **MM 92** and **MM 64**) series exhibited strong inhibition of cell proliferation. Interestingly, the introduction of other halogens (fluorine atoms) into the phenyl ring resulted in a decrease of the cytotoxicity, when compared with their chlorine analogues. In addition, regarding the compounds with a five-membered heteroring (furan and thiophene) (entries 21-27 and 48-50, Table V.2) and the pyridyl ring (entry 28, Table V.2) instead of the six-membered benzene ring, they also did not lead to a marked reduction of cell proliferation. Although there was a decrease of the percentage of relative HepaRG cell proliferation for a

significant number of compounds, it should be mentioned that the four evaluated AEDs also significantly decreased the proliferation of HepaRG cells.

Due to the strong cytotoxicity found in HepaRG cells for some compounds, the *in vitro* antiproliferative activity of the most cytotoxic DHPM(t)s (relative cell proliferation lower than 50%) was further investigated by determining the corresponding concentration inducing 50% inhibition of cell growth (IC_{50}) (Table V.3). This allowed us to draw a more reliable structure-cytotoxicity activity relationship of the compounds against this cell line. Within the thiourea series, compound **MM 36**, containing a methoxy group attached to the aromatic ring at *para*-position, was the unique molecule evaluated that did not include a chlorine atom into its structure and appeared to be the less cytotoxic (IC_{50} = 41.48 μM) towards the HepaRG cells. Additionally, compounds derived from acetylacetone (entries 10 and 13, Table V.3) showed relatively weak cytotoxicity in the HepaRG cell line (IC_{50} = 31.86 μM and IC_{50} = 25.49 μM, respectively), which can suggest that small lateral chains afford less cytotoxicity. Additionally, when comparing compounds **MM 46** and **MM 90** (2,3-dichloro derivatives) with compounds **MM 60** and **MM 92** (2,4-dichloro derivatives), a higher cytotoxicity was observed for compounds **MM 46** and **MM 90**. In this group, compound **MM 46** was the most potent compound, displaying the strongest cytotoxicity (IC_{50} = 0.75 μM). Regarding the DHPMs (urea series), from the analysis of the data obtained in Table V.3, it can be observed that no marked differences were found regarding the position of the chlorine atoms. However, interestingly, contrarily to the compounds belonging to thiourea series, the results suggest that small lateral chains at the position 5 of the pyrimidinone ring (IC_{50} = 5.47 μM for **MM 54** and IC_{50} = 5.28 μM for **MM 56**) afford higher toxicity than longer lateral chains (IC_{50} = 9.76 μM for **MM 55**, IC_{50} = 13.33 μM for **MM 57** and IC_{50} = 15.96 μM for **MM 81**). The unique compound (**MM 106**) evaluated in this context that incorporated two heterocycles in its structure (5-chloro-thiophenyl and dyhidropyrimidinone rings) was the less cytotoxic derivative of this series, which indicated that the presence of the phenyl ring, together with the chlorine atoms could be a requirement for the toxicity of these compounds against these cells.

Table V.3 – Cytotoxicity (IC_{50} μM) of the most cytotoxic compounds, distributed respectively into the urea and thiourea series, against HepaRG cell line.[a]

Entry	Compound	IC_{50} (μM)	R^2	Entry	Compound	IC_{50} (μM)	R^2
	Urea series				**Thiourea series**		
				7	MM 36	41.48	0.82
1	MM 55	9.76	0.99	8	MM 46	0.75	0.97
				9	MM 90	6.53	0.96
2	MM 57	13.33	0.99	10	MM 48	31.86	0.99
3	MM 54	5.47	0.97	11	MM 60	14.31	0.99
4	MM 81	15.96	0.99	12	MM 92	25.07	0.91
5	MM 56	5.28	0.99	13	MM 64	25.49	0.99
6	MM 106	31.21	0.88				
				14	5-fluorouracil	2.02	0.93

[a]The cells were treated with a variety of concentrations (0.01, 0.1, 1, 10, 50 and 100 μM) during 72 h. The cytotoxicity was determined by the MTT assay and the IC_{50} values were calculated by sigmoidal fitting. The data shown are representative of at least two independent experiments.

In addition to N27 and HepaRG cell lines, the potential intestinal cytotoxicity was also evaluated using Caco-2 cells, because the oral route is the desirable route of administration for anticonvulsant drug candidates. In general, the values of relative cell proliferation were much higher than those observed for HepaRG cells. However, as can be seen in Table V.4, some DHPMts still exhibited marked cytotoxicity against Caco-2 cells, such as **MM 90**, **MM 60** and **MM 92** (IC_{50} = 25.36 μM, 30.21 μM and 39.27 μM, respectively). On the other hand, the results of the compound **MM 95** (a DHPM), which has a pyridine ring in its chemical structure, should be highlighted because a significant increase of the Caco-2 cells growth was found (relative cell proliferation of 122.17%).

Table V.4 – Relative cell proliferation in percentage of the synthesized compounds, distributed respectively into the urea and thiourea series, and standard antiepileptic drugs (lamotrigine, carbamazepine, phenytoin and clonazepam), at 30 μM, in cancer intestinal (Caco-2) cells.

Entry	Compound	Relative cell proliferation (%)	Entry	Compound	Relative cell proliferation (%)
	Urea series			**Thiourea series**	
1	MM 18	98.25 ± 6.30	29	MM 26	105.20 ± 8.56
2	MM 72	98.83 ± 1.37	30	MM 83	87.28 ± 16.49
3	MM 17	98.29 ± 4.04	31	MM 25	94.14 ± 12.75
4	MM 22	89.41 ± 11.12	32	MM 28	81.87 ± 4.89*
5	MM 73	87.07 ± 3.46	33	MM 84	79.80 ± 8.45
6	MM 19	96.41 ± 7.88	34	MM 29	97.42 ± 6.86
7	MM 23	89.50 ± 8.08			
8	MM 82	98.48 ± 5.74			
9	MM 24	91.63 ± 7.22	35	MM 30	104.19 ± 5.56
10	MM 34	88.58 ± 9.33	36	MM 36	72.38 ± 3.67**
11	MM 74	89.70 ± 4.28	37	MM 85	91.35 ± 17.36
12	MM 35	85.89 ± 6.87	38	MM 37	94.08 ± 5.53
13	MM 55	51.74 ± 10.37***	39	MM 46	51.97 ± 2.26****
			40	MM 90	**25.36 ± 3.65*** **
14	MM 54	54.85 ± 2.73***	41	MM 48	73.83 ± 3.38*
15	MM 57	51.43 ± 1.55***	42	MM 60	**30.21 ± 3.14*** **
16	MM 81	63.65 ± 5.73***	43	MM 92	**39.27 ± 0.72*** **
17	MM 56	55.57 ± 6.27***	44	MM 64	88.11 ± 5.52
18	MM 59	86.36 ± 6.24***	45	MM 61	88.56 ± 8.55
19	MM 75	76.10 ± 2.88***	46	MM 86	92.53 ± 11.28
20	MM 58	97.56 ± 8.88	47	MM 63	91.55 ± 6.57
21	MM 65	83.39 ± 6.73	48	MM 68	90.11 ± 11.26
22	MM 76	96.64 ± 7.31	49	MM 88	103.02 ± 25.27
23	MM 66	83.17 ± 1.85	50	MM 67	91.38 ± 22.26
24	MM 93	89.33 ± 6.12*			
25	MM 99	85.07 ± 13.00		**Antiepileptic drugs**	
26	MM 96	107.86 ± 14.57	51	Lamotrigine	97.14 ± 3.98
27	MM 106	99.92 ± 10.49	52	Carbamazepine	94.64 ± 6.87
28	MM 95	122.17 ± 4.58***	53	Phenytoin	94.15 ± 6.62
			54	Clonazepam	97.80 ± 8.62

Results are expressed as mean ± SD (standard deviation) after 72 h of treatment. Each experiment was performed in quadruplicate and at least two independent experiments were carried out. The control were untreated cells. *p < 0.05 *versus* control; **p < 0.01 *versus* control; ***p < 0.001 *versus* control. Bold values correspond to the compounds that exhibited a relative cell proliferation lower than 50%.

Finally, the effects of these compounds in normal human dermal fibroblasts (NHDF) were also studied because, contrarily to both hepatic and colon cell lines, NHDF are non-cancerous cells and contrarily to N27 cells, NHDF is a human cell line. Thus, the demonstration of the absence of relevant cytotoxicity in this kind of cells is also an important finding. Moreover,

this cell line also allows to evaluate the selectivity of these compounds between cancerous *versus* non-cancerous cells. In general, the compounds did not show marked cytotoxicity in these dermal cells (relative cell proliferation higher than 50% at 30 μM). However, a number of molecules containing chlorine atoms in their structure, in C2 and C3 positions (entries 13 and 14, Table V.5) and C2 and C4 positions (entries 15, 17 and 43, Table V.5) of the aromatic ring, showed the lowest values of the percentage of relative cell proliferation (lower than 60%) (Table V.5).

Considering the results of the cytotoxicity of these compounds in these cell lines, it is clear that in general molecules containing no substituents in the phenyl ring or the methyl, nitro or methoxy groups at *para*-position of both series did not show notable cytotoxicity in all the cell lines used at 30 μM. Additionally, values lower than 50% of HepaRG, Caco-2 and NHDF cell proliferation were also not observed when a different heteroaromatic ring replaced the phenyl ring.

Overall, mainly the chlorinated compounds appeared to have significant cytotoxicity in the hepatic (HepaRG), neuronal (N27) and/or intestinal (Caco-2) cancer cell lines, which suggest that the presence of chlorine atoms could play an important role on the effects of these compounds in the *in vitro* growth of these cell lines. In this context, no marked differences between series, lateral chain and chlorine position were found in the screening against neuronal cells at 30 μM. Moreover, comparing with the results in HepaRG and Caco-2 cells, the cytotoxicity regarding N27 cells seems to be less marked. On the other hand, the major reduction of cell growth was observed in the hepatic cell line. Through Table V.3 it is also perceptible that DHPMs are more toxic than the corresponding DHPMts (with exception of compound **MM 46**). However, DHPMts showed additional marked cytotoxicity in Caco-2 cells, contrarily to DHPMs. Hence, the structures of the present molecules containing chlorine atoms appeared to be the most problematic in all these cell lines.

Table V.5 – Relative cell proliferation in percentage of the synthesized compounds, distributed respectively into the urea and thiourea series, and standard antiepileptic drugs (lamotrigine, carbamazepine, phenytoin and clonazepam), at 30 μM, in normal dermal fibroblasts (NHDF).

Entry	Compound	Relative cell proliferation (%)	Entry	Compound	Relative cell proliferation (%)
	Urea series			**Thiourea series**	
1	MM 18	76.90 ± 4.46*	29	MM 26	70.67 ± 7.29*
2	MM 72	92.40 ± 4.10	30	MM 83	83.03 ± 2.16**
3	MM 17	84.78 ± 3.04***	31	MM 25	83.89 ± 1.94
4	MM 22	67.20 ± 3.79*	32	MM 28	70.12 ± 8.07
5	MM 73	83.36 ± 2.40**	33	MM 84	76.31 ± 2.46*
6	MM 19	79.06 ± 7.97	34	MM 29	76.31 ± 6.18
7	MM 23	60.37 ± 3.44*			
8	MM 82	76.15 ± 1.44***			
9	MM 24	79.34 ± 6.17**	35	MM 30	67.37 ± 10.41
10	MM 34	67.04 ± 2.07	36	MM 36	69.50 ± 1.44***
11	MM 74	86.28 ± 5.06	37	MM 85	87.68 ± 1.79
12	MM 35	86.94 ± 5.27	38	MM 37	96.63 ± 0.84**
13	MM 55	52.91 ± 9.81***	39	MM 46	67.26 ± 15.69***
			40	MM 90	88.81 ± 8.20
14	MM 54	60.63 ± 3.04***	41	MM 48	69.56 ± 1.76*
15	MM 57	53.26 ± 2.46***	42	MM 60	65.06 ± 8.41***
16	MM 81	54.35 ± 2.38***	43	MM 92	56.87 ± 14.02**
17	MM 56	62.65 ± 1.75	44	MM 64	85.19 ± 2.93***
18	MM 59	70.65 ± 3.25***	45	MM 61	69.15 ± 7.06**
19	MM 75	59.63 ± 3.88***	46	MM 86	69.58 ± 5.37**
20	MM 58	83.25 ± 4.47***	47	MM 63	96.20 ± 1.55***
21	MM 65	86.99 ± 16.03*	48	MM 68	97.54 ± 6.80
22	MM 76	93.72 ± 8.80	49	MM 88	104.10 ± 2.43
23	MM 66	88.17 ± 4.85***	50	MM 67	93.85 ± 3.81
24	MM 93	69.31 ± 3.41***			
25	MM 99	65.21 ± 4.03***		**Antiepileptic drugs**	
26	MM 96	99.56 ± 9.70	51	Lamotrigine	88.95 ± 1.90*
27	MM 106	71.94 ± 5.42	52	Carbamazepine	91.19 ± 1.16
28	MM 95	102.68 ± 5.34***	53	Phenytoin	77.64 ± 9.82**
			54	Clonazepam	85.64 ± 10.12

Results are expressed as mean ± SD (standard deviation) after 72 h of treatment. Each experiment was performed in quadruplicate and at least two independent experiments were carried out. The control were untreated cells. *p < 0.05 *versus* control; **p < 0.01 *versus* control; ***p < 0.001 *versus* control.

Taking into consideration that the structure of the synthesized molecules is similar to monastrol (a DHPMt that exhibits antitumor properties by reversibly inhibiting the Kinesin-like protein KIF11), supplementary research work was performed in order to understand the potential antiproliferative activity of the compounds. They included additional studies of cytotoxicity in human breast adenocarcinoma (MCF-7), human breast ductal carcinoma (T47D) and human prostatic carcinoma (LNCaP) cell lines as well as the determination of cell death and a cell cycle distribution assay in order to clarify the mechanism of cytotoxicity. Moreover, analysis of the relationships between *in silico* calculated molecular descriptors and bioactivity by QSAR modelling was also performed (Appendix D).

V.3.2. Kinetic parameters

As already referred, DHPM(t)s have attracted considerable attention in organic and medicinal chemistry because they exhibit multiple pharmacological and therapeutic properties that are

worthy to be explored as a new hope for treating several pathologies. However, up to date, to the best of our knowledge, the pharmacokinetics of these compounds has never been investigated. Considering that the authentic efficacy of a molecule is strongly dependent of their pharmacokinetic properties, the early ADME assessment is required in order to predict the success as a new drug candidate. Indeed, poor pharmacokinetic properties are considered one of the main causes of compounds failure in drug development programmes. To fulfil this gap in the rational DHPM(t)s design and development, some relevant kinetic properties of the DHPM(t)s were explored with the purpose of understanding which are, from the kinetic point of view, the structural features that should be (or not) considered in further studies when searching for more potent anticonvulsant drug candidates.

Several *in vitro* permeability screening methodologies are being employed in the discovery settings to predict drug absorption (Feng et al., 2014). The concept of PAMPA was born in 1998 with the publication of the first flux based assay in the microtiter-plate format by Kansy and collaborators, using an artificial membrane of egg lecithin dissolved in *n*-dodecane (Kansy et al., 1998). Due to its relative versatility, the PAMPA technology has rapidly gained popularity within the pharmaceutical industry and a variety of PAMPA assays have appeared since then. Indeed, 10 years after the pioneering work of the Roche group, more than 100 publications referring to PAMPA have appeared and a number of research works about PAMPA have been highly cited in the literature (Faller, 2008). Indeed, this assay is an easy, fast, highly reproducible and relatively inexpensive technique, offering a high throughput approach to measure artificial membrane permeability and to assess the absorption potential of a large number of compounds (Reis et al., 2010) Moreover, it has been widely used for the selection of drug lead compounds for more advanced preclinical studies (early ADME screening), demonstrating a good correlation with *in vivo* absorption rates (Avdeef, 2005).

In this assay, a donor compartment and an acceptor compartment are separated by a filter supporting an artificial membrane consisting of ingredients found in biological membranes. A schematic representation of a PAMPA assay setup is shown in Figure V.1. Initially, the PAMPA system was developed to model the passive permeability through gastrointestinal epithelium. However, nowadays, different synthetic phospholipids and fatty acids are employed in order to mimic different biological barriers. Thus, for instance, this methodology has been modified for BBB permeability predictions by using porcine brain lipid as the phospholipid component (a PAMPA system called as PAMPA-BBB) (Sjöstedt et al., 2014). This motivated us to explore the potential of the DHPM(t)s to permeate either the intestine epithelium or the BBB, which are two important anatomophysiological barriers that can limit the efficacy of the DHPM(t)s as anticonvulsant drug candidates.

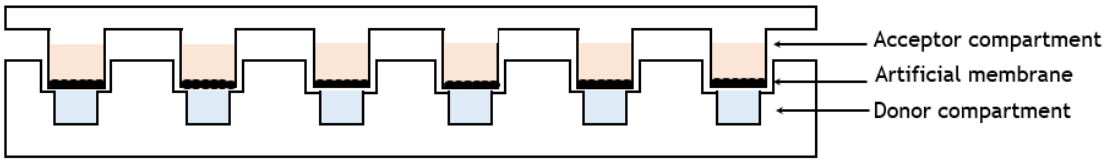

Figure V.1 - Schematic representation of a parallel artificial membrane permeability assay (PAMPA).

Thus, using L-α-phosphatidylcholine and *in-house* porcine brain lipid extract, the present work estimated, respectively, the intestinal absorption and the brain penetration of the DHPM(t)s under investigation. The Papp values found for each test compound and for the three commercial AEDs (lamotrigine, carbamazepine and phenytoin) are listed in Table V.6. The low variability obtained for the majority of the results indicates the good reproducibility of both PAMPA methodologies (intestinal PAMPA model and PAMPA-BBB model).

Table V.6 – Experimental apparent permeability (Papp) values of the synthesized dihydropyrimidin(thi)ones, distributed respectively into the urea and thiourea series, and the antiepileptic drugs lamotrigine, carbamazepine and phenytoin, tested in intestinal PAMPA and PAMPA-BBB models. Results are expressed as mean ± standard deviation, *n* = 6.

Compound	Intestinal PAMPA	PAMPA-BBB	Compound	Intestinal PAMPA	PAMPA-BBB
	P_{app} (× 10^{-6} cm/s)	P_{app} (× 10^{-6} cm/s)		P_{app} (× 10^{-6} cm/s)	P_{app} (× 10^{-6} cm/s)
Urea series			**Thiourea series**		
MM 18	5.00 ± 0.16	2.86 ± 0.28	MM 26	9.41 ± 0.90	4.47 ± 0.50
MM 72	3.33 ± 0.07	0.37 ± 0.01	MM 83	8.19 ± 0.60	4.11 ± 0.18
MM 17	1.16 ± 0.04	0.46 ± 0.02	MM 25	2.16 ± 0.41	1.03 ± 0.05
MM 22	3.86 ± 0.15	4.08 ± 0.14	MM 28	4.12 ± 0.59	3.87 ± 0.45
MM 73	5.79 ± 0.16	2.02 ± 0.23	MM 84	9.79 ± 0.90	5.43 ± 0.05
MM 19	2.54 ± 0.09	1.18 ± 0.04	MM 29	7.07 ± 0.23	2.40 ± 0.08
MM 23	6.16 ± 0.74	3.14 ± 0.44			
MM 82	5.71 ± 0.21	2.07 ± 0.06			
MM 24	2.36 ± 0.10	0.91 ± 0.04	MM 30	3.19 ± 0.12	1.43 ± 0.04
MM 34	5.50 ± 0.17	3.07 ± 0.10	MM 36	8.40 ± 1.72	4.18 ± 0.66
MM 74	3.43 ± 0.05	1.67 ± 0.02	MM 85	6.87 ± 1.96	3.70 ± 0.11
MM 35	1.35 ± 0.06	0.52 ± 0.01	MM 37	2.47 ± 0.04	1.08 ± 0.04
MM 55	0.76 ± 0.10	1.07 ± 0.14	MM 46	0.58 ± 0.09	1.46 ± 0.11
			MM 90	4.39 ± 0.30	2.33 ± 0.14
MM 54	2.57 ± 0.21	2.23 ± 0.13	MM 48	1.28 ± 0.41	2.43 ± 0.15
MM 57	0.95 ± 0.12	1.35 ± 0.30	MM 60	1.87 ± 0.16	2.06 ± 0.11
MM 81	0.77 ± 0.09	3.74 ± 0.61	MM 92	0.62 ± 0.05	3.09 ± 0.30
MM 56	5.85 ± 0.13	3.46 ± 0.08	MM 64	9.21 ± 1.35	4.65 ± 0.22
MM 59	2.66 ± 0.25	3.20 ± 0.44	MM 61	5.66 ± 0.35	3.32 ± 1.02
MM 75	2.15 ± 0.16	0.80 ± 0.07	MM 86	7.25 ± 0.27	3.69 ± 0.12
MM 58	1.58 ± 0.08	0.64 ± 0.01	MM 63	1.09 ± 0.04	1.36 ± 0.10
MM 65	1.96 ± 0.08	1.29 ± 0.05	MM 68	3.78 ± 0.10	2.56 ± 0.08
MM 76	1.22 ± 0.04	0.68 ± 0.02	MM 88	2.14 ± 0.07	0.92 ± 0.05
MM 66	0.35 ± 0.02	0.21 ± 0.02	MM 67	0.82 ± 0.18	0.49 ± 0.01
MM 93	3.83 ± 0.18	2.72 ± 0.06			
MM 99	2.83 ± 0.17	5.93 ± 0.17	**Antiepileptic drugs**		
MM 96	4.21 ± 0.09	2.46 ± 0.31	Lamotrigine	3.83 ± 0.05	1.20 ± 0.03
MM 106	1.85 ± 0.07	4.02 ± 0.26	Carbamazepine	7.72 ± 0.02	3.41 ± 0.12
MM 95	0.82 ± 0.03	0.97 ± 0.03	Phenytoin	2.56 ± 0.01	2.81 ± 0.32

In the intestinal PAMPA assay, two different pH values were considered in donor (pH 6.5) and acceptor (pH 7.4) compartments in order to simulate the proximal small intestine and blood pH environment, respectively. After 16 h of incubation, the majority of the compounds of both series presented a Papp higher than 1.1×10^{-6} cm/s through the artificial membrane, in the same range of the marketed AEDs (Figure V.2), suggesting that they are absorbed in the intestine through passive transcellular pathway. The urea derivatives **MM 55**, **MM 57**, **MM 81**, **MM 66** and **MM 95** and the thiourea derivatives **MM 46**, **MM 92**, **MM 63** (borderline value) and **MM 67** displayed a Papp value lower than 1.1×10^{-6} cm/s, which suggests a low passive transcellular permeability.

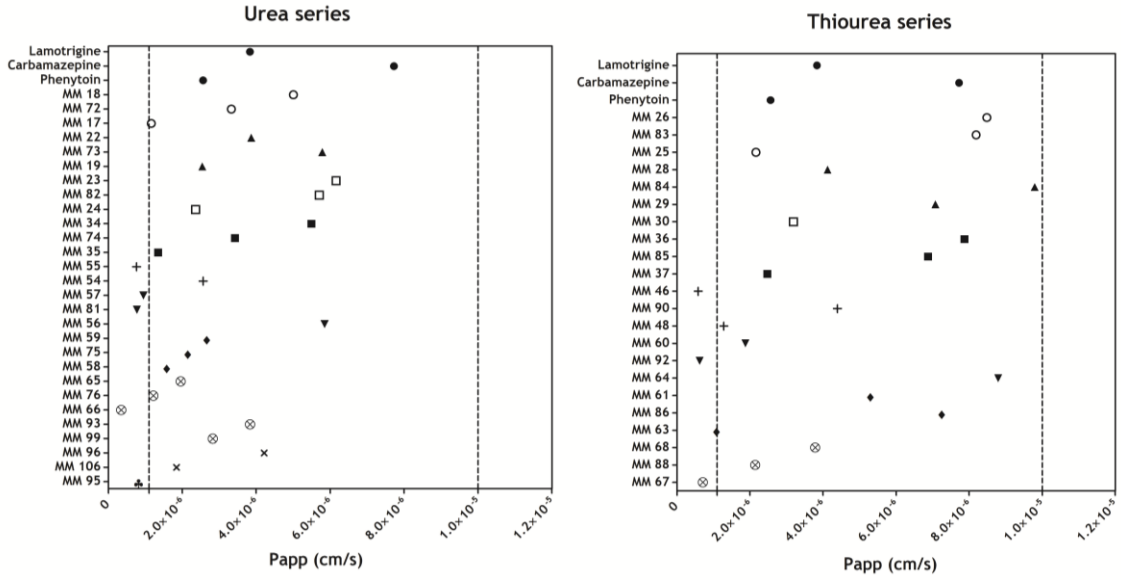

Figure V.2 – Experimental apparent permeability (Papp) values of the tested compounds and the marketed antiepileptic drugs lamotrigine, carbamazepine and phenytoin, obtained employing intestinal PAMPA model with 2% of L-α-phosphatidylcholine in *n*-dodecane and 16 h of incubation. Vertical dashed lines correspond to Papp = 1.1×10^{-6} cm/s and Papp = 1×10^{-5} cm/s, respectively from the left to right. Compounds between the two vertical dashed lines present a predicted intestinal absorption fraction higher than 85% and plasma protein binding lower than 90%. The main structural characteristics are portrayed as: ● antiepileptic drugs; ○ unsubstituted phenyl ring; ▲ 4-methyl; □ 4-nitro; ■ 4-methoxy; + 2,3-dichloro; ▼ 2,4-dichloro; ♦ 2,3-difluoro; ⊗ furyl; × thiophenyl; ♣ pyridil.

According to Fortuna *et al.* (Fortuna et al., 2012), the intestinal PAMPA model herein employed can be used not only to predict the human intestinal absorption fraction (Fa), but also the extent of plasma protein binding (PPB) of compounds. For compounds with values of Papp higher than 1.1×10^{-6} cm/s, a high Fa (≥ 85%) can be anticipated, whereas compounds with Papp values smaller than 1.1×10^{-6} cm/s are expected to present a Fa lower than 85% in humans. However, if Papp is equal to or higher than 1.0×10^{-5} cm/s, compounds are expected to exhibit a percentage of PPB higher than 90% in humans, which may be critical in clinical practice. Therefore, taking into account the obtained data, almost all compounds are expected to present a Fa equal to or greater than 85% and a PPB lower than 90%, which are

favourable indicators for its clinical development (Figure V.2 and Table V.6). Thus, overall, only nine out of fifty DHPM(t)s (**MM 46**, **MM 55**, **MM 57**, **MM 63**, **MM 66**, **MM 67**, **MM 81**, **MM 92** and **MM 95**) exhibited Papp values lower than 1.1×10^{-6} cm/s and, consequently, are expected to have a low Fa in humans (Table V.7). On the other hand, a special attention should be given to compound **MM 84**, which exhibited the highest Papp value obtained for the tested compounds and it is positioned in the limit between low and high PPB, as can be observed in Figure V.2 and Table V.6.

Table V.7 – Classification of the synthesized dihydropyrimidin(thi)ones and the antiepileptic drugs lamotrigine, carbamazepine, phenytoin regarding their human intestinal absorption fraction (Fa) and plasma protein binding (PPB), predicted by the intestinal PAMPA model used. The compounds are grouped as urea and thiourea series.

Compound	Fa	PPB	Compound	Fa	PPB
Urea series			**Thiourea series**		
MM 18	High	Low	MM 26	High	Low
MM 72	High	Low	MM 83	High	Low
MM 17	High	Low	MM 25	High	Low
MM 22	High	Low	MM 28	High	Low
MM 73	High	Low	MM 84	High	Low
MM 19	High	Low	MM 29	High	Low
MM 23	High	Low			
MM 82	High	Low			
MM 24	High	Low	MM 30	High	Low
MM 34	High	Low	MM 36	High	Low
MM 74	High	Low	MM 85	High	Low
MM 35	High	Low	MM 37	High	Low
MM 55	Low	Low	MM 46	Low	Low
			MM 90	High	Low
MM 54	High	Low	MM 48	High	Low
MM 57	Low	Low	MM 60	High	Low
MM 81	Low	Low	MM 92	Low	Low
MM 56	High	Low	MM 64	High	Low
MM 59	High	Low	MM 61	High	Low
MM 75	High	Low	MM 86	High	Low
MM 58	High	Low	MM 63	Low	Low
MM 65	High	Low	MM 68	High	Low
MM 76	High	Low	MM 88	High	Low
MM 66	Low	Low	MM 67	Low	Low
MM 93	High	Low			
MM 99	High	Low	**Antiepileptic drugs**		
MM 96	High	Low	Lamotrigine	High	Low
MM 106	High	Low	Carbamazepine	High	Low
MM 95	Low	Low	Phenytoin	High	Low

Since these DHPM(t)s were synthesized as potential anticonvulsant drug candidates (Matias et al., 2017b), their ability to cross the BBB is an essential requirement. For this reason, their BBB permeability was also predicted, using a PAMPA-BBB model. In this case, the membrane was impregnated with a lipid extracted directly from a fresh pig brain (*in-house* brain lipid extract) as already described in the literature (Abbott et al., 2013). The extraction method was previously optimized, being concluded that the implemented lipid extraction process was reproducible, cost-effective and reliable when compared to the commercialized polar brain porcine (Bicker et al., 2016), which is the main lipid used in the PAMPA-BBB assay. Firstly, the phospholipid content in the lipid extracts from the brain tissue was approximately 35.73 ±

2.83 μg phospholipids per mg wet brain weight (n = 4 extracts) in phosphorus assay. This result was coherent with those previously obtained, indicating a good reproducibility of the lipid extraction method. Concerning the PAMPA-BBB procedure, the assays were conducted at pH 7.4 in both sides of the artificial membrane in order to mimic the physiological conditions of blood and brain extracellular fluid. Similarly to intestinal PAMPA, the incubation time was 16 h, which allowed, in this case, the discrimination between BBB^- (low BBB permeation) and BBB^+ (high BBB permeation) compounds. However, due to the high permeability of the compounds **MM 48**, **MM 59** and **MM 106**, they were further measured after 3 h of incubation. In this assay, the Papp cut-off value of 2.0×10^{-6} cm/s was defined to discriminate BBB^+ compounds (Papp > 2.0×10^{-6} cm/s) and BBB^- (Papp < 2.0×10^{-6} cm/s) (Bicker et al., 2016). As illustrated in Figure V.3, approximately 50% of urea derivatives (Papp ranges from 2.15×10^{-6} cm/s to 6.16×10^{-6} cm/s) and 70% of thiourea derivatives (Papp ranges from 2.14×10^{-6} cm/s to 9.79×10^{-6} cm/s) were considered BBB^+. Using the present PAMPA-BBB model, lamotrigine was classified as BBB^- (Papp = 1.20×10^{-6} cm/s), which is consistent with results found in the literature (Di et al., 2009). This can suggest that the transport of lamotrigine across the BBB probably involves other mechanisms rather than passive transcellular diffusion, such as the active uptake mediated by organic cation transporter 1 (Dickens et al., 2012).

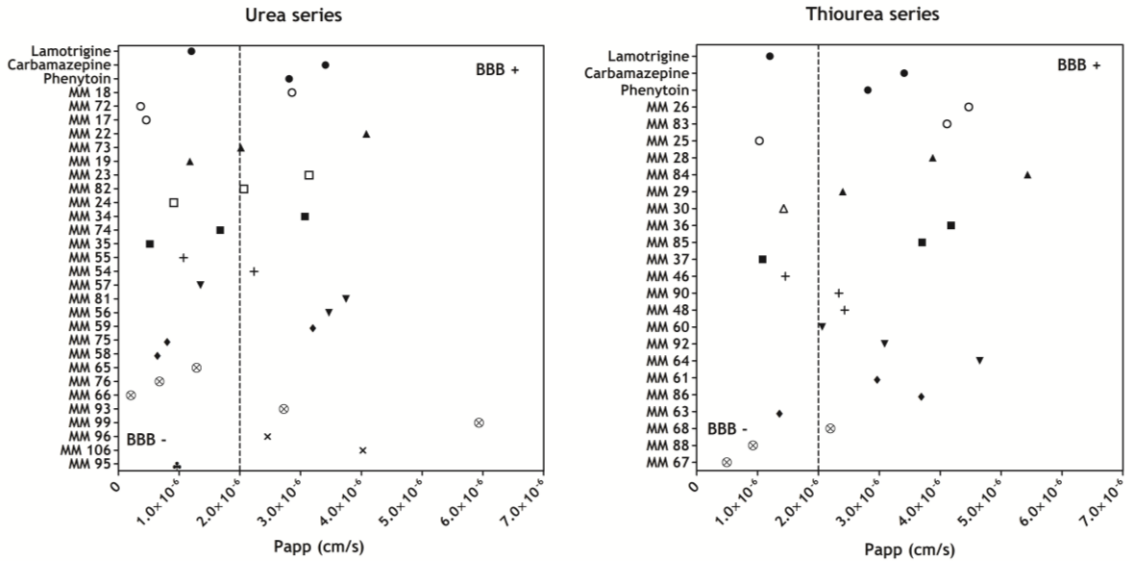

Figure V.3 – Experimental apparent permeability (Papp) values of the tested compounds and the marketed antiepileptic drugs lamotrigine, carbamazepine and phenytoin, obtained employing the PAMPA-BBB model with 2% of *in-house* brain lipid extract in *n*-dodecane and 16 h of incubation. Compounds **MM 48**, **MM 59** and **MM 106** were evaluated after 3 h of incubation. The vertical dashed line corresponds to Papp = 2×10^{-6} cm/s. Compounds with higher values of Papp were classified as BBB^+ and compounds with lower values of Papp were classified as BBB^-. The main structural characteristics are portrayed as: ● antiepileptic drugs; ○ unsubstituted phenyl ring; ▲ 4-methyl; □ 4-nitro; ■ 4-methoxy; + 2,3-dichloro; ▼ 2,4-dichloro; ♦ 2,3-difluoro; ⊗ furyl; × thiophenyl; ♣ pyridil.

Overall, it was verified that 82% of the compounds displayed good intestinal permeability, 66% of which also presented good BBB permeability. In both experiments, compounds belonging to thiourea series presented higher permeability values in comparison with the respective analogues of the urea series. This could be explained, in part, by their higher lipophilic nature.

Due to the fact that the results obtained in PAMPA assays do not include the effect of efflux transporters, an additional study was carried out in order to understand the interference of DHPM(t)s on the P-gp-mediated efflux activity. For that, the fifty chemical compounds were herein investigated for the first time regarding their effect on the P-gp-mediated efflux transport in MDCK-MDR1 cells using as surrogate marker the intracellular accumulation of Rh123 (a well-known fluorescent P-gp probe substrate) (Barthomeuf et al., 2005; Jouan et al., 2016). In fact, probe substrate accumulation assays have been applied since they were successfully used in HTS methodologies to assess the inhibition/induction potency of P-gp modulators (Jouan et al., 2016). The negative control consisted of evaluating the accumulation of Rh123 in untreated cells while the positive control corresponded to that quantification in cells treated with the classical P-gp inhibitor, verapamil. Lamotrigine, carbamazepine and phenytoin were also evaluated for comparative purposes. All compounds were tested at both concentrations of 10 μM and 50 μM (Bharate et al., 2015; Juvale et al., 2012).

To prevent misrepresentation of the results due to toxic effects, the intrinsic cytotoxicity of the tested compounds against MDCK-MDR1 cells was evaluated by the MTT assay at the same concentrations used in the intracellular Rh123 accumulation assay. The cytotoxicity activity of the compounds is listed in Table V.8 and it is expressed in percentage as the relative cell proliferation in comparison with the negative control. In general, as discussed in the literature (Wu et al., 2016), the compounds did not demonstrate marked cytotoxicity (relative cell proliferation higher than 50%) after 4 h of incubation.

Table V.8 – Relative cell proliferation resulted from MTT assay (expressed as the mean value ± standard deviation) of the synthesized dihydropyrimidin(thi)ones and lamotrigine, carbamazepine, phenytoin and verapamil, at concentrations of 10 and 50 μM, against Madin-Darby canine kidney cells expressing the efflux transporter P-glycoprotein (MDCK-MDR1).

Compound	Relative cell proliferation (%)		Compound	Relative cell proliferation (%)	
	10 μM	50 μM		10 μM	50 μM
Urea series			**Thiourea series**		
MM 18	98.35 ± 3.86	94.95 ± 5.61	MM 26	98.66 ± 8.01	96.42 ± 3.86
MM 72	103.95 ± 5.85	104.40 ± 7.59	MM 83	89.92 ± 13.48	93.23 ± 11.66
MM 17	98.88 ± 0.67	100.00 ± 6.09	MM 25	94.70 ± 3.50	96.21 ± 7.22
MM 22	102.16 ± 4.10	108.08 ± 1.07*	MM 28	92.52 ± 1.39*	86.40 ± 4.02***
MM 73	99.65 ± 5.35	91.12 ± 4.68	MM 84	98.53 ± 7.49	104.11 ± 14.13
MM 19	98.89 ± 2.76	88.96 ± 2.03**	MM 29	100.55 ± 8.22	99.02 ± 5.54
MM 23	108.28 ± 5.83*	103.16 ± 2.11			
MM 82	104.78 ± 9.29	99.69 ± 8.11			
MM 24	99.20 ± 1.86	91.77 ± 2.41*	MM 30	100.87 ± 9.90	100.32 ± 5.31
MM 34	96.18 ± 12.18	89.97 ± 3.36**	MM 36	95.17 ± 9.91	86.41 ± 7.00**
MM 74	89.44 ± 3.90	98.80 ± 4.98	MM 85	107.34 ± 10.07	96.27 ± 11.14
MM 35	100.12 ± 9.61	95.65 ± 14.00	MM 37	89.22 ± 5.74*	70.12 ± 9.06***
MM 55	94.78 ± 4.62	81.55 ± 2.42***	MM 46	83.52 ± 7.46**	88.47 ± 2.42*
			MM 90	90.49 ± 12.78	76.10 ± 4.38***
MM 54	90.25 ± 7.14*	79.75 ± 9.21***	MM 48	92.89 ± 7.65	91.59 ± 2.95
MM 57	78.20 ± 2.22***	77.41 ± 4.71***	MM 60	76.81 ± 8.89***	62.82 ± 4.95***
MM 81	95.10 ± 4.08	99.50 ± 8.06	MM 92	75.04 ± 4.36***	66.48 ± 6.35***
MM 56	88.77 ± 4.17**	89.21 ± 7.35*	MM 64	91.69 ± 2.92*	89.03 ± 2.94**
MM 59	96.47 ± 6.66	94.16 ± 2.26	MM 61	99.62 ± 3.77	102.45 ± 4.41
MM 75	93.44 ± 3.16	91.82 ± 8.95	MM 86	92.28 ± 9.10	88.26 ± 4.94**
MM 58	96.17 ± 4.20	99.22 ± 2.46	MM 63	99.89 ± 2.65	101.11 ± 6.54
MM 65	92.69 ± 5.06	106.42 ± 5.30	MM 68	100.00 ± 7.95	103.05 ± 1.92
MM 76	92.19 ± 11.72	88.74 ± 6.77	MM 88	100.90 ± 1.65	110.54 ± 7.27
MM 66	103.33 ± 8.66	102.42 ± 6.22	MM 67	97.20 ± 17.07	95.62 ± 3.60
MM 93	95.94 ± 3.28	106.66 ± 7.35			
MM 99	97.94 ± 4.25	100.22 ± 4.48	**Antiepileptic drugs**		
MM 96	101.07 ± 7.01	95.94 ± 8.62	Lamotrigine	95.52 ± 6.08	94.90 ± 7.75
MM 106	100.07 ± 6.96	94.95 ± 6.06	Carbamazepine	98.81 ± 1.92	99.21 ± 3.32
MM 95	111.34 ± 12.31	102.59 ± 9.47	Phenytoin	103.00 ± 2.58	98.98 ± 4.04
			Verapamil	95.74 ± 5.28	91.88 ± 2.91

Results are expressed as mean ± standard deviation after 4 h of incubation (n=4). Untreated cells were the control. *p < 0.05 *versus* control; **p < 0.01 *versus* control; ***p < 0.001 *versus* control.

Concerning the interference of the DHPM(t)s in P-gp modulation (induction or inhibition), they presented very distinct results. If a cut-off value of ± 20% regarding to control (100%) is applied, it can be verified that around half of the compounds (**MM 18**, **MM 72**, **MM 83**, **MM 25**, **MM 22**, **MM 84**, **MM 19**, **MM 24**, **MM 30**, **MM 34**, **MM 85**, **MM 35**, **MM 57**, **MM 56**, **MM 64**, **MM 61**, **MM 75**, **MM 86**, **MM 63**, **MM 65**, **MM 68**, **MM 66**, **MM 67**, **MM 93**, **MM 96** and **MM 106**) presented similar values to the negative control (Table V.9), suggesting that they did not modulate P-gp at both concentrations tested (10 and 50 μM). On the one hand, the derivatives **MM 82**, **MM 59**, **MM 58**, **MM 99** and **MM 95** (entries 8, 18, 20, 25 and 28, Table V.9) showed at 50 μM a negative effect on intracellular Rh123 accumulation (69-79%) similar to the observed with lamotrigine, carbamazepine and phenytoin (68-79%), suggesting the induction of the P-gp functional activity. In addition, a similar inducing effect was also observed for compounds **MM 17**, **MM 73**, **MM 74** and **MM 76** (entries 3, 5, 11 and 22, Table V.9) (intracellular Rh123 accumulation ranging from 69-79%) at 10 μM. On the other hand, interestingly, the compounds incorporating chlorine atoms in their structure (entries 13-17 and 39-44, Table V.9), in general, seemed to inhibit the P-gp transport at 50 μM (intracellular

Rh123 accumulation ranging from 122-350%); among them, compounds **MM 46** and **MM 60** stand out with increased levels of Rh123 around, respectively, 3.4- and 2.8-fold in relation to negative control. At the concentration of 50 μM, compounds **MM 26**, **MM 28**, **MM 29**, **MM 36**, **MM 37** and **MM 88** were also able to increase the amount of Rh123 intracellularly accumulated in MDCK-MDR1 cells (122-160%), suggesting their inhibition of the P-gp activity in these cells. Indeed, from Table V.9, it is evident that the urea derivatives showed a trend to induce the P-gp activity whereas the thiourea derivatives seem to have a trend to inhibit the P-gp activity.

Table V.9 – Intracellular accumulation of rhodamine 123 (Rh123) induced by tested dihydropyrimidin(thi)ones at the concentrations of 10 μM and 50 μM. The verapamil and the antiepileptic drugs lamotrigine, carbamazepine and phenytoin were also used for comparison.

Entry	Compound	Rh123 accumulation (%)		Entry	Compound	Rh123 accumulation (%)	
		10 μM	50 μM			10 μM	50 μM
	Urea series				**Thiourea series**		
1	MM 18	100.18 ± 7.34	86.61 ± 16.43	29	MM 26	104.15 ± 15.48	**135.93 ± 28.09***
2	MM 72	83.54 ± 13.47	83.68 ± 9.10*	30	MM 83	91.03 ± 30.21	88.72 ± 13.70
3	MM 17	**77.29 ± 17.58***	87.90 ± 20.56	31	MM 25	95.05 ± 11.80	88.58 ± 8.18
4	MM 22	95.93 ± 11.73	102.50 ± 32.40	32	MM 28	115.83 ± 11.37	**142.20 ± 5.31***
5	MM 73	**79.25 ± 17.78***	81.15 ± 10.19*	33	MM 84	81.07 ± 11.56*	97.70 ± 17.41
6	MM 19	90.38 ± 6.53	113.62 ± 53.94	34	MM 29	116.88 ± 63.69	**128.14 ± 15.07**
7	MM 23	**123.76 ± 25.56**	104.56 ± 15.15				
8	MM 82	81.29 ± 7.20*	**75.54 ± 2.56***				
9	MM 24	85.59 ± 10.29	110.10 ± 27.39	35	MM 30	103.45 ± 31.44	117.41 ± 12.81*
10	MM 34	102.65 ± 15.01	110.55 ± 14.01	36	MM 36	**122.12 ± 23.82**	**160.45 ± 9.51***
11	MM 74	**72.95 ± 4.61***	91.28 ± 6.41	37	MM 85	81.99 ± 13.56*	86.27 ± 6.21*
12	MM 35	82.53 ± 15.13*	103.86 ±13.31	38	MM 37	103.39 ± 8.72	**122.12 ± 18.25***
13	MM 55	104.77 ± 8.48	**148.39 ± 16.22***	39	MM 46	**122.29 ± 16.03***	**350.32 ± 26.43***
				40	MM 90	108.65 ± 18.59	**187.26 ± 16.58***
14	MM 54	116.41 ± 119.20	**123.28** ± 29.87	41	MM 48	110.39 ± 14.78	**131.01 ± 31.00***
15	MM 57	100.60 ± 2.25	114.32 ± 8.83*	42	MM 60	**130.02 ± 13.16***	**283.29 ± 19.34***
16	MM 81	99.01 ± 8.17	**154.68 ± 43.61***	43	MM 92	84.39 ± 7.53*	**160.82 ± 24.54***
17	MM 56	89.63 ± 9.31	117.76 ± 18.61	44	MM 64	95.60 ± 9.97	106.63 ± 18.38
18	MM 59	94.30 ± 12.02	**75.45 ± 6.92**	45	MM 61	87.64 ± 17.44	106.63 ± 13.71
19	MM 75	89.03 ± 15.29	91.85 ± 8.92	46	MM 86	95.36 ± 20.74	97.56 ± 7.79
20	MM 58	113.28 ± 26.27	**74.49 ± 10.11***	47	MM 63	90.53 ± 12.59	109.68 ± 7.98
21	MM 65	88.54 ± 16.73	96.26 ± 28.25	48	MM 68	90.68 ± 19.09	105.29 ± 23.23
22	MM 76	**68.67 ± 12.94***	93.99 ± 13.99	49	MM 88	**131.03 ± 19.04***	**128.17 ± 22.46***
23	MM 66	81.94 ± 15.66*	92.03 ± 18.23	50	MM 67	117.35 ± 42.50	86.17 ± 11.16
24	MM 93	107.41 ± 18.23	86.96 ± 19.43				
25	MM 99	91.39 ± 14.27	**69.20 ± 5.57***		**Antiepileptic drugs**		
26	MM 96	98.05 ± 12.87	90.04 ± 26.93	51	Lamotrigine	108.80 ± 28.45	**67.59 ± 4.84***
27	MM 106	91.88 ± 16.45	89.15 ± 24.98	52	Carbamazepine	102.74 ± 4.67	**77.67 ± 16.92***
28	MM 95	91.22 ± 8.17	**79.21 ± 14.47***	53	Phenytoin	105.11 ± 8.70	**78.51 ± 22.26**
				54	Verapamil	**512.22 ± 39.46***	**458.75 ± 21.87***

Results are expressed as means ± standard deviation (n = 5-6). Untreated cells were the control. The bold values correspond to the compounds that presented values ± 20% regarding to control (100%). * $p < 0.05$ versus control.

Overall, the *in vitro* results herein obtained revealed that 52% of the compounds did not modulate this efflux transporter. This is an important finding since P-gp is physiologically expressed in tissues and organs decisively influencing the pharmacokinetics and, therefore, its inhibition or induction may cause important changes in the pharmacokinetics of several drugs (Hitchcock, 2012), leading to DDIs, disturbance of drug efficacy and potentiation of toxicity.

As P-gp induction can be beneficial to efflux out of P-gp substrate toxins from the body and, particularly, from the CNS by hampering their access to the brain, efforts have been made to find new chemical entities capable of acting as P-gp inducers (Padala et al., 2016; Silva et al., 2015). However, when developing DHPM(t)s as anticonvulsant drug candidates it may be favourable to select for further development those compounds that do not interfere with P-gp or those that exhibit a moderate P-gp inhibition. Furthermore, as the overexpression of this drug efflux transporter at the level of the BBB has been proposed as one of the major mechanisms responsible for multidrug resistance in epilepsy (Aronica et al., 2012), a certain level of P-gp inhibition is expected to increase the AED concentrations in epileptogenic brain areas by therapy with AEDs that are substrates of the P-gp. Nevertheless, development of drug tolerance or potentiation of side effects can become barriers to this kind of modulation (Potschka, 2012).

In conclusion, the kind of data herein presented are crucial for decision-making processes during the drug discovery and development steps. The results of the present study allowed to draw some conclusions about the structural features of DHPM(t)s derivatives which are important from the pharmacokinetic perspective for further hit-to-lead optimization. Overall, within this group of compounds, thiourea derivatives containing an unsubstituted or a *p*-monosubstituted (-NO_2, -CH_3, -OCH_3) phenyl attached to the position 4 of the dihydropyrimidine represent the most promising structures from the kinetic point of view and they should be considered in subsequent studies of development of new drug candidates. Particularly, in the case of anticonvulsant drug development, as studies of efficacy are usually performed by means of *in vivo* animal models of seizures and/or epilepsy, the need of the evaluation of ADMET properties as part of the screening process during the selection of drug candidates is reinforced.

CHAPTER VI

IN SILICO STUDIES:

Pharmacokinetic and toxicity predictions

VI.1. Introduction

To assess the biological activity of drug candidates, *in vivo* and *in vitro* models are widely used; however, in the last decades, computational (*in silico*) methods have also been extensively applied in drug discovery and development programmes.

A wide range of computational approaches have been used to investigate various aspects of interest in the drug discovery and development, in particular because it has been proposed that the extensive use of computational tools could reduce the cost of drug development by up to 50%. *In silico* models are particularly useful during the early stages of a drug discovery/development programme when thousands of compounds must be screened for either interactions with a specific target or for the appropriate physicochemical properties. As consequence, these computational strategies are able to decrease the number of molecules to only few hit compounds, which are then synthesized and tested in *in vitro* and/or *in vivo* models (Passeleu-Le Bourdonnec et al., 2013). According to Wang *et al*. (Wang et al., 2015) the rational drug design methods can be divided into two major classes:

- methods for lead discovery and optimization, which often play an important role in the early state of research and development and help scientists to identify compounds with higher potency and selectivity to one or a few targets. In this context, the integration of experimental and computational methods allows the identification and development of new chemical starting points from collections of real or virtual compounds. Virtual screening can be based on ligand structure or based on the target structure, namely employing the use of molecular docking, which includes, for example, the prediction of the binding mode of a small molecule in a binding site of the target (Andrade et al., 2016);
- methods for predicting compounds' druggability, which aim to prioritize lead molecules for further development by a comprehensive assessment of their therapeutic properties. Notwithstanding the development of faster and more reliable *in vitro* screening technologies, it is expected that in the future the *in silico* tools will play a decisive role for rationalising and predicting the ADMET properties of compounds in the drug discovery (Eddershaw et al., 2000). In fact, the *in silico* prediction of ADMET characteristics has provided an easy and accessible high throughput method to improve the screening ability of compounds and reducing the time and costs of the drug discovery process (Zhou et al., 2016). Moreover, *in silico* methods have also greatly increased the ability to predict human pharmacokinetics properties based on physicochemical, *in vitro* and whole-animal data (Pellegatti, 2012). The establishment of high-quality *in silico* models permits the optimization of compounds druggability properties in parallel with the evaluation of their efficacy, which is expected not only to improve the overall quality of drug candidates and therefore the probability of their success, but also to reduce the expenses due to a reduced downstream attrition rate (Wang et al., 2015).

Hence, *in silico* studies afford the advantages of speed of execution, low cost and ability to reduce the use of animals and can include the study of the SAR, toxicity, pharmacodynamics and pharmacokinetics (Andrade et al., 2016). The computational approaches have application in all stages of the drug discovery and development process. The challenges in computer simulation of biopharmaceutical properties of small-molecule compounds has been particularly successful through implementation of models using predicted and measured biopharmaceutical data (Leucuta, 2014). Thus, a set of physicochemical, pharmacokinetic and toxicity properties of the synthesized DHPM(t)s was estimated in order to better understand their druggabillity.

VI.2. Experimental section

VI.2.1. Physicochemical properties

A computational study was performed to estimate several physicochemical and molecular properties for all compounds [synthesized DHPM(t)s and commercial reference compounds]. Molecular descriptors such as *n*-octanol/water partition coefficient (Log *P*), topological polar surface area (TPSA), number of rotatable bonds (*n*-ROTB), number of hydrogen bond donors (*n*-OHNH donors), number of hydrogen bond acceptors (*n*-OH acceptors) and violations of Lipinski's rule of five were calculated by using ACD/Percepta 2015 ("ACD/Percepta, 2015). Log *P* was calculated using GALAS algorithm. Hydrophilic factor (Hy) was calculated using E-Dragon online 1.0 (Tetko et al., 2005). The percentage of oral absorption (%ABS) was calculated using the formula 109-0.345*TPSA (Zhao et al., 2002) and molecular volume (MV) was calculated using the formula molecular weight (MW)/density, which were also obtained through ACD/Percepta 2015.

VI.2.2. Pharmacokinetic and toxicity properties

The ADMET properties were generated from SMILES string for all synthesized compounds and commercial AEDs lamotrigine, carbamazepine, phenytoin, clonazepam and sodium valproate. The properties were determined through the freely accessible web server pkCSM, which use graph-based signatures (http://structure.bioc.cam.ac.uk/pkcsm). The specific parameters were selected for their importance in development of AEDs.

VI.3. Results and discussion

The information about the druglikeness of compounds is useful in decision-making process to improve the success rate in drug discovery. Important physicochemical properties of a drug compound include lipophilicity, aqueous solubility, ionization, topology, and molecular mass. These properties may affect the ADMET profile of the compounds, their potency, selectivity against targets, and the 'screenability' in HTS. Therefore, multiple methods and tools exist to assess the physicochemical properties of a molecule that are able to affect the pharmacokinetic and pharmacodynamic properties (Mignani et al., 2016; Wang et al., 2015). Thus, a computational study for the prediction of the relevant properties influencing bioactivity of the target compounds was performed, and the *in silico* molecular parameters of the synthesized DHPM(t)s and several AEDs are summarized in Table VI.1.

Firstly, the TPSA has been recognized as a good indicator that enables the prediction of transport properties of drugs in the intestine and the BBB (Ertl et al., 2000). This descriptor allowed the calculation of the percentage of oral absorption (%ABS). It was observed that an acceptable oral absorption ranging from 68.89 to 88.92% was estimated for the target compounds. Additionally, for drugs that have to cross the BBB, their activity has been correlated with an optimum lipophilicity (Log *P*) near 2 (Van de Waterbeemd et al., 1998), as also demonstrated by the commercial AEDs tested (Table VI.1). In the context of anticonvulsant activity, some authors suggest that increased lipophilicity does not necessarily enhance the anticonvulsant properties and, conversely, it may sometimes lead to a reduction or loss of activity (Liao et al., 2017). On the other hand, other authors refer that the duration of anticonvulsant protection of the tested compounds depends on the lipophilic properties of the molecules, namely, the higher log *P* value, the longer activity was observed (Kamiński et al., 2016). In fact, the lipophilicity of compounds should be high enough to allow a good affinity to lipid membranes, but it should not be too high so as to avoid trapping of the compound inside the membrane and bioaccumulation. Due to the hydrophobic nature of the biomembranes, ionisation also greatly affects the drug diffusion because ionised compounds are highly hydrophilic and therefore can have poor interactions with the biomembrane components. The *in silico* results obtained for the synthesized DHPM(t)s predicted a large range of Log *P* values among the tested compounds. For example, compounds containing chlorine atoms attached to the phenyl ring presented higher lipophilicity (2.94-3.56). On the other hand, the predicted Log *P* values for compounds possessing an unsubstituted furan ring and the pyridine pharmacophore were clearly lower (0.52-0.87 and 0.57, respectively), suggesting a poor ability to cross biological barriers. These results led to the introduction of the Hy in the calculated parameters, which gives the hydrophilic profile for the compounds. However, in this case, it was not verified a great difference of values among the compounds (0.36-0.53).

Table VI.1 – Molecular properties of tested dihydropyrimidin(thi)ones and antiepileptic drugs lamotrigine, carbamazepine, phenytoin, clonazepam and sodium valproate.[a]

Compound	%ABS	TPSA	*n*-ROTB	MW	MV	Log *P*	Hy	*n*-OHNH donors	*n*-OH acceptors	Lipinski's violation[b]
MM 18	85.74	67.43	4	260.29	222.47	1.79	0.39	2	5	0
MM 26	80.55	82.45	4	276.36	219.33	1.66	0.39	2	4	0
MM 72	85.74	67.43	3	246.26	205.22	1.48	0.43	2	5	0
MM 83	80.55	82.45	3	262.33	203.36	1.51	0.43	2	4	0
MM 17	88.92	58.20	2	230.26	200.23	1.46	0.41	2	4	0
MM 25	83.74	73.22	2	246.33	197.06	1.42	0.41	2	3	0
MM 22	85.74	67.43	4	274.32	238.54	2.13	0.36	2	5	0
MM 28	80.55	82.45	4	290.38	236.08	2.01	0.36	2	4	0
MM 73	85.74	67.43	3	260.29	222.47	1.88	0.39	2	5	0
MM 84	80.55	82.45	3	276.36	219.33	1.59	0.39	2	4	0
MM 19	88.92	58.20	2	244.29	216.19	1.84	0.37	2	4	0
MM 29	83.74	73.22	2	260.36	213.41	1.93	0.37	2	3	0
MM 23	68.89	116.26	5	305.29	234.84	1.74	0.44	2	8	0
MM 82	68.89	116.26	4	291.26	217.36	1.41	0.47	2	8	0
MM 24	72.07	107.03	3	275.26	211.74	1.34	0.46	2	7	0
MM 30	66.89	122.05	3	291.33	209.59	1.33	0.46	2	6	0
MM 34	82.55	76.66	5	290.31	246.03	1.57	0.38	2	6	0
MM 36	77.37	91.68	5	306.38	241.24	1.51	0.38	2	5	0
MM 74	82.55	76.66	4	276.29	230.24	1.34	0.41	2	6	0
MM 85	77.37	91.68	4	292.35	226.63	1.29	0.41	2	5	0
MM 35	85.74	67.43	3	260.29	224.39	1.38	0.39	2	5	0
MM 37	80.55	82.45	3	276.36	219.33	1.32	0.39	2	4	0
MM 55	85.74	67.43	4	329.18	245.66	3.31	0.43	2	5	0
MM 46	80.55	82.45	4	345.24	241.43	3.52	0.43	2	4	0
MM 90	80.55	82.45	3	331.22	225.32	2.95	0.46	2	4	0
MM 54	88.92	58.20	2	299.15	223.25	3.03	0.45	2	4	0
MM 48	83.74	73.22	2	315.22	218.90	3.50	0.45	2	3	0
MM 57	85.74	67.43	4	329.18	245.66	3.25	0.43	2	5	0
MM 60	80.55	82.45	4	345.24	241.43	3.53	0.43	2	4	0
MM 81	85.74	67.43	3	315.15	230.04	2.94	0.46	2	5	0
MM 92	80.55	82.45	3	331.22	225.32	3.09	0.46	2	4	0
MM 56	88.92	58.20	2	299.15	223.25	3.12	0.45	2	4	0
MM 64	83.74	73.22	2	315.22	218.90	3.56	0.45	2	3	0
MM 59	85.74	67.43	4	296.27	231.46	1.95	0.43	2	5	0
MM 61	80.55	82.45	4	312.34	229.66	1.66	0.43	2	4	0
MM 75	85.74	67.43	3	282.24	213.82	1.27	0.46	2	5	0
MM 86	80.55	82.45	3	298.31	213.08	1.32	0.46	2	4	0

Table VI.1 *(continued)*

Compound	%ABS	TPSA	*n*-ROTB	MW	MV	Log *P*	Hy	*n*-OHNH donors	*n*-OH acceptors	Lipinski's violation[b]
MM 58	88.92	58.20	2	266.24	208.00	1.71	0.45	2	4	0
MM 63	83.74	73.22	2	282.31	207.58	1.43	0.45	2	3	0
MM 65	81.20	80.57	4	250.25	205.12	0.87	0.48	2	6	0
MM 68	76.02	95.59	4	266.32	201.76	0.88	0.48	2	5	0
MM 76	81.20	80.57	3	236.22	188.98	0.52	0.53	2	6	0
MM 88	76.02	95.59	3	252.29	185.51	0.67	0.53	2	5	0
MM 66	84.39	71.34	2	220.22	182.00	0.69	0.51	2	5	0
MM 67	79.21	86.36	2	236.29	180.37	0.66	0.51	2	4	0
MM 93	81.20	80.57	4	264.28	222.08	1.17	0.45	2	6	0
MM 99	81.20	80.57	4	284.70	217.33	1.89	0.50	2	6	0
MM 96	75.99	95.67	4	266.32	211.37	1.48	0.48	2	5	0
MM 106	75.99	95.67	4	300.76	224.45	2.31	0.50	2	5	0
MM 95	81.29	80.32	4	261.28	215.93	0.57	0.45	2	6	0
Lamotrigine	77.71	90.71	1	256.09	163.11	2.33	2.32	4	5	0
Carbamazepine	93.02	46.33	0	236.27	186.04	2.17	0.32	2	3	0
Phenytoin	88.92	58.20	2	252.27	200.21	2.38	0.34	2	4	0
Clonazepam	77.85	90.29	2	315.71	210.47	2.57	-0.22	1	6	0
Sodium valproate	96.13	37.30	5	144.21	155.06	2.64	-0.16	1	2	0

[a]%ABS, percentage of oral absorption; TPSA, topological polar surface area (Å^2); *n*-ROTB, number of rotatable bonds; MW, molecular weight (Da); MV, molecular volume (cm^3/mol); Hy, hydrophilic factor; *n*-OHNH donors, number of hydrogen bond donors; *n*-OH acceptors, number of hydrogen bond acceptors.

[b]Lipinski rule of five: no more than 5 hydrogen bond donors; no more than 10 hydrogen bond acceptors; molecular weight less than 500 Da and octanol-water partition coefficient log *P* not greater than 5. A maximum of 1 violation is permitted (Lipinski, 2000).

Thus, lipophilicity has been considered as a main factor in determining the pharmacokinetic properties of drug candidates, contributing to the solubility, permeability, potency, selectivity, and promiscuity of the compounds (Wang et al., 2015). The Lipinski's rule-of-five is a rule of thumb to evaluate the druglikeness of a molecule based on some important molecular descriptors for ADME properties. This rule is widely used as filter to prioritize the compounds that are more likely to be drug candidates. Hence, low bioavailability is encountered in some molecular compounds with high molecular weight (> 500 Da), high value of log *P* (> 5), high number of hydrogen bond donors (> 5) and hydrogen bond acceptor (> 10) sites. In addition, a high number of rotatable bonds on the molecule also disfavors oral absorption (Leucuta, 2014; Lipinski, 2000). Therefore, these parameters were calculated for the DHPM(t)s and are summarized in Table VI.1. Hence, it was verified that MV (182.00-246.03 cm^3/mol), MW (220.22-345.24 Da), number of rotatable bonds (2-5), hydrogen bond donor (2) and hydrogen bond acceptor (3-8) were in acceptable range, being comparable with the standard AEDs. Consequently, none of the compounds violated Lipinski's rule-of-five, suggesting that they possess favourable properties that fulfil the criteria of druglikeness. In addition, the values predicted also comply with the criteria suggested by Veber *et al.* (Veber et al., 2002), which proposed that compounds with 10 or fewer rotatable bonds and 12 or fewer hydrogen bond donors and acceptors will have a high probability of good oral bioavailability. According to the authors, the commonly applied MW cut-off of 500 Da is not significant by itself to distinguish the compounds with poor oral bioavailability from those with acceptable values. On the other hand, reduced molecular flexibility, as measured by the number of rotatable bonds, and low polar surface area/total hydrogen bond count would be important predictors of good oral bioavailability, independently of the MW (Veber et al., 2002).

Due to the fact that the experimental evaluation of a large number of molecules is highly expensive and a time-consuming process, which lead with frequency to low success rates (Barton and Riley, 2016; Kola and Landis, 2004; Page, 2016), this study also intended to predict several additional pharmacokinetic and toxicity properties to complement the *in vitro* studies performed, using a freely available informatics tool. In addition to the advantages already mentioned, the computational studies can also have a role in the reduction of animal testing, thereby gaining even greater relevance in therapeutic areas where preclinical research in whole-animals is so demanding (Dudai and Evers, 2014; Raies and Bajic, 2016). In fact, computational prediction of pharmacokinetics and toxicity has become a complementary approach in early stages of drug discovery and development, contributing for the decision-making process. For this reason, ADMET properties were estimated for the DHPM(t)s test compounds using the pkCSM database, which is an integrated platform to rapidly predict a large number of pharmacokinetic and toxicity parameters based on molecular structure. This is a very recent tool, which performs as well or better than the similar methods currently available (Pires et al., 2015) and it has been used by several

authors with the purpose of predicting physicochemical, pharmacokinetic and toxicity properties (Guo et al., 2016; Junker et al., 2016; Rosseto et al., 2015).

The results of the *in silico* prediction of ADMET properties of the DHPM(t)s with the pkCSM database are listed in Table VI.2. Regarding the permeability through the Caco-2 cells, the Papp values were higher for thiourea derivatives comparatively to the corresponding analogues of urea series (e.g. Papp = 18.62×10^{-6} cm/s for compound **MM 83** *versus* Papp = 0.62×10^{-6} cm/s for compound **MM 72**); these findings are similar to those obtained in the experimental intestinal PAMPA assay previously described (Table V.6). Notwithstanding, some compounds presented higher (e.g. **MM 25**, **MM 67** and several halogenated compounds, with estimated Papp values between 19.05×10^{-6} cm/s and 70.79×10^{-6} cm/s) or lower (e. g. compounds with a nitro group, with estimated Papp values between 0.79×10^{-6} cm/s and 0.81×10^{-6} cm/s) *in silico* Papp values in comparison to those experimentally found. As PAMPA only measures the intrinsic ability of compounds to transcellularly permeate lipophilic barriers through passive diffusion, these differences suggest that those compounds can also be transported *via* influx or efflux mediated mechanisms, which can be expressed by Caco-2 cells.

Regarding the intestinal absorption potential of the DHPM(t)s, the *in* silico model estimated values of human intestinal absorption around 90%, in agreement with the results experimentally generated using the intestinal PAMPA model. The apparent volume of distribution (V_D), which provides information about the extent of distribution of the compounds in the body fluids and tissues (Mifsud, 2009), was also estimated *in silico*. Theoretically, higher membrane permeation leads to higher values of V_D, while compounds extensively bound to plasma proteins exhibit small values of V_D (Fortuna et al., 2012). Using the pkCSM tool, the V_D values at steady-state predicted for the tested compounds (0.33-2.04 L/kg) are in accordance with those obtained for the marketed AEDs lamotrigine, carbamazepine and phenytoin (0.63-2.51 L/kg). The unbound drug fraction estimated for all tested compounds is also depicted in Table VI.2 and ranged from 0.13 to 0.59, corroborating the low PPB of the DHPM(t)s predicted from the PAMPA screening. Therefore, these compounds probably do not raise major concerns on drug-drug PPB interactions, which usually occur when two or more that bind extensively to plasma proteins (> 90%) are co-administered (Mifsud, 2009; Patsalos and Perucca, 2003). These *in silico* prediction corroborate the *in vitro* results obtained with the intestinal PAMPA model.

Table VI.2 – Pharmacokinetic and toxicological parameters of the target dihydropyrimidin(thi)ones and the drugs lamotrigine, carbamazepine, phenytoin, clonazepam and sodium valproate using the pkCSM predictive database.

Compound	Absorption		Distribution				Metabolism							Toxicity	
							Substrate		Inhibitor[b]						
	P_{Caco} (Papp x10^{-6} cm/s)	Abs (%)	V_{Dss} (L/kg)	Fu	P_{BBB} (log BB)	P_{CNS}[a]	CYP2D6	CYP3A4	CYP1A2	CYP2C19	CYP2C9	CYP2D6	CYP3A4	AMES test	Hepatic
MM 18	7.08	93.49	0.66	0.29	-0.19	$CNS^{\pm}$	No	No	No	No	No	No	No	No	No
MM 26	19.50	93.28	1.07	0.29	0.23	$CNS^{\pm}$	No	No	No	No	No	No	No	No	Yes
MM 72	0.62	93.91	0.58	0.31	-0.16	$CNS^{\pm}$	No	No	No	No	No	No	No	No	No
MM 83	18.62	93.70	0.93	0.31	0.25	$CNS^{\pm}$	No	No	No	No	No	No	No	No	No
MM 17	18.62	93.41	0.63	0.36	-0.03	CNS^{-}	No	No	No	No	No	No	No	No	No
MM 25	37.15	93.42	0.93	0.35	0.16	CNS^{+}	No	No	No	Yes	No	No	No	No	Yes
MM 22	7.08	93.28	0.71	0.26	-0.18	$CNS^{\pm}$	No	No	No	No	No	No	No	No	No
MM 28	20.42	93.08	1.15	0.27	0.25	$CNS^{\pm}$	No	No	No	No	No	No	No	No	Yes
MM 73	7.24	93.70	0.62	0.29	-0.16	$CNS^{\pm}$	No	No	No	No	No	No	No	No	No
MM 84	19.50	93.50	1.00	0.29	0.26	$CNS^{\pm}$	No	No	No	No	No	No	No	No	Yes
MM 19	19.50	93.21	0.68	0.34	-0.02	CNS^{+}	No	No	No	Yes	No	No	No	No	Yes
MM 29	37.15	93.22	1.00	0.32	0.17	CNS^{+}	No	No	No	Yes	No	No	No	No	Yes
MM 23	0.81	80.15	0.41	0.13	-0.37	$CNS^{\pm}$	No	Yes	No	No	No	No	No	Yes	No
MM 82	0.79	79.39	0.36	0.15	-0.36	$CNS^{\pm}$	No	No	No	No	No	No	No	Yes	No
MM 24	8.51	81.97	0.62	0.29	-0.31	$CNS^{\pm}$	No	No	No	No	No	No	No	Yes	Yes
MM 30	7.41	89.98	1.07	0.23	-0.22	$CNS^{\pm}$	No	No	Yes	Yes	No	No	No	Yes	No
MM 34	9.12	93.39	0.51	0.28	-0.15	$CNS^{\pm}$	No	No	No	No	No	No	No	No	No
MM 36	19.50	93.28	0.78	0.28	-0.13	$CNS^{\pm}$	No	No	No	No	No	No	No	No	Yes
MM 74	3.24	93.80	0.98	0.35	-0.49	$CNS^{\pm}$	No	Yes	No	No	No	No	No	No	Yes
MM 85	16.98	93.73	1.48	0.33	0.13	$CNS^{\pm}$	No	Yes	No	No	No	No	No	No	No
MM 35	9.12	93.33	1.32	0.33	-0.19	$CNS^{\pm}$	No	Yes	No	No	No	No	No	No	Yes
MM 37	18.62	93.37	2.04	0.31	0.11	$CNS^{\pm}$	No	Yes	Yes	No	No	No	No	No	Yes
MM 55	7.41	89.66	0.65	0.19	-0.28	$CNS^{\pm}$	No	Yes	No	No	No	No	No	No	Yes
MM 46	25.12	89.45	0.85	0.22	0.15	$CNS^{\pm}$	No	Yes	No	Yes	No	No	No	No	No
MM 90	23.99	89.87	0.74	0.24	0.16	$CNS^{\pm}$	No	Yes	No	No	No	No	No	No	No
MM 54	22.91	90.09	0.56	0.29	-0.03	CNS^{-}	No	No	Yes	Yes	No	No	No	No	No
MM 48	38.90	90.10	0.85	0.27	0.16	CNS^{+}	No	No	Yes	Yes	No	No	No	No	No
MM 57	6.46	90.17	0.56	0.20	-0.19	$CNS^{\pm}$	No	No	No	No	No	No	No	No	No
MM 60	23.99	89.96	0.93	0.21	0.23	$CNS^{\pm}$	No	No	No	No	No	No	No	No	No

Table VI.2 *(continued)*

Compound	Absorption		Distribution				Metabolism							Toxicity	
							Substrate		Inhibitor[b]						
	P_{Caco} (Papp x10^{-6} cm/s)	Abs (%)	V_{Dss} (L/kg)	Fu	P_{BBB} (log BB)	P_{CNS}[a]	CYP2D6	CYP3A4	CYP1A2	CYP2C19	CYP2C9	CYP2D6	CYP3A4	AMES test	Hepatic
MM 81	6.61	90.58	0.49	0.23	-0.17	$CNS^{\pm}$	No	No	No	No	No	No	No	No	No
MM 92	22.91	90.38	0.79	0.23	0.25	$CNS^{\pm}$	No	No	No	No	No	No	No	No	No
MM 56	22.91	90.09	0.56	0.29	-0.03	CNS^{-}	No	No	Yes	Yes	No	No	No	No	Yes
MM 64	38.90	90.10	0.85	0.27	0.16	CNS^{+}	No	No	Yes	Yes	No	No	No	No	Yes
MM 59	11.75	91.99	0.38	0.26	-0.76	$CNS^{\pm}$	No	No	No	No	No	No	No	Yes	Yes
MM 61	20.89	91.78	0.56	0.27	-0.10	$CNS^{\pm}$	No	No	No	Yes	No	No	No	No	Yes
MM 75	12.02	92.41	0.33	0.28	-0.75	$CNS^{\pm}$	No	No	No	No	No	No	No	Yes	Yes
MM 86	19.95	92.20	0.48	0.29	-0.09	$CNS^{\pm}$	No	No	No	No	No	No	No	No	Yes
MM 58	20.42	91.80	0.38	0.35	-0.13	CNS^{-}	No	No	No	No	No	No	No	No	Yes
MM 63	70.79	91.81	0.55	0.33	0.06	CNS^{+}	No	No	No	No	No	No	No	No	Yes
MM 65	2.95	93.74	0.60	0.56	-0.40	CNS^{-}	No	No	No	No	No	No	No	No	No
MM 68	3.16	93.69	0.83	0.56	0.09	CNS^{-}	No	No	No	No	No	No	No	No	Yes
MM 76	2.57	70.01	0.54	0.58	-0.37	CNS^{-}	No	No	No	No	No	No	No	No	No
MM 88	2.82	76.40	0.74	0.59	-0.22	CNS^{-}	No	No	No	No	No	No	No	No	Yes
MM 66	4.90	93.54	0.42	0.57	-0.33	CNS^{-}	No	No	No	No	No	No	No	No	No
MM 67	19.05	93.56	0.60	0.55	0.05	CNS^{-}	No	No	No	No	No	No	No	No	No
MM 93	5.75	93.54	0.63	0.53	-0.39	CNS^{-}	No	No	No	No	No	No	No	No	Yes
MM 99	8.91	91.85	0.51	0.48	-0.72	CNS^{-}	No	No	No	No	No	No	No	No	Yes
MM 96	6.61	91.91	0.51	0.34	-0.21	$CNS^{\pm}$	No	No	No	No	No	No	No	No	No
MM 106	7.08	89.99	0.56	0.27	-0.33	$CNS^{\pm}$	No	No	Yes	No	No	No	No	No	No
MM 95	2.14	67.73	0.38	0.48	-0.41	CNS^{-}	No	No	No	No	No	No	No	No	Yes
Lamotrigine	21.88	89.30	0.63	0.24	-0.15	$CNS^{\pm}$	No	No	No	No	No	No	No	No	Yes
Carbamazepine	22.39	94.32	2.51	0.05	0.15	CNS^{+}	No	Yes	Yes	No	No	No	No	Yes	No
Phenytoin	19.05	94.31	1.03	0.11	0.06	$CNS^{\pm}$	No	Yes	No	No	No	No	No	No	No
Clonazepam	6.59	91.23	1.09	0.00	-0.32	$CNS^{\pm}$	No	Yes	Yes	Yes	Yes	No	No	Yes	No
Sodium valproate	28.64	97.45	0.10	0.70	-0.09	CNS^{+}	No	No	No	No	No	No	No	No	No

P_{Caco}, Caco-2 permeability; Abs, intestinal absorption (human); V_{Dss}, steady-state volume of distribution (human); Fu, unbound fraction (human); P_{BBB}, blood-brain barrier permeability; P_{CNS}, central nervous system permeability.

[a]A compound is considered CNS^{+} when the calculated logarithm of blood-brain permeability–surface area product (log PS) > -2; CNS^{-} when log PS < -3 and $CNS^{\pm}$ between these values.

[b]A compound is considered to be a CYP450 inhibitor if the concentration required to lead to 50% of inhibition is less than 10 μM.

Concerning the brain penetration, two parameters were estimated *in silico*: the BBB permeability and CNS permeability. Regarding the first one, which gives the ability of a compound to cross the BBB, once again, higher values were observed for the target compounds of thiourea series, which is also in agreement with the obtained experimental PAMPA-BBB results. This property is given through the logarithm of the brain-to-blood concentration ratio (log BB) of drugs, which is the most used parameter for predicating BBB penetration and a higher ratio is related to a higher concentration that reaches the brain (Zhou et al., 2016). However, this parameter merely reflects the total drug concentration in the brain rather than providing any insight on the free drug concentration. On the other hand, the logarithm of blood-brain permeability-surface area product (log PS) has been suggested by some authors as a more appropriate index because it eliminates the effect of PPB or non-specific brain binding and provides a direct measure of BBB apparent permeability (Wang et al., 2015). Therefore, the second parameter calculated (CNS permeability) is related with the direct measurement of the BBB permeability and does not consider the effects of the systemic distribution. This parameter is calculated using the log PS and the compounds were classified as CNS^{+}, CNS^{-} and $CNS^{\pm}$, as specified in Table VI.2. The compounds that appeared to have a better CNS permeability were **MM 25**, **MM 19**, **MM 29**, **MM 48**, **MM 64** and **MM 63**. Interestingly, all these compounds share the shortest lateral chain in their structures.

Equally important is the prediction of metabolic issues of new chemical entities, which must be early screened, particularly focusing on the CYP450 isoenzymes, which are considered to be the most relevant drug-metabolizing enzymes for majority of currently marketed drugs (Walsh and Miwa, 2011). In fact, most AEDs are metabolized by the CYP450 system, being also inducers or inhibitors of specific CYP450 isoenzymes, and thus are associated to important pharmacokinetic-based drug interactions (Landmark and Patsalos, 2010). Moreover, although this enzymatic system is important for detoxification processes, sometimes, it can also be responsible for the production of toxic metabolites (Matias et al., 2014), reinforcing the need of studying the metabolism of new drug candidates in early stages of drug development. In this context, pkCSM tool identified substrates and inhibitors of several important drug-metabolizing CYP450 isoenzymes among the target DHPM(t)s. According to the results obtained, theoretically, compounds **MM 18**, **MM 26**, **MM 72**, **MM 83**, **MM 17**, **MM 22**, **MM 28**, **MM 73**, **MM 84**, **MM 82**, **MM 24**, **MM 34**, **MM 36**, **MM 57**, **MM 60**, **MM 81**, **MM 92**, **MM 59**, **MM 75**, **MM 86**, **MM 58**, **MM 63**, **MM 65**, **MM 68**, **MM 76**, **MM 88**, **MM 66**, **MM 67**, **MM 93**, **MM 99**, **MM 96** and **MM 95** are not metabolized by CYP2D6 or CYP3A4 and do not inhibit the CYP1A2, CYP2C19, CYP2C9, CYP2D6 and CYP3A4 isoenzymes, similarly to lamotrigine. This suggests that a large amount of compounds of the DHPM(t)s class is not expected to be involved in clinically important metabolism-based drug interactions. However, in more advanced stages, experimental data are required to confirm these results, at least for the most promising molecules.

With regard to toxicity, it remains as one of the most significant reasons for failure in late stages of drug development. A critical priority in drug development is the early identification of compounds that cause severe toxicity, applying the current paradigm "fail early fail cheap" (Wang et al., 2015). The toxicity evaluation of new compounds starts at the early stages of drug discovery and development and continues even after the drug has been launched into the market. In order to complement the information obtained in *in vitro* studies of cytotoxicity, it was also predicted the mutagenicity and hepatotoxicity of the compounds. The first one was obtained based on Ames test data (Naven et al., 2010). The estimated results suggested that just a limited number of compounds, those possessing the nitro group (**MM 23**, **MM 82**, **MM 24** and **MM 30**) and two compounds incorporating fluorine atoms (**MM 61** and **MM 75**), are more likely mutagenic effects. However, the prediction of the disrupted normal function of the liver suggested that this class of compounds should deeply and carefully studied in more reliable liver models because half of them presented a trend to cause hepatotoxicity.

CHAPTER VII

GENERAL DISCUSSION

In this section, a more integrative discussion of the various topics explored within the previous chapters will be addressed. A critical overview of the key subjects covering the overall research work carried out to achieve the main objectives proposed at the beginning of this thesis will be herein provided.

In spite of the technological progresses and the better understanding of biology systems, drug discovery is still a protracted, expensive, difficult and inefficient process with low rate of success. When the drug discovery process follows the target-based approach, the next steps regarding efficacy evaluation and assessment of the mechanism of action become far simpler. However, when the drug discovery processes follow phenotypic-based screening approaches and there is no direct evidence about the therapeutic target, the mechanism of action can then be determined during the preclinical drug development, or when the candidate drug is already being evaluated in clinical trials or even after reaching the market. Moreover, it is also possible that the drug's mechanism of action may not be fully clarified but that the drug is approved for marketing. Indeed, drug regulatory agencies have approved many drugs with unknown mechanism of action or target identification (Andrade et al., 2016). The majority of AEDs belongs to this group of drugs, which means that one of the main challenges that a scientist faces when intends to start the discovery of a new AED candidate is exactly in the beginning of the discovery process.

Thus, without a specific target to drive the process, different other approaches have been currently used to obtain new leads. Within these, the consideration of the structure of an existing lead or a drug (sometimes the "best-in-class" molecules) is possibly the most common strategy to produce new drug candidates. Indeed, this approach has been highly successful in generating incremental improvements in the pharmacotherapeutic armamentarium. However, the main challenge is to identify a compound and/or specific pharmacophores with significant pharmacological activity (Murray and Rees, 2009). As a consequence, the DHPM(t)s herein reported were chosen based on the structure of lamotrigine (an established broad-spectrum AED). Moreover, it was also verified that the DHPM(t)s structures could include several pharmacophoric groups present in other clinically available AEDs, namely phenobarbital and possibly retigabine (as illustrated in Figure VII.1). Taking into account the different mechanisms of action that have been attributed to each of these AEDs, the synthesized molecules could be considered as approximations of hybrid compounds. Thus, it could be expected the potentiation of the anticonvulsant activity.

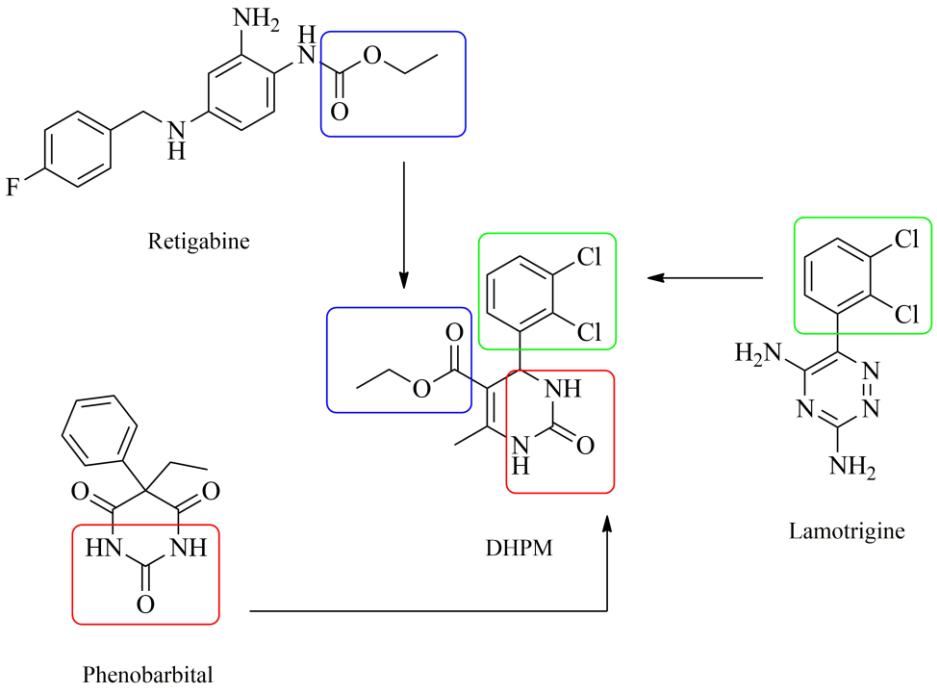

Figure VII.1 – Representative chemical structure of a 3,4-dihydropyrimidin-2(1*H*)-one (DHPM) and their structural similarities with the clinically available antiepileptic drugs lamotrigine, phenobarbital and retigabine.

As mentioned in Chapter IV, the functionalized DHPM(t)s possess a broad spectrum of biological and pharmacological activities, further arousing the interest of both synthetic and medicinal chemists. For this reason, it is quite astonishing the lack of information on the anticonvulsant potential of this class of heterocycles. However, at the same time, such situation opened the door for this work, aiming to fulfil this gap in the rational design and development of DHPM(t)s as potential anticonvulsant agents. Hence, fifty different DHPM(t)s were synthesized through the well-known Biginelli reaction. This MCR is not new, as the synthesis of DHPMs was reported for the first time in the literature over than 100 years ago, and throughout the years several other approaches to perform it have been described, involving, for example, the use of microwaves, sonication, ionic liquids, and a wide array of different catalysts. As required, in laboratory practice it was rapidly noted that this reaction is fast, simple and cost-effective, leading to the generation of a large set of compounds with structural diversity, which were posteriorly evaluated.

As the large majority of anticonvulsant pharmacophores includes at least one heterocycle, which can display a role in the anticonvulsant activity, several Biginelli products were developed incorporating a second heteroaromatic group instead of the phenyl at the 4-position of the dihydropyrimidine ring. The heterocyclics were selected considering the evidence of their anticonvulsant potential. Specifically, the clinically available AED tiagabine has two thiophene rings in its chemical structure and in the literature it can also be found chemical structures containing a furan ring associated with anticonvulsant activity (Ozdemir

et al., 2007). This motivated us to include furan and thiophene rings in the DHPMs structure. Moreover, taking into account that the chlorine atoms could be relevant for the activity of lamotrigine, compounds containing a chlorine atom attached to these 5-membered heterocycles were also synthesized. In addition, the discovery of the new AED perampanel opened new doors for the development of new AED candidates with pyridine as a possible anticonvulsant pharmacophore (Boehlen et al., 2013), which also led us to add a pyridine ring to the 4-position of the dihydropyrimidine nucleus.

Once synthesized, purified and characterised, all DHPM(t)s were subject to further evaluation of their pharmacodynamic (*in vivo* anticonvulsant activity), toxicity (*in vivo* neuromotor toxicity, *in vitro* cytotoxicity and *in silico* predictions) and pharmacokinetic (*in vitro* permeability and P-gp modulation, and *in silico* predictions) properties. The obtained results are summarized in Table VII.1, considering the main functional groups that were successfully varied.

Concerning the *in vivo* experiments, they began with the careful selection of an appropriate delivery/administration vehicle devoid of intrinsic neuromotor toxicity (minimal neurological deficit) and that enable the suitable formulation of the test compounds. At this level formulation issues are relevant, but it would not be less important to ensure the absence of neurotoxicity of the formulation vehicle itself when the use of the rotarod performance test is required. Having this in mind, and taking into consideration the results obtained, CMC 0.5%/DMSO (50%/50%, *v*/*v*) was shown to be the suitable vehicle to deliver the test compounds during initial screening assays in mice (30 mg/kg, 100 mg/kg and 300 mg/kg). This vehicle was also experimentally tested in the standard models of anticonvulsant efficacy (MES and scPTZ) as the negative control to check whether it was not a bias factor of the results. Regarding the compounds administered by oral route to rats, as the dose tested was the lowest one tested in mice (30 mg/kg), it was still possible to reduce the percentage of DMSO (5%) contained in the vehicle.

Table VII.1 – Summary of the structure-anticonvulsant activity and structure-kinetic profile relationships of the synthesized dihydropyrimidin(thi)ones.

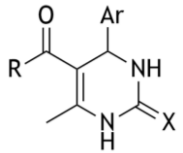

	Modification	Anticonvulsant activity (MES model)[a]	Motor impairment[b]	Cytotoxicity[c]	Rh123 accumulation[d]	Intestinal PAMPA[e]	PAMPA-BBB[f]	Predicted parameters[g]
Ar	Ph	Yes	No	Relatively low	No pronounced	High	Low	Trend to low VD_{ss}
	4-methyl-Ph	Yes	Yes	Relatively low	No pronounced	High	High	Trend to be hepatotoxic
	4-nitro-Ph	No	No	Relatively low	No pronounced	High	High	Trend to low Caco-2 permeability Trend to low VD_{ss} AMES positive
	4-methoxy-Ph	No	No	Relatively low	No pronounced	High	High	Trend to be CYP450 substrate Trend to be hepatotoxic
	2,3-dichloro-Ph	No	Yes	Marked in N27 and HepaRG cells	Trend to inhibition (high concentration)	High	Low	Trend to CYP inhibition Trend to be CYP450 substrate
	2,4-dichloro-Ph	No	Yes	Marked in N27 and HepaRG cells	Trend to inhibition (high concentration)	Low	Low	Trend to low VD_{ss}
	2,3-difluoro-Ph	No	No	Relatively low	No pronounced	High	Low	Trend to low VD_{ss} Trend to be hepatotoxic
	2-furyl	No	No	Relatively low	No pronounced	High	Low	Trend to low Caco-2 permeability Trend to low VD_{ss}
	5-methyl-2-furyl	No	Yes	Marked in N27 cells	No pronounced	High	High	Trend to low Caco-2 permeability Trend to low VD_{ss} Trend to be hepatotoxic
	5-chloro-2-furyl	No	Yes	Marked in N27 cells	No pronounced	High	High	Trend to low VD_{ss} Trend to be hepatotoxic

Table VII.1 *(continued)*

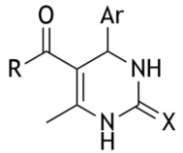

	Modification	Anticonvulsant activity (MES model)[a]	Motor impairment[b]	Cytotoxicity[c]	Rh123 accumulation[d]	Intestinal PAMPA[e]	PAMPA-BBB[f]	Predicted parameters[g]
Ar	2-thiophenyl	No	Yes	Relatively low	No pronounced	High	High	Trend to low Caco-2 permeability Trend to low VD_{ss}
	5-chloro-2-thiophenyl	No	Yes	Relatively low	No pronounced	High	High	Trend to low Caco-2 permeability Trend to low VD_{ss} Trend to CYP450 inhibition
	Pyridyl	No	Yes	Relatively low	Trend to induction (high concentration)	Low	Low	Trend to low Caco-2 permeability Trend to low VD_{ss} Trend to be hepatotoxic
R	Methyl	No	No	Relatively low	No pronounced	High	Low	Trend to CYP inhibition Trend to be hepatotoxic
	Methoxy	No	Yes	Relatively low	Trend to induction or inhibition (low/high concentration)	High	High	Trend to low Caco-2 permeability
	Ethoxy	No	No	Relatively low	No pronounced	High	High	Trend to low Caco-2 permeability

Table VII.1 *(continued)*

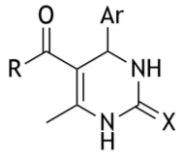

	Modification	Anticonvulsant activity (MES model)[a]	Motor impairment[b]	Cytotoxicity[c]	Rh123 accumulation[d]	Intestinal PAMPA[e]	PAMPA-BBB[f]	Predicted parameters[g]
X	Urea	No	No	Relatively low	No pronounced	High	Low	Trend to low VD_{ss}
	Thiourea	No	Yes	Relatively low	Trend to induction or inhibition (low/high concentration)	High	High	Trend to be hepatotoxic

[a]A group of compounds was considered as having anticonvulsant activity when half or more of the compounds belonging to the respective group showed protection against electrically-induced seizures at the lowest dose tested (30 mg/kg)
[b]A group of compounds was considered as having marked motor impairment when half or more of the compounds belonging to the respective group showed neuromotor deficit at the lowest dose tested (30 mg/kg)
[c]A group of compounds was considered as having marked toxicity when half or more of the compounds belonging to the respective group showed relative cell proliferation lower than 50%
[d]A group of compounds was considered as having pronounced activity when half or more of the compounds belonging to the respective group showed induction or inhibition in the intracellular rhodamine123 accumulation assay applying a cut-off of ± 20% regarding the control (100%)
[e]A group of compounds was considered as having low permeability when half or more of the compounds belonging to the respective group showed apparent permeability lower than 1.1×10^{-6} cm/s in the intestinal PAMPA assay
[f]A group of compounds was considered as having low permeability when half or more of the compounds belonging to the respective group showed apparent permeability lower than 2×10^{-6} cm/s in the PAMPA-BBB assay
[g]When half or more of the compounds belonging to a specific group showed:
- values lower than 8×10^{-6} cm/s, they were considered as having low Caco-2 permeability
- values lower than 0.71 L/kg, they were considered as having low VD_{ss}

In Table VII.1 the results of scPTZ test are not represented because no anticonvulsant protection has been observed with the compounds tested. On the other hand, it is evident that an unsubstituted or *para*-substituted phenyl ring with a methyl group seem to be the most relevant functional groups involved in the anticonvulsant activity against electrically induced seizures. According to the criterion stated in Table VII.1, it does not seem to have major differences among other functional groups. However, the chemical structures of the most potent compounds, i.e. the compounds that showed anticonvulsant protection in half or more of the animals at 30 mg/kg, are illustrated in Figure VII.2; analysing such molecular structures, it is evident that other relevant structural parts of the evaluated DHPM(t)s could contribute to the anticonvulsant properties observed in MES test. Thus, the structural characteristics more related to the anticonvulsant activity are highlighted in this figure: smaller chains at the position 5 of the dihydropyrimidine ring (i.e. derived from acetylacetone and methyl acetoacetate) and thiourea derivatives. It is worth noting that although compound **MM 82** presents good anticonvulsant activity and is devoid of neurotoxicity until the dose of 300 mg/kg, the difficulty of chemical synthesis of the compounds possessing a nitro group should not be forgotten in the decision-making process. In fact, in the future, more efforts should be done regarding the optimization of the reactional conditions, because the thiourea analogues with a nitro group were not successfully synthesized and/or the yields were too low to allow their evaluation in animal models. This is an important limitation of this group of compounds as various thiourea derivatives seem to be most promising as anticonvulsant agents than their corresponding urea analogues. Concerning the potential neurotoxicity, several functional groups seem be responsible for a marked neuromotor impairment in the rotarod performance test. In this context, compounds with a methyl group, having chlorine atoms, possessing a second heteroring (exception for unsubstituted furan ring), a lateral chain derived from methyl acetoacetate, and belonging to the thiourea series could be the most toxic ones. Among the mentioned groups, a highlight goes to thiourea derivatives and compounds incorporating the methyl group in their structure, because these functional groups are suggested as relevant for the anticonvulsant activity of the DHPM(t)s.

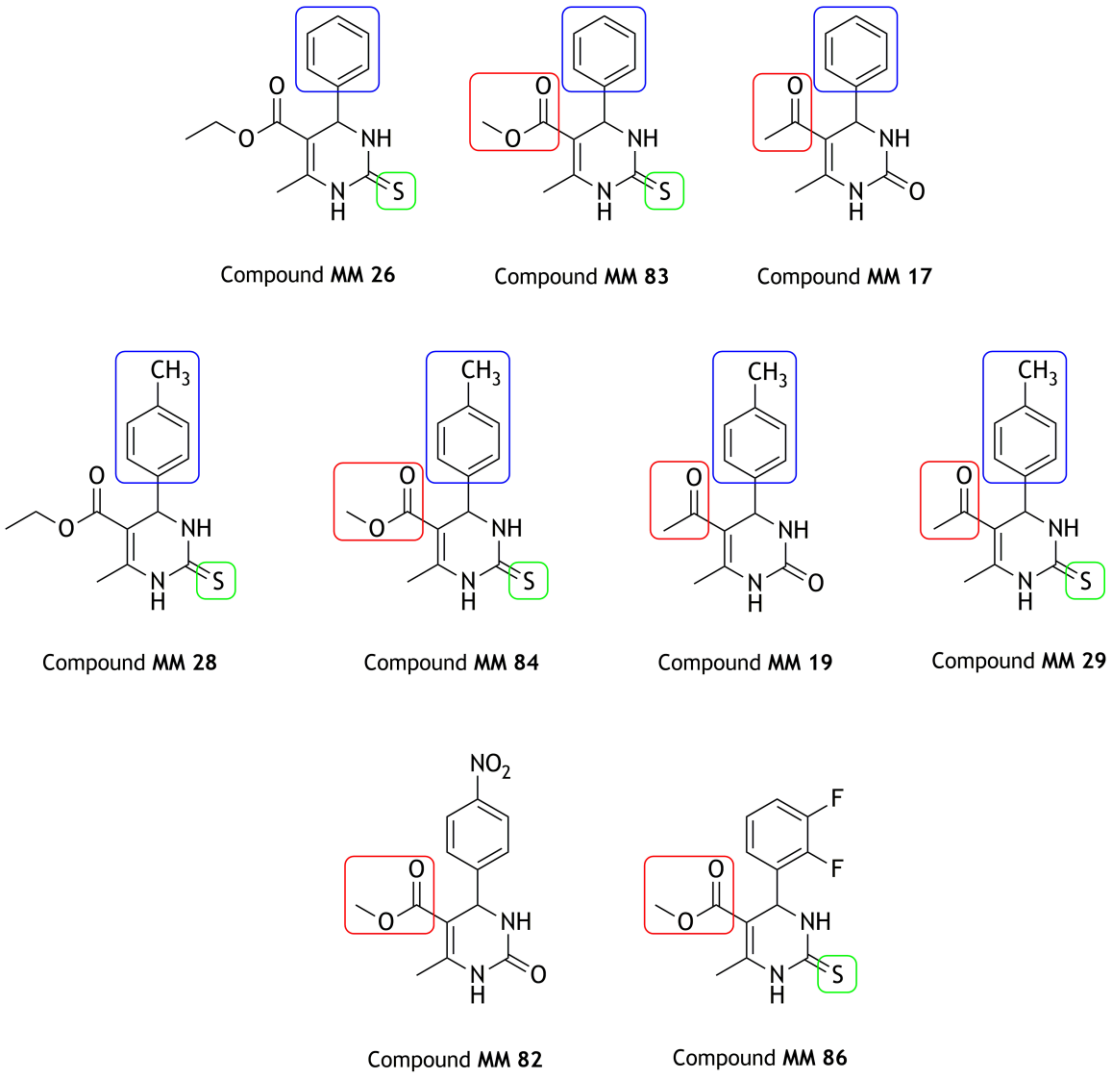

Figure VII.2 – Structural features of the dihydropyrimidin(thi)ones that are suggested to be responsible for the anticonvulsant activity: red rectangle represents the small and intermediate chains at the position 5 of the dihydropyrimidine ring; green rectangle represents the portion from thiourea; and blue rectangle represents the unsubstituted and para-substituted phenyl ring with a methyl group.

Unlike the standard models used in the screening of anticonvulsant activity, the remaining research was performed using *in vitro* and *in silico* systems. This strategy intended to contribute to promote the 3Rs principle (Replacement, Reduction and Refinement) initiated by Russell and Burch in 1959, which encourages the use of alternative assays to animal testing (Ferdowsian and Beck, 2011).

As aforementioned, it is true that DHPM(t)s have attracted considerable attention in organic and medicinal chemistry but, to the best of our knowledge, the pharmacokinetics of these compounds has not been investigated. Nevertheless, as it is widely recognised today, poor pharmacokinetic properties and toxicity are the main causes of compound failure in drug development programmes, thus the early ADMET assessment of new drug candidates is required (Wang et al., 2015). Hence, to fulfil this gap in the rational DHPM(t)s design and

development, we intended to also investigate some important ADMET properties of the DHPM(t)s. Therefore, in this work several kinetic and toxicity properties were simultaneously studied through *in vitro* and *in silico* techniques in order to obtain as much information as possible about the synthesized DHPM(t)s.

However, it is important to note that, in spite of the advances in the computational field, the *in vitro* assays are more reliable than the *in silico* assays, the later providing only some indications on important aspects of ADMET of the compounds that are difficult to obtain for a large number of compounds in *in vitro* assays. Unfortunately, *in silico* tools are not consistently employed, possible due to several factors, such as the fact that *in silico* methods are becoming more numerous and sophisticated and their use requires appropriate expertise that the researchers frequently do not have; many computational models have been heavily criticized in the literature due to deficiencies in producing reliable predictions; and the interpretation of the data should be done carefully due to the common inaccurate nature underlying all this research. However, an integration of *in silico* tools with *in vitro* and/or *in vivo* methods at the various stages of the drug discovery and development process is one proposal to improve the general rate of success (Caldwell, 2015).

Thus, one possible main application of the computational models in this context has been in the preclinical assessment in order to find promising molecules when a strong linkage between a particular molecular target and a pathologic event has been demonstrated. However, in the field of AED development, the current lack of evidence about which are the most relevant molecular targets adds a persistent and major obstacle to apply these kind of tools (Easter et al., 2009; Talevi, 2016). On the other hand, over the past decade, significant efforts have been devoted to modelling and predicting various ADME-related issues of interest for drug research.

In this section, the most important aspect is the integration of the results obtained in *in vitro* experiments with those of *in silico* predictions, which are summarised in Table VII.1. Thus, regarding the measured intestinal permeability, almost all compounds showed a possible high passive transcellular permeability. These results were consistent with the data of the compounds orally administered to rats (gastrointestinal absorption of the compounds **MM 17**, **MM 19** and **MM 83**). However, in the case of the brain penetration, several structural modifications showed a trend to impair the passage through the BBB by transcellular pathway. The compounds that exhibited a better brain penetration were the derivatives with a methyl, a nitro and a methoxy groups attached at the *para*-position of the aromatic ring, some of those possessing a second heterocycle, and the derivatives having longer chains at the position 5 of the dihydropyrimidine ring and belonging to thiourea series. However, it is worthy to note that the *in vitro* technique utilized (PAMPA-BBB model) only measures the intrinsic ability of compounds to permeate lipophilic barriers through passive transcellular absorption and does not consider the action of influx or efflux transporters which are present

in the BBB. This motivated the inclusion of the predicted values of the Caco-2, BBB and CNS-permeability in this study as explored in the Chapter VI of this thesis. In general, the permeability is enhanced in the thiourea derivatives comparatively with the corresponding analogues of urea series, similarly to what was observed in *in vitro* assays. Particularly in the case of the estimated permeability through Caco-2 cells, some compounds presented higher or lower values of Papp *in silico* in comparison to those found experimentally, which suggest that some compounds could be substrates of influx or efflux transporters, respectively.

In addition to permeability, preliminary experimental studies of P-gp modulation were performed to afford some indications about the modulation of this efflux transporter by the synthesized DHPM(t)s. In this context, changes in transporter activity or expression could theoretically alter drug disposition, including intestinal absorption and BBB penetration (Bagal and Bungay, 2014). An interesting finding (as demonstrated in Table VII.1) is that when the compounds showed trend to P-gp induction, this was verified in urea derivatives, whereas the trend to P-gp inhibition was particularly observed with thiourea derivatives. The chlorinated compounds were those that evidenced the strongest inhibitory action. However, possibly, the concentration used is very high to be clinically significant. Most worrying is the fact that these results can suggest that these compounds could be competitive substrates of P-gp. Further studies should be performed to establish the substrate *status* of these compounds (e.g. *in vitro* bidirectional transport assays and *in vivo* assays), considering essentially those that showed promising anticonvulsant activity.

Among the ADMET properties, metabolism is probably the most challenging one to evaluate and predict, considering the multiple enzyme systems that can be involved. Metabolism is crucial in determining the formation of metabolites of a drug in the body, which has implications in terms of safety and efficacy. Particularly, metabolism can play a key role in a number of issues, such as poor bioavailability, toxic effects, and DDI (Matias et al., 2014; Zhou et al., 2016). Therefore, metabolic data can offer prospective advice for drug development, for example, to guide the design of a pro-drug for some metabolically unstable drug to enhance bioavailability. Currently, the models to predict the metabolism are mainly focused on interaction models of enzymes with xenobiotics, which are often used to distinguish whether a xenobiotic is a substrate or inhibitor of CYP450 isoenzymes; clearance models of the liver that could quantitatively predict the metabolic stability of xenobiotics; the site of metabolism that can be used to predict the 'soft spots' on xenobiotics; and metabolite prediction models (Wang et al., 2015). In this context, the predictions using the pkCSM tool provide some indications for some compounds that could be substrates and/or inhibitors of specific isoenzymes of CYP450, such as chlorinated compounds (mainly the 2,3-dichloro derivatives) and derivatives with a methoxy group at the *para*-position of the phenyl ring. Moreover, just 14% of the urea derivatives showed tendency for CYP450 inhibition *versus* 36% of the thiourea derivatives. Due to the maximum importance of this thematic, the most promising compounds should be experimentally evaluated later.

Finally, integrating all data obtained, several "hits" can be identified for further optimization to lead anticonvulsant compounds. Once the discovery of new chemical entities for the management of epileptic seizures is based on the empirical screening against acute seizure rodent models, it can be suggested that the active compounds possess intrinsic physicochemical properties that permitted the *in vivo* crossing of biological barriers, specially the BBB, in order to obtain the intended CNS action. Therefore, accordingly to the *in vivo* experiments, the two main groups that showed a better potential anticonvulsant (particularly at 30 mg/kg) were those that included molecules with an unsubstituted phenyl ring or this ring substituted with a methyl group in the *para*-position. Interestingly, these compounds showed good additional properties, namely the relative low cytotoxicity in all tested cell lines (values of relative cell proliferation similar to those obtained for the AEDs) and good permeability. One exception was compound **MM 17** that exhibited low values of intestinal permeability and poor brain penetration in *in vitro* assays, but demonstrated interesting anticonvulsant protection against the electrically induced seizures (MES model), either after ip or oral administration. However, so far, it is unknown whether this compound is subject to uptake by influx transporters. In the context, after oral administration to rats, it was observed that compound **MM 83** showed higher anticonvulsant activity (75% of protection) than the urea derivatives **MM 17** and **MM 19** (50% of protection). In fact, **MM 83** is a thiourea derivative and could be hypothesized that the better results could be associated with the higher permeation of the membranes, as proved by the PAMPA assay. On the other hand, **MM 17** was the compound that provoked less neuromotor impairment in the rotarod assay among these three selected compounds. Moreover, it was also found that the percentage of intracellular Rh123 accumulation for this compound was very similar to that observed in untreated cells, which could represent lesser probability of interactions, toxicity and changes of efficacy related to P-gp. Regarding the lateral chain elected for further experiments, it should be mentioned that longer chains in the position 5 of the pyrimidine ring lead to better permeability, but are likely to reduce the desired anticonvulsant potential. Considering the two series (urea and thiourea), at first sight, the results show that thiourea derivatives seem to be most promising in terms of the anticonvulsant activity and pharmacokinetic properties. However, these compounds are more difficult to synthesize.

It also was found that the introduction of halogens into the basic scaffold of the DHPM(t)s (molecules with the unsubstituted phenyl ring) does not seem to be advantageous. In general, these molecules presented difficulties in crossing barriers based on the experimental results of intestinal PAMPA model and mainly PAMPA-BBB model, limiting their application as CNS-active molecules. In fact, kind of these molecules appeared to be the most problematic in almost all the studies. Particularly in the MTT assays, the chlorinated compounds showed to be highly cytotoxic for the hepatic cell line, exhibiting values of IC_{50} similar to those found in anticancer agents (e.g. 5-fluorouracil). Although less marked, the cytotoxicity of these compounds was also obvious in the neuronal cell line and some of them (thiourea derivatives)

presented cytotoxic effects at low concentrations in Caco-2 cell line. Still in relation to hepatic toxicity, it was predicted that the DHPM(t)s seem to have a tendency to disrupt the normal function of the liver, particularly in the presence of 4-methyl, 4-methoxy and 2,3-difluoro substituents, a 5-membered ring furan, small chains at the position 5 of the dihydropyrimidine ring and even among the thiourea derivatives. Surprisingly, the chlorinated compounds were not included in this group of hepatotoxic compounds. A painstaking and rigorous study in this scope should be carried out later.

Other chemical structures that disappointed were the DHPM(t)s incorporating a second heterocycle. In spite of they did not show pronounced modulation of the P-gp efflux transporter, the majority of the compounds appeared to have problems of permeation (and probably of distribution) mainly in the PAMPA-BBB assay. In addition, most of these compounds showed strong neurotoxicity in the rotarod assay even at the lowest dose (30 mg/kg). Moreover, contrarily to the thiophenyl derivatives, all the compounds having a furan and the compound incorporating the pyridyl moiety in the position 4 of the pyrimidine ring were considered CNS^- (unable to penetrate the CNS accordingly to the *in silico* model used). Thus, the poor pharmacokinetic profile of these compounds could explain, at least in part, the unexpected failure of anticonvulsant activity in the animal models. Indeed, at this level, an important aspect to consider is a clear distinction between BBB penetration and CNS activity. For example, in *in vivo* systems if a compound is active in CNS, it definitely permeates. However, the opposite is not necessarily true. In this case, the absence of central effects may be attributed either to inability to cross BBB, or the lack of target within the brain (Lanevskij et al., 2013). Furthermore, it was reported that compounds containing a furan ring could produce reactive metabolites during the biotransformation process (Peterson, 2013). Specifically in the case of thiophenyl and pyridyl moieties, there may be necessary to increase the spectrum of compounds in order to obtain a better structure-activity/kinetic profile relationship.

Finally, this integrated data would be relevant in the decision-making process about the structural properties that should be maintained or better explored in order to produce more active analogues in subsequent steps of research of new DHPM(t)s as potential AEDs candidates.

CHAPTER VIII

CONCLUSIONS AND FUTURE PERSPECTIVES

Epilepsy is a complex brain disorder that affects million people worldwide. A range of structurally diverse drugs are currently being used for management of epileptic seizures, acting through different molecular mechanisms of action. Nevertheless, despite the availability of many AEDs already in clinical use, just 60-70% of the patients with epilepsy remains seizure-free when properly treated with the current drugs. Therefore, the development of safer and more effective AEDs is required to fulfil an unmet medical need in this therapeutic area. Thus, in this work, the assessment of the anticonvulsant potential of fifty DHPM(t)s was investigated, as well as several of their pharmacokinetic and toxicity properties.

The results obtained in this study provide new information on the anticonvulsant activity of this class of heterocycles, which still remains underexploited. The structural design of the target molecules under investigation in this work was based on the pharmacophoric pattern of clinical relevant AEDs, aiming at improving the anticonvulsant activity of the synthesized compounds. More than half of the DHPM(t)s showed anticonvulsant protection against electrically-induced seizures, in the MES model, confirming the interest of this pharmacophoric strutural features for designing of new pharmacotherapeutic agents. Based on the anticonvulsant screening in mice, important structural features of this attractive scaffold potentially responsible for the anticonvulsant activity were identified, which should be considered in further hit-to-lead optimization. Thus, DHPM(t)s bearing small or intermediate chains at the position 5 of the dihydropyrimidine ring (derived from acetylacetone and methyl acetoacetate, respectively), belonging to thiourea series and possessing an unsubstituted or a substituted phenyl ring at the *para*-position with a methyl group seem to be the most promising structures. Additionally to the anticonvulsant activity demonstrated, these DHPM(t)s derivatives also showed a good profile of cytotoxicity and the generality of the most active compounds exhibited potentially favourable pharmacokinetic properties, namely good permeation through intestinal membrane and BBB models. Moreover, it was suggested that these specific chemical entities are not strong modulators of the efflux transporter P-gp. Furthermore, none of the compounds violated the Lipinski's rule-of-five, which make them as template structures for future design, modification and investigation.

The dataset herein generated is crucial for decision-making processes during the next steps of the discovery and development programme of DHPM(t)s as AEDs. Thus, the interesting anticonvulsant activity found in MES model justifies further research. Hence, accordingly with the main conclusions of this research work, as well as additional proposals for future work are described below:

- The set of DHPM(t)s was obtained after partial optimization of procedures in both chemical reactions and work up stages, and these results can be useful for future preparation of new derivatives. However, particularly in the case of thiourea derivatives (the series that showed higher anticonvulsant potential), an alternative route to produce DHPMts with higher yields should be considered and developed;

- Futhermore, based on the biological results, other structural modifications can be carried out in order to obtain molecules with optimized anticonvulsant activity. Some examples are: change the position of the methyl group in the aromatic ring (e.g. *ortho* or *meta*) and increase the number of methyl groups. In fact, the corresponding aldehydes are commercially available and they are cost-effective. In addition, the synthesis of thiourea analogues using the second heterocycle can also be performed; this strategy could increase the lipophilicity of the compounds and consequently enhance their efficacy. In turn, once the compounds with small lateral chains seem to be more active, the synthesis of these analogues using acetylacetone as starting material should also be attempted. Finally, regarding the structural modifications, it is also proposed new efforts to synthesize new compounds from Meldrum's acid because the approximation to the structure of phenobarbital could be promising;
- Considering the compounds herein evaluated, it is important to mention that the initial anticonvulsant screening used is not enough to discriminate the anticonvulsant potency of the compounds. In this context, such studies should be carried out after the estimation of the time of peak effect (studies considered in the phase 2 of the Anticonvulsant Screening Program). These quantitative studies comprise the calculation of the ED_{50}, which measures the dose of a drug candidate that is effective in 50% of the tested animals. Moreover, taking into account the results obtained in the rotarod performance test, it would be primordial to calculate the median toxic dose (TD_{50}), which is nedeed to the estimation of the protective index (TD_{50}/ED_{50}) of the compounds of interest. These results will not only permit to understand which is the most potent compound, but also to compare these new agents with reference AEDs;
- The use of acute seizure models for the identification of compounds with potential anticonvulsant activity presents the limitations that were previously explained. Thus, the further use of a chronic animal model of epilepsy (e.g. kindling) is also one of the next steps to consider in the evaluation of the most potent compounds. The 6-Hz model is also important to be considered because, despite some controversy, has been referred to as a model of pharmacoresistant epilepsy;
- The possible mechanisms of action of these DHPM(t)s should also be investigated as part of further development for the most promising compounds in order to understand as much as possible the putative mechanism(s) underlying their anticonvulsant activity;
- Although some *in vitro* and *in silico* findings on the pharmacokinetic properties of the synthesized DHPM(t)s have been antecipated, more robust pharmacokinetic studies (*in vitro* and *in vivo*) are required for the most promising molecules;
- Finally, it is clear that the synthesized DHPM(t)s were designed and produced as anticonvulsant compounds. However, during the evaluation phase of their general cytotoxicity in *in vitro* conditions, it was found that several chlorinated derivatives (in

general not considered to be promising anticonvulsant agents) could be better explored for their cytotoxic activity. Although this type of studies is out of the scope of this thesis, the findings already obtained can be seen as a starting point for a different research area, such as the cancer pharmacotherapy.

In fact, this research work showed the potentiality of developing new agents with anticonvulsant properties considering the DHPM(t)s scaffold. Overall, the results presented in this doctoral thesis are just a "tip of the iceberg" in the process of discovery and development of the DHPM(t)s as new AEDs, and there is still a long way to go before they can be translated into clinical setting.

CHAPTER IX

REFERENCES

Abbasi, M., Martinez, F., Jouyban, A., 2014. Prediction of deferiprone solubility in aqueous mixtures of ethylene glycol, propylene glycol and polyethylene glycol 400 at various temperatures. J. Mol. Liq. 197, 171–175.

Abbott, S.K., Jenner, A.M., Mitchell, T.W., Brown, S.H.J., Halliday, G.M., Garner, B., 2013. An Improved High-Throughput Lipid Extraction Method for the Analysis of Human Brain Lipids. Lipids. 48, 307-318

ACD/Percepta, 2015 release, Advanced Chemistry Development, Inc., Toronto, ON, Canada, www.acdlabs.com, 2015,

Ahmed, B., Khan, R.A., Habibullah, Keshari, M., 2009. An improved synthesis of Biginelli-type compounds via phase-transfer catalysis. Tetrahedron Lett. 50, 2889–2892.

Alam, O., Mullick, P., Verma, S.P., Gilani, S.J., Khan, S.A., Siddiqui, N., Ahsan, W., 2010. Synthesis, anticonvulsant and toxicity screening of newer pyrimidine semicarbazone derivatives. Eur. J. Med. Chem. 45, 2467–2472.

Ali, F., Khan, K.M., Salar, U., Iqbal, S., Taha, M., Ismail, N.H., Perveen, S., Wadood, A., Ghufran, M., Ali, B., 2016. Dihydropyrimidones: As novel class of ß-glucuronidase inhibitors. Bioorg. Med. Chem. 24, 3624–3635.

Ali, I.A.I., 2013. One-pot Synthesis of 3,4-dihydropyrimidin-2-(1H)-one/thiones bearing Sugar Side Chain Using Samarium Chloride as a Catalyst. Rev. Chim. 64, 1413–1415.

Ali, R., Siddiqui, N., 2015. New Benzo[d]thiazol-2-yl-aminoacetamides as Potential Anticonvulsants: Synthesis, Activity and Prediction of Molecular Properties. Arch. Pharm. Chem. Life Sci. 348, 254–265.

Allen, D.D., Caviedes, R., Cárdenas, A.M., Shimahara, T., Segura-Aguilar, J., Caviedes, P.A., 2005. Cell lines as in vitro models for drug screening and toxicity studies. Drug Dev. Ind. Pharm. 31, 757–768.

Almasirad, A., Mousavi, Z., Tajik, M., Assarzadeh, M.J., Shafiee, A., 2014. Synthesis, analgesic and anti-inflammatory activities of new methyl-imidazolyl-1,3,4-oxadiazoles and 1,2,4-triazoles. Daru J. Pharm. Sci. 22, 22.

Almeida, L., Soares-da-Silva, P., 2007. Eslicarbazepine Acetate (BIA 2-093). Neurotherapeutics 4, 88–96.

Alqahtani, S., Mohamed, L.A., Kaddoumi, A., 2013. Experimental models for predicting drug absorption and metabolism. Expert Opin. Drug Metab. Toxicol. 9, 469–485.

Amato, G., Roeloffs, R., Rigdon, G.C., Antonio, B., Mersch, T., McNaughton-Smith, G., Wickenden, A.D., Fritch, P., Suto, M.J., 2011. N-pyridyl and pyrimidine benzamides as KCNQ2/Q3 potassium channel openers for the treatment of epilepsy. ACS Med. Chem. Lett. 2, 481–484.

Ambrósio, A.F., Silva, A.P., Araújo, I., Malva, J.O., Soares-da-Silva, P., Carvalho, A.P.,

Carvalho, C.M., 2000. Neurotoxic/neuroprotective profile of carbamazepine, oxcarbazepine and two new putative antiepileptic drugs, BIA 2-093 and BIA 2-024. Eur. J. Pharmacol. 406, 191–201.

Ambrósio, A.F., Silva, A.P., Malva, J.O., Soares-da-Silva, P., Carvalho, A.P., Carvalho, C.M., 2001. Inhibition of glutamate release by BIA 2-093 and BIA 2-024, two novel derivatives of carbamazepine, due to blockade of sodium but not calcium channels. Biochem. Pharmacol. 61, 1271–1275.

Amenta, P.S., Jallo, J.I., Tuma, R.F., Elliott, M.B., 2012. A cannabinoid type 2 receptor agonist attenuates blood-brain barrier damage and neurodegeneration in a murine model of traumatic brain injury. J. Neurosci. Res. 90, 2293–2305.

Amir, M., Ali, I., Hassan, M.Z., 2013. Design and synthesis of some new quinazolin-4-(3H)-ones as anticonvulsant and antidepressant agents. Arch. Pharm. Res. 36, 61–68.

Andrade, E.L., Bento, A.F., Cavalli, J., Oliveira, S.K., Freitas, C.S., Marcon, R., Schwanke, R.C., Siqueira, J.M., Calixto, J.B., 2016. Non-clinical studies required for new drug development – Part I: early in silico and in vitro studies, new target discovery and validation, proof of principles and robustness of animal studies. Brazilian J. Med. Biol. Res. 49, e5644.

Aronica, E., Sisodiya, S.M., Gorter, J.A., 2012. Cerebral expression of drug transporters in epilepsy. Adv. Drug Deliv. Rev. 64, 919–929.

Arunkhamkaew, S., Athipornchai, A., Apiratikul, N., Suksamrarn, A., Ajavakom, V., 2013. Novel racemic tetrahydrocurcuminoid dihydropyrimidinone analogues as potent acetylcholinesterase inhibitors. Bioorg. Med. Chem. Lett. 23, 2880–2882.

Asif, M., 2015. Anticonvulsant Activities of Various Series of Heterocyclic Compounds Containing Triazole, Thiadiazine, Benzo-triazole, Benzothiazole, Oxadiazole Ring Systems. Am. J. Curr. Org. Chem. 1, 37–59.

Astashkina, A., Mann, B., Grainger, D.W., 2012. A critical evaluation of in vitro cell culture models for high-throughput drug screening and toxicity. Pharmacol. Ther. 134, 82–106.

Ator, M.A., Mallamo, J.P., Williams, M., 2006. Overview of drug discovery and development. Curr. Protoc. Pharmacol. 9, Supplement 35.

Atwal, K.S., Swanson, B.N., Unger, S.E., Floyd, D.M., Moreland, S., Hedberg, A., O'Reilly, B.C., 1991. Dihydropyrimidine calcium channel blockers. 3. 3-Carbamoyl-4-aryl-1,2,3,4-tetrahydro-6-methyl-5-pyrimidinecarboxylic acid esters as orally effective antihypertensive agents. J. Med. Chem. 34, 806–811.

Auta, J., Kadriu, B., Giusti, P., Costa, E., Guidotti, A., 2010. Anticonvulsant, anxiolytic, and non-sedating actions of imidazenil and other imidazo-benzodiazepine carboxamide derivatives. Pharmacol. Biochem. Behav. 95, 383–389.

Authier, N., Dupuis, E., Kwasiborski, A., Eschalier, A., Coudore, F., 2002. Behavioural

assessment of dimethylsulfoxide neurotoxicity in rats. Toxicol. Lett. 132, 117–121.

Avdeef, A., 2005. The rise of PAMPA. Expert Opin. Drug Metab. Toxicol. 1, 325–342.

Ayati, A., Emami, S., Foroumadi, A., 2016. The importance of triazole scaffold in the development of anticonvulsant agents. Eur. J. Med. Chem. 109, 380–392.

Azizian, J., Mohammadi, M.K., Firuzi, O., Mirza, B., Miri, R., 2010. Microwave-assisted solvent-free synthesis of bis(dihydropyrimidinone) benzenes and evaluation of their cytotoxic activity. Chem. Biol. Drug Des. 75, 375–380.

Bagal, S., Bungay, P., 2014. Restricting CNS penetration of drugs to minimise adverse events: Role of drug transporters. Drug Discov. Today Technol. 12, e79–e85.

Baggs, J.E., Hughes, M.E., Hogenesch, J.B., 2010. The network as the target. Syst. Biol. Med. 2, 127–133.

Bakar, B., Kose, E.A., Sonal, S., Alhan, A., Kilinc, K., Keskil, I.S., 2012. Evaluation of the neurotoxicity of DMSO infused into the carotid artery of rat. Injury 43, 315–22.

Banach, M., Czuczwar, S.J., Borowicz, K.K., 2014. Statins - Are they anticonvulsant? Pharmacol. Reports 66, 521–528.

Banerjee, J., Shi, Y., Azevedo, H.S., 2016. In vitro blood–brain barrier models for drug research: state-of-the-art and new perspectives on reconstituting these models on artificial basement membrane platforms. Drug Discov. Today 21, 1367–1386.

Banerjee, P.N., Filippi, D., Hauser, W.A., 2009. The descriptive epidemiology of epilepsy - a review. Epilepsy Res. 85, 31–45.

Banfor, P.N., Gintant, G.A., Lipari, J.M., Zocharski, P.D., 2016. A novel intravenous vehicle for preclinical cardiovascular screening of small molecule drug candidates in rat. J. Pharmacol. Toxicol. Methods 82, 62–67.

Bansal, Y., Silakari, O., 2014. Multifunctional compounds: Smart molecules for multifactorial diseases. Eur. J. Med. Chem. 76, 31–42.

Bao, D., Chen, M., Wang, H., Wang, J., Liu, C., Sun, R., 2014. Preparation and characterization of double crosslinked hydrogel films from carboxymethylchitosan and carboxymethylcellulose. Carbohydr. Polym. 110, 113–120.

Barker-Haliski, M.L., Friedman, D., French, J.A., White, H.S., 2015. Disease modification in epilepsy: From animal models to clinical applications. Drugs 75, 749–767.

Barthomeuf, C., Grassi, J., Demeule, M., Fournier, C., Boivin, D., Béliveau, R., 2005. Inhibition of P-glycoprotein transport function and reversion of MDR1 multidrug resistance by cnidiadin. Cancer Chemother. Pharmacol. 56, 173–181.

Barton, P., Riley, R.J., 2016. A new paradigm for navigating compound property related drug attrition. Drug Discov. Today 21, 72–81.

Baumstark-Khan, C., Hellweg, C.E., Reitz, G., 2010. Cytotoxicity and genotoxicity reporter systems based on the use of mammalian cells. Adv. Biochem. Eng. Biotechnol. 118, 113–151.

Bellot, F., Coslédan, F., Vendier, L., Brocard, J., Meunier, B., Robert, A., 2010. Trioxaferroquines as new hybrid antimalarial drugs. J. Med. Chem. 53, 4103–4109.

Ben-Menachem, E., 2014. Medical management of refractory epilepsy - Practical treatment with novel antiepileptic drugs. Epilepsia 55, 3–8.

Benes, J., Parada, A., Figueiredo, A.A., Alves, P.C., Freitas, A.P., Learmonth, D.A., Cunha, R.A., Garrett, J., Soares-da-Silva, P., 1999. Anticonvulsant and sodium channel-blocking properties of novel 10,11-dihydro-5H-dibenz[b,f]azepine-5-carboxamide derivatives. J. Med. Chem. 42, 2582–2587.

Berg, A.T., 2015. New classification efforts in epilepsy: Opportunities for clinical neurosciences. Epilepsy Behav. 64, 304-305.

Berube, G., 2016. An overview of molecular hybrids in drug discovery. Expert Opin. Drug Discov. 11, 281–305.

Bharate, J.B., Singh, S., Wani, A., Sharma, S., Joshi, P., Khan, I.A., Kumar, A., Vishwakarma, R.A., Bharate, S.B., 2015. Discovery of 4-acetyl-3-(4-fluorophenyl)-1-(p-tolyl)-5-methylpyrrole as a dual inhibitor of human P-glycoprotein and Staphylococcus aureus Nor A efflux pump. Org. Biomol. Chem. 13, 5424–5431.

Bialer, M., 2012. Chemical properties of antiepileptic drugs (AEDs). Adv. Drug Deliv. Rev. 64, 887–895.

Bialer, M., 2006. New antiepileptic drugs that are second generation to existing antiepileptic drugs. Expert Opin. Investig. Drugs 15, 637–647.

Bialer, M., Johannessen, S.I., Levy, R.H., Perucca, E., Tomson, T., White, H.S., 2017. Progress report on new antiepileptic drugs: A summary of the Thirteenth Eilat Conference on New Antiepileptic Drugs and Devices (EILAT XIII). Epilepsia 58, 181–221.

Bialer, M., Johannessen, S.I., Levy, R.H., Perucca, E., Tomson, T., White, H.S., 2015. Progress report on new antiepileptic drugs: A summary of the Twelfth Eilat Conference (EILAT XII). Epilepsy Res. 111, 85–141.

Bialer, M., White, H.S., 2010. Key factors in the discovery and development of new antiepileptic drugs. Nat. Rev. Drug Discov. 9, 68–82.

Bicker, J., Alves, G., Fortuna, A., Soares-Da-Silva, P., Falcão, A., 2016. A new PAMPA model using an in-house brain lipid extract for screening the blood-brain barrier permeability of drug candidates. Int. J. Pharm. 501, 102–111.

Bidwell, J., Khuwatsamrit, T., Askew, B., Ehrenberg, J.A., Helmers, S., 2015. Seizure reporting technologies for epilepsy treatment: A review of clinical information needs

and supporting technologies. Seizure 32, 109–117.

Biggs-Houck, J.E., Younai, A., Shaw, J.T., 2010. Recent advances in multicomponent reactions for diversity-oriented synthesis. Curr. Opin. Chem. Biol. 14, 371–382.

Bisi, A., Rampa, A., Budriesi, R., Gobbi, S., Belluti, F., Ioan, P., Valoti, E., Chiarini, A., Valenti, P., 2003. Cardiovascular hybrid drugs: new benzazepinone derivatives as bradycardic agents endowed with selective ß1-Non-competitive antagonism. Bioorg. Med. Chem. 11, 1353–1361.

Björnsson, E., 2008. Hepatotoxicity associated with antiepileptic drugs. Acta Neurol. Scand. 118, 281–290.

Boehlen, A., Schwake, M., Dost, R., Kunert, A., Fidzinski, P., Heinemann, U., Gebhardt, C., 2013. The new KCNQ2 activator 4-Chlor-N-(6-chlor-pyridin-3-yl)-benzamid displays anticonvulsant potential. Br. J. Pharmacol. 168, 1182–1200.

Bose, A.K., Pednekar, S., Ganguly, S.N., Chakraborty, G., Manhas, M.S., 2004. A simplified green chemistry approach to the Biginelli reaction using "Grindstone Chemistry." Tetrahedron Lett. 45, 8351–8353.

Botros, S., Khalil, N.A., Naguib, B.H., El-Dash, Y., 2013. Synthesis and Anticonvulsant Activity of New Phenytoin Derivatives. Eur. J. Med. Chem. 60, 57–63.

Brodie, M.J., 2016. Pharmacological treatment of drug-resistant epilepsy in adults: a practical guide. Curr. Neurol. Neurosci. Rep. 16, 82.

Brodie, M.J., 2010. Antiepileptic drug therapy the story so far. Seizure 19, 650–655.

Brodie, M.J., Covanis, A., Gil-Nagel, A., Lerche, H., Perucca, E., Sills, G.J., White, H.S., 2011. Antiepileptic drug therapy: Does mechanism of action matter? Epilepsy Behav. 21, 331–341.

Brown, C., 2016. Pharmacological management of epilepsy. Prog. Neurol. Psychiatry 20, 27–34.

Bum, E.N., Taiwe, G.S., Nkainsa, L.A., Moto, F.C.O., Seke Etet, P.F., Hiana, I.R., Bailabar, T., Rouyatou, Seyni, P., Rakotonirina, A., Rakotonirina, S. V., 2009. Validation of anticonvulsant and sedative activity of six medicinal plants. Epilepsy Behav. 14, 454–458.

Bunel, V., Ouedraogo, M., Nguyen, A.T., Stévigny, C., Duez, P., 2014. Methods applied to the in vitro primary toxicology testing of natural products: State of the art, strengths, and limits. Planta Med. 80, 1210–1226.

Caldwell, G.W., 2015. In silico tools used for compound selection during target-based drug discovery and development. Expert Opin. Drug Discov. 10, 901–923.

Cao, X., Chen, Y., Zhang, Y., Lan, Y., Zhang, J., Xu, X., Qiu, Y., Zhao, S., Liu, X., Liu, B.-F., Zhang, G., 2016. Synthesis and biological evaluation of novel sigma1 receptor ligands for

treating neuropathic pain: 6-Hydroxypyridazinones. J. Med. Chem. 59, 2942–2961.

Caron, G., Ermondi, G., 2017. Updating molecular properties during early drug discovery. Drug Discov. Today 22, 835–840.

Castel-Branco, M.M., Alves, G.L., Figueiredo, I. V., Falcão, A.C., Caramona, M.M., 2009. The maximal electroshock seizure (MES) model in the preclinical assessment of potential new antiepileptic drugs. Methods Find. Exp. Clin. Pharmacol. 31, 101–106.

Cavaletti, G., Oggioni, N., Sala, F., Pezzoni, G., Cavalletti, E., Marmiroli, P., Petruccioli, M.G., Frattola, L., Tredici, G., 2000. Effect on the peripheral nervous system of systemically administered dimethylsulfoxide in the rat: a neurophysiological and pathological study. Toxicol. Lett. 118, 103–107.

Cernecka, H., Veizerova, L., Mensikova, L., Svetlik, J., Krenek, P., 2012. Selective inhibitory action of Biginelli-type dihydropyrimidines on depolarization-induced arterial smooth muscle contraction. J. Pharm. Pharmacol. 64, 735–741.

Chandra, N., Padiadpu, J., 2013. Network approaches to drug discovery. Expert Opin. Drug Discov. 8, 7–20.

Chari, M.A., Shobha, D., Kumar, T.K., Dubey, P.K., 2005. Bismuth (III) nitrate catalyzed one-pot synthesis of 3 , 4-dihydro-pyrimidin-2-(1H)-ones: an improved protocol for the Biginelli reaction. Arkivoc 2005, 74–80.

Chaudhary, G.R., Bansal, P., Mehta, S.K., 2014. Recyclable CuS quantum dots as heterogeneous catalyst for Biginelli reaction under solvent free conditions. Chem. Eng. J. 243, 217–224.

Chen, Y., Liu, L., 2012. Modern methods for delivery of drugs across the blood-brain barrier. Adv. Drug Deliv. Rev. 64, 640–665.

Chiang, A.N., Valderramos, J.-C., Balachandran, R., Chovatiya, R.J., Mead, B.P., Schneider, C., Bell, S.L., Klein, M.G., Huryn, D.M., Chen, X.S., Day, B.W., Fidock, D.A., Wipf, P., Brodsky, J.L., 2009. Select pyrimidinones inhibit the propagation of the malarial parasite, Plasmodium falciparum. Bioorg. Med. Chem. 17, 1527–1533.

Chong, D.J., Lerman, A.M., 2016. Practice update: Review of anticonvulsant therapy. Curr. Neurol. Neurosci. Rep. 16, 39.

Ciociola, A.A., Cohen, L.B., Kulkarni, P., 2014. How drugs are developed and approved by the FDA: Current process and future directions. Am. J. Gastroenterol. 109, 620–623.

Colucci, M., Maione, F., Bonito, M.C., Piscopo, A., Di Giannuario, A., Pieretti, S., 2008. New insights of dimethyl sulphoxide effects (DMSO) on experimental in vivo models of nociception and inflammation. Pharmacol. Res. 57, 419–425.

Cox, J.H., Seri, S., Cavanna, A.E., 2014. Zonisamide as a treatment for partial epileptic seizures: A systematic review. Adv. Ther. 31, 276–288.

Curia, G., Longo, D., Biagini, G., Jones, R.S.G., Avoli, M., 2008. The pilocarpine model of temporal lobe epilepsy. J. Neurosci. Methods 172, 143–157.

Da Silva, D.L., Reis, F.S., Muniz, D.R., Ruiz, A.L.T.G., De Carvalho, J.E., Sabino, A.A., Modolo, L. V., De Fátima, Â., 2012. Free radical scavenging and antiproliferative properties of Biginelli adducts. Bioorg. Med. Chem. 20, 2645–2650.

Dahlin, J.L., Inglese, J., Walters, M.A., 2015. Mitigating risk in academic preclinical drug discovery. Nat. Rev. Drug Discov. 14, 279–294.

Dalkara, S., Karakurt, A., 2012. Recent progress in anticonvulsant drug research: Strategies for anticonvulsant drug development and applications of antiepileptic drugs for non-epileptic central nervous system disorders. Curr. Top. Med. Chem. 12, 1033–1071.

Dawood, K.M., Abdel-Gawad, H., Rageb, E.A., Ellithey, M., Mohamed, H.A., 2006. Synthesis, anticonvulsant, and anti-inflammatory evaluation of some new benzotriazole and benzofuran-based heterocycles. Bioorg. Med. Chem. 14, 3672–3680.

De Fátima, Â., Braga, T.C., Neto, L. da S., Terra, B.S., Oliveira, B.G.F., da Silva, D.L., Modolo, L. V., 2015. A mini-review on Biginelli adducts with notable pharmacological properties. J. Adv. Res. 6, 363–373.

DeGorter, M.K., Xia, C.Q., Yang, J.J., Kim, R.B., 2012. Drug transporters in drug efficacy and toxicity. Annu. Rev. Pharmacol. Toxicol. 52, 249–273.

Desai, B., Dallinger, D., Kappe, C.O., 2006. Microwave-assisted solution phase synthesis of dihydropyrimidine C5 amides and esters. Tetrahedron 62, 4651–4664.

Di, L., Fish, P. V., Mano, T., 2012. Bridging solubility between drug discovery and development. Drug Discov. Today 17, 486–495.

Di, L., Kerns, E.H., Bezar, I.F., Petusky, S.L., Huang, Y., 2009. Comparison of blood–brain barrier permeability assays: In situ brain perfusion, MDR1-MDCKII and PAMPA-BBB. J. Pharm. Sci. 98, 1980–1991.

Dickens, D., Owen, A., Alfirevic, A., Giannoudis, A., Davies, A., Weksler, B., Romero, I.A., Couraud, P.-O., Pirmohamed, M., 2012. Lamotrigine is a substrate for OCT1 in brain endothelial cells. Biochem. Pharmacol. 83, 805–814.

Dong, F., Jun, L., Xinli, Z., Zhiwen, Y., Zuliang, L., 2007. One-pot green procedure for Biginelli reaction catalyzed by novel task-specific room-temperature ionic liquids. J. Mol. Catal. A Chem. 274, 208–211.

Dong, S., Wang, T., Hu, C., Chen, X., Jin, Y., Wang, Z., 2017. Design and synthesis of 5-substituted benzo[d][1,3]dioxole derivatives as potent anticonvulsant agents. Arch. Pharm. Chem. Life Sci. 349, e1600274.

Doumlele, K., Conway, E., Hedlund, J., Tolete, P., Devinsky, O., 2016. A case report on the efficacy of vigabatrin analogue (1S, 3S)-3-amino-4-difluoromethylenyl-1-cyclopentanoic

acid (CPP-115) in a patient with infantile spasms. Epilepsy Behav. Case Rep. 6, 67–69.

Dudai, Y., Evers, K., 2014. To simulate or not to simulate: What are the questions? Neuron 84, 254–261.

Easter, A., Bell, M.E., Damewood Jr., J.R., Redfern, W.S., Valentin, J.-P., Winter, M.J., Fonck, C., Bialecki, R.A., 2009. Approaches to seizure risk assessment in preclinical drug discovery. Drug Discov. Today 14, 876–884.

Eddershaw, P.J., Beresford, A.P., Bayliss, M.K., 2000. ADME/PK as part of a rational approach to drug discovery. Drug Discov. Today 5, 409–414.

Ekstein, D., 2015. Issues and promise in clinical studies of botanicals with anticonvulsant potential. Epilepsy Behav. 52, 329–332.

El-Azab, A.S., Eltahir, K.E.H., 2012. Synthesis and anticonvulsant evaluation of some new 2,3,8-trisubstituted-4(3H)-quinazoline derivatives. Bioorg. Med. Chem. Lett. 22, 327–333.

Elder, D., Holm, R., 2013. Aqueous solubility: Simple predictive methods (in silico, in vitro and bio-relevant approaches). Int. J. Pharm. 453, 3–11.

EMA, 2012. Guideline on the investigation of drug interactions. Guid. Doc. 44, 59.

Epilepsy Foundation, 2017. Accessed on 21 January 2017: http://www.epilepsy.com/accelerating-new-therapies/new-therapies-pipeline#drugs

Ertl, P., Rohde, B., Selzer, P., 2000. Fast calculation of molecular polar surface area as a sum of fragment-based contributions and its application to the prediction of drug transport properties. J. Med. Chem. 43, 3714–3717.

Faller, B., 2008. Artificial membrane assays to assess permeability. Curr. Drug Metab. 9, 886–892.

Faught, E., 2014. BGG492 (selurampanel), an AMPA/kainate receptor antagonist drug for epilepsy. Expert Opin. Investig. Drugs 23, 107–113.

FDA, 2012. Guidance for industry. Drug interaction studies study design, data analysis, implications for dosing, and labeling recommendations. Guid. Doc. 79.

Feng, B., Varma, M. V., Costales, C., Zhang, H., Tremaine, L., 2014. In vitro and in vivo approaches to characterize transporter-mediated disposition in drug discovery. Expert Opin. Drug Discov. 9, 873–890.

Ferdowsian, H.R., Beck, N., 2011. Ethical and scientific considerations regarding animal testing and research. PLoS One 6, e24059.

Fishburn, C.S., 2013. Translational research: The changing landscape of drug discovery. Drug Discov. Today 18, 487–494.

Fisher, R.S., 2017a. The new classification of seizures by the International League Against

Epilepsy 2017. Curr. Neurol. Neurosci. Rep. 17, 48.

Fisher, R.S., 2017b. An overview of the 2017 ILAE operational classification of seizure types. Epilepsy Behav. 70, 271–273.

Fisher, R.S., Acevedo, C., Arzimanoglou, A., Bogacz, A., Cross, J.H., Elger, C.E., Engel Jr., J., Forsgren, L., French, J.A., Glynn, M., Hesdorffer, D.C., Lee, B.I., Mathern, G.W., Moshé, S.L., Perucca, E., Scheffer, I.E., Tomson, T., Watanabe, M., Wiebe, S., 2014. A practical clinical definition of epilepsy. Epilepsia 55, 475–482.

Fisher, R.S., Cross, J.H., D'Souza, C., French, J.A., Haut, S.R., Higurashi, N., Hirsch, E., Jansen, F.E., Lagae, L., Moshé, S.L., Peltola, J., Roulet Perez, E., Scheffer, I.E., Schulze-Bonhage, A., Somerville, E., Sperling, M., Yacubian, E.M., Zuberi, S.M., 2017. Instruction manual for the ILAE 2017 operational classification of seizure types. Epilepsia 58, 531–542.

Fishman, M.C., Porter, J.A., 2005. A new grammar for drug discovery. Nature 437, 491–493.

Fortuna, A., Alves, G., Soares-da-Silva, P., Falcão, A., 2012. Optimization of a Parallel Artificial Membrane Permeability Assay for the Fast and Simultaneous Prediction of Human Intestinal Absorption and Plasma Protein Binding of Drug Candidates: Application to Dibenz[b,f]Azepine-5-Carboxamide Derivatives. J. Pharm. Sci. 101, 530–540.

Franco, V., French, J.A., Perucca, E., 2016. Challenges in the clinical development of new antiepileptic drugs. Pharmacol. Res. 103, 95–104.

Gad, S., Cassidy, C.D., Aubert, N., Spainhour, B., Robbe, H., 2006. Nonclinical Vehicle Use in Studies by Multiple Routes in Multiple Species. Int. J. Toxicol. 25, 499–521.

Galvao, J., Davis, B., Tilley, M., Normando, E., Duchen, M.R., Cordeiro, M.F., 2014. Unexpected low-dose toxicity of the universal solvent DMSO. FASEB J. 28, 1317–1330.

Ganem, B., 2009. Strategies for innovation in multicomponent reaction design. Acc. Chem. Res. 42, 463–472.

Gangwar, N., Kasana, V.K., 2012. 3,4-Dihydropyrimidin-2(1H)-one derivatives: Organocatalysed microwave assisted synthesis and evaluation of their antioxidant activity. Med. Chem. Res. 21, 4506–4511.

Garro Martinez, J.C., Vega-Hissi, E.G., Andrada, M.F., Estrada, M.R., 2015. QSAR and 3D-QSAR studies applied to compounds with anticonvulsant activity. Expert Opin. Drug Discov. 10, 37–51.

Geldenhuys, W.J., Schyf, C.J. Van Der, 2013. Designing drugs with multi-target activity: the next step in the treatment of neurodegenerative disorders. Expert Opin. Drug Discov. 8, 115–129.

Ghodasara, H.B., Trivedi, A.R., Kataria, V.B., Patel, B.G., Shah, V.H., 2013. Synthesis and antimicrobial evaluation of novel substituted pyrimidine scaffold. Med. Chem. Res. 22,

6121–6128.

Ghogare, J.G., Bhandari, S. V., Bothara, K.G., Madgulkar, A.R., Parashar, G.A., Sonawane, B.G., Inamdar, P.R., 2010. Design, synthesis and pharmacological screening of potential anticonvulsant agents using hybrid approach. Eur. J. Med. Chem. 45, 857–863.

Ghosh, B., Antonio, T., Zhen, J., Kharker, P., Reith, M.E.A., Dutta, A.K., 2010. Development of (S)-N6-(2-(4-(Isoquinolin-1-yl)piperazin-1-yl)ethyl)-N6-propyl-4,5,6,7-tetrahydrobenzo[d]-thiazole-2,6-diamine and its analogue as a D3 receptor preferring agonist: Potent in vivo activity in Parkinson's disease animal models. J. Med. Chem. 53, 1–35.

Giacomini, K.M., Huang, S.-M., Tweedie Donald J., Benet, L.Z., Brouwer, K.L.R., Chu, X., Dahlin, A., Evers, R., Fischer, V., Hillgren, K.M., Hoffmaster, K.A., Ishikawa, T., Keppler, D., Kim, R.B., Lee, C.A., Niemi, M., Polli, J.W., Sugiyama, Y., Swaan, P.W., Ware, J.A., Wright, S.H., Yee, S.W., Zamek-Gliszczynski, M.J., Zhang, L., 2010. Membrane transporters in drug development. Nat. Rev. Drug Discov. 9, 215–236.

Gireesh, T., Kamble, R.R., Kattimani, P.P., Dorababu, A., Manikantha, M., Hoskeri, J.H., 2013. Synthesis of Sydnone Substituted Biginelli Derivatives as Hyaluronidase Inhibitors. Arch. Pharm. Chem. Life Sci. 346, 645–653.

Glass, H.E., DiFrancesco, J.J., Glass, L.M., Tran, P., 2015. Are Phase 3 Clinical Trials Really Becoming More Complex? Ther. Innov. Regul. Sci. 49, 852–860.

Godhani, D.R., Dobariya, P.B., Jogel, A.A., Sanghani, A.M., Mehta, J.P., 2014. An efficient synthesis, characterization, and antimicrobial screening of tetrahydropyrimidine derivatives. Med. Chem. Res. 23, 2417–2425.

Golyala, A., Kwan, P., 2017. Drug development for refractory epilepsy: The past 25 years and beyond. Seizure 44, 147–156.

Gómez-Lechón, M.J., Tolosa, L., Conde, I., Donato, M.T., 2014. Competency of different cell models to predict human hepatotoxic drugs. Expert Opin. Drug Metab. Toxicol. 10, 1553–1568.

Gong, L.-Z., Chen, X.-H., Xu, X.-Y., 2007. Asymmetric organocatalytic Biginelli reactions: A new approach to quickly access optically active 3,4-dihydropyrimidin-2-(1H)-ones. Chem. Eur. J. 13, 8920–8926.

Goodfellow, V.S., Loweth, C.J., Ravula, S.B., Wiemann, T., Nguyen, T., Xu, Y., Todd, D.E., Sheppard, D., Pollack, S., Polesskaya, O., Marker, D.F., Dewhurst, S., Gelbard, H.A., 2013. Discovery, synthesis, and characterization of an orally bioavailable, brain penetrant inhibitor of mixed lineage kinase 3. J. Med. Chem. 56, 8032–8048.

Goss, J.M., Schaus, S.E., 2008. Enantioselective synthesis of SNAP-7941: Chiral dihydropyrimidone inhibitor of MCH1-R. J. Org. Chem. 73, 7651–7656.

Greenwood, J., Valdes, J., 2016. Perampanel (Fycompa): A Review of Clinical Efficacy and

Safety in Epilepsy. Pharm. Ther. 41, 683–688.

Grever, M.R., 2013. Accelerating safe drug development: an ideal approach to approval. Hematol. Am. Soc. Hematol. Educ. Progr. 2013, 24–29.

Gschwind, M., Seeck, M., 2016. Modern management of seizures and epilepsy. Swiss Med. Wkly. 146, w14310.

Guo, R., Zhang, Y., Li, X., Song, X., Li, D., Zhao, Y., 2016. Discovery of ERBB3 inhibitors for non-small cell lung cancer (NSCLC) via virtual screening. J. Mol. Model. 22, 135.

Habib, M.M.W., Abdelfattah, M.A.O., Abadi, A.H., 2015. Design and Synthesis of Novel Phenylpiperazine Derivatives as Potential Anticonvulsant Agents. Arch. Pharm. Chem. Life Sci. 348, 868–874.

Hamdi, N., Medyouni, R., Bilel, H., Mansour, L., Romerosa, A., 2017. An Efficient One-Pot Protocol for the Synthesis of Substituted 3,4-Dihydropyrimidin-2(1H)-ones Using Metallophthalocyanines (MPcs) as Potent Heterogeneous Catalysts: Synthesis, Characterization, Aggregation and Antimicrobial Activity. Molecules 22, 605.

Hammer, H., Bader, B.M., Ehnert, C., Bundgaard, C., Bunch, L., Hoestgaard-Jensen, K., Schroeder, O.H.-U., Bastlund, J.F., Gramowski-Voß, A., Jensen, A.A., 2015. A Multifaceted GABAA Receptor Modulator: Functional Properties and Mechanism of Action of the Sedative-Hypnotic and Recreational Drug Methaqualone (Quaalude). Mol. Pharmacol. 88, 401–420.

Hanslick, J.L., Lau, K., Noguchi, K.K., Olney, J.W., Zorumski, C.F., Mennerick, S., Farber, N.B., 2009. Dimethyl sulfoxide (DMSO) produces widespread apoptosis in the developing central nervous system. Neurobiol. Dis. 34, 1–10.

Harada, A., Suzuki, K., Kimura, H., 2017. TAK-063, a novel phosphodiesterase 10A inhibitor, protects from striatal neurodegeneration and ameliorates behavioral deficits in the R6/2 mouse model of Huntington's disease. J. Pharmacol. Exp. Ther. 360, 75–83.

Harford-Wright, E., Thornton, E., Vink, R., 2010. Angiotensin-converting enzyme (ACE) inhibitors exacerbate histological damage and motor deficits after experimental traumatic brain injury. Neurosci. Lett. 481, 26–29.

Hasebe, M., Matsumoto, I., Imagawa, T., Uehara, M., 2008. Effects of an anti-thyroid drug, methimazole, administration to rat dams on the cerebellar cortex development in their pups. Int. J. Devl. Neurosci. 26, 409–414.

Hassan, M.Z., Khan, S.A., Amir, M., 2012. Design, synthesis and evaluation of N-(substituted benzothiazol-2-yl)amides as anticonvulsant and neuroprotective. Eur. J. Med. Chem. 58, 206–213.

Hayon, T., Dvilansky, A., Shpilberg, O., Nathan, I., 2003. Appraisal of the MTT-based assay as a useful tool for predicting drug chemosensitivity in leukemia. Leuk. Lymphoma 44, 1957–1962.

Hendriksen, H., Groenink, L., 2015. Back to the future of psychopharmacology: A perspective on animal models in drug discovery. Eur. J. Pharmacol. 759, 30–41.

Hidalgo-Figueroa, S., Ramírez-Espinosa, J.J., Estrada-Soto, S., Almanza-Pérez, J.C., Román-Ramos, R., Alarcón-Aguilar, F.J., Hernández-Rosado, J. V., Moreno-Díaz, H., Díaz-Coutiño, D., Navarrete-Vázquez, G., 2013. Discovery of thiazolidine-2,4-dione/biphenylcarbonitrile hybrid as dual PPAR α/γ modulator with antidiabetic effect: in vitro, in silico and in vivo approaches. Chem. Biol. Drug Des. 81, 474–483.

Hitchcock, S.A., 2012. Structural modifications that alter the P-glycoprotein efflux properties of compounds. J. Med. Chem. 55, 4877–4895.

Holmes, L.B., Hernandez-Diaz, S., 2012. Newer anticonvulsants: Lamotrigine, topiramate and gabapentin. Birth Defects Res. Part A - Clin. Mol. Teratol. 94, 599–606.

Hosseini, N., Mokhtari, S., Momeni, E., Vossoughi, M., Barekatian, M., 2016. Effect of motivational interviewing on quality of life in patients with epilepsy. Epilepsy Behav. 55, 70–74.

Hughes, J.P., Rees, S., Kalindjian, S.B., Philpott, K.L., 2011. Principles of early drug discovery. Br. J. Pharmacol. 162, 1239–1249.

Hulme, C., Gore, V., 2003. "Multi-component reactions: emerging chemistry in drug discovery" "from xylocain to crixivan". Curr. Med. Chem. 10, 51–80.

Ibrahim, M.-K., El-Adl, K., Al-Karmalawy, A.A., 2015. Design, synthesis, molecular docking and anticonvulsant evaluation of novel 6-iodo-2-phenyl-3-substituted-quinazolin-4(3H)-ones. Bull. Fac. Pharmacy, Cairo Univ. 53, 101–116.

Jenner, G., 2004. Effect of high pressure on Biginelli reactions. Steric hindrance and mechanistic considerations. Tetrahedron Lett. 45, 6195–6198.

Jetti, S.R., Upadhyaya, A., Jain, S., 2014. 3,4-Hydropyrimidin-2-(1H)one derivatives: Solid silica-based sulfonic acid catalyzed microwave-assisted synthesis and their biological evaluation as antihypertensive and calcium channel blocking agents. Med. Chem. Res. 23, 4356–4366.

Jiang, B., Rajale, T., Wever, W., Tu, S.-J., Li, G., 2010. Multicomponent Reactions for the Synthesis of Heterocycles. Chem. Asian J. 5, 2318–2335.

Jouan, E., Le Vée, M., Mayati, A., Denizot, C., Parmentier, Y., Fardel, O., 2016. Evaluation of P-glycoprotein inhibitory potential using a rhodamine 123 accumulation assay. Pharmaceutics 8, 1–13.

Junker, A., Balasubramanian, R., Ciancetta, A., Uliassi, E., Kiselev, E., Martiriggiano, C., Trujillo, K., Mtchedlidze, G., Birdwell, L., Brown, K.A., Harden, T.K., Jacobson, K.A., 2016. Structure-Based Design of 3-(4-Aryl-1H-1,2,3-triazol-1-yl)-Biphenyl Derivatives as P2Y14 Receptor Antagonists. J. Med. Chem. 59, 6149–6168.

Juvale, K., Pape, V.F.S., Wiese, M., 2012. Investigation of chalcones and benzochalcones as inhibitors of breast cancer resistance protein. Bioorg. Med. Chem. 20, 346–355.

Kaitin, K.I., 2010. Deconstructing the Drug Development Process: The New Face of Innovation. Clin. Pharmacol. Ther. 87, 356–361.

Kalita, H.R., Phukan, P., 2007. CuI as reusable catalyst for the Biginelli reaction. Catal. Commun. 8, 179–182.

Kamiński, K., Rapacz, A., Łuszczki, J.J., Latacz, G., Obniska, J., Kieć-Kononowicz, K., Filipek, B., 2015. Design, synthesis and biological evaluation of new hybrid anticonvulsants derived from N-benzyl-2-(2,5-dioxopyrrolidin-1-yl)propanamide and 2-(2,5-dioxopyrrolidin-1-yl)butanamide derivatives. Bioorg. Med. Chem. 23, 2548–2561.

Kamiński, K., Zagaja, M., Rapacz, A., Łuszczki, J.J., Andres-Mach, M., Abram, M., Obniska, J., 2016. New hybrid molecules with anticonvulsant and antinociceptive activity derived from 3-methyl- or 3,3-dimethyl-1-[1-oxo-1-(4-phenylpiperazin-1-yl)propan-2-yl]pyrrolidine-2,5-diones. Bioorg. Med. Chem. 24, 606–618.

Kaminski, R.M., Rogawski, M.A., Klitgaard, H., 2014. The Potential of Antiseizure Drugs and Agents that Act on Novel Molecular Targets as Antiepileptogenic Treatments. Neurotherapeutics 11, 385–400.

Kandratavicius, L., Alves Balista, P., Lopes-Aguiar, C., Ruggiero, R.N., Umeoka, E.H., Garcia-Cairasco, N., Bueno-Junior, L.S., Leite, J.P., 2014. Animal models of epilepsy: Use and limitations. Neuropsychiatr. Dis. Treat. 10, 1693–1705.

Kang, S., Cooper, G., Dunne, S.F., Luan, C.-H., James Surmeier, D., Silverman, R.B., 2013. Antagonism of L-type Ca(2+) channels CaV1.3 and CaV1.2 by 1,4-dihydropyrimidines and 4H-pyrans as dihydropyridine mimics. Bioorg. Med. Chem. 21, 4365–4373.

Kansy, M., Senner, F., Gubernator, K., 1998. Physicochemical High Throughput Screening: Parallel Artificial Membrane Permeation Assay in the Description of Passive Absorption Processes. J. Med. Chem. 41, 1007–1010.

Kappe, C.O., 2003. The Generation of Dihydropyrimidine Libraries Utilizing Biginelli Multicomponent Chemistry. QSAR Comb. Sci. 22, 630–645.

Kashaw, S.K., Kashaw, V., Mishra, P., Jain, N.K., Stables, J.P., 2009. Synthesis, anticonvulsant and CNS depressant activity of some new bioactive 1-(4-substituted-phenyl)-3-(4-oxo-2-phenyl/ethyl-4H-quinazolin-3-yl)-urea. Eur. J. Med. Chem. 44, 4335–4343.

Kaur, R., Chaudhary, S., Kumar, K., Gupta, M.K., Rawal, R.K., 2017. Recent synthetic and medicinal perspectives of dihydropyrimidinones: A review. Eur. J. Med. Chem. 132, 108–134.

Kerr, M.P., 2012. The impact of epilepsy on patients' lives. Acta Neurol. Scand. 126, 1–9.

Khodaei, M.M., Khosropour, A.R., Beygzadeh, M., 2004. An Efficient and Environmentally Friendly Method for Synthesis of 3,4-Dihydropyrimidin-2(1H)-ones Catalyzed by Bi(NO3)3 ·5H2O. Synth. Commun. 34, 1551–1557.

Kikuchi, R., de Morais, S.M., Kalvass, J.C., 2013. In vitro P-glycoprotein efflux ratio can predict the in vivo brain penetration regardless of biopharmaceutics drug disposition classification system class. Drug Metab. Dispos. 41, 2012–2017.

Kim, J., Park, C., Ok, T., So, W., Jo, M., Seo, M., Kim, Y., Sohn, J.-H., Park, Y., Ju, M.K., Kim, J., Han, S.-J., Kim, T.-H., Cechetto, J., Nam, J., Sommer, P., No, Z., 2012. Discovery of 3,4-dihydropyrimidin-2(1H)-ones with inhibitory activity against HIV-1 replication. Bioorg. Med. Chem. Lett. 22, 2119–2124.

Kim, S., Kim, Y., Kong, Y., Kim, H., Kang, J., 2009. Synthesis and in vitro biological activity of retinyl polyhydroxybenzoates, novel hybrid retinoid derivatives. Bioorg. Med. Chem. Lett. 19, 508–512.

Kinfe, H.H., Belay, Y.H., Joseph, J.S., Mukwevho, E., 2013. Evaluation of the Influence of thiosemicarbazone-triazole hybrids on genes implicated in lipid oxidation and accumulation as potential anti-obesity agents. Bioorg. Med. Chem. Lett. 23, 5275–5278.

Kola, I., Landis, J., 2004. Can the pharmaceutical industry reduce attrition rates? Nat. Rev. Drug Discov. 3, 711–715.

Kolosov, M.A., Orlov, V.D., Beloborodov, D.A., Dotsenko, V. V., 2009. A chemical placebo: NaCl as an effective, cheapest, non-acidic and greener catalyst for Biginelli-type 3,4-dihydropyrimidin-2(1H)-ones (-thiones) synthesis. Mol. Divers. 13, 5–25.

Koppel, S.J., Swerdlow, R.H., 2017. Neuroketotherapeutics: A modern review of a century-old therapy. Neurochem. Int. 1–12.

Kostewicz, E.S., Abrahamsson, B., Brewster, M., Brouwers, J., Butler, J., Carlert, S., Dickinson, P.A., Dressman, J., Holm, R., Klein, S., Mann, J., McAllister, M., Minekus, M., Muenster, U., Müllertz, A., Verwei, M., Vertzoni, M., Weitschies, W., Augustijns, P., 2014. In vitro models for the prediction of in vivo performance of oral dosage forms. Eur. J. Pharm. Sci. 57, 342–366.

Kowalczyk, P., Sałat, K., Höfner, G.C., Mucha, M., Rapacz, A., Podkowa, A., Filipek, B., Wanner, K.T., Kulig, K., 2014. Synthesis, biological evaluation and structure-activity relationship of new GABA uptake inhibitors, derivatives of 4-aminobutanamides. Eur. J. Med. Chem. 83, 256–273.

Kowski, A.B., Weissinger, F., Gaus, V., Fidzinski, P., Losch, F., Holtkamp, M., 2016. Specific adverse effects of antiepileptic drugs — A true-to-life monotherapy study. Epilepsy Behav. 54, 150–157.

Krasowski, M.D., 2010. Therapeutic Drug Monitoring of the Newer Anti-Epilepsy Medications. Pharmaceuticals 3, 1909–1935.

Krasowski, M.D., Mcmillin, G.A., 2014. Advances in anti-epileptic drug testing. Clin. Chim. Acta 436, 224–236.

Kshirsagar, A., Toraskar, M.P., Kulkarni, V.M., Dhanashire, S., Kadam, V., 2009. Microwave assisted synthesis of potential anti infective and anticonvulsant thiosemicarbazones. Int. J. ChemTech Res. 1, 696–701.

Kuhlmann, L., Grayden, D.B., Wendling, F., Schiff, S.J., 2015. The role of multiple-scale modelling of epilepsy in seizure forecasting. J. Clin. Neurophysiol. 32, 220–226.

Kulandasamy, R., Adhikari, A.V., Taranalli, A., Venkataswamy, T., 2010. New Hydrazides and Thiosemicarbazides Derived from Ethylenedioxythiophene as Potential Anticonvulsants. Phosphorus, Sulfur Silicon Relat. Elem. 185, 1358–1368.

Kumar, D., Sharma, V.K., Kumar, R., Singh, T., Singh, H., Singh, A.D., Roy, R.K., 2013. Design, synthesis and anticonvulsant activity of some new 5,7-dibromoisatin semicarbazone derivatives. EXCLI J. 12, 628–640.

Kumar, P., Shrivastava, B., Pandeya, S.N., Stables, J.P., 2011. Design, synthesis and potential 6 Hz psychomotor seizure test activity of some novel 2-(substituted)-3-{[substituted]amino}quinazolin-4(3H)-one. Eur. J. Med. Chem. 46, 1006–1018.

Kumari, S., Mishra, C.B., Tiwari, M., 2016. Pharmacological evaluation of novel 1-[4-(4-benzo[1,3]dioxol-5-ylmethyl-piperazin-1-yl)-phenyl]-3-phenyl-urea as potent anticonvulsant and antidepressant agent. Pharmacol. Rep. 68, 250–258.

Kupferberg, H., 2001. Animal Models Used in the Screening of Antiepileptic Drugs. Epilepsia 42, 7–12.

Kwan, P., Arzimanoglou, A., Berg, A.T., Brodie, M.J., Hauser, W.A., Mathern, G., Moshé, S.L., Perucca, E., Wiebe, S., French, J., 2010. Definition of drug resistant epilepsy: Consensus proposal by the ad hoc Task Force of the ILAE Commission on Therapeutic Strategies. Epilepsia 51, 1069–1077.

Lacotte, P., Buisson, D.A., Ambroise, Y., 2013. Synthesis, evaluation and absolute configuration assignment of novel dihydropyrimidin-2-ones as picomolar sodium iodide symporter inhibitors. Eur. J. Med. Chem. 62, 722–727.

Łączkowski, K.Z., Sałat, K., Misiura, K., Podkowa, A., Malikowska, N., 2016. Synthesis and anticonvulsant activities of novel 2-(cyclopentylmethylene)hydrazinyl-1,3-thiazoles in mouse models of seizures. J. Enzym. Inhib. Med. Chem. 31, 1576–1582.

Landmark, C.J., Patsalos, P.N., 2010. Drug interactions involving the new second- and third-generation antiepileptic drugs. Expert Rev. Neurother. 10, 119–140.

Lanevskij, K., Japertas, P., Didziapetris, R., 2013. Improving the prediction of drug disposition in the brain. Expert Opin. Drug Metab. Toxicol. 9, 473–486.

Larsen, J., Gasser, K., Hahin, R., 1996. An Analysis of Dimethylsulfoxide-Induced Action

Potential Block: A Comparative Study of DMSO and Other Aliphatic Water Soluble Solutes. Toxicol. Appl. Pharmacol. 140, 296–314.

Lau, K., Swiney, B.S., Reeves, N., Noguchi, K.K., Farber, N.B., 2012. Propylene glycol produces excessive apoptosis in the developing mouse brain, alone and in combination with phenobarbital. Pediatr. Res. 71, 54–62.

Lennernäs, H., Aarons, L., Augustijns, P., Beato, S., Bolger, M., Box, K., Brewster, M., Butler, J., Dressman, J., Holm, R., Julia Frank, K., Kendall, R., Langguth, P., Sydor, J., Lindahl, A., McAllister, M., Muenster, U., Müllertz, A., Ojala, K., Pepin, X., Reppas, C., Rostami-Hodjegan, A., Verwei, M., Weitschies, W., Wilson, C., Karlsson, C., Abrahamsson, B., 2014. Oral biopharmaceutics tools - Time for a new initiative - An introduction to the IMI project OrBiTo. Eur. J. Pharm. Sci. 57, 292–299.

Leo, A., Russo, E., Elia, M., 2016. Cannabidiol and epilepsy: Rationale and therapeutic potential. Pharmacol. Res. 107, 85–92.

Leucuta, S.E., 2014. Selecting oral bioavailability enhancing formulations during drug discovery and development. Expert Opin. Drug Discov. 9, 139–150.

Lévesque, M., Avoli, M., 2013. The kainic acid model of temporal lobe epilepsy. Neurosci. Biobehav. Rev. 37, 2887–2899.

Lewis, R.W., Mabry, J., Polisar, J.G., Eagen, K.P., Ganem, B., Hess, G.P., 2010. Dihydropyrimidinone positive modulation of delta-subunit-containing gamma-aminobutyric acid type A receptors, including an epilepsy-linked mutant variant. Biochemistry 49, 4841–4851.

Li, J.-T., Han, J.-F., Yang, J.-H., Li, T.-S., 2003. An efficient synthesis of 3,4-dihydropyrimidin-2-ones catalyzed by NH2SO3H under ultrasound irradiation. Ultrason. Sonochem. 10, 119–122.

Li, J., Lou, J., Wang, Z., Wang, T., Xiao, Y., Hu, X., Liu, P., Hong, X., 2015. Design, synthesis and pharmacological evaluation of novel N-(2-(1, 1-dimethyl-5, 7-dioxo-4, 6-diazaspiro[2.4]heptan-6-yl)ethyl) sulfonamide derivatives as potential anticonvulsant agents. Eur. J. Med. Chem. 92, 370–376.

Li, S., Shen, C., Guo, W., Zhang, X., Liu, S., Liang, F., Xu, Z., Pei, Z., Song, H., Qiu, L., Lin, Y., Pang, J., 2013. Synthesis and neuroprotective action of xyloketal derivatives in Parkinson's disease models, Mar. Drugs 11, 5159-5189.

Li, W., Zhou, J., Xu, Y., 2015. Study of the in vitro cytotoxicity testing of medical devices. Biomed. Rep. 3, 617–620.

Liang, B., Wang, X., Wang, J.X., Du, Z., 2007. New three-component cyclocondensation reaction: microwave-assisted one-pot synthesis of 5-unsubstituted-3,4-dihydropyrimidin-2(1H)-ones under solvent-free conditions. Tetrahedron 63, 1981–1986.

Liao, A.-M., Wang, T., Cai, B., Jin, Y., Cheon, S., Chun, C., Wang, Z., 2017. Design, synthesis

and evaluation of 5-substituted 1-H-tetrazoles as potent anticonvulsant agents. Arch. Pharm. Res. 40, 435–443.

Lidster, K., Jefferys, J.G., Blümcke, I., Crunelli, V., Flecknell, P., Frenguelli, B.G., Gray, W.P., Kaminski, R., Pitkänen, A., Ragan, I., Shah, M., Simonato, M., Trevelyan, A., Volk, H., Walker, M., Yates, N., Prescott, M.J., 2015. Opportunities for improving animal welfare in rodent models of epilepsy and seizures. J. Neurosci. Methods 260, 2–25.

Lipinski, C.A., 2000. Drug-like properties and the causes of poor solubility and poor permeability. J. Pharmacol. Toxicol. Methods 44, 235–249.

Litvić, M., Večenaj, I., Ladišić, Z.M., Lovrić, M., Vinković, V., Filipan-Litvić, M., 2010. First application of hexaaquaaluminium (III) tetrafluoroborate as a mild, recyclable, non-hygroscopic acid catalyst in organic synthesis: a simple and efficient protocol for the multigram scale synthesis of 3,4-dihydropyrimidinones by Biginelli reaction. Tetrahedron 66, 3463–3471.

Liu, A., Huang, L., Wang, Z., Luo, Z., Mao, F., Shan, W., Xie, J., Lai, K., Li, X., 2013. Hybrids consisting of the pharmacophores of salmeterol and roflumilast or phthalazinone: dual ß$_2$-adrenoceptor agonists-PDE4 inhibitors for the treatment of COPD. Bioorg. Med. Chem. Lett. 23, 1548–1552.

Löscher, W., 2016. Fit for purpose application of currently existing animal models in the discovery of novel epilepsy therapies. Epilepsy Res. 126, 157–184.

Löscher, W., 2011. Critical review of current animal models of seizures and epilepsy used in the discovery and development of new antiepileptic drugs. Seizure 20, 359–368.

Löscher, W., Klitgaard, H., Twyman, R.E., Schmidt, D., 2013. New avenues for anti-epileptic drug discovery and development. Nat. Rev. Drug Discov. 12, 757–776.

Löscher, W., Schmidt, D., 2011. Modern antiepileptic drug development has failed to deliver: Ways out of the current dilemma. Epilepsia 52, 657–678.

Löscher, W., Schmidt, D., 2006. New horizons in the development of antiepileptic drugs: Innovative strategies. Epilepsy Res. 69, 183–272.

Łukawski, K., Gryta, P., Łuszczki, J., Czuczwar, S.J., 2016. Exploring the latest avenues for antiepileptic drug discovery and development. Expert Opin. Drug Discov. 11, 369–382.

Malik, S., Khan, S.A., 2014. Design and evaluation of new hybrid pharmacophore quinazolino-tetrazoles as anticonvulsant strategy. Med. Chem. Res. 23, 207–223.

Margineanu, D.G., 2014. Systems biology, complexity, and the impact on antiepileptic drug discovery. Epilepsy Behav. 38, 131–142.

Martínez-Jiménez, F., Marti-Renom, M.A., 2016. Should network biology be used for drug discovery? Expert Opin. Drug Discov. 11, 1135–1137.

Matias, M., Campos, G., Santos, A.O., Falcao, A., Silvestre, S., Alves, G., 2017a. Synthesis, in

vitro evaluation and QSAR modelling of potential antitumoral 3,4- dihydropyrimidin-2-(1H)-thiones. Arab. J. Chem. *In Press*.

Matias, M., Campos, G., Santos, A.O., Falcão, A., Silvestre, S., Alves, G., 2016a. Potential antitumoral 3,4-dihydropyrimidin-2-(1H)-ones: synthesis, in vitro biological evaluation and QSAR studies. RSC Adv. 6, 84943–84958.

Matias, M., Campos, G., Silvestre, S., Falcão, A., Alves, G., 2017b. Early preclinical evaluation of dihydropyrimidin(thi)ones as potential anticonvulsant drug candidates. Eur. J. Pharm. Sci. 102, 264–274.

Matias, M., Canário, C., Silvestre, S., Falcão, A., Alves, G., 2014. Cytochrome P450-mediated toxicity of therapeutic drugs, in: Cytochrome P450 Enzymes: Biochemistry, Pharmacology and Health Implications. 13–50.

Matias, M., Silvestre, S., Falcão, A., Alves, G., 2016b. Gastrodia elata and epilepsy: Rationale and therapeutic potential. Phytomedicine 23, 1511–1526.

Matias, M., Silvestre, S., Falcão, A., Alves, G., 2017c. Recent Highlights on Molecular Hybrids Potentially Useful in Central Nervous System Disorders. Mini Rev. Med. Chem. 17, 486-517.

Mayer, T.U., Kapoor, T.M., Haggarty, S.J., King, R.W., Schreiber, S.L., Mitchison, T.J., 1999. Small molecule inhibitor of mitotic spindle bipolarity identified in a phenotype-based screen. Science 286, 971–974.

McGovern, R.A., Banks, G.P., McKhann, G.M., 2016. New Techniques and Progress in Epilepsy Surgery. Curr. Neurol. Neurosci. Rep. 16, 65.

Mehta, S., Pavana, R.K., Yogeeswari, P., Sriram, D., Stables, J., 2006. Heteroaryl-substuted Semicarbazones: Synthesis and Anticonvulsant Activity of N-(3-Methylpyridin-2-yl)-substituted Semicarbazones. J. Heterocycl. Chem. 43, 1287–1293.

Meunier, B., 2008. Hybrid molecules with a dual mode of action: dream or reality? Acc. Chem. Res. 41, 69–77.

Mifsud, J., 2009. The clinical relevance of pharmacokinetics and drug interactions with anti epileptic drugs. J. Malta Coll. Pharm. Pract. 1, 23–28.

Mignani, S., Huber, S., Tomás, H., Rodrigues, J., Majoral, J.-P., 2016. Compound high-quality criteria: A new vision to guide the development of drugs, current situation. Drug Discov. Today 21, 573–584.

Milelli, A., Turrini, E., Catanzaro, E., Maffei, F., Fimognari, C., 2016. Perspectives in Designing Multifunctional Molecules in Antipsychotic Drug Discovery. Drug Dev. Res. 77, 437–443.

Mills, A.D., Yoo, C., Butler, J.D., Yang, B., Verkman, A.S., Kurth, M.J., 2010. Design and synthesis of a hybrid potentiator-corrector agonist of the cystic fibrosis mutant protein

DeltaF508-CFTR. Bioorg. Med. Chem. Lett. 20, 87–91.

Mintzer, S., French, J.A., Perucca, E., Cramer, J.A., Messenheimer, J.A., Blum, D.E., Rogawski, M.A., Baulac, M., 2015. Is a separate monotherapy indication warranted for antiepileptic drugs? Lancet Neurol. 14, 1229–1240.

Mishra, N.K., 2011. Computational modeling of P450s for toxicity prediction. Expert Opin. Drug Metab. Toxicol. 7, 1211–1231.

Miziak, B., Chroscinska-Krawczyk, M., Błaszczyk, B., Radzik, I., Czuczwar, S.J., 2012. Novel approaches to anticonvulsant drug discovery. Expert Opin. Drug Discov. 7, 417–428.

Mizoule, J., Meldrum, B., Mazadier, M., Croucher, M., Ollat, C., Uzan, A., Legrand, J.J., Gueremy, C., Le Fur, G., 1985. 2-Amino-6-trifluoromethoxy benzothiazole, a possible antagonist of excitatory amino acid neurotransmission - I. Anticonvulsant properties. Neuropharmacology 24, 767–773.

Mosmann, T., 1983. Rapid colorimetric assay for cellular growth and survival: application to proliferation and cytotoxicity assays. J. Immunol. Methods 65, 55–63.

Mozaffari, S., Ghasemi, S., Baher, H., Khademi, H., Amini, M., Sakhteman, A., Foroumadi, A., Ebrahimabadi, A.H., Sharifzadeh, M., 2012. Synthesis and evaluation of some novel methylene-bridged aryl semicarbazones as potential anticonvulsant agents. Med. Chem. Res. 21, 3797–3808.

Mula, M., 2016a. Third generation antiepileptic drug monotherapies in adults with epilepsy. Expert Rev. Neurother. 16, 1087–1092.

Mula, M., 2016b. Investigational new drugs for focal epilepsy. Expert Opin. Investig. Drugs 25, 1–5.

Mula, M., Cock, H.R., 2015. More than seizures: Improving the lives of people with refractory epilepsy. Eur. J. Neurol. 22, 24–30.

Murray, C.W., Rees, D.C., 2009. The rise of fragment-based drug discovery. Nat. Chem. 1, 187–192.

Narahari, S.R., Reguri, B.R., Gudaparthi, O., Mukkanti, K., 2012. Synthesis of dihydropyrimidinones via Biginelli multi-component reaction. Tetrahedron Lett. 53, 1543–1545.

Naven, R.T., Louise-May, S., Greene, N., 2010. The computational prediction of genotoxicity. Expert Opin. Drug Metab. Toxicol. 6, 797–807.

NICE, 2016. National Institute for Health and Care Excellence. Accessed on 23 January 2017: https://pathways.nice.org.uk/pathways/epilepsy.

Nicita, F., Spalice, A., Raucci, U., Iannetti, P., Parisi, P., 2016. The possible use of the L-type calcium channel antagonist verapamil in drug-resistant epilepsy. Expert Rev. Neurother. 16, 9–15.

Nicolaou, K.C., 2014. Advancing the drug discovery and development process. Angew. Chem. Int. Ed. Engl. 53, 9128–9140.

Nierode, G., Kwon, P.S., Dordick, J.S., Kwon, S.-J., 2016. Cell-based Assay Design for High-Content Screening of Drug Candidates. J. Microbiol. Biotechnol. 26, 213–225.

Nikalje, A.P.G., Shaikh, A.N., Shaikh, S.I., Kalam Khan, F.A., Sangshetti, J.N., Shinde, D.B., 2014. Microwave assisted synthesis and docking study of N-(2-oxo-2-(4-oxo-2-substituted thiazolidin-3ylamino)ethyl)benzamide derivatives as anticonvulsant agents. Bioorg. Med. Chem. Lett. 24, 5558–5562.

Niles, A.L., Moravec, R.A., Riss, T.L., 2008. Update on in vitro cytotoxicity assays for drug development. Expert Opin. Drug Discov. 3, 655–669.

NINDS, 2016. National Institute of Neurological Disorders and Stroke. Accessed on 3 January 2017: http://www.ninds.nih.gov/research/asp/index.htm#testing_services.

Nusrat, B., Ali, R., Siddiqui, N., Habib, A., 2014. Some heterocyclics with anticonvulsant properties. Bull. Pharm. Res. 4, 21–36.

Obniska, J., Chlebek, I., Kamiñski, K., Bojarski, A.J., Sataa, G., 2012. Synthesis, anticonvulsant activity and 5-HT1A/5-HT7 receptors affinity of 1-[(4-arylpiperazin-1-yl)-propyl]-succinimides. Pharmacol. Rep. 64, 326–335.

Obniska, J., Rapacz, A., Rybka, S., Góra, M., Kamiński, K., Sałat, K., Zmudzki, P., 2016. Synthesis, and anticonvulsant activity of new amides derived from 3-methyl- or 3-ethyl-3-methyl-2,5-dioxo-pyrrolidin-1-yl-acetic acids. Bioorg. Med. Chem. 24, 1598–1607.

Ozdemir, Z., Kandilci, H.B., Gumusel, B., Calis, U., Bilgin, A.A., 2007. Synthesis and studies on antidepressant and anticonvulsant activities of some 3-(2-furyl)-pyrazoline derivatives. Eur. J. Med. Chem. 42, 373–379.

Padala, A.K., Wani, A., Vishwakarma, R.A., Kumar, A., Bharate, S.B., 2016. Functional induction of P-glycoprotein efflux pump by phenyl benzenesulfonamides: Synthesis and biological evaluation of T0901317 analogs. Eur. J. Med. Chem. 122, 744–755.

Page, K.M., 2016. Validation of Early Human Dose Prediction: A Key Metric for Compound Progression in Drug Discovery. Mol. Pharm. 13, 609–620.

PANACHE, 2017. Models currently in active use. Acessed on 3 January 2017: https://panache.ninds.nih.gov/CurrentModels.aspx

Pandey, S., Sonar, P.K., Saraf, S.K., 2016. Synthesis and characterization of novel conjugates of 4-[3-(aryl/heteroaryl)-3-oxo-propenyl]-benzaldehyde with thiazole and thiazolidinones as possible voltage-gated sodium channel blockers. Med. Chem. Res. 25, 1484–1496.

Pandeya, S.N., Yogeeswari, P., Stables, J.P., 2000. Synthesis and anticonvulsant activity of 4-bromophenyl substituted aryl semicarbazones. Eur. J. Med. Chem. 35, 879–886.

Passeleu-Le Bourdonnec, C., Carrupt, P.-A., Scherrmann, J.M., Martel, S., 2013. Methodologies to assess drug permeation through the blood-brain barrier for pharmaceutical research. Pharm. Res. 30, 2729–2756.

Patel, H.M., Noolvi, M.N., Shirkhedkar, A., Kulkarni, A., Pardeshi, C. V., Surana, S., 2016. Anti-convulsant potential of quinazolinones. RSC Adv. 6, 44435–44455.

Patrick, G.L., 2009. An Introduction to Medicinal Chemistry, 4th ed. Oxford.

Patsalos, P.N., Perucca, E., 2003. Clinically important drug interactions in epilepsy: General features and interactions between antiepileptic drugs. Lancet Neurol. 2, 347–356.

Pavlović, D., Fajdetić, A., Mutak, S., 2010. Novel hybrids of 15-membered 8a- and 9a-azahomoerythromycin A ketolides and quinolones as potent antibacterials. Bioorg. Med. Chem. 18, 8566–8582.

Pellegatti, M., 2012. Preclinical in vivo ADME studies in drug development: a critical review. Expert Opin. Drug Metab. Toxicol. 8, 161–172.

Perucca, E., French, J., Bialer, M., 2007. Development of new antiepileptic drugs: challenges, incentives, and recent advances. Lancet Neurol. 6, 793–804.

Perucca, P., Mula, M., 2013. Antiepileptic drug effects on mood and behavior: molecular targets. Epilepsy Behav. 26, 440–449.

Pessah, N., Yagen, B., Hen, N., Shimshoni, J.A., Wlodarczyk, B., Finnell, R.H., Bialer, M., 2011. Design and pharmacological activity of glycinamide and N-methoxy amide derivatives of analogs and constitutional isomers of valproic acid. Epilepsy Behav. 22, 461–468.

Peterson, L.A., 2013. Reactive Metabolites in the Biotransformation of Molecules Containing a Furan Ring. Chem. Res. Toxicol. 26, 6–25.

Pires, D.E. V., Blundell, T.L., Ascher, D.B., 2015. pkCSM: Predicting small-molecule pharmacokinetic and toxicity properties using graph-based signatures. J. Med. Chem. 58, 4066–4072.

Potschka, H., 2012. Role of CNS efflux drug transporters in antiepileptic drug delivery: Overcoming CNS efflux drug transport. Adv. Drug Deliv. Rev. 64, 943–952.

Powell, K.L., Cain, S.M., Snutch, T.P., O'Brien, T.J., 2013. Low threshold T-type calcium channels as targets for novel epilepsy treatments. Br. J. Clin. Pharmacol. 77, 729–739.

Prashantha Kumar, B.R., Sankar, G., Nasir Baig, R.B., Chandrashekaran, S., 2009. Novel Biginelli dihydropyrimidines with potential anticancer activity: A parallel synthesis and CoMSIA study. Eur. J. Med. Chem. 44, 4192–4198.

Putatunda, S., Chakraborty, S., Ghosh, S., Nandi, P., Chakraborty, S., Sen, P.C., Chakraborty, A., 2012. Regioselective N1-alkylation of 3,4-dihydropyrimidine-2(1H)-ones: Screening of their biological activities against Ca2+-ATPase. Eur. J. Med. Chem. 54, 223–231.

Quan, Z.-J., Da, Y.-X., Zhang, Z., Wang, X.-C., 2009. PS-PEG-SO3H as an efficient catalyst for 3,4-dihydropyrimidones via Biginelli reaction. Catal. Commun. 10, 1146–1148.

Ragavendran, J.V., Sriram, D., Patel, S.K., Reddy, I.V., Bharathwajan, N., Stables, J., Yogeeswari, P., 2007. Design and synthesis of anticonvulsants from a combined phthalimide-GABA-anilide and hydrazone pharmacophore. Eur. J. Med. Chem. 42, 146–151.

Raies, A.B., Bajic, V.B., 2016. In silico toxicology: computational methods for the prediction of chemical toxicity. WIREs Comput. Mol. Sci. 6, 147–172.

Rapacz, A., Rybka, S., Obniska, J., Sałat, K., Powroźnik, B., Pękala, E., Filipek, B., 2016. Evaluation of anticonvulsant and antinociceptive properties of new N-Mannich bases derived from pyrrolidine-2,5-dione and 3-methylpyrrolidine-2,5-dione. Naunyn. Schmiedebergs. Arch. Pharmacol. 389, 339–348.

Rashid, U., Batool, I., Wadood, A., Khan, A., ul-Haq, Z., Chaudhary, M.I., Ansari, F.L., 2013. Structure based virtual screening-driven identification of monastrol as a potent urease inhibitor. J. Mol. Graph. Model. 43, 47–57.

Raub, T.J., 2006. P-glycoprotein recognition of substrates and circumvention through rational drug design. Mol. Pharm. 3, 3–25.

Reddy, V., Mahesh, M., Raju, P.V.K., Babu, T.R., Reddy, V.V.N., 2002. Zirconium (IV) chloride catalyzed one-pot synthesis of 3, 4-dihydropyrimidin-2(1H)-ones. Tetrahedron Lett. 43, 2657–2659.

Reddy, Y.T., Rajitha, B., Reddy, P.N., Kumar, B.S., Rao, V.P., 2004. Bismuth Subnitrate Catalyzed Efficient Synthesis of 3,4-Dihydropyrimidin-2(1H)-Ones: An Improved Protocol for the Biginelli Reaction. Synth. Commun. 34, 3821–3825.

Reis, J.M., Sinkó, B., Serra, C.H.R., 2010. Parallel artificial membrane permeability assay (PAMPA) - Is it better than Caco-2 for human passive permeability prediction? Mini Rev. Med. Chem. 10, 1071–1076.

Rodríguez-Domínguez, J.C., Bernardi, D., Kirsch, G., 2007. ZrCl4 or ZrOCl2 under neat conditions: optimized green alternatives for the Biginelli reaction. Tetrahedron Lett. 48, 5777–5780.

Rogawski, M.A., 2006. Molecular targets versus models for new antiepileptic drug discovery. Epilepsy Res. 68, 22–28.

Rosseto, L.A., Pires, M.E.L., Melchior, A.C.B., Bosquesi, P.L., Pavan, A.R., Marcondes, S., Chung, M.C., dos Santos, J.L., 2015. Synthesis and preliminary evaluation of N-oxide derivatives for the prevention of atherothrombotic events. Molecules 20, 18185–18200.

Rouf, A., Tanyeli, C., 2015. Bioactive thiazole and benzothiazole derivatives. Eur. J. Med. Chem. 97, 911–927.

Rowley, N.M., Madsen, K.K., Schousboe, A., Steve White, H., 2012. Glutamate and GABA synthesis, release, transport and metabolism as targets for seizure control. Neurochem. Int. 61, 546–558.

Rubio, C., Rubio-Osornio, M., Retana-Márquez, S., López, M., Custodio, V., Paz, C., 2010. In vivo experimental models of epilepsy. Cent. Nerv. Syst. Agents Med. Chem. 10, 298–309.

Ruijter, E., Scheffelaar, R., Orru, R.V.A., 2011. Multicomponent reaction design in the quest for molecular complexity and diversity. Angew. Chem. Int. Ed. Engl. 50, 6234–6246.

Russowsky, D., Canto, R.F.S., Sanches, S.A.A., D'Oca, M.G.M., de Fátima, Â., Pilli, R.A., Kohn, L.K., Antônio, M.A., de Carvalho, J.E., 2006. Synthesis and differential antiproliferative activity of Biginelli compounds against cancer cell lines: Monastrol, oxo-monastrol and oxygenated analogues. Bioorg. Chem. 34, 173–182.

Sabitha, G., Reddy, G.S.K.K., Reddy, K.B., Yadav, J.S., 2003. Vanadium (III) chloride catalyzed Biginelli condensation: Solution phase library generation of dihydropyrimidin-(2H)-ones. Tetrahedron Lett. 44, 6497–6499.

Sachdeva, H., Dwivedi, D., 2012. Lithium-acetate-mediated Biginelli one-pot multicomponent synthesis under solvent-free conditions and cytotoxic activity against the human lung cancer cell line A549 and breast cancer cell line MCF7. Sci. World J. 2012, 109432.

Sakkaki, S., Gangarossa, G., Lerat, B., Françon, D., Forichon, L., Chemin, J., Valjent, E., Lerner-Natoli, M., Lory, P., 2016. Blockade of T-type calcium channels prevents tonic-clonic seizures in a maximal electroshock seizure model. Neuropharmacology 101, 320–329.

Salim, S.D., Akamanchi, K.G., 2011. Sulfated tungstate: An alternative, eco-friendly catalyst for Biginelli reaction. Catal. Commun. 12, 1153–1156.

Salvador, J.A.R., Figueiredo, S.A.C., Pinto, R.M.A., Silvestre, S.M., 2012. Bismuth compounds in medicinal chemistry. Future Med. Chem. 4, 1495–1523.

Sams-Dodd, F., 2006. Drug discovery: selecting the optimal approach. Drug Discov. Today 11, 465–472.

Sander, J.W., 2003. The epidemiology of epilepsy revisited. Curr. Opin. Neurol. 16, 165–170.

Santos, N.C., Figueira-Coelho, J., Martins-Silva, J., Saldanha, C., 2003. Multidisciplinary utilization of dimethyl sulfoxide: pharmacological, cellular, and molecular aspects. Biochem. Pharmacol. 65, 1035–1041.

Santulli, L., Coppola, A., Balestrini, S., Striano, S., 2016. The challenges of treating epilepsy with 25 antiepileptic drugs. Pharmacol. Res. 107, 211–219.

Sarkisian, M.R., 2001. Overview of the Current Animal Models for Human Seizure and Epileptic Disorders. Epilepsy Behav. 2, 201–216.

Sashidhara, K. V., Modukuri, R.K., Choudhary, D., Bhaskara Rao, K., Kumar, M., Khedgikar,

V., Trivedi, R., 2013. Synthesis and evaluation of new coumarin-pyridine hybrids with promising anti-osteoporotic activities. Eur. J. Med. Chem. 70, 802–810.

Schnell, B., Krenn, W., Faber, K., Kappe, C.O., 2000. Synthesis and reactions of Biginelli-compounds. Part 23. Chemoenzymatic syntheses of enantiomerically pure 4-aryl-3,4-dihydropyrimidin-2(1H)-ones. J. Chem. Soc., Perkin Trans. 1 2, 4382–4389.

Schulze-Bonhage, A., 2013. Pharmacokinetic and pharmacodynamic profile of pregabalin and its role in the treatment of epilepsy. Expert Opin. Drug Metab. Toxicol. 9, 105–115.

Shanmugam, P., Boobalan, P., Perumal, P.T., 2007. A novel method for the synthesis of highly functionalized 3,4-dihydropyrimidin-2(1H)-ones through the 1,4-addition on pyrimidin-2(1H)-ones. Tetrahedron 63, 12215–12219.

Shekh-Ahmad, T., Bialer, M., Yavin, E., 2012. Synthesis and anticonvulsant evaluation of dimethylethanolamine analogues of valproic acid and its tetramethylcyclopropyl analogue. Epilepsy Res. 98, 238–246.

Shetty, A.K., Upadhya, D., 2016. GABA-ergic cell therapy for epilepsy: Advances, limitations and challenges. Neurosci. Biobehav. Rev. 62, 35–47.

Shillingford, C.A., Vose, C.W., 2001. Effective decision-making: Progressing compounds through clinical development. Drug Discov. Today 6, 941–946.

Siddiqui, N., Akhtar, M.J., Yar, M.S., Ahuja, P., Ahsan, W., Ahmed, S., 2014. Substituted phenyl containing 1,3,4-oxadiazole-2-yl-but-2-enamides: Synthesis and preliminary evaluation as promising anticonvulsants. Med. Chem. Res. 23, 4915–4925.

Silva, R., Vilas-Boas, V., Carmo, H., Dinis-Oliveira, R.J., Carvalho, F., De Lourdes Bastos, M., Remião, F., 2015. Modulation of P-glycoprotein efflux pump: Induction and activation as a therapeutic strategy. Pharmacol. Ther. 149, 1–123.

Simonato, M., Brooks-Kayal, A.R., Engel Jr, J., Galanopoulou, A.S., Jensen, F.E., Moshé, S.L., O'Brien, T.J., Pitkanen, A., Wilcox, K.S., French, J.A., 2014. The challenge and promise of anti-epileptic therapy development in animal models. Lancet Neurol. 13, 949–960.

Simonato, M., French, J.A., Galanopoulou, A.S., O'Brien, T.J., 2013. Issues for new antiepilepsy drug development. Curr. Opin. Neurol. 26, 195–200.

Simonato, M., Löscher, W., Cole, A.J., Dudek, F.E., Engel Jr, J., Kaminski, R.M., Loeb, J.A., Scharfman, H., Staley, K.J., Velisek, L., Klitgaard, H., 2012. Finding a better drug for epilepsy: Preclinical screening strategies and experimental trial design. Epilepsia 53, 1860–1867.

Singh, K., Arora, D., Poremsky, E., Lowery, J., Moreland, R.S., 2009. N1-Alkylated 3,4-dihydropyrimidine-2(1H)-ones: Convenient one-pot selective synthesis and evaluation of their calcium channel blocking activity. Eur. J. Med. Chem. 44, 1997–2001.

Singh, K., Singh, K., Trappanese, D.M., Moreland, R.S., 2012. Highly regioselective synthesis

of N-3 organophosphorous derivatives of 3,4-dihydropyrimidin-2(1H)-ones and their calcium channel binding studies. Eur. J. Med. Chem. 54, 397–402.

Singh, M., Kaur, M., Chadha, N., Silakari, O., 2015. Hybrids: a new paradigm to treat Alzheimer's disease. Mol. Divers. 20, 271–297.

Sjöstedt, N., Kortejärvi, H., Kidron, H., Vellonen, K.S., Urtti, A., Yliperttula, M., 2014. Challenges of using in vitro data for modeling P-glycoprotein efflux in the blood-brain barrier. Pharm. Res. 31, 1–19.

SLAS, 2016. Society for Laboratory Automation and Screening. Accessed on 20 December 2017: https://www.slas.org/resources/information/academic-screening-facilities/

Smith, M., Wilcox, K.S., White, H.S., 2007. Discovery of Antiepileptic Drugs. Neurotherapeutics 4, 12–17.

Sośnicki, J.G., Struk, Ł., Kurzawski, M., Perużyńska, M., Maciejewska, G., Droździk, M., 2014. Regioselective synthesis of novel 4,5-diaryl functionalized 3,4-dihydropyrimidine-2(1H)-thiones via a non-Biginelli-type approach and evaluation of their in vitro anticancer activity. Org. Biomol. Chem. 12, 3427.

Stadler, A., Kappe, C.O., 2001. Automated library generation using sequential microwave-assisted chemistry. Application toward the Biginelli multicomponent condensation. J. Comb. Chem. 3, 624–630.

Stegemann, S., Leveiller, F., Franchi, D., de Jong, H., Lindén, H., 2007. When poor solubility becomes an issue: From early stage to proof of concept. Eur. J. Pharm. Sci. 31, 249–261.

Stępień, K.M., Tomaszewski, M., Tomaszewska, J., Czuczwar, S.J., 2012. The multidrug transporter P-glycoprotein in pharmacoresistance to antiepileptic drugs. Pharmacol. Rep. 64, 1011–1019.

Sucher, N.J., Carles, M.C., 2015. A pharmacological basis of herbal medicines for epilepsy. Epilepsy Behav. 52, 308–318.

Suresh, Sandhu, J.S., 2012. Past, present and future of the Biginelli reaction: a critical perspective. Arkivoc 2012, 66–133.

Talevi, A., 2016. Computational approaches for innovative antiepileptic drug discovery. Expert Opin. Drug Discov. 11, 1001–1016.

Tamimi, N.A.M., Ellis, P., 2009. Drug development: From concept to marketing! Nephron. Clin. Pr. 113, 125–131.

Tatum, W.O., 2013. Recent and emerging anti-seizure drugs: 2013. Curr. Treat. Options Neurol. 15, 505–518.

Taylor, A.P., Robinson, R.P., Fobian, Y.M., Blakemore, D.C., Jones, L.H., Fadeyi, O., 2016. Modern advances in heterocyclic chemistry in drug discovery. Org. Biomol. Chem. 14, 6611–6637.

Tetko, I. V., Gasteiger, J., Todeschini, R., Mauri, A., Livingstone, D., Ertl, P., Palyulin, V.A., Radchenko, E. V., Zefirov, N.S., Makarenko, A.S., Tanchuk, V.Y., Prokopenko, V. V., 2005. Virtual computational chemistry laboratory - design and description. J. Comput. Aided Mol. Des. 19, 453–463.

Thackaberry, E.A., Wang, X., Schweiger, M., Messick, K., Valle, N., Dean, B., Sambrone, A., Bowman, T., Xie, M., 2014. Solvent-based formulations for intravenous mouse pharmacokinetic studies: tolerability and recommended solvent dose limits. Xenobiotica 44, 235–241.

Theoduloz, C., Bravo, I., Pertino, M.W., Schmeda-Hirschmann, G., 2013. Diterpenylquinone hybrids: synthesis and assessment of gastroprotective mechanisms of action in human cells. Molecules 18, 11044–11066.

Thore, S.N., Gupta, S. V., Baheti, K.G., 2015. Synthesis and Pharmacological Evaluation of Novel Triazolo [4,3-a] tetrahydrobenzo(b)thieno [3,2-e] pyrimidine-5(4H)-ones. J. Heterocycl. Chem. 52, 142–149.

Thurman, D.J., Beghi, E., Begley, C.E., Berg, A.T., Buchhalter, J.R., Ding, D., Hesdorffer, D.C., Hauser, W.A., Kazis, L., Kobau, R., Kroner, B., Labiner, D., Liow, K., Logroscino, G., Medina, M.T., Newton, C.R., Parko, K., Paschal, A., Preux, P.-M., Sander, J.W., Selassie, A., Theodore, W., Tomson, T., Wiebe, S., 2011. Standards for epidemiologic studies and surveillance of epilepsy. Epilepsia 52, 2–26.

Torregrosa, R., Yang, X.-F., Dustrude, E.T., Cummins, T.R., Khanna, R., Kohn, H., 2015. Chimeric derivatives of functionalized amino acids and a-aminoamides: Compounds with anticonvulsant activity in seizure models and inhibitory actions on central, peripheral, and cardiac isoforms of voltage-gated sodium channels. Bioorg. Med. Chem. 23, 3655–3666.

Touré, B.B., Hall, D.G., 2009. Natural Product Synthesis Using Multicomponent Reaction Strategies. Chem. Rev. 109, 4439–4486.

Tripathi, L., Kumar, P., Singh, R., Stables, J.P., 2012. Design, synthesis and anticonvulsant evaluation of novel N-(4-substituted phenyl)-2-[4-(substituted) benzylidene]-hydrazinecarbothio amides. Eur. J. Med. Chem. 47, 153–166.

Vafaeezadeh, M., Hashemi, M.M., 2015. Polyethylene glycol (PEG) as a green solvent for carbon-carbon bond formation reactions. J. Mol. Liq. 207, 73–79.

Vajda, F.J.E., Eadie, M.J., 2014. The clinical pharmacology of traditional antiepileptic drugs. Epileptic Disord. 16, 395–408.

Val, C., Crespo, A., Yaziji, V., Coelho, A., Azuaje, J., El Maatougui, A., Carbajales, C., Sotelo, E., 2013. Three-Component Assembly of Structurally Diverse 2-Aminopyrimidine-5-carbonitriles. ACS Comb. Sci. 15, 370–378.

Van de Waterbeemd, H., Camenisch, G., Folkers, G., Chretien, J.R., Raevsky, O.A., 1998.

Estimation of blood-brain barrier crossing of drugs using molecular size and shape, and H-bonding descriptors. J. Drug Target. 6, 151–165.

Varvel, N.H., Jiang, J., Dingledine, R., 2015. Candidate Drug Targets for Prevention or Modification of Epilepsy. Annu. Rev. Pharmacol. Toxicol. 55, 229–247.

Veber, D.F., Johnson, S.R., Cheng, H.-Y., Smith, B.R., Ward, K.W., Kopple, K.D., 2002. Molecular Properties That Influence the Oral Bioavailability of Drug Candidates. J. Med. Chem. 45, 2615–2623.

Verrotti, A., Prezioso, G., Stagi, S., Paolino, M.C., Parisi, P., 2016. Pharmacological considerations in the use of stiripentol for the treatment of epilepsy. Expert Opin. Drug Metab. Toxicol. 12, 345–352.

Villalba, M.L., Enrique, A. V., Higgs, J., Castaño, R.A., Goicoechea, S., Taborda, F.D., Gavernet, L., Lick, I.D., Marder, M., Bruno Blanch, L.E., 2016. Novel sulfamides and sulfamates derived from amino esters: Synthetic studies and anticonvulsant activity. Eur. J. Pharmacol. 774, 55–63.

Walker, L.E., Mirza, N., Yip, V.L.M., Marson, A.G., Pirmohamed, M., 2015. Personalized medicine approaches in epilepsy. J. Intern. Med. 277, 218–234.

Walsh, J.S., Miwa, G.T., 2011. Bioactivation of drugs: risk and drug design. Annu. Rev. Pharmacol. Toxicol. 51, 145–167.

Wan, H., 2013. What ADME tests should be conducted for preclinical studies? ADMET DMPK 1, 19–28.

Wang, G.-X., Wang, D.-W., Liu, Y., Ma, Y.-H., 2016. Intractable epilepsy and the P-glycoprotein hypothesis. Int. J. Neurosci. 126, 385–392.

Wang, S.-B., Deng, X.-Q., Liu, D.-C., Zhang, H.-J., Quan, Z.-S., 2014. Synthesis and evaluation of anticonvulsant and antidepressant activities of 7-alkyl-7H-tetrazolo[1,5-g]purine derivatives. Med. Chem. Res. 23, 4619–4626.

Wang, X., Cattaneo, F., Ryno, L., Hulleman, J., Reixach, N., Buxbaum, J.N., 2014. The systemic amyloid precursor transthyretin (TTR) behaves as a neuronal stress protein regulated by HSF1 in SH-SY5Y human neuroblastoma cells and APP23 Alzheimer's disease model mice. J. Neurosci. 34, 7253–7765.

Wang, Y., Xing, J., Xu, Y., Zhou, N., Peng, J., Xiong, Z., Liu, X., Luo, X., Luo, C., Chen, K., Zheng, M., Jiang, H., 2015. In silico ADME/T modelling for rational drug design. Q. Rev. Biophys. 48, 488–515.

Wang, Z.-T., Xu, L.-W., Xia, C.-G., Wang, H.-Q., 2004. Novel Biginelli-like three-component cyclocondensation reaction: Efficient synthesis of 5-unsubstituted 3,4-dihydropyrimidin-2(1H)-ones. Tetrahedron Lett. 45, 7951–7953.

Weaver, D.F., 2013. Design of innovative therapeutics for pharmacoresistant epilepsy:

challenges and needs. Epilepsia 54, 56–59.

Wei, C.-X., Bian, M., Gong, G.-H., 2015. Current Research on Antiepileptic Compounds. Molecules 20, 20741–20776.

Wells B.G.; Dipiro J.T.; Schwinghammer T.L.; Dipiro C.V., 2009, 7th Ed. Pharmacotherapy handbook. MC Graw Hill Medical, US.

White, H.S., Smith, M.D., Wilcox, K.S., 2007. Mechanisms of Action of Antiepileptic Drugs. Int. Rev. Neurobiol. 81, 85–110.

Williams, C.T., 2016. Food and Drug Administration Drug Approval Process. A History and Overview. Nurs. Clin. North Am. 51, 1–11.

Williams, M., 2011. Qualitative pharmacology in a quantitative world: Diminishing value in the drug discovery process. Curr. Opin. Pharmacol. 11, 496–500.

Wilson, J.R., Fehlings, M.G., 2014. Riluzole for acute traumatic spinal cord injury: A promising neuroprotective treatment strategy. World Neurosurg. 81, 825–829.

Wu, Y., Pan, M., Dai, Y., Liu, B., Cui, J., Shi, W., Qiu, Q., Huang, W., Qian, H., 2016. Design, synthesis and biological evaluation of LBM-A5 derivatives as potent P-glycoprotein-mediated multidrug resistance inhibitors. Bioorg. Med. Chem. 24, 2287–2297.

Yang, H.N., Park, J.S., Jeon, S.Y., Park, K.H., 2015. Carboxymethylcellulose (CMC) formed nanogels with branched poly(ethyleneimine) (bPEI) for inhibition of cytotoxicity in human MSCs as a gene delivery vehicles. Carbohydr. Polym. 122, 265–275.

Yasam, V.R., Jakki, S.L., Senthil, V., Eswaramoorthy, M., Shanmuganathan, S., Arjunan, K., Nanjan, M.J., 2016. A pharmacological overview of lamotrigine for the treatment of epilepsy. Expert Rev. Clin. Pharmacol. 9, 1533–1546.

Yogeeswari, P., Sriram, D., Sahitya, P., Ragavendran, J.V., Ranganadh, V., 2007. Synthesis and anticonvulsant activity of 4-(2-(2,6-dimethylphenylamino)-2-oxoethylamino)-N-(substituted)butanamides: a pharmacophoric hybrid approach. Bioorg. Med. Chem. Lett. 17, 3712–3715.

Yoo, Y.J., Nam, D.H., Jung, S.Y., Jang, J.W., Kim, H.J., Jin, C., Pae, A.N., Lee, Y.S., 2011. Synthesis of cinnamoyl ketoamides as hybrid structures of antioxidants and calpain inhibitors. Bioorg. Med. Chem. Lett. 21, 2850–2854.

Yuan, C., Gao, J., Guo, J., Bai, L., Marshall, C., Cai, Z., Wang, L., Xiao, M., 2014. Dimethyl sulfoxide damages mitochondrial integrity and membrane potential in cultured astrocytes. PLoS One 9, e107447.

Zaccara, G., Schmidt, D., 2016. Do traditional anti-seizure drugs have a future? A review of potential anti-seizure drugs in clinical development. Pharmacol. Res. 104, 38–48.

Zakeri-Milani, P., Valizadeh, H., 2014. Intestinal transporters: enhanced absorption through P-glycoprotein-related drug interactions. Expert Opin. Drug Metab. Toxicol. 10, 859–871.

Zanni, R., Galvez-Llompart, M., García-Domenech, R., Galvez, J., 2015. Latest advances in molecular topology applications for drug discovery. Expert Opin. Drug Discov. 10, 945–957.

Zar, T., Graeber, C., Perazella, M.A., 2007. Recognition, treatment, and prevention of propylene glycol toxicity. Semin. Dial. 20, 217–219.

Zeng, Z.-S., He, Q.-Q., Liang, Y.-H., Feng, X.-Q., Chen, F.-E., De Clercq, E., Balzarini, J., Pannecouque, C., 2010. Hybrid diarylbenzopyrimidine non-nucleoside reverse transcriptase inhibitors as promising new leads for improved anti-HIV-1 chemotherapy. Bioorg. Med. Chem. 18, 5039–5047.

Zhang, C., Kwan, P., Zuo, Z., Baum, L., 2012. The transport of antiepileptic drugs by P-glycoprotein. Adv. Drug Deliv. Rev. 64, 930–942.

Zhang, L.-M., Zhao, N., Guo, W.-Z., Jin, Z.-L., Qiu, Z.-K., Chen, H.-X., Xue, R., Zhang, Y.-Z., Yang, R.-F., Li, Y.-F., 2014. Antidepressant-like and anxiolytic-like effects of YL-IPA08, a potent ligand for the translocator protein (18 kDa). Neuropharmacology 81, 116–125.

Zhao, Y., Abraham, M., Le, J., Hersey, A., Luscombe, C., Beck, G., Sherbone, B., Cooper, I., 2002. Rate-limited steps of human oral absorption and QSAR studies. Pharm. Res. 19, 1446–1457.

Zhou, W., Wang, Y., Lu, A., Zhang, G., 2016. Systems Pharmacology in Small Molecular Drug Discovery. Int. J. Mol. Sci. 17, 246.

APPENDICES

APPENDIX A

A.1. Optimization of the Biginelli reaction

Previously to the final protocol used to synthesize the compounds, the procedure was partially optimized. In Tables A.1 (solvent-free) and A.2 (use of solvent) are specified the main conditions studied.

Table A.1 – Reactional conditions (solvent-free) during the initial partial optimization of the Biginelli reaction.

Compound	Reagents	Specific conditions	Time	Yield (%)
Urea series				
MM 10	Benzaldehyde Acetylacetone	Catalyst: $Bi(NO_3)_3.5H_2O$ (10 mol%), 70 ºC extraction with dichlorometane (without recrystallization)	26 min	68[a]
MM 12	Benzaldehyde Acetylacetone	Without catalyst, room temperature, extraction with ethyl acetate (without recrystallization)	193 min	-
MM 13	Benzaldehyde Acetylacetone	Without catalyst, 70 ºC, extraction with ethyl acetate (without recrystallization)	40 min	-
MM 14	Benzaldehyde Acetylacetone	Catalyst: $Bi(NO_3)_3.5H_2O$ (10 mol%), room temperature, extraction with ethyl acetate (without recrystallization)	90 min	-
MM 16	Benzaldehyde Acetylacetone	Catalyst: $Bi(NO_3)_3.5H_2O$ (10 mol%), 45 ºC, extraction with ethyl acetate (without recrystallization)	30 min	55
MM 17	Benzaldehyde Acetylacetone	Catalyst: $Bi(NO_3)_3.5H_2O$ (10 mol%), 70 ºC wash with cold water followed by recrystallization	6 min	93
MM 11	Benzaldehyde Ethyl acetoacetate	Catalyst: $Bi(NO_3)_3.5H_2O$ (10 mol%), 70 ºC extraction with ethyl acetate (without recrystallization)	15 min	67
MM 18	Benzaldehyde Ethyl acetoacetate	Catalyst: $Bi(NO_3)_3.5H_2O$ (10 mol%), 70 ºC wash with cold water followed by recrystallization	7 min	81
Thiourea series				
MM 20	Benzaldehyde Acetylacetone	Catalyst: $Bi(NO_3)_3.5H_2O$ (10 mol%), 70 ºC, extraction with ethyl acetate (without recrystallization)	24 h	-
MM 25	Benzaldehyde Acetylacetone	Catalyst: $ZrCl_4$ (5 mol%), 70 ºC wash with cold water followed by recrystallization	8 min	80
MM 21	Benzaldehyde Ethyl acetoacetate	Catalyst: $Bi(NO_3)_3.5H_2O$ (10 mol%), 70 ºC, extraction with ethyl acetate (without recrystallization)	62 h	-
MM 26	Benzaldehyde Ethyl acetoacetate	$ZrCl_4$ (5 mol%), 70 ºC, wash with cold water followed by recrystallization	14 min	70

[a]yield = 41% with recrystallization

Regarding the work up, the extraction with organic solvents such as ethyl acetate and dichloromethane (compounds **MM 10**, **MM 11** and **MM 16**) did not show benefits comparatively to the work up described in the experimental section of the Chapter II (compounds **MM 17**,

MM 18, **MM 25** and **MM 26**) as it was proved by the yields obtained. However, when the compounds were extracted with organic solvents, the recrystallization step did not seem crucial for purification as observed in ^{1}H-nuclear magnetic resonance spectra (NMR).

In the cases of the reactions carried out at room temperature (compounds **MM 12** and **MM 14**) or without catalyst (compounds **MM 12** and **MM 13**), the final product was an oil and the ^{1}H-NMR spectra were inconclusive, which suggests the importance of the temperature and the use of catalyst.

Regarding the thiourea series, in solvent-free conditions (Table A.1), the compounds were not successfully synthesized using $Bi(NO_3)_3.5H_2O$ as catalyst (compounds **MM 20** and **MM 21**). However, using zirconium tetrachloride ($ZrCl_4$) as catalyst the reaction was successful, as observed by NMR data. With regard to the use of solvent, in the case of this series, it was tested the use of ethanol 99.9%, particularly to afford the products with a nitro group attached to the aromatic ring because previous experiments were unsuccessful (solvent-free conditions). However, all these trials have failed. Moreover, using 2,3-dichlorobenzaldehyde as starting material, it was tested the reaction in a microwaves with and without solvent (ethanol). The reactions irradiated with microwaves were carried out using a single reactor (monomode) of the microwave apparatus (Milestone® MultiSYNTH), which consists of a system of continuous release of focused microwaves energy. All reactions were performed in sealed glass tubes (10 ml) and the temperature was controlled inside the reaction tube and in the surrounding environment. Using a maximum power of 250 W, the reaction mixture was irradiated for 15 minutes, ramp heating from room temperature to 120 ºC for 5 minutes, and then mantainedat this temperature for 10 minutes, followed by cooling. In these reactions, the NMR spectra showed much more impurities than the spectra of the same compounds obtained through the traditional procedure.

Table A.2 – Reactional conditions, using solvent, during the initial partial optimization of the Biginelli reaction for urea series.

Compound	Reagents	Solvent	Specific conditions	Time (h)	Yield (%)
MM 15	Benzaldehyde Acetylacetone	Acetonitrile	Catalyst: $Bi(NO_3)_3.5H_2O$ (5 mol%), 70 ºC, extraction with ethyl acetate (without recrystallization)	24	-
MM 39	Benzaldehyde Ethyl acetoacetate	Ethanol	Catalyst: $ZrCl_4$ (5 mol%), 80-90 ºC, wash with cold water followed by recrystallization	41	51
MM 47	Benzaldehyde Ethyl acetoacetate	Ethanol	Catalyst: $ZrCl_4$ (10 mol%), 80-90 ºC, wash with cold water followed by recrystallization	49	53
MM 42	*p*-Tolualdehyde Acetylacetone	Ethanol	Catalyst: $ZrCl_4$ (10 mol%), 80-90 ºC, wash with cold water followed by recrystallization	22	-
MM 49	*p*-Tolualdehyde Ethyl acetoacetate	Ethanol	Catalyst: $ZrCl_4$ (10 mol%), 80-90 ºC, wash with cold water followed by recrystallization	72	39
MM 43	4-Nitrobenzaldehyde Ethyl acetoacetate	Ethanol	Catalyst: $ZrCl_4$ (10 mol%), 80-90 ºC, wash with cold water followed by recrystallization	21	36
MM 44	4-Nitrobenzaldehyde Acetylacetone	Ethanol	Catalyst: $ZrCl_4$ (10 mol%), 80-90 ºC, wash with cold water followed by recrystallization	73	-
MM 45	2,3-Dichlorobenzaldehyde Ethyl acetoacetate	Ethanol	Catalyst: $ZrCl_4$ (10 mol%), 80-90 ºC, wash with cold water followed by recrystallization	25	28
MM 110	2,3-Dichlorobenzaldehyde Methyl acetoacetate	Ethanol	Catalyst: $ZrCl_4$ (10 mol%), 80-90 ºC, wash with cold water followed by recrystallization	26	-
MM 112	2,3-Dichlorobenzaldehyde Acetylacetone	Ethanol	Catalyst: $ZrCl_4$ (10 mol%), 80-90 ºC, wash with cold water followed by recrystallization	84	37
MM 114	2,4-Dichlorobenzaldehyde Methyl acetoacetate	Ethanol	Catalyst: $ZrCl_4$ (10 mol%), 80-90 ºC, wash with cold water followed by recrystallization	60	45
MM 50	Anisaldehyde Acetylacetone	Ethanol	Catalyst: $ZrCl_4$ (10 mol%), 80-90 ºC, wash with cold water followed by recrystallization	47	-

The Biginelli reaction was also carried out using acetonitrile as solvent as reported by Chari and collaborators (Chari et al., 2005) for urea series, employing the same catalyst (Table A.2). However, as ^{1}H-NMR spectrum was inconclusive, another solvent (ethanol) was tried. Following the procedure described in the experimental section of the Chapter II ("*Alternative procedure for chlorinated compounds for urea series*"), several compounds listed in Table A.2

were synthesized. Comparing with the reactions performed without solvent, in this case, the reactions were longer (21-84 h) and the yields were slightly lower. It was also verified that the different amounts of the catalyst employed ($ZrCl_4$, 5 mol% and 10 mol%) did not markedly affect the yields (compounds **MM 39** and **MM 47**).

Surprisingly, in some cases (compounds **MM 42**, **MM 44**, **MM 50** and **MM 110**), compounds that were not structurally related, were not synthesized with success as demonstrated by NMR spectra, which were inconclusive or exhibited many impurities.

On the other hand, it should be highlighted that the use of solvent (ethanol) was employed to obtain chlorinated compounds of the urea series when large quantities were needed to perform the *in vivo* experiments and in the cases that little impurities were demonstrated in NMR spectra after the compounds had been produced by the general procedure.

A.2. References

Chari, M.A., Shobha, D., Kumar, T.K., Dubey, P.K., 2005. Bismuth (III) nitrate catalyzed one-pot synthesis of 3,4-dihydro-pyrimidin-2-(1H)-ones: an improved protocol for the Biginelli reaction. Arkivoc 2005, 74–80.

APPENDIX B

B.1. Synthesis of molecular hybrids of lamotrigine and GABAergic compounds

B.1.1. Synthesis of lamotrigine-aminoacids

Taking into consideration the design and preparation of molecular hybrids as an encouraging research field in the development of new antiepileptic drug candidates, we aimed to synthesize hybrid molecules combining lamotrigine, a voltage-dependent sodium channel blocker, with linear [γ-aminobutyric-acid (GABA)] and cyclic (isonipecotic acid) GABAergic compounds. In order to prepare lamotrigine–GABAergic compounds, the simplest synthetic strategy was applied as it is described below.

B.1.1.1. Experimental section

Synthesis of protected aminoacids: To a mixture of an aminoacid [isonipecotic acid (Acros Organics, New Jersey, USA) or GABA (Sigma-Aldrich, St. Louis, MO, USA] (1 mmol), and di-*tert*-butyl dicarbonate (Boc_2O, Acros Organics, New Jersey, USA, 1.2 mmol) was added finely grinded $Bi(NO_3)_3.5H_2O$ (5 mol%) and the reaction was stirred at room temperature for an appropriate period of time, using methanol as solvent (Table B.1). After completion of the reaction as monitored by thin layer chromatography (TLC), water (10 mL) was added to the reaction mixture and the product was extracted with ethyl acetate (3 x 20 mL). The combined organic layer was washed with brine, dried with anhydrous sodium sulphate and concentrated in vacuum to give the product which was then characterised by ^{1}H- and ^{13}C-nuclear magnetic resonance (NMR).

1-(*tert*-butoxycarbonyl)piperidine-4-carboxylic acid (compound **MM 1**) (Winkler et al., 2007). White powder, yield: 88%, ^{1}H-NMR (400 MHz, $CDCl_3$) δ: 1.45 (s, 9H), 1.57-1.67 (m, 2H), 1.86-1.91 (m, 2H), 2.43-2.51 (m, 1H), 2.80-2.87 (m, 2H), 4.00 (d, *J* = 13.06, 2H); ^{13}C-NMR (100 MHz, $CDCl_3$) δ: 27.73, 28.42, 40.77, 42.96, 79.76, 154.75, 179.96.

4-((*tert*-butoxycarbonyl)amino)butanoic acid (compound **MM 2**) (Ceruso et al., 2014). Colourless oil, yield: 86%, ^{1}H-NMR (400 MHz, $CDCl_3$) δ: 1.33 (s, 9H), 1.67-1.74 (m, 2H), 2.273 (t, *J* = 7.25, 2H), 3.01-3.07 (m, 2H), 8.97 (brs, 1H); ^{13}C-NMR (100 MHz, $CDCl_3$) δ: 25.11, 28.38, 31.32, 39.82, 79.46, 156.41, 177.81.

Synthesis of lamotrigine-protected aminoacids: Lamotrigine (0.25 mmol) was dissolved in 10 mL of dry dichloromethane (DCM), followed by addition of the protected aminoacid (0.25 mmol) and *N*,*N*'-dicyclohexylcarbodiimide (DCC; Acros Organics, New Jersey, USA; 0.25 mmol). The reaction mixture was stirred at room temperature for 24 h, being followed by TLC. Afterwards, the reaction mixture was filtered and the product was extracted with DCM (3 x 60 mL). The combined organic layer was washed with brine, dried with anhydrous sodium

sulphate and then concentrated in vacuum. The product was chromatographed through silica gel (0.060-0.200 mm) using ethyl acetate:petroleum ether (5:1) as eluent, aiming to obtain the pure products that were characterised by ^{1}H- and ^{13}C-NMR.

B.1.1.2. Results and discussion

The synthesis of lamotrigine–aminoacids (isonipecotic acid and GABA) was started with the protection of the amine group of the referred aminoacids with Boc. This procedure was based on the work of Suryakiran and collaborators (Suryakiran et al., 2006) and, as demonstrated by NMR spectra, the products were successfully synthesized and with good yields (Table B.1).

Table B.1 – Step of protection of aminoacids with Boc_2O at room temperature, catalysed by $Bi(NO_3)_3.5H_2O$.

Product	Time (h)	Yield (%)
Boc-isonipecotic acid	4	88
Boc-GABA	7	86

Then, the reaction of these *N*-protected compounds with lamotrigine was performed by using DCC as coupling agent, based on the reported by Kamal *et al*. (Kamal et al., 2003). Analysing the structures and expected chemical reactivity of the involved compounds, it was anticipated that the desired products could be prepared by a coupling reaction involving the 3-amine group of the 3,5-diaminetriazine moiety of lamotrigine and the activated carboxylic acid group of the compound that would be introduced. In fact, the study carried out by Edmeades *et al*. supported this reactivity, describing a procedure to prepare *N*-[5-amino-6-(2,3-dichlorophenyl)-1,2,4-triazine-3-yl]-2,3-dichlorobenzamide by the direct reaction of lamotrigine and 2,3-dichlorobenzoyl chloride in pyridine (Edmeades et al., 2002). In this context, in synthesis proposed by us, the major products expected were the 3-acylated-lamotrigine derivatives (Products 1.1 and 2.1, Figure B.1, Panel A and B, respectively), probably due to steric effects.

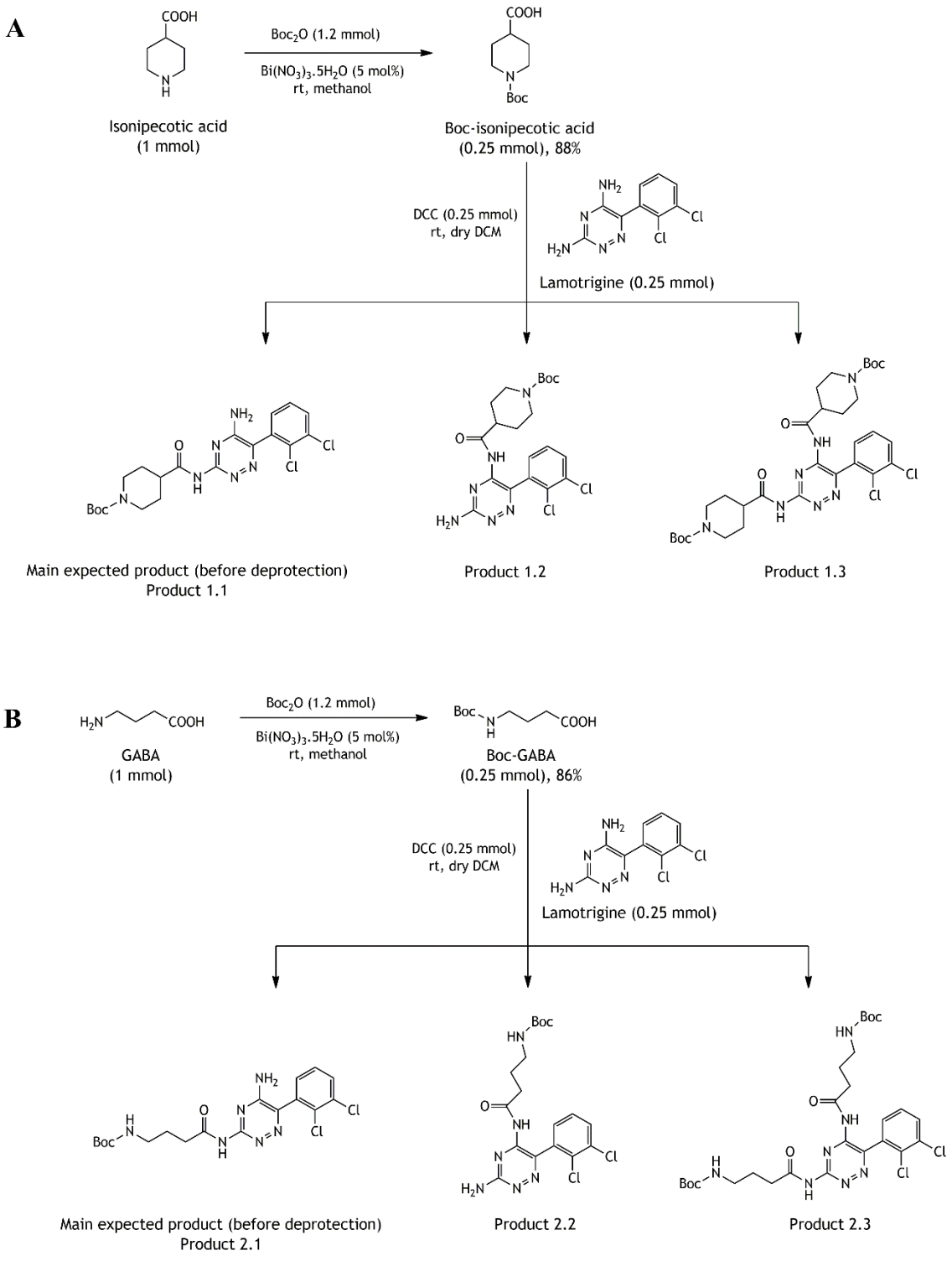

Figure B.1 – Schematic reaction of the protection of the aminoacids with the Boc_2O and, after, the step of synthesis of the molecular hybrids combining lamotrigine with the protected GABAergic compounds: **A** – cyclic aminoacid, isonipecotic acid; **B** – linear aminoacid, GABA.

However, the other mono- (Products 1.2 and 2.2, Figure B.1, Panel A and B, respectively) and also the diacylated (Products 1.3 and 2.3, Figure B.1, Panel A and B, respectively) compounds possibly were also produced in similar quantities than the Products 1.1 and 2.1, as suggested

by NMR data. Different conditions were employed, such as different temperatures and reaction times (17 h – 4 days), and the changes of eluents introduced in the chromatographic column with or without gradient [e.g. ethyl acetate:methanol (15:1), DCM:acetone (3:1)] intending to isolate the products produced. However, the reactions were not completed under any of the conditions tested, and thus the amount of the isolated products was so small, which became unfeasible their characterisation using the standard NMR techniques.

Overall, the next experiments were carried out in order to understand the chemical reactivity of lamotrigine through reactions of acylation.

B.1.2. Studies on the acylation of lamotrigine

As referred, aiming to better understand the chemical reactivity of lamotrigine, different reactions were carried out, namely its acylation with acyl chlorides possessing different sizes, such as acetyl chloride and palmitoyl chloride and interesting functional groups like *p*-toluene sulfonyl chloride.

B.1.2.1. Experimental section

Lamotrigine acylation: Triethylamine (TEA, 66 µL; Fisher Scientific, New Hampshire, USA) was added to a suspension of lamotrigine (0.25 mmol) in dry DCM at a temperature of 0-5 ºC. Afterwards, an excess of acyl chloride (0.30 mmol) in DCM was slowly added and the reaction mixture was heated to 25-30 ºC, being monitored by TLC. The work up was performed extracting the products with DCM, drying with anhydrous sodium sulphate and concentrating in vacuum. Subsequently, the products were introduced in a chromatographic column (silica gel), eluting with a gradient of ethyl acetate and petroleum ether.

B.1.2.2. Results and discussion

The proposed structural modifications were conducted accordingly to the procedure reported by Rao and collaborators (Rao et al., 2012), who described the selective acylation of lamotrigine with 2,3-dichlorobenzoyl chloride. For this reason, the procedure was adapted for different acyl chlorides (Figure B.2). Taking into account the long chain of palmitoyl chloride or the bulky *p*-toluene sulfonyl chloride, it was expected the production of an isolated product due to the steric hindrance, contrarily to the products obtained with acetyl chloride, which is a much smaller group. However, similarly to the reactions between lamotrigine and the *N*-protected aminoacids (section B.1.1.), the NMR spectra indicated that probably a mixture of three possible products was obtained for the products linking the acetyl and palmitoyl chlorides to lamotrigine. Regarding the product(s) obtained using the *p*-toluene

sulfonyl chloride, the NMR spectra were inconclusive. Given these results, other options were considered in order to produce compounds with anticonvulsant potential and structurally related lamotrigine. Among them, emerged the synthesis of Biginelli products, which have shown interesting pharmacological activities.

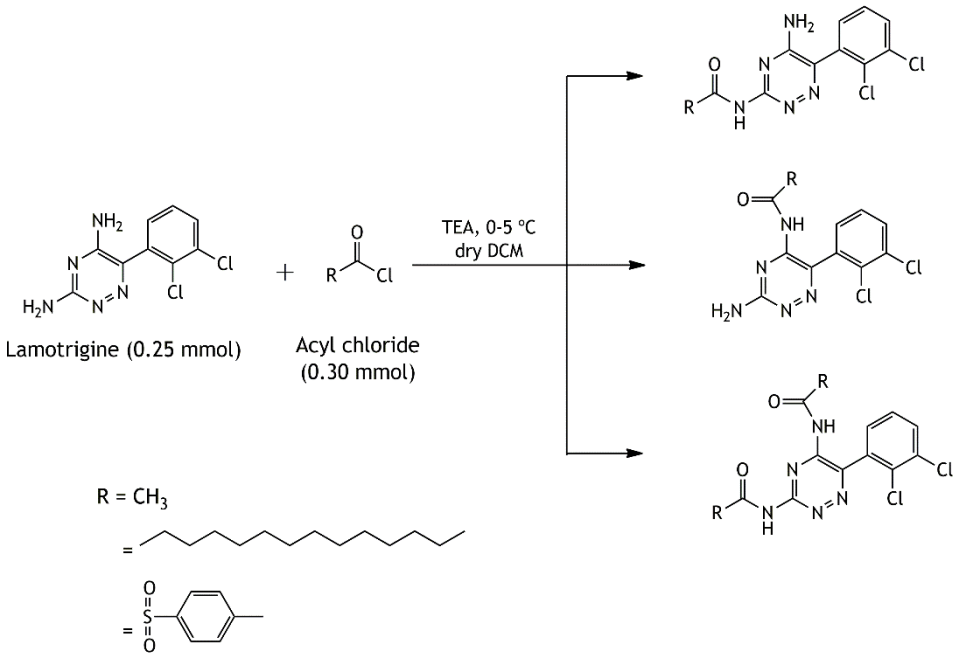

Figure B.2 – Schematic reaction of the acylation of lamotrigine with acetyl, palmitoyl and *p*-toluene sulfonyl chlorides and the possible products obtained.

B.1.3. Synthesis of lamotrigine-valproic acid hybrids

Additionally to GABAergic aminoacids, it was also intended to link valproic acid to lamotrigine (Figure B.3) by acylation of this compound with valproic acid chloride in the presence of a base such as TEA, similarly to the procedure reported in section B.1.2.1. On contrary to the previously described synthesis of lamotrigine–aminoacid compounds, valproic acid must be activated as acyl halides, namely valproic acid chloride, by the reaction of the carboxylic acid with thionyl chloride, previous to the acylation reaction. This first step was carried out under 0 ºC in dry DCM due to the high reactivity of the thionyl chloride (Acros Organics, New Jersey, USA) (Pessah et al., 2009). After, the reaction was conducted either at room temperature or at 50 ºC and monitored by TLC. Unfortunately, the valproic acid chloride was not detected in the NMR spectra, which can be partially explained by the instability of this intermediate.

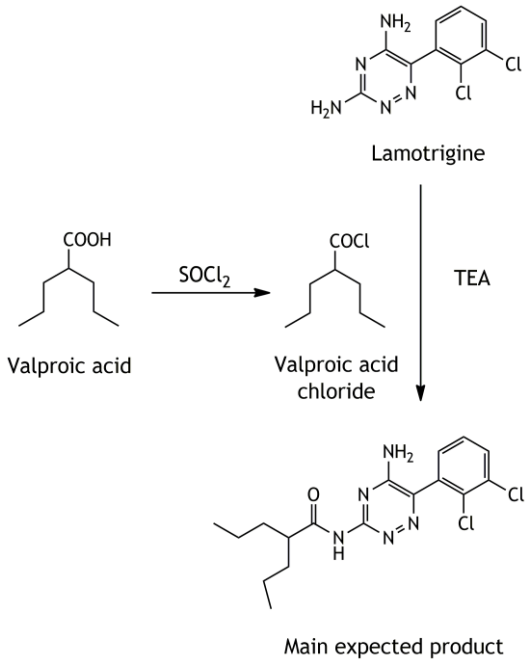

Figure B.3 – Schematic reaction of the synthesis of the lamotrigine-valproic acid hybrid.

B.2. References

Ceruso, M., Antel, S., Vullo, D., Scozzafava, A., Supuran, C.T., 2014. Inhibition studies of new ureido-substituted sulfonamides incorporating a GABA moiety against human carbonic anhydrase isoforms I-XIV. Bioorg. Med. Chem. 22, 6768–6775.

Edmeades, L.M., Griffith-Skinner, N.A., Hill, D.A., Hill, G.T., Packham, T.W., 2002. 1,2,4-Triazine derivative, its preparation and its use as reference marker for testing purity and stability of "lamotrigine."

Kamal, A., Kumar, B.A., Arifuddin, M., Dastidar, S.G., 2003. Synthesis of 4-amido and 4-sulphonamido analogues of podophyllotoxin as potential antitumour agents. Bioorg. Med. Chem. 11, 5135–5142.

Pessah, N., Bialer, M., Wlodarczyk, B., Finnell, R.H., Yagen, B., 2009. Fluoro-2,2,3,3-Tetramethylcyclopropanecarboxamide, a Novel Potent Anticonvulsant Derivative of a Cyclic Analogue of Valproic Acid. J. Med. Chem. 52, 2233–2242.

Rao, S.N., Somaiah, S., Ravisankar, T., Babu, K.S., 2012. Synthesis and characterization of impurities of an anticonvulsant drug, Lamotrigine. Int. J. Pharm. Pharm. Sci. 4, 133–136.

Suryakiran, N., Prabhakar, P., Reddy, T.S., Rajesh, K., Venkateswarlu, Y., 2006. Facile N-tert-butoxycarbonylation of amines using La(NO3)3·6H2O as a mild and efficient catalyst under solvent-free conditions. Tetrahedron Lett. 47, 8039–8042.

Winkler, M., Meischler, D., Klempier, N., 2007. Nitrilase-catalyzed enantioselective synthesis of pyrrolidine- And piperidinecarboxylic acids. Adv. Synth. Catal. 349, 1475–1480.

APPENDIX C

C.1. Additional reactions to produce other compounds more similar to lamotrigine

C.1.1. Experimental section

Procedure 1: To a mixture of benzaldehyde (1 mmol), ethyl acetoacetate (1 mmol) and guanidine thiocyanate (1.3 mmol; Sigma-Aldrich, St. Louis, MO, USA) was added zirconium tetrachloride ($ZrCl_4$, 5 mol%). The reaction was heated, under stirring, at 70 ºC in a preheated oil bath for 6 h. The reaction was considered completed when solidified and, after being cooled to room temperature, was poured onto cold water and stirred from 20-30 min. The crude product was washed with ice-cold water, dried and then recrystallized from ethanol 99.9%.

Procedure 2: To a mixture of benzaldehyde (1 mmol), ethyl acetoacetate/acetylacetone (1 mmol) and guanidine thiocyanate (1.3 mmol) was added zinc oxide (ZnO, 10 mol%) and the mixture was stirred at 60 ºC under solvent-free conditions for 23/43 h. Afterwards, 30 mL of ethyl acetate was added and the precipitated of ZnO was filtered off. The resulting organic solution was washed with 15 mL of 10% sodium bicarbonate and 15 mL of brine, dried over anhydrous sodium sulfate and evaporated.

Procedure 3: Benzaldehyde (1 mmol), ethyl acetoacetate (1 mmol) and guanidine hydrochloride (1 mmol; Sigma-Aldrich, St. Louis, MO, USA) were mixed together followed by addition of tetra-*n*-butylammonium hydrogen sulfate (TBHS, 15 mol%; Alfa Aesar, Karlsruhe, Germany). The reaction mixture was heated, under stirring, at 100 ºC in a preheated oil bath for 3 h. After the completion of the reaction, the resultant mass was poured into crushed ice and the solid obtained was filtered and then recrystallized from ethanol 99.9%.

Procedure 4: To a suspension of the compound **MM 26** (0.25 mmol) in chlorobenzene (Acros Organics, New Jersey, USA) at 0-5 ºC was added methyl trifluoromethanesulfonate (0.275 mmol; Sigma-Aldrich, St. Louis, MO, USA) in one portion. The reaction mixture was allowed to warm to room temperature and stirred for 3.5 h. Then, ammonium acetate (2.5 mmol) was added at 0-5 ºC to the mixture reaction for 10 min. The reaction was heated at 95-100 ºC for 17 h. After that, it was cooled to room temperature, diluted with a saturated solution of sodium carbonate (20 mL) and water (20 mL), extracted with ethyl acetate (3 x 40 mL), dried with anhydrous sodium sulfate, filtered and concentrated under reduced pressure. The crude residue was then recrystallized from *n*-hexane:ethanol 99.9% (1:1).

Procedure 5: A mixture of Meldrum's acid (1.05 mmol; Acros Organics, New Jersey, USA), benzaldehyde (1 mmol) and guanidine thiocyanate (1 mmol) in dimethylformamide (Sigma-Aldrich, St. Louis, MO, USA) was stirred at 120-130 ºC for 4 h. The mixture was cooled to the room temperature, diluted with 20 mL of acetone-water (50/50%, *v*/*v*) and then refluxed for

10 min and was kept overnight at room temperature. The solid formed was filtered off, washed with 40 mL of the acetone-water mixture and dried.

Procedure 6: To a solution of Meldrum's acid (1 mmol), benzaldehyde (1 mmol) and guanidine hydrochloride (1 mmol) in dimethylformamide was added anhydrous potassium carbonate (1 mmol; Fisher Scientific, New Hampshire, USA) or sodium ethoxide (1 mmol; Sigma-Aldrich, St. Louis, MO, USA). The reaction mixture was heated at 120 ºC for 6 h. After completion of the reaction, the mixture was poured into crushed ice while stirring, filtered and washed by ethyl acetate:hexane (1:3). Then, it was recrystallized from ethanol 99.9%.

Procedure 7: A solution of compound **MM 18** (0.25 mmol) in ethanol and KOH (0.5 mmol; Chem-Lab, Zedelgem, Belgium) dissolved in 1 mL of water was mixed and heated at 85 ºC, and magnetically stirred for 21 h. The progress of the reaction was monitored by thin layer chromatography (TLC). The reaction mixture was cooled and concentrated under vacuum to remove the solvent. To the residue obtained was added 25 mL of ice-cold water and then it was extracted with chloroform (3 x 10 mL), dried with anhydrous sodium sulphate and evaporated under vacuum to give the crude product. Finally, it was recrystallized from ethanol 99.9%.

Procedure 8: A solution of compound **MM 18** (0.5 mmol) in methanol and NaOH (1 mmol) dissolved in 1 mL of water was heated at 60 ºC, and magnetically stirred for 14 h. The progress of the reaction was monitored by TLC. The reaction mixture was cooled and concentrated under vacuum to remove the solvent. To the residue obtained was added 25 mL of ice-cold water and it was extracted with chloroform (3 x 10 mL) to remove the unreacted ester. The aqueous layer was acidified to pH 2 using HCl (10% *v*/*v*) and then extracted with ethyl acetate (3 x 15 mL), dried with anhydrous sodium sulphate and evaporated under vacuum to give the crude product. After that, it was recrystallized from ethanol 99.9%.

C.1.2. Results and discussion

Several attempts were made in order to produce compounds with a structure closer to lamotrigine. To start with, the first structural modification considered was the replacement of the ketone/thioketone by an amine in the dihydropyrimidine ring (Figure C.1). To achieve this goal, the general procedure was applied (Procedure 1), but the final desired product was not obtained according to the ^{1}H-nuclear magnetic resonance (NMR) spectrum. Further, based on the literature, different catalysts were used, such as ZnO (Procedure 2) (Tamaddon and Moradi, 2013) and TBHS (Procedure 3) (Ahmed et al., 2009), but similarly to the procedure 1, the product was also not obtained.

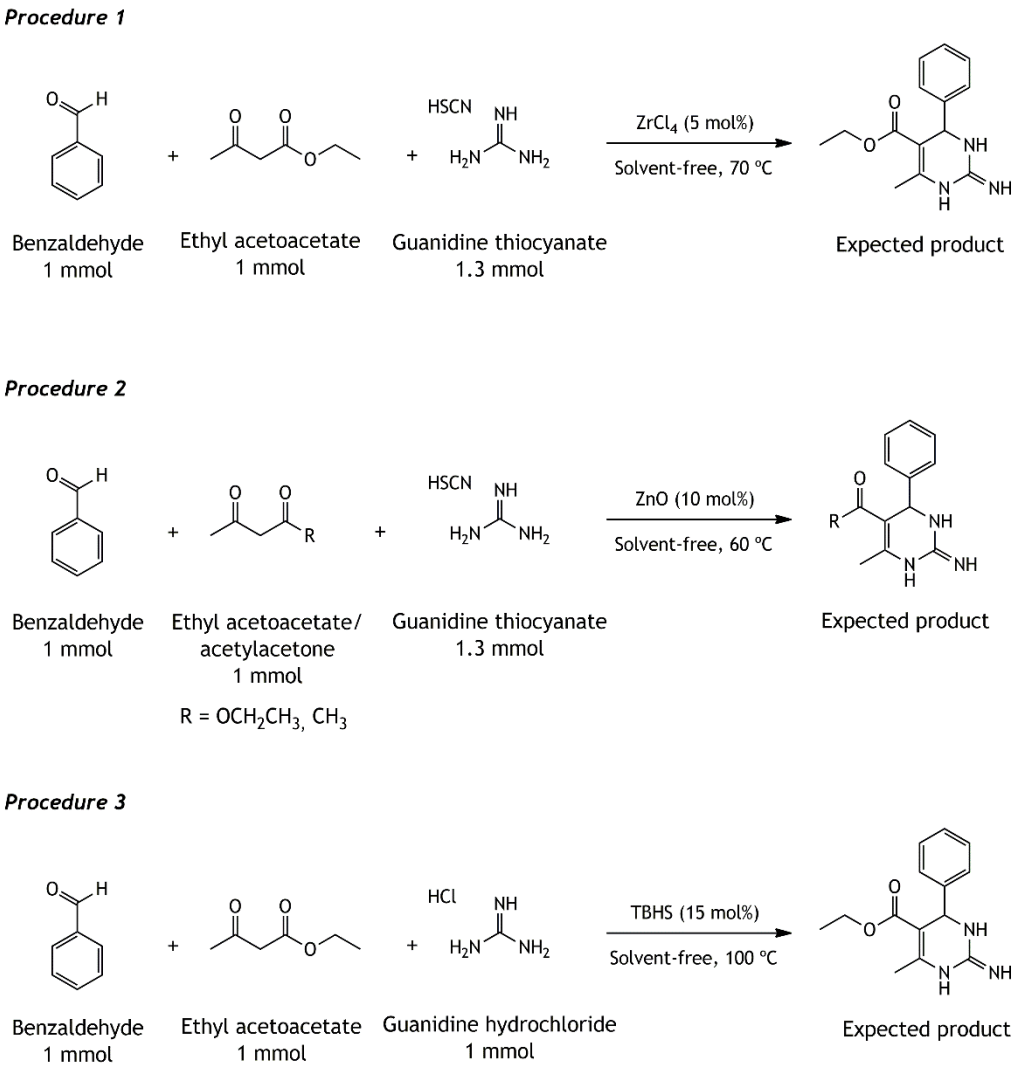

Figure C.1 – Schemes of one-pot synthesis of dihydropyrimidines employing the procedures 1, 2 and 3.

In fact, whereas the use of urea and thiourea as starting materials in the Biginelli reaction is well documented, similar transformations employing guanidine derivatives are comparatively less well-developed. However, according to the literature, one reason for the failure of the reactions using the procedures 1, 2 and 3 could be related with the fact that probably direct three-component Biginelli reactions with guanidine can lead to the formation of a bicyclic byproduct, as illustrated in Figure C.2 (Nilsson and Overman, 2006). It was also suggested that these bicyclic derivatives arise from Michael-type condensations between two molecules of ester and the guanidine backbone (Eynde et al., 2001). On the other hand, some reports have shown that guanidine can be used in a traditional three-component Biginelli reaction when the ß-ketoester possesses a phenyl substituent, giving Biginelli adducts in satisfactory yields and avoiding double Biginelli byproducts (Akbas et al., 2010). Other modifications have been explored such as the use of substituted guanidine (Val et al., 2013) and the production of 2-imino-5-carboxy-3,4-dihydropyrimidines by combination of pyrazole carboxamidine, a ß-ketoester, and an aldehyde in an initial Biginelli reaction followed by Boc protection,

aminolysis and acidic deprotection. Moreover, the same products can also be obtained using a triazone-protected guanidine, a ß-ketoester, and an aldehyde in a Biginelli reaction, followed by the acidic cleavage of the triazone (Nilsson and Overman, 2006).

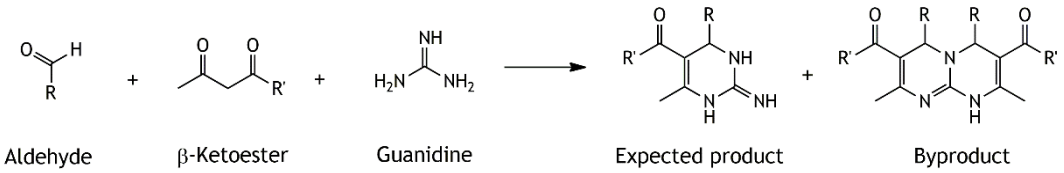

Figure C.2 – Scheme of one-pot synthesis of dihydropyrimidines plus the bicyclic byproduct probably produced.

A different approach to obtain dihydropyrimidines with a primary amine was also applied (*Procedure 4*) involving the methylation of a 3,4-dihydropyrimidin-2-(1*H*)-thione (compound **MM 26**) followed by aminolysis, as described by Arnold and collaborators (Arnold et al., 2013) (Figure C.3). In this case, the first step was concluded with success (compound **MM 62**), but the desired aminolysis, unfortunately, did not occur.

Procedure 4

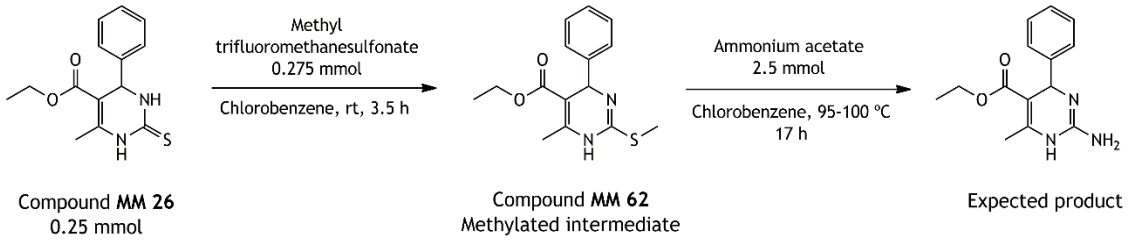

Figure C.3 – Scheme of compound **MM 26** methylation followed by aminolysis of the thioimidate to afford the 2-aminodihydropyrimidine.

Ethyl 6-methyl-2-(methylthio)-4-phenyl-1,4-dihydropyrimidine-5-carboxylate (compound **MM 62**). White solid, yield: 63%, IR (υ_{max}/cm^{-1}): 2979, 2901, 1705, 1656, 1238, 1089; ^{1}H-NMR (400 MHz, DMSO-d_6) δ: 1.08 (t, 3H, *J* = 7.06 Hz, OCH_2CH_3), 1.79 (s, 3H, CH_3), 2.27 (s, 3H, SCH3) 3.97 (q, 2H, *J* = 7.06 Hz, OCH_2), 5.27 (s, 1H, CH), 7.21-7.37 (m, 5H, ArH); ^{13}C-NMR (100 MHz, DMSO-d_6) δ:14.14, 20.32, 22.80, 52.37, 58.90, 99.42, 126.31, 127.40, 128.44, 144.86, 153.51, 165.43, 174.55.

Meldrum's acid has also been used in Biginelli reactions, leading to the production of interesting structures (Svetlik and Veizerova, 2011). Looking for the expected structures in the Figure C.4, the final products contain the desired primary amine and they do not have the

lateral chain and thus are more similar to lamotrigine. In addition, the ketone in the tetrahydropyrimidine ring could afford an additional point to establish interactions with the biological targets. These reasons led us to do the procedures 5 (Ostras et al., 2006) and 6 (Mirza-Aghayan et al., 2010). Unfortunately, the NMR spectra were inconclusive or the amount of the product obtained was so small to allow the NMR characterisation, which suggested the necessity of future optimization of the reactional conditions and work up.

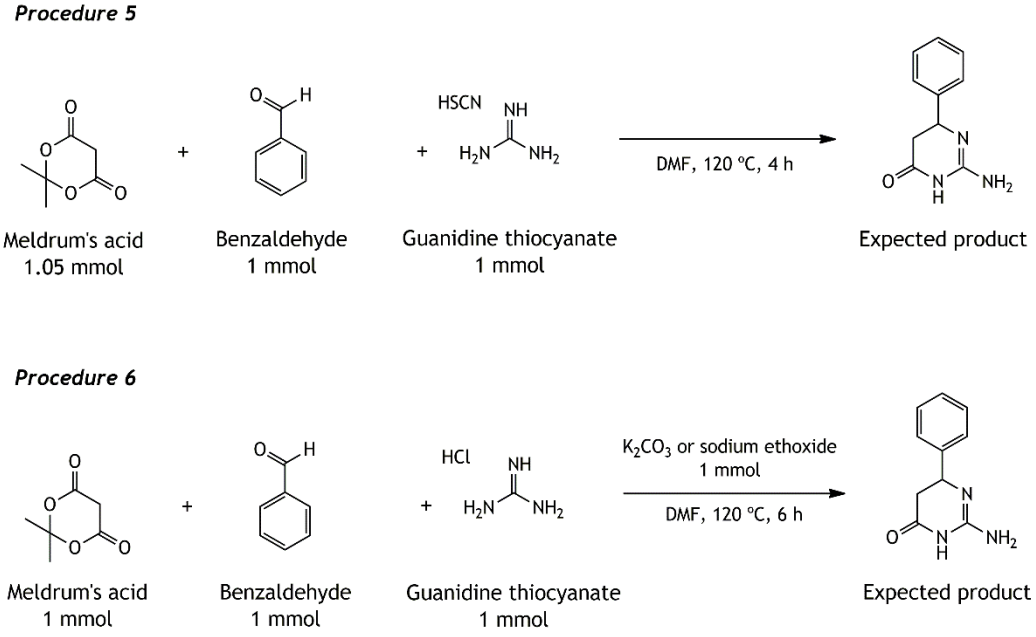

Figure C.4 – Scheme of one-pot synthesis of 2-amino-5,6-dihydropyrimidin-4(3*H*)-one, using Meldrum's acid as starting material.

Based on the literature, additional reactions were performed to obtain products with different lateral chains either by decarboxylation (Procedure 7) or hydrolysis (Procedure 8) (Soumyanarayanan et al., 2012) of the compound **MM 18** as demonstrated in Figure C.5. However, NMR data indicated the presence of the substrate in the first case and were inconclusive in the second one.

All these reactions were performed using the simplest starting materials in order to understand the conditions and characteristics of each reaction. However, the aim would be the use of the 2,3-dichlorobenzaldehyde (Procedures 1, 2, 3, 5 and 6) or the respective analogues of compound MM 26 (Procedure 4) or compound MM 18 (Procedures 7 and 8) with the chlorine atoms at position 2 and 3 of the aromatic ring similarly to lamotrigine. Moreover, the salt of guanidine used could also be determinant for the success/failure of the reactions, due to the fact that in general, the salt of guanidine usually found in the literature is the carbonate (Šíša et al., 2009).

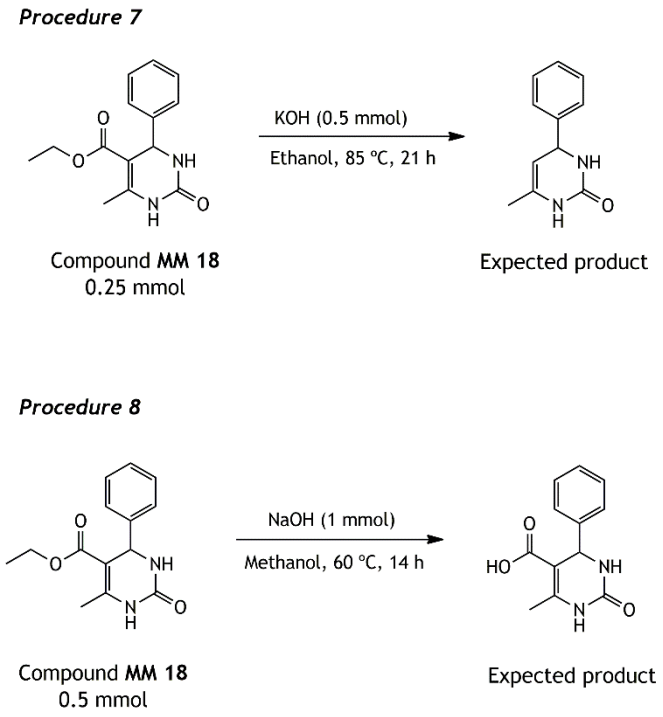

Figure C.5 – Scheme of the reactions of decarboxylation (Procedure 7) and hydrolysis (Procedure 8) of the compound **MM 18**.

C.2. References

Ahmed, B., Khan, R. a., Keshari, M., 2009. An improved synthesis of Biginelli-type compounds via phase-transfer catalysis. Tetrahedron Lett. 50, 2889–2892.

Akbas, E., Levent, A., Gumus, S., Sumer, M.R., Akyazi, I., 2010. Synthesis of Some Novel Pyrimidine Derivatives and Investigation of their Electrochemical Behavior. Bull. Korean Chem. Soc. 31, 3632–3638.

Arnold, D.M., Laporte, M.G., Anderson, S.M., Wipf, P., 2013. Condensation reactions of guanidines with bis-electrophiles: Formation of highly nitrogenous heterocycles. Tetrahedron 69, 7719–7731.

Eynde, J.J. Vanden, Hecq, N., Kataeva, OlgaKappe, C.O., 2001. Microwave-mediated regioselective synthesis of novel pyrimido [1,2-a] pyrimidines under solvent-free conditions. Tetrahedron 57, 1785–1791.

Mirza-Aghayan, M., Lashaki, T.B., Rahimifard, M., Boukherroub, R., Tarlani, A.A., 2010. Amino-Functionalized MCM-41 Base-Catalyzed One-Pot Synthesis of 2-Amino-5,6-dihydropyrimidin-4(3H)-ones. J. Iran. Chem. Soc. 8, 280–286.

Nilsson, B.L., Overman, L.E., June, R. V, 2006. Concise Synthesis of Guanidine-Containing Heterocycles Using the Biginelli Reaction. J. Org. Chem. 71, 7706–7714.

Ostras, K.S., Gorobets, N.Y., Desenko, S.M., Musatov, V.I., 2006. An easy access to 2-Amino-

5,6-dihydro-3H-pyrimidin-4-one building blocks: The reaction under conventional and microwave conditions. Mol. Divers. 10, 483–489.

Soumyanarayanan, U., Bhat, V.G., Kar, S.S., Mathew, J. a, 2012. Monastrol mimic Biginelli dihydropyrimidinone derivatives: synthesis, cytotoxicity screening against HepG2 and HeLa cell lines and molecular modeling study. Org. Med. Chem. Lett. 2, 23.

Svetlik, J., Veizerova, L., 2011. A Different Role of Meldrum's Acid in the Biginelli Reaction. Helv. Chim. Acta 94, 199–205.

Tamaddon, F., Moradi, S., 2013. Controllable selectivity in Biginelli and Hantzsch reactions using nanoZnO as a structure base catalyst. J. Mol. Catal. A Chem. 370, 117–122.

Val, C., Crespo, A., Yaziji, V., Coelho, A., Azuaje, J., El Maatougui, A., Carbajales, C., Sotelo, E., 2013. Three-Component Assembly of Structurally Diverse 2-Aminopyrimidine-5-carbonitriles. ACS Comb. Sci. 2–10.

APPENDIX D

D.1. Additional *in vitro* evaluation

In addition to evaluating the cytotoxicity in rat mesencephalic dopaminergic (N27) normal human dermal fibroblasts (NHDF), human hepatocellular carcinoma (HepaRG) and human colorectal adenocarcinoma (Caco-2) cell lines, the cytotoxicity of the synthesized DHPM(t)s was also investigated in other available cell lines: human breast adenocarcinoma (MCF-7), human breast ductal carcinoma (T47D) and human prostatic carcinoma (LNCaP) cell lines. This was performed in order to obtain the most complete spectrum of cytotoxicity for the target compounds. Moreover, analysis of cell death and cell cycle distribution were also performed using HepaRG and MCF-7 cell lines as described below.

D.1.1. Experimental section

D.1.1.1. MTT assay

The additional cytotoxicity studies were performed according to the experimental procedure described in section V.2.1 of the Chapter V.

D.1.1.2. Cell viability

The analysis of cell viability was performed by flow cytometry after staining dead cells with propidium iodide (PI) (solution of PI 1 mg/ml in 0.1% of azide and water; Sigma Aldrich, St. Louis, MO, USA). Briefly, 3 mL of cells suspension were seeded in 6-well plates (cell density of 3×10^4 cells/mL for HepaRG and MCF-7 cell lines) in complete culture medium. After 48 h they were treated with 50 μM of the compounds **MM 81**, **MM 83** and **MM 92**. Untreated cells were used as negative control. At the end of 24 h of incubation, the supernatant of each well was collected, cells were harvested by trypsinization and pooled with the supernatants. The resulting cell suspension was kept on ice, pelleted by centrifugation and resuspended in 400 μL of complete medium. Afterwards, 395 μL of the cell suspension was transferred to a FACS tube and 5 μL of PI was added. A minimum of 10000 events was acquired using a FACSCalibur flow cytometer in the channels forward scatter (FSC), side scatter (SSC) and fluorescence channel-3 (FL3, for PI). Acquisition and analysis was performed with CellQuest™ Pro Software. In the FSC/FL3 contour plot, two regions were created, one corresponding to viable cells (R1) and another to dead cells (R2) to exclude debris which were not considered in the analysis. The percentage of viability is the percentage of cells in R1 as compared to the total number of events in R1 and R2.

D.1.1.3. Cell cycle distribution

Cell cycle distribution of cells was determined through PI staining of DNA in fixed and permeabilized cells using a flow cytometry assay. In brief, 3 mL of cells suspension were seeded in 6-well plates (cell density of 2×10^4 cells/mL for HepaRG and MCF-7 cell lines) in complete culture medium. After 48 h they were treated with 50 µM of compounds **MM 81**, **MM 83** and **MM 92**. For comparison, untreated cells were used as negative control and cells treated with 5-fluorouracil (5-FU) at 50 µM were used as positive control. After 48 h of incubation, the cells were trypsinized, centrifuged and resuspended in 450 µL of a cold solution of 0.5% bovine serum albumin (BSA; Amresco, USA) in PBS. The resulting cell suspension was kept on ice and then fixed by gently adding ice-cold 70% ethanol (-20 ºC) with simultaneous gentle vortex agitation. After at least 2 days at –20 ºC, fixed cells were washed twice with PBS and resuspended in a solution of PI (50 µg/mL) prepared in 0.5% BSA in PBS and sequentially incubated with Ribonuclease A from bovine pancreas at a final concentration of 7.1 µg/mL (solution in 50% glycerol, 10 mM Tris-HCl, pH8, Sigma Aldrich, St. Louis, MO, USA) for 15 min in the dark. The data were analysed using ModFit software (Becton Dickinson, San Jose, CA, USA). A region (R1) was created on the FL3-Width/FL3-Area contour plot to exclude cell aggregates and another region (R2) was created on the FL1-Height/FL3-Area contour plot to exclude part of the debris.

D.1.1.4. Statistics

The data were expressed as a mean ± standard deviation (SD). Comparison among multiple groups of one factor was analysed by using one-way ANOVA followed by Dunnett's post hoc tests to determine significant differences among the means. Difference between groups was considered statistically significant for a *p*-value lower than 0.05 ($p < 0.05$). The determination of the IC_{50} was done by sigmoidal fitting analysis considering a 95% confidence interval.

D.1.2. Results and discussion

The cytotoxicity of the synthesized DHPM(t)s was additionally evaluated in MCF-7, T47D and LNCaP human cancer cell lines, using the MTT assay. A single concentration of 30 µM was used to perform the screening of the antiproliferative properties and the results correspond to the relative cell proliferation, in percentage, after 72 h of incubation with the compounds of interest (Table D.1).

Table D.1 – Relative cell proliferation in percentage of the synthesized compounds and standard antiepileptic drugs, at 30 μM, in MCF-7, T47D and LNCaP cells.

Compound	MCF-7 (%)	T47D (%)	LNCaP (%)	Compound	MCF-7 (%)	T47D (%)	LNCaP (%)
Urea series				**Thiourea series**			
MM 18	94.57 ± 8.07	77.82 ± 13.79	59.82 ± 7.42***	MM 26	75.42 ± 15.26**	87.14 ± 3.28	62.67 ± 12.79***
MM 72	98.32 ± 12.02	82.71 ± 7.79	81.67 ± 6.41*	MM 83	76.87 ± 22.85	78.97 ± 22.71	68.23 ± 11.73***
MM 17	84.37 ± 7.30*	82.01 ± 4.66	75.09 ± 19.54**	MM 25	85.05 ± 10.02*	80.60 ± 4.26	72.11 ± 11.27***
MM 22	97.65 ± 4.02	87.34 ± 3.80	55.16 ± 13.43***	MM 28	78.74 ± 4.70**	80.51 ± 8.48	54.64 ± 5.64***
MM 73	87.31 ± 2.68	98.30 ± 2.33	83.13 ± 7.65*	MM 84	69.63 ± 4.58	70.44 ± 4.54**	69.50 ± 5.19***
MM 19	91.00 ± 4.37	88.78 ± 8.10	62.15 ± 5.01***	MM 29	94.86 ± 7.74	94.70 ± 5.62	73.40 ± 17.33***
MM 23	50.86 ± 3.53***	73.94 ± 6.16	50.89 ± 8.55***				
MM 82	50.69 ± 4.74	66.80 ± 6.58	72.27 ± 5.81**				
MM 24	58.98 ± 7.61***	70.12 ± 5.37	70.56 ± 12.80***	MM 30	81.01 ± 6.69**	96.29 ± 2.83	62.54 ± 7.23***
MM 34	79.71 ± 5.26**	89.83 ± 2.39	57.36 ± 8.13***	MM 36	93.39 ± 6.40	69.02 ± 7.81***	64.77 ± 8.81***
MM 74	97.71 ± 34.16	91.31 ± 11.08	79.77 ± 12.58*	MM 85	66.83 ± 15.26	68.63 ± 9.60***	73.31 ± 3.95**
MM 35	69.12 ± 14.52	86.32 ± 4.62	85.63 ± 9.60	MM 37	98.07 ± 11.02	77.24 ± 20.30**	82.06 ± 14.73*
MM 55	50.94 ± 5.13***	53.45 ± 3.91***	53.74 ± 5.93***	MM 46	62.42 ± 15.87*	77.30 ± 8.10**	61.40 ± 20.47
				MM 90	**36.96 ± 5.48****	59.26 ± 4.88***	61.88 ± 5.93***
MM 54	53.59 ± 5.73***	50.33 ± 1.55***	64.09 ± 4.41*	MM 48	60.24 ± 6.64*	56.41 ± 5.15***	72.43 ± 4.32***
MM 57	66.94 ± 5.25***	50.22 ± 4.67***	53.09 ± 1.66***	MM 60	**19.86 ± 3.55*****	59.05 ± 7.46***	60.12 ± 6.93***
MM 81	65.98 ± 30.33	50.36 ± 4.31*	74.95 ± 11.43**	MM 92	**31.11 ± 2.78*****	52.02 ± 1.61***	52.49 ± 5.01***
MM 56	64.17 ± 5.32***	59.11 ± 2.80***	57.68 ± 13.42*	MM 64	83.05 ± 8.83*	91.46 ± 3.28	76.52 ± 4.97**
MM 59	67.33 ± 17.12**	66.86 ± 8.55***	89.78 ± 13.28	MM 61	56.60 ± 9.43*	80.99 ± 4.88*	73.61 ± 6.52**
MM 75	61.16 ± 19.92	60.17 ± 4.16*	60.06 ± 12.29***	MM 86	55.61 ± 14.22	70.50 ± 4.79***	78.30 ± 19.59*
MM 58	82.05 ± 15.06*	79.70 ± 10.50**	78.17 ± 7.04	MM 63	103.39 ± 4.99	98.11 ± 11.10	81.43 ± 18.86
MM 65	104.14 ± 4.80	84.25 ± 1.58**	85.90 ± 11.42	MM 68	69.91 ± 9.65	78.45 ± 8.11	83.28 ± 3.65*
MM 76	84.79 ± 14.42	78.73 ± 9.47	74.62 ± 7.19**	MM 88	84.68 ± 9.88	95.76 ± 7.35	82.40 ± 5.70*
MM 66	92.30 ± 18.21	83.69 ± 7.10	92.20 ± 14.90	MM 67	74.68 ± 20.52	80.84 ± 8.98*	82.70 ± 6.84*
MM 93	54.37 ± 2.66***	93.22 ± 2.75	79.90 ± 4.99				
MM 99	83.65 ± 10.23	95.20 ± 8.27	84.54 ± 3.19	**Antiepileptic drugs**			
MM 96	89.56 ± 6.31	102.69 ± 9.02	92.03 ± 6.76	Lamotrigine	69.80 ± 8.54	83.89 ± 9.90	108.75 ± 28.11
MM 106	74.35 ± 13.27	105.38 ± 11.03	82.79 ± 6.78	Carbamazepine	72.89 ± 2.74	75.73 ± 6.14	109.68 ± 18.00
MM 95	98.14 ± 9.97	108.54 ± 4.09	96.41 ± 9.80	Phenytoin	69.88 ± 12.93	83.64 ± 4.46	93.35 ± 15.15
				Clonazepam	79.76 ± 5.91	86.08 ± 7.49*	89.50 ± 8.29

Results are expressed as mean ± SD (standard deviation) after 72 h of treatment. Each experiment was performed in quadruplicate and at least two independent experiments were carried out. The control were untreated cells. *$p < 0.05$ *versus* control; **$p < 0.01$ *versus* control; ***$p < 0.001$ *versus* control. Bold values correspond to the compounds that exhibited a relative cell proliferation lower than 50%.

The screening in these cell lines showed that the compounds did not exhibit marked cytotoxicity in the prostatic and breast T47D cells (relative cell proliferation higher than 50% at 30 μM). However, several compounds incorporating chlorine atoms presented relative cell proliferation around 50% against these cells. In contrast, it was found that compounds **MM 90**, **MM 60** and **MM 92** (chlorinated derivatives from thiourea series) exhibited relevant cytotoxicity in the screening at 30 μM against MCF-7 cells, which was confirmed by the calculation of the respective IC_{50} values (IC_{50} = 4.30 μM; 2.95 μM; and 10.89 μM, respectively). These results reinforce the fact that compounds incorporating chlorine atoms in their structures can constitute problematic compounds when the anticonvulsant effect is desired. Due to the fact that the commercial anticancer drug 5-FU was also tested for comparison in the following assays, its cytotoxicity was also assessed in all cell lines used (IC_{50} = 1.71 μM for MCF-7; IC_{50} = 0.54 μM for T47D; IC_{50}= 7.80 μM for LNCaP; IC_{50} = 3.61 μM for NHDF; IC_{50} = 1.15 μM for Caco-2; IC_{50} = 1.70 μM for N27 cells).

Intending to obtain some data on the possible mechanism of cytotoxicity of the chlorinated compounds both cell survival and cell cycle distribution were determined using flow cytometry in MCF-7 and HepaRG cells. Compound **MM 92** was chosen because it previously showed marked cytotoxicity in both cell lines and compound **MM 83**, without substituents in the aromatic ring, was also evaluated to understand if chlorine atoms present on compound **MM 92** have influence in the cell death and cycle distribution. Moreover, compound **MM 81**, the DHPM analogue of **MM 92**, was also evaluated in order to observe possible differences between the two series.

Firstly, a PI flow cytometric assay was used to identify death cells with compromised cell membrane, and the results showed that all the compounds evaluated (**MM 90**, **MM 60** and **MM 92**) at the concentration of 50 μM did not induce important cell death after 24 h of incubation in both MCF-7 and HepaRG cell lines (Figure D.1).

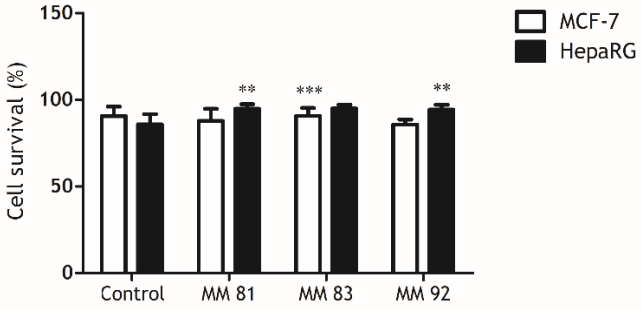

Figure D.1 – Percentage of cell survival after 24 h treatment with 50 μM of compounds **MM 81**, **MM 83** and **MM 92** in MCF-7 and HepaRG cell lines through propidium iodide flow cytometric assay. The control corresponds to untreated cells. The percentage of survival is the percentage of live cells as compared to the total number of events of both live and dead cells. Each bar represents the mean (standard deviation). $^{**}p < 0.01$ *versus* control; $^{***}p < 0.001$ *versus* control.

As monastrol affects the cell cycle, mainly as a specific inhibitor of the human motor protein Eg5 (Asraf et al., 2015), this encouraged the evaluation of the cell cycle distribution induced by the compounds in MCF-7 (Figure D.2) and HepaRG (Figure D.3) cell lines. Untreated cells and 5-FU-treated cells were used as negative and positive controls, respectively. Interestingly, compound **MM 92** at 50 μM for 48 h arrested MCF-7 cells in G_0/G_1 phase (the phase before DNA replication), increasing the proportion of cells in this cell cycle phase from 65.96% ± 1.01% (control) to 89.63% ± 0.92% (Figure D.2, Panel B). This phenomenon was accompanied by a 4.4-fold decrease in the populations of cells in S phase (the DNA synthesis phase where DNA replication occurs) and a 2.1-fold decrease of cells in G_2/M phase (phase where cell division occurs). This is in contrast with the monastrol effect, which is described to induce mitotic arrest in several cell lines (Asraf et al., 2015), and did not seem to significantly affect the distribution of the cell cycle of MCF-7 cells even at 1 mM (Guido et al., 2015). Although less pronounced, compounds **MM 81** and **MM 83** also had effect on the percentage of cells in G_0/G_1 phase (79.29% ± 3.88% and 77.06% ± 2.61%, respectively).

As expected, in HepaRG cells, the synthesized compounds did not share the effect of 5-FU either, which strongly arrested the cells in S phase (68.97% ± 2.06% *versus* the control 17.01% ± 2.508%) (Figure D.3, Panel B). As in MCF-7 cell line, the compounds significantly increased the number of cells in G_0/G_1 stage (81.67% ± 4.03% for compound **MM 81**; 86.16% ± 1.66% for compound **MM 83** and 84.99% ± 1.42% for compound **MM 92** *versus* the control 72.31% ± 3.92%) after treatment with 50 μM for 48 h (Figure D.3, Panel B). Although in the case of HepaRG cell line the cell cycle distribution does not discriminate structural aspects of the molecules evaluated, in the case of MCF-7 cells, the effects seem to be stronger for compound **MM 92** than their analogues, which is concordant with the results obtained in the screening of MTT assay at 30 μM. In spite of the obtained data suggest that cell cycle arrest in G_0/G_1 stage could contribute to the antiproliferative effects of the compounds in MCF-7 and HepaRG cells, this hypothesis does not exclude that other mechanisms may be involved.

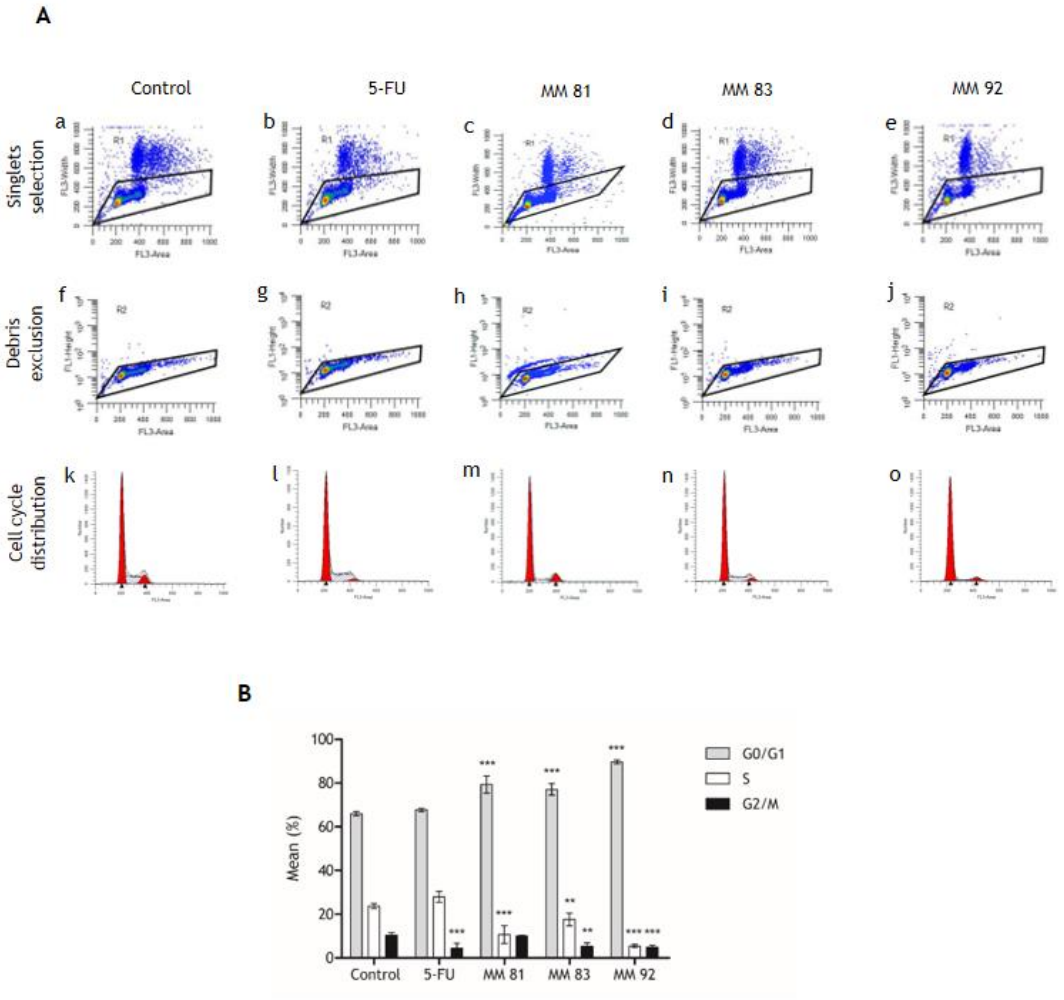

Figure D.2 - Cell cycle distribution analysis of MCF-7 breast cancer cells after treatment with compounds **MM 81**, **MM 83** and **MM 92** (50 μM) for 48 h. A negative control (untreated cells) and a positive control (5-FU, 50 μM) were included. The analysis of the cell cycle distribution was performed using the PI staining and by flow cytometry. **A** – representative cell cycle distribution analysis showing in a, b, c, d and e, gating of singlets by region R1 created on the FL3-Width/FL3-Area contour plot; in f, g, h, i and j, debris exclusion by region (R2) created on the FL1-Height/FL3-Area contour plot; and in k, l, m, n and o, cell cycle distribution fit, respectively for negative control, 5-FU, compound **MM 81**, compound **MM 83** and compound **MM 92**. **B** – quantification of the proportion of cells in G_0/G_1, S, and G_2/M phases of the cell cycle. Each bar represents the mean ± SD of four samples (originating from two independent experiments). $^{**}p < 0.01$ *versus* control; $^{***}p < 0.001$ *versus* control.

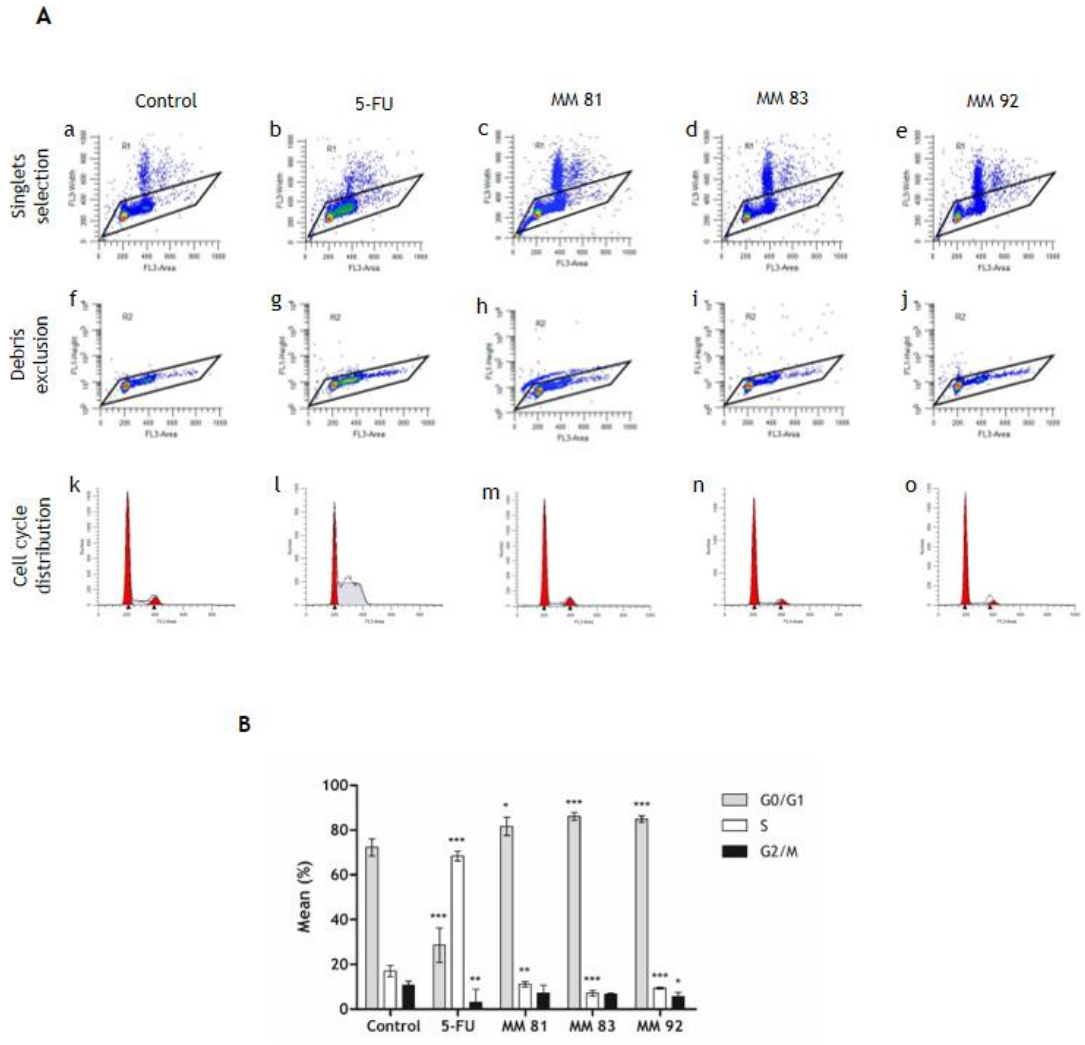

Figure D.3 - Cell cycle distribution analysis of HepaRG hepatic cancer cells after treatment with compounds **MM 81**, **MM 83** and **MM 92** (50 μM) for 48 h. A negative control (untreated cells) and a positive control (5-FU, 50 μM) were included. The analysis of the cell cycle distribution was performed using the PI staining and by flow cytometry. **A** – representative cell cycle distribution analysis showing in a, b, c, d and e, gating of singlets by region R1 created on the FL3-Width/FL3-Area contour plot; in f, g, h, i and j, debris exclusion by region (R2) created on the FL1-Height/FL3-Area contour plot; and in k, l, m, n and o, cell cycle distribution fit, respectively for negative control, 5-FU, compound **MM 81**, compound **MM 83** and compound **MM 92**. **B** – quantification of the proportion of cells in G_0/G_1, S, and G_2/M phases of the cell cycle. Each bar represents the mean ± SD of four samples (originating from two independent experiments). **p* < 0.05 *versus* control; ***p* < 0.01 *versus* control; ****p* < 0.001 *versus* control.

D.2. Quantitative structure-activity relationship model for cytotoxicity of dihydropyrimidin(thi)ones

Using the cell proliferation experimental data obtained in the initial screening of cytotoxicity of the synthesized DHPM(t)s, a quantitative structure-activity relationship (QSAR) analysis was performed employing Bayesian regularized artificial neural networks (BRANNs) to relate *in silico* calculated molecular descriptors and bioactivity of the compounds across the tested cell lines in order to predict the cytotoxicity of new related compounds.

D.2.1. Experimental section

D.2.1.1. Data handling and *in silico* calculation of the molecular descriptors

The *in vitro* cell antiproliferative activity (expressed as the relative cell proliferation in percentage) of the target compounds at a concentration of 30 μM against the human cell lines (NHDF, HepaRG, Caco-2, MCF-7, T47D and LNCaP) was initially log transformed (base 10). In order to increase the available data and the usefulness of the developed QSAR model, all bioactivity measurements were combined using a three bit codification system to distinguish between the six tested cell lines. Using these three binary inputs, a total of six different combinations (out of 8 possible) were selected, with no particular order, which represent each of the cell lines employed (Table D.2). Comparatively with the use of a dummy inputs system, an important reduction in required inputs for cell line distinction was obtained. The two series were analysed separately. Thus, for the thiourea series 132 cases were available for QSAR modelling, in which 112 cases (85%) were randomly selected as the training set for model development and the remaining 20 cases (15%) as the test set for external validation purposes. The random selection was performed in a way that the minimum and maximum relative cell proliferation values for each cell line were not selected for the test set, and the test set selected cases were well distributed between both cell lines and range of values in each cell line. For the urea series 138 cases were available for QSAR development. Within these, using the Kennard–Stone design, 100 cases were selected for training of the model (training group) and the remaining 38 cases were used to externally validate the QSAR model and assess its predictive performance (test group). For the *in silico* calculation of the molecular descriptors, the titled compounds were first manually drawn in ACD/ChemSketch 2015 Pack 2 ("ACD/ChemSketch, 2015 release, Advanced Chemistry Development, Inc., Toronto, ON, Canada, www.acdlabs.com, 2015," n.d.), and the SMILES notation was obtained and used for tautomer and ionization state check and the calculation of the GALAS log *P* in

ACD/Percepta 2015 ("ACD/Percepta, 2015 release, Advanced Chemistry Development, Inc., Toronto, ON, Canada, www.acdlabs.com, 2015," n.d.). The remaining molecular descriptors were calculated using E-Dragon online version 1. No molecular descriptor dependent on the 3D conformation of the molecules was calculated, since the antitumoral bioactive conformations of this family of compounds is not known and due to the fact that the simpler selected descriptors are more easily interpreted.

Table D.2 – Three bit representation for the NHDF, HepaRG, Caco-2, MCF-7, T47D and LNCaP cell lines used for QSAR modelling.

Cell line	Binary variables		
	Bit 1	Bit 2	Bit 3
NHDF	1	0	0
HepaRG	0	1	0
Caco-2	0	0	1
MCF-7	1	1	0
T47D	1	0	1
LNCaP	0	1	1

D.2.1.2. BRANN modelling for QSAR development

QSAR development was performed using an *in-house* developed tool based on BRANNs in MATLAB R2014a (MATLAB, 2014), which allowed process automation, data analysis and the use of cross-validation procedures. All calculations and modelling were performed on a 3.5 Ghz Intel i7 CPU running Windows 7 operating system. Commonly selected parameters were "trainbr" as the training function, pre-processing of input and output variables to [-1, 1] range, "tansig" transfer function in the hidden layer and "purelin" in the output layer. The remaining parameters were kept at their default value. The molecular descriptors and the three bits used for cell line identification were used as independent variables (inputs), and the log(relative cell proliferation) was used as the dependent variable (output). Prior to BRANN modelling, the UFS algorithm was employed in the training set for the thiourea series, in order to remove multicollinear and insufficiently discriminative molecular descriptors (selected parameters were maximum multiple correlation value of 0.9 and minimum standard deviation value of 0.01). For the urea series training set, molecular descriptors that were repetitive or insufficiently discriminatory (minimum standard deviation value of 0.05) or highly correlated with other descriptors (maximum correlation coefficient value of 0.9) for QSAR analysis were removed.

Following this initial input reduction, a forward selection method was performed using a repeated 10-fold cross-validation procedure with the BRANN models, starting with the three bit inputs. Each iteration was repeated 10 times with random splits of the available data, and the average statistical evaluation was taken. For each iteration, the selected molecular descriptor was the one that returned the best average Q^2 and $RMSE_{CV}$ values. After selection of the most relevant molecular descriptors (the ones that returned the best average cross-

validated statistics), and for simplicity sake, the same 10-fold cross-validation procedure with 10 duplicates was used to determine the optimal number of neurons in a single hidden layer between 0 (linear model) and 10 (non-linear models). After determination of the best parameters regarding the molecular descriptors and model complexity (internal validation), a y-scrambling procedure was performed to verify the absence of chance correlations between the input and output variables. The final QSAR models were then trained on all available training data. The final QSAR models were further validated using the hold-out test sets (external validation), by comparison of the QSAR predicted values with those observed experimentally for the cases not used to train the models.

Finally, to elucidate the relationships between the selected molecular descriptors and relative cell proliferation, the Lek Profile method was employed individually for each cell line, by varying each molecular descriptor across 11 data points (10 equal intervals over the entire range of the molecular descriptor) and holding the remaining molecular descriptors at 5 different data range splits (minimum, first quartile, median, third quartile and maximum value). The average predicted responses across the five split predictions were taken as the relationship between the molecular descriptor and the response variable, and the relative importance of each molecular descriptor is taken as the maximum range between the calculated predictions (maximum predicted value – minimum predicted value).

D.2.1.3. Internal and external statistical evaluation

For both internal and external validation purposes, the coefficient of determination (R^2 or Q^2 in cross-validation) was used as a measurement of the goodness of fit of the model. Also, the root mean squared error (RMSE) between predicted and observed values was used as a measurement of accuracy.

D.2.2. Results and discussion

In order to develop a QSAR model to relate the *in silico* calculated molecular descriptors of the synthesized compounds with their experimentally obtained antiproliferative activity, and predict the given response of hypothetical related compounds, BRANN models coupled with an optimization process for the selection of the most relevant molecular descriptors and required model complexity were used.

Since a QSAR model that can reliably predict the bioactivity of compounds in multiple cell lines is of greater utility, and that the use of larger data sets for training (Tables D.3 and D.4) can generate better predictive models, the available data of the six cell lines were incorporate in a single output QSAR model, separately for the urea and thiourea series (Tropsha, 2010). Given the importance of external validation to ultimately validate a QSAR

model, the available data for both series was split as described in the experimental section to ensure that the test sets were representative both across cell lines and experimental value ranges.

Table D.3 – QSAR predicted antiproliferative activity (as the relative cell proliferation in percentage) of the urea derivatives at concentration of 30 μM, against normal human dermal fibroblasts (NHDF) and against hepatic (HepaRG), colon (Caco-2), breast (MCF-7 and T47D) and prostatic (LNCaP) human cancer cell lines. The cases used in the external validation of the QSAR model are underlined.

Compound	NHDF	HepaRG	Caco-2	MCF-7	T47D	LNCaP
MM 18	83.41	60.27	95.74	86.57	78.69	84.89
MM 72	86.95	67.23	99.66	89.33	81.13	87.80
MM 17	90.34	70.38	100.88	93.28	84.75	91.62
MM 22	77.52	47.68	87.33	81.62	75.45	78.50
MM 73	82.33	59.27	94.86	86.25	77.86	85.15
MM 19	85.78	61.44	95.74	90.05	81.51	88.20
MM 23	65.99	54.05	79.90	59.25	66.02	64.14
MM 82	68.31	57.94	82.10	61.11	67.57	65.47
MM 24	73.23	58.80	86.44	66.71	70.91	68.11
MM 34	79.71	53.83	88.85	74.60	76.79	70.48
MM 74	82.65	59.07	92.70	77.80	78.60	73.69
MM 35	86.52	60.46	95.90	84.08	81.92	78.85
MM 55	45.16	18.87	45.44	52.29	57.72	47.71
MM 54	58.26	30.15	62.72	66.97	64.73	65.09
MM 57	47.05	19.83	47.96	54.21	58.69	49.87
MM 81	59.90	33.37	68.39	67.71	64.25	68.96
MM 56	55.64	27.86	58.89	64.35	63.49	61.82
MM 59	66.71	57.99	87.19	64.63	64.85	71.98
MM 75	69.14	60.47	86.10	63.54	67.21	68.49
MM 58	72.05	63.94	94.08	73.52	67.98	79.96
MM 65	88.48	64.97	97.83	84.39	83.38	79.14
MM 76	90.50	65.59	98.08	84.98	85.74	78.74
MM 66	93.59	70.40	102.05	92.12	88.13	87.12

Table D.4 – QSAR predicted antiproliferative activity (as the relative cell proliferation in percentage) of the thiourea derivatives at concentration of 30 μM, against normal human dermal fibroblasts (NHDF) and against hepatic (HepaRG), colon (Caco-2), breast (MCF-7 and T47D) and prostatic (LNCaP) human cancer cell lines. The cases used in the external validation of the QSAR model are underlined.

Compound	NHDF	HepaRG	Caco-2	MCF-7	T47D	LNCaP
MM 26	68.43	60.18	93.91	71.51	78.66	62.89
MM 83	69.96	64.84	97.17	75.27	81.11	65.13
MM 25	83.89	73.14	84.29	87.52	89.02	82.20
MM 28	67.17	56.01	88.87	69.39	77.23	61.28
MM 84	68.24	61.19	94.08	73.01	79.61	63.01
MM 29	82.71	71.88	84.71	86.80	88.56	80.76
MM 30	89.02	83.55	87.63	90.32	90.80	88.43
MM 36	79.18	48.98)	79.76	65.12	75.31	71.11
MM 85	77.27	57.16	91.73	68.22	77.07	70.32
MM 37	82.47	83.14	101.51	85.84	88.00	80.24
MM 46	59.45	19.24	29.30	46.35	64.01	49.28
MM 90	63.28	21.32	33.12	48.18	64.85	52.86
MM 48	77.33	40.96	67.12	61.46	72.96	68.40
MM 60	62.68	20.57	31.73	47.95	65.14	52.18
MM 92	65.96	22.71	35.63	49.65	65.88	55.36
MM 64	79.98	49.82	81.04	65.50	75.60	71.93
MM 61	82.87	48.53	79.08	65.22	75.71	74.31
MM 86	81.49	55.37	89.32	67.63	77.01	73.92
MM 63	79.55	85.10	112.07	82.95	86.19	76.46
MM 68	85.00	70.20	109.91	72.25	80.02	78.56
MM 88	82.15	79.99	121.33	75.04	81.54	76.78
MM 67	76.08	77.17	106.74	80.51	84.59	72.35

Regarding DHPMts, following the optimization procedure described in the experimental section, the initially calculated 632 calculated descriptors were reduced to 14 by removal of multicollinear and insufficiently discriminative molecular descriptors using the Unsupervised Forward Selection (UFS) algorithm (Whitley et al., 2000). Further selection of the most relevant descriptors using a forward selection method, by maximizing the 10-fold cross-validated coefficient of determination (Q^2), returned three molecular descriptors as the most relevant: BLI (Kier benzene-likeliness index), GATS1m (Geary autocorrelation of lag 1 weighted by mass) and GATS5v (Geary autocorrelation of lag 5 weighted by van der Waals volume). The calculated descriptors values for the titled compounds are given in Table D.5. In the case of the urea series, with the initial removal of collinear and insufficiently discriminative molecular descriptors, 7 out of the initial 16 molecular descriptors were removed, resulting in 9 descriptors available for further optimization. Further removal of molecular descriptors using a forward selection method, by maximizing the 10-fold cross-validation statistics, Log *P* (GALAS predicted octanol:water partition coefficient), AMR (Ghose-Crippen molar refractivity) and Ss (sum of Kier-Hall electrotopological states) (Table D.5) were selected as the most relevant, since they generated the best average values of Q^2 and $RMSE_{CV}$.

Table D.5 – Selected *in silico* calculated molecular descriptors values for the synthesized compounds (urea and thiourea series) in both QSAR models.

Compound	Log *P*[a]	AMR[b]	Ss[c]	Compound	BLI[d]	GATS1m[e]	GATS5v[f]
Urea series				**Thiourea series**			
MM 18	1.79	71.43	47.67	MM 26	0.981	0.540	1.158
MM 72	1.48	66.69	46.17	MM 83	0.940	0.541	1.195
MM 17	1.46	65.47	42.67	MM 25	0.974	0.508	1.041
MM 22	2.13	76.47	49.33	MM 28	0.993	0.539	1.166
MM 73	1.88	71.73	47.83	MM 84	0.955	0.540	1.202
MM 19	1.84	70.51	44.33	MM 29	0.987	0.508	1.047
MM 23	1.74	78.76	63.33				
MM 82	1.41	74.01	61.83				
MM 24	1.34	72.79	58.33	MM 30	0.906	0.518	0.850
MM 34	1.57	77.90	52.83	MM 36	0.964	0.571	1.032
MM 74	1.34	73.15	51.33	MM 85	0.926	0.573	1.067
MM 35	1.38	71.93	47.83	MM 37	0.955	0.540	0.890
MM 55	3.31	81.04	55.22	MM 46	1.024	0.572	1.115
				MM 90	0.989	0.576	1.141
MM 54	3.03	75.08	50.22	MM 48	1.022	0.561	1.016
MM 57	3.25	81.04	55.22	MM 60	1.023	0.572	1.098
MM 81	2.94	76.29	53.72	MM 92	0.988	0.576	1.126
MM 56	3.12	75.08	50.22	MM 64	1.021	0.561	0.968
MM 59	1.94	71.87	63.00	MM 61	0.921	0.584	1.034
MM 75	1.27	67.12	61.50	MM 86	0.881	0.588	1.066
MM 58	1.71	65.90	58.00	MM 63	0.908	0.555	0.984
MM 65	0.87	63.82	47.17	MM 68	0.952	0.577	0.913
MM 76	0.52	59.08	45.67	MM 88	0.907	0.580	0.952
MM 66	0.69	57.86	42.17	MM 67	0.940	0.544	1.063

[a]Log *P*, Galas predicted octanol:water partition coefficient; [b]AMR, Ghose-Crippen molar refractivity; [c]Ss, sum of Kier-Hall electrotopological states; [d]BLI: Kier benzene-likeliness index; [e]GATS1m: Geary autocorrelation of lag 1 weighted by mass; [f]GATS5v: Geary autocorrelation of lag 5 weighted by van der Waals volume.

The Pearson linear correlation matrix for the molecular descriptors and tested cell lines for each series is presented in Tables D.6 and D.7. It can be observed that the chosen descriptors are poorly correlated between them, which is a requirement for a valid QSAR model (Dearden et al., 2009). The final models 6-3-1 for the urea series and 6-2-1 for the thiourea series, trained on all training cases, contain six inputs (three bits for cell line identification and the three selected molecular descriptors in each series), three or two neurons in one hidden layer (respectively) and one output neuron which returns the logarithm of the relative cell proliferation.

Table D.6 – Pearson linear correlation matrix for the *in silico* calculated molecular descriptors for compounds belonging to urea series and tested NHDF, HepaRG, Caco-2, MCF-7, T47D and LNCaP cell lines relative cell proliferation.

Correlation	LogP[a]	AMR[b]	Ss[c]
LogP	1.000		
AMR	0.764	1.000	
Ss	0.212	0.476	1.000
NHDF	-0.797	-0.769	-0.534
HepaRG	-0.740	-0.540	-0.170
Caco-2	-0.789	-0.501	-0.145
MCF-7	-0.471	-0.533	-0.694
T47D	-0.669	-0.414	-0.475
LNCaP	-0.540	-0.657	-0.278

[a]LogP: Galas predicted octanol:water partition coefficient; [b]AMR: Ghose-Crippen molar refractivity; [c]Ss: sum of Kier-Hall electrotopological states.

Table D.7 – Pearson linear correlation matrix for the *in silico* calculated molecular descriptors for compounds belonging to thiourea series and tested NHDF, HepaRG, Caco-2, MCF-7, T47D and LNCaP cell lines relative cell proliferation.

Correlation	BLI[a]	GATS1m[b]	GATS5v[c]
BLI	1.000		
GATS1m	-0.086	1.000	
GATS5v	0.310	0.036	1.000
NHDF	-0.350	-0.019	-0.391
HepaRG	-0.651	-0.341	-0.369
Caco-2	-0.565	-0.427	-0.422
MCF-7	-0.307	-0.529	-0.414
T47D	-0.377	-0.446	-0.426
LNCaP	-0.487	0.050	-0.551

[a]BLI: Kier benzene-likeliness index; [b]GATS1m: Geary autocorrelation of lag 1 weighted by mass; [c]GATS5v: Geary autocorrelation of lag 5 weighted by van der Waals volume.

The internal validation statistics (coefficient of determination and RMSE) of the developed QSAR models, both for cross-validation and training, are presented in Table D.8.

Table D.8 – Statistical evaluation of the developed QSAR models for the cross-validation, training and test data.

Parameter	Urea series	Thiourea series
Train cases	100	112
Q^2 (10-fold cross-validation)	0.663	0.686
$RMSE_{CV}$ (10-fold cross-validation)	0.071	0.086
R^2 (non cross-validated)	0.839	0.764
RMSE (non cross-validated)	0.049	0.074
Test cases	38	20
R^2_{pred}	0.740	0.699
RMSE	0.077	0.087

In this table are also shown the external validation statistics obtained when comparing the predicted output of the cases left out of the training process, for which the experimental result is known. Analysing the obtained cross-validated statistics (Q^2 of 0.663 and $RMSE_{CV}$ of

0.071 for DHPM and Q^2 of 0.686 and $RMSE_{CV}$ of 0.086 for DHPMts), and external test set statistics (R^2_{pred} of 0.740 and RMSE of 0.077 for DHPM and R^2_{pred} of 0.699 and RMSE of 0.087 for DHPMts), it can be concluded that the models present great predictive ability, generating reliable predictions. Through Figures D.4 and D.5, it is noticeable that the predicted log(relative cell proliferation) of both training and test set cases is similar to the respective experimental results for the majority of the cases. Also, for the y-scrambling procedure, the highest value of Q^2 achieved in 10 trials was 0.024 (DHPMs) and 0.006 (DHPMts), which confirms the absence of chance correlations between the molecular descriptors and the response.

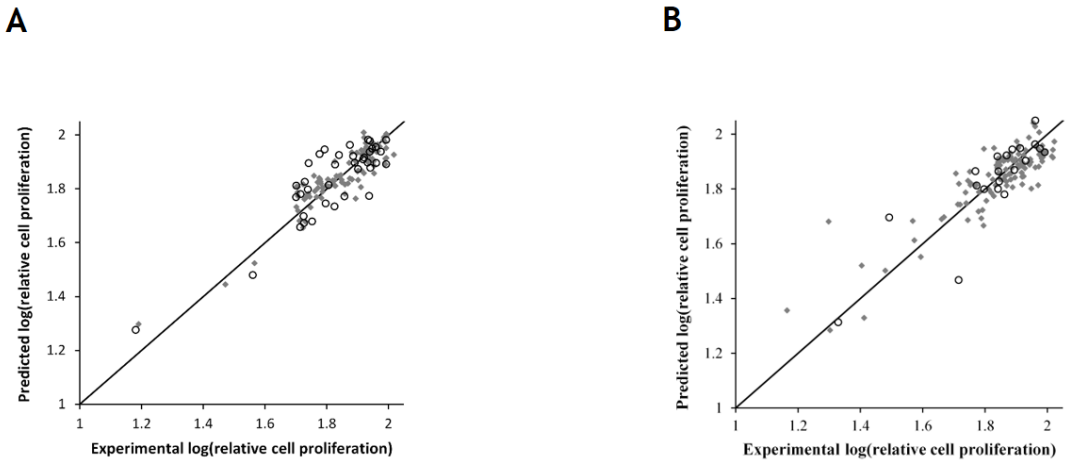

Figure D.4 – Plot of the experimental and predicted log(relative cell proliferation) for the developed BRANN QSAR models. Solid line represents the line of unity, grey marks indicate cases used for training and open circles represent cases used for external testing. **A** – Urea series; **B** – Thiourea series.

Although artificial neural networks are commonly known as "black-boxes" due to the challenging interpretation of the inputs used (Olden and Jackson, 2002), several approaches have been developed to overcome this limitation (Olden et al., 2004). In this work, it was employed the Lek profile method as depicted in the experimental section. Figures D.5 and D.6 contain the obtained trends between the molecular descriptors of each series and the response variable for each cell line.

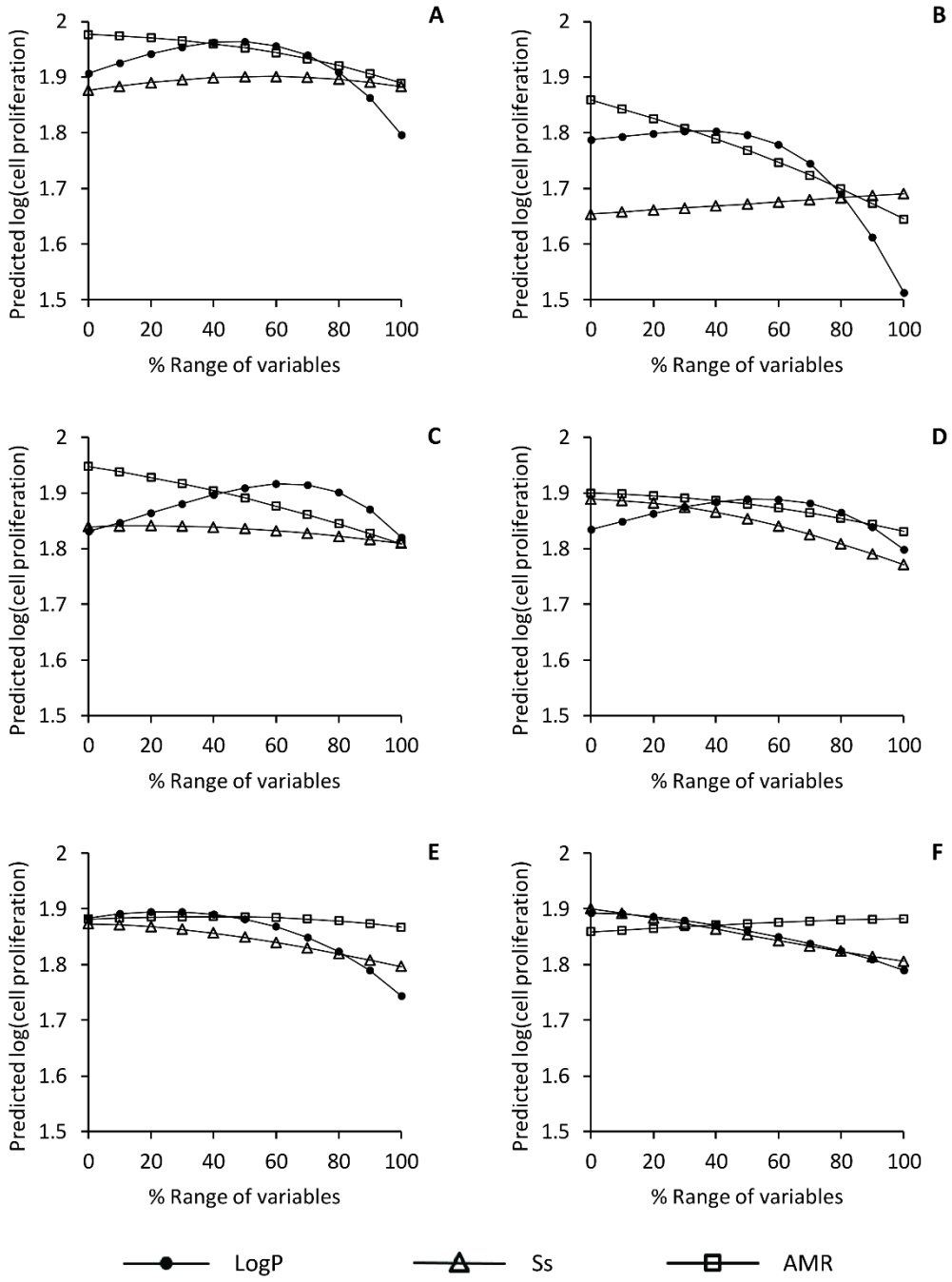

Figure D.5 – Contribution profile of the *in silico* calculated molecular descriptors Log *P* (Galas predicted octanol:water partition coefficient), Ss (sum of Kier-Hall electrotopological states) and AMR (Ghose-Crippen molar refractivity) to the prediction of the log(relative cell proliferation) of urea series by the BRANN QSAR model for the (**A**) Caco-2, (**B**) HepaRG, (**C**) LNCaP, (**D**) MCF-7, (**E**) NHDF and (**F**) T47D cell lines. Each data point is obtained as the average predicted output when each variable is varied across its minimum and maximum value and the remaining variables are fixed at their minimum, first quartile, median, third quartile and maximum value.

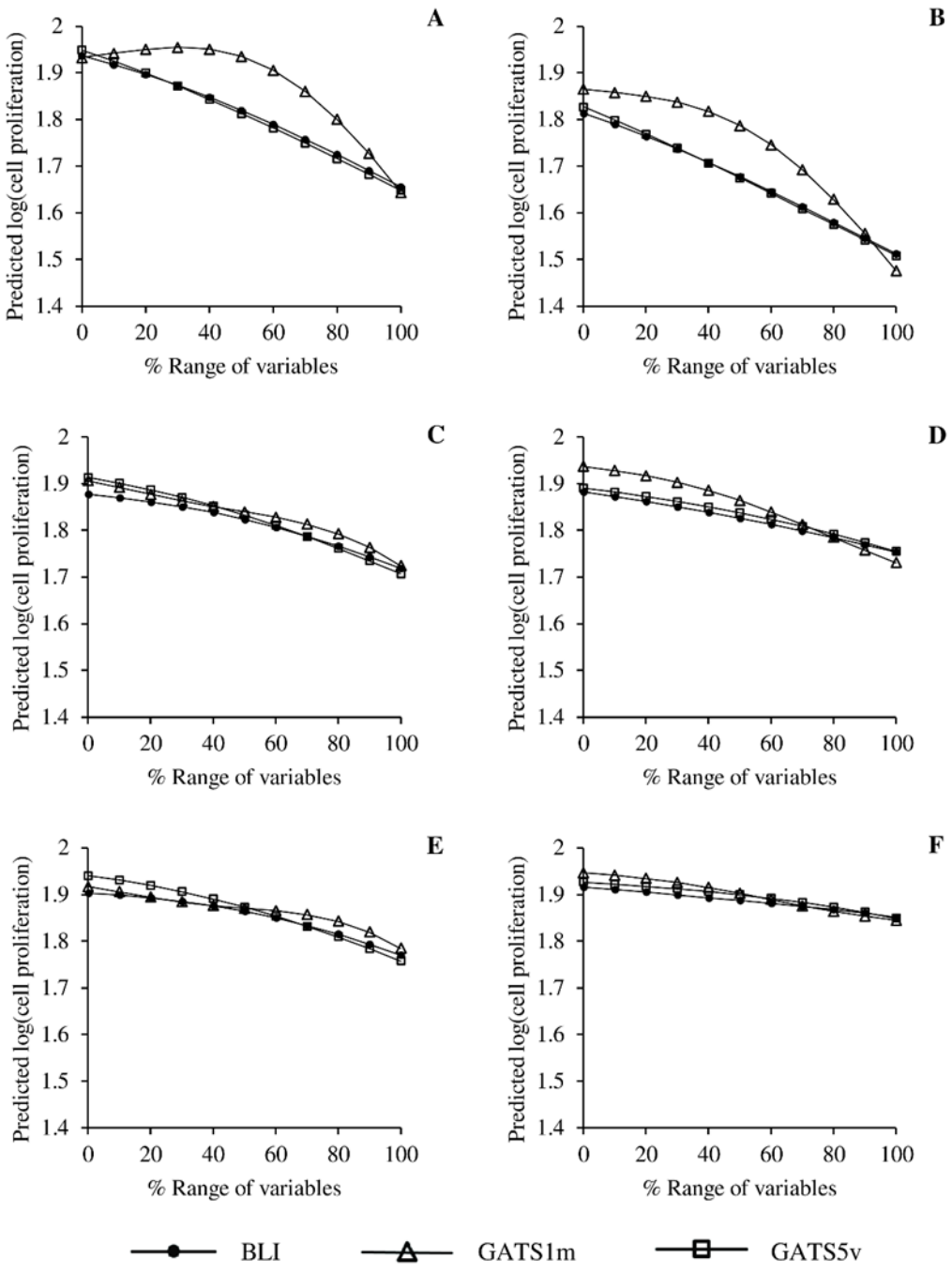

Figure D.6 – Contribution profile of the molecular descriptors BLI, Kier benzene-likeliness index; GATS1m, Geary autocorrelation of lag 1 weighted by mass; and GATS5v, Geary autocorrelation of lag 5 weighted by van der Waals volume, to the prediction of the log(relative cell proliferation) of thiourea series by the BRANN QSAR model for the (**A**) Caco-2, (**B**) HepaRG, (**C**) LNCaP, (**D**) MCF-7, (**E**) NHDF and (**F**) T47D cell lines. Each data point is obtained as the average predicted output when each variable is varied across its minimum and maximum value and the remaining variables are fixed at their minimum, first quartile, median, third quartile and maximum value.

For both series, although the trends obtained differ between the cell lines, as would be expected, there are some similarities between them. Regarding urea series, as shown in Figure D.6, Log *P* appears to have a parabolic relationship with the output, in which higher values of Log *P* generate lower values of relative cell proliferation. This observation is in

accordance with the experimental findings, in which the more lipophilic compounds (compounds containing chlorine atoms in their structure) are the most cytotoxic, particularly in the HepaRG cell line. In some cell lines (Caco-2, LNCaP and MCF-7), lower values of Log *P* also produce lower values of relative cell proliferation, and thus, higher cytotoxicity. For the molecular descriptor Ss, in general higher values generate lower values of relative cell proliferation. As an exception, for the cell lines Caco-2 and HepaRG, the relationship is positive (higher values generate higher values of relative cell proliferation). Finally, higher values of AMR tend to produce lower values of relative cell proliferation, with T47D cell line being the exception. Again, this observation is in accordance with the experimental findings, in which the bulkier chlorine-containing compounds are the most cytotoxic. This is particularly evident in the HepaRG cell line. Thus, in general, this QSAR study suggests that more lipophilic and bulky related molecules, with higher values for Ss, can generate compounds with improved cytotoxicity. This can be partially confirmed in Table D.8 by the obtained negative values for the Pearson's linear correlation coefficients between the molecular descriptors and the relative cell proliferation in each cell line (negative relationships). Although Log *P* appears to be negatively correlated with the response variable, the trend for all cell lines is not linear, and thus a direct conclusion cannot be drawn from the correlation coefficient directly without further investigation (as done in the Lek profile method). In general, Log *P* appears to be the most relevant molecular descriptor, followed by AMR, and Ss. Nevertheless, high variability exists in the relative relevance of each molecular descriptor in each cell line.

Concerning thiourea derivatives, in general, as the value of the molecular descriptors BLI, GATS1m and GATS5v increases, the relative cell proliferation decreases, and this relationship is similar to the Pearson's linear correlation coefficient values. BLI is a measure of aromaticity calculated from molecular topology, obtained by dividing the first-order valence connectivity index ${}^{1}\chi^{v}$ by the number of bonds in the molecule (excluding hydrogen bonds). The value is normalized on the benzene molecule, for which BLI takes a value of 1. Thus, as suggested by the Lek trends obtained, an increase in molecular aromaticity favours the antiproliferative activity (Kier and Hall, 1986; Todeschini and Consonni, 2000). GATS1m and GATS5v belong to the 2D autocorrelation group of molecular descriptors, which employ the Geary algorithm. These molecular descriptors describe the distribution of a specific atomic property in a molecule. Higher values are obtained when pairs of atoms in a molecule at a specified topological distance present differences in the selected atomic property. Thus, as suggested by the Lek trends obtained, larger differences in atomic weight and van der Waals volume of atom pairs at a topological distance of 1 and 5, respectively, tend to favour the antiproliferative activity (Geary, 1954; Todeschini and Consonni, 2000). In terms of relative importance of each molecular descriptor to the prediction of the antiproliferative activity, it appears that GATS1m is the most relevant input, followed by GATS5v, and finally BLI.

Overall, the developed models can be effectively used to guide future efforts in improving activity of new hypothetical related compounds, by predicting the relative cell proliferation in any of the used cell lines, given that the required molecular descriptors for the new compounds are calculated. Since only *in silico* molecular descriptors are used, there is no prior requirement of synthesis of new compounds for model prediction, and future synthesized and assayed compounds can be used to validate even further the developed model.

D.3. References

ACD/ChemSketch, 2015 release, Advanced Chemistry Development, Inc., Toronto, ON, Canada, www.acdlabs.com, 2015.

ACD/Percepta, 2015 release, Advanced Chemistry Development, Inc., Toronto, ON, Canada, www.acdlabs.com, 2015.

Asraf, H., Avunie-Masala, R., Hershfinkel, M., Gheber, L., 2015. Mitotic slippage and expression of survivin are linked to differential sensitivity of human cancer cell-lines to the Kinesin-5 inhibitor monastrol. PLoS One 10, e0129255.

Dearden, J.C., Cronin, M.T.D., Kaiser, K.L.E., 2009. How not to develop a quantitative structure-activity or structure-property relationship (QSAR/QSPR). SAR QSAR Env. Res. 20, 241–266.

Geary, R.C., 1954. The Contiguity Ratio and Statistical Mapping. Inc. Stat. 5, 115–127.

Guido, B.C., Ramos, L.M., Nolasco, D.O., Nobrega, C.C., Andrade, B.Y., Pic-Taylor, A., Neto, B.A., Corrêa, J.R., 2015. Impact of kinesin Eg5 inhibition by 3,4-dihydropyrimidin-2(1H)-one derivatives on various breast cancer cell features. BMC Cancer 15, 283.

Kier, L.B., Hall, L.H., 1986. Molecular Connectivity in Structure-Activity Analysis, in: Wiley-VCH (Ed.), Research Studies Press. UK.

MATLAB and Neural Network Toolbox Release 2014a, The MathWorks, Inc., Natick, Massachusetts, United States, 2014.

Olden, J.D., Jackson, D.A., 2002. Illuminating the “black box”: a ramdomization approach for understanding variable contributions in artificial neuronal networks. Ecol. Modell. 154, 135–150.

Olden, J.D., Joy, M.K., Death, R.G., 2004. An accurate comparison of methods for quantifying variable importance in artificial neural networks using simulated data. Ecol. Modell. 178, 389–397.

Todeschini, R., Consonni, V., 2000. Handbook of Molecular Descriptors. Wiley-VCH, UK.

Tropsha, A., 2010. Best practices for QSAR model development, validation, and exploitation.

Mol. Inf. 29, 476–488.

Whitley, D.C., Ford, M.G., Livingstone, D.J., 2000. Unsupervised forward selection: a method for eliminating redundant variables. J. Chem. Inf. Comput. Sci. 40, 1160–1168.